ISSN: 2067-3809

ACTA TECHNICA CORVINIENSIS

BULLETIN OF ENGINEERING

fascicule 4

[October-December]

TOME VI

[2013]

ACTA TECHNICA CORVINIENSIS
– BULLETIN of ENGINEERING
ISSN: 2067-3809 [CD-Rom, online]

http://acta.fih.upt.ro

UNIVERSITY "POLITEHNICA" TIMISOARA

FACULTY OF ENGINEERING – HUNEDOARA

5, Revolutiei,
331128 – Hunedoara,
ROMANIA

Aims & Scope

General Aims:

ACTA TECHNICA CORVINIENSIS - BULLETIN OF ENGINEERING is an international and interdisciplinary journal which reports on scientific and technical contributions.

Every year, in four online issues (fascicules 1 - 4), ACTA TECHNICA CORVINIENSIS - Bulletin of Engineering [e-ISSN: 2067-3809] publishes a series of reviews covering the most exciting and developing areas of engineering. Each issue contains papers reviewed by international researchers who are experts in their fields. The result is a journal that gives the scientists and engineers the opportunity to keep informed of all the current developments in their own, and related, areas of research, ensuring the new ideas across an increasingly the interdisciplinary field.

ACTA TECHNICA CORVINIENSIS - BULLETIN OF ENGINEERING publishes invited review papers covering the full spectrum of engineering. The reviews, both experimental and theoretical, provide general background information as well as a critical assessment on topics in a state of flux. We are primarily interested in those contributions which bring new insights, and papers will be selected on the basis of the importance of the new knowledge they provide.

Topical reviews in materials science and engineering, each including:

- *surveys of work accomplished to date*
- *current trends in research and applications*
- *future prospects.*

As an open-access journal ACTA TECHNICA CORVINIENSIS - Bulletin of Engineering will serve the whole engineering research community, offering a stimulating combination of the following:

- *Research Papers - concise, high impact original research articles,*
- *Scientific Papers - concise, high impact original theoretical articles,*
- *Perspectives - commissioned commentaries highlighting the impact and wider implications of research appearing in the journal.*

ACTA TECHNICA CORVINIENSIS - BULLETIN OF ENGINEERING encourages the submission of comments on papers published particularly in our journal. The journal publishes articles focused on topics of current interest within the scope of the journal and coordinated by invited guest editors. Interested authors are invited to contact one of the Editors for further details.

ACTA TECHNICA CORVINIENSIS - Bulletin of Engineering has been published since 2008, as an online supplement of the ANNALS OF FACULTY ENGINEERING HUNEDOARA - INTERNATIONAL JOURNAL OF ENGINEERING.

Now, the ACTA TECHNICA CORVINIENSIS - Bulletin of Engineering is a free-access, online, international and multidisciplinary publication of the Faculty of Engineering Hunedoara.

ACTA TECHNICA CORVINIENSIS - BULLETIN OF ENGINEERING exchange similar publications with similar institutions of our country and from abroad.

Audience & Coverage:

Scientists and engineers with an interest in the respective interfaces of engineering fields, technology and materials, information processes, research in various industrial applications. It publishes articles of interest to researchers and engineers and to other scientists involved with materials phenomena and computational modeling.

ACTA TECHNICA CORVINIENSIS - Bulletin of Engineering is a good opportunity for the researchers to exchange information and to present the results of their research activity. Scientists and engineers with an interest in the respective interfaces of engineering fields, technology and materials, information processes, research in various industrial applications are the target and audience of ACTA TECHNICA CORVINIENSIS - Bulletin of Engineering. It publishes articles of interest to researchers and engineers and to other scientists involved with materials phenomena and computational modeling.

The journal's coverage will reflect the increasingly interdisciplinary nature of engineering, recognizing wide-ranging contributions to the development of methods, tools and evaluation strategies relevant to the field. Numerical modeling or simulation, as well as theoretical and experimental approaches to engineering will form the core of ACTA TECHNICA CORVINIENSIS - Bulletin of Engineering's content, however approaches from a range of environmental science and economics are strongly encouraged.

ACTA TECHNICA CORVINIENSIS - Bulletin of Engineering appear in four issues per year and is open to the reviews, papers, short communications and breakings news inserted as Scientific Events, in the field of engineering.

Mission:

ACTA TECHNICA CORVINIENSIS - Bulletin of Engineering is an international and interdisciplinary journal which reports on scientific and technical contributions. The ACTA TECHNICA CORVINIENSIS - Bulletin of Engineering advances the understanding of both the fundamentals of engineering science and its application to the solution of challenges and problems in engineering and management, dedicated to the publication of high quality papers on all aspects of the engineering sciences and the management.

You are invited to contribute review or research papers as well as opinion in the fields of science and technology including engineering. We accept contributions (full papers) in the fields of applied sciences and technology including all branches of engineering and management.
Submission of a paper implies that the work described has not been published previously (except in the form of an abstract or as part of a published lecture or academic thesis) that it is not under consideration for publication elsewhere. It is not accepted to submit materials which in any way violate copyrights of third persons or law rights. An author is fully responsible ethically and legally for breaking given conditions or misleading the Editor or the Publisher.
The Editor reserves the right to return papers that do not conform to the instructions for paper preparation and template as well as papers that do not fit the scope of the journal, prior to refereeing. The Editor reserves the right not to accept the paper for print in the case of a negative review made by reviewers and also in the case of not paying the required fees if such will be fixed and in the case time of waiting for the publication of the paper would extend the period fixed by the Editor as a result of too big number of papers waiting for print. The decision of the Editor in that matter is irrevocable and their aim is care about the high content-related level of that journal.
The mission of the ACTA TECHNICA CORVINIENSIS - Bulletin of Engineering is to disseminate academic knowledge across the scientific realms and to provide applied research knowledge to the appropriate stakeholders. We are keen to receive original contributions from researchers representing any Science related field.
We strongly believe that the open access model will spur research across the world especially as researchers gain unrestricted access to high quality research articles. Being an Open Access Publisher, Academic Journals does not receive payment for subscription as the journals are freely accessible over the internet.

General Topics:

ENGINEERING
- ☐ Mechanical Engineering
- ☐ Metallurgical Engineering
- ☐ Agricultural Engineering
- ☐ Control Engineering
- ☐ Electrical Engineering
- ☐ Civil Engineering
- ☐ Biomedical Engineering
- ☐ Transport Engineering
- ☐ Nanoengineering

CHEMISTRY
- ☐ General Chemistry
- ☐ Analytical Chemistry
- ☐ Inorganic Chemistry
- ☐ Materials Science & Metallography
- ☐ Polymer Chemistry
- ☐ Spectroscopy
- ☐ Thermo-chemistry

ECONOMICS
- ☐ Agricultural Economics
- ☐ Development Economics
- ☐ Environmental Economics
- ☐ Industrial Organization
- ☐ Mathematical Economics
- ☐ Monetary Economics
- ☐ Resource Economics
- ☐ Transport Economics
- ☐ General Management
- ☐ Managerial Economics
- ☐ Logistics

AGRICULTURE
- ☐ Agricultural & Biological Engineering
- ☐ Food Science & Engineering
- ☐ Horticulture

COMPUTER & INFORMATION SCIENCES
- ☐ Computer Science
- ☐ Information Science

EARTH SCIENCES
- ☐ Geodesy
- ☐ Geology
- ☐ Hydrology
- ☐ Seismology
- ☐ Soil science

ENVIRONMENTAL
- ☐ Environmental Chemistry
- ☐ Environmental Science & Ecology
- ☐ Environmental Soil Science
- ☐ Environmental Health

BIOMECHANICS & BIOTECHNOLOGY
- ☐ Biomechanics
- ☐ Biotechnology
- ☐ Biomaterials

MATHEMATICS
- ☐ Applied mathematics
- ☐ Modeling & Optimization
- ☐ Foundations & Methods

Invitation:

We are looking forward to a fruitful collaboration and we welcome you to publish in our ACTA TECHNICA CORVINIENSIS - Bulletin of Engineering. You are invited to contribute review or research papers as well as opinion in the fields of science and technology including engineering. We accept contributions (full papers) in the fields of applied sciences and technology including all branches of engineering and management.
Submission of a paper implies that the work described has not been published previously (except in the form of an abstract or as part of a published lecture or academic thesis) that it is not under consideration for publication elsewhere. It is not accepted to submit materials which in any way violate copyrights of third persons or law rights. An author is fully responsible ethically and legally for breaking given conditions or misleading the Editor or the Publisher.

5th Anniversary Celebration:

We are very pleased to inform that our journal ACTA TECHNICA CORVINIENSIS - Bulletin of Engineering completed its five years of publication successfully [2008-2012, Tome I-V]. In a very short period it has acquired global presence and scholars from all over the world have taken it with great enthusiasm.
We are extremely grateful and heartily acknowledge the kind of support and encouragement from all contributors and all collaborators!

ACTA TECHNICA CORVINIENSIS - BULLETIN of ENGINEERING

ISSN: 2067-3809 [CD-Rom, online]

ACTA TECHNICA CORVINIENSIS – Bulletin of Engineering
Tome VI (Year 2013) – FASCICULE 4 [October–December]
ISSN 2067–3809

Editorial & Advisory Board

Review process & Editorial Policy

ACTA TECHNICA CORVINIENSIS - Bulletin of Engineering is dedicated to publishing material of the highest engineering interest, and to this end we have assembled a distinguished Editorial Board and Scientific Committee of academics, professors and researchers.

ACTA TECHNICA CORVINIENSIS - Bulletin of Engineering publishes invited review papers covering the full spectrum of engineering. The reviews, both experimental and theoretical, provide general background information as well as a critical assessment on topics in a state of flux. We are primarily interested in those contributions which bring new insights, and papers will be selected on the basis of the importance of the new knowledge they provide.

The editorial policy of ACTA TECHNICA CORVINIENSIS - Bulletin of Engineering is to serve its readership in two ways. Firstly, it provides a critical overview of the current issues in a well-defined area of immediate interest to materials scientists. Secondly, each review contains an extensive list of references thus providing an invaluable pointer to the primary research literature available on the topic. This policy is implemented by the Editorial Board which consists of outstanding scientists in their respective disciplines. The Board identifies the topics of interest and subsequently invites qualified authors. In order to ensure speedy publication, each material will be report to authors, separately, thought Report of the Scientific Committee. For an overview of recent dispatched issues, see the ACTA TECHNICA CORVINIENSIS - Bulletin of Engineering issues.

ACTA TECHNICA CORVINIENSIS - Bulletin of Engineering encourages the submission of comments on papers published particularly in our journal. The journal publishes articles focused on topics of current interest within the scope of the journal and coordinated by invited guest editors. Interested authors are invited to contact one of the Editors for further details.

The members of the Editorial Board may serve as reviewers. The reports of the referees and the Decision of the Editors regarding the publication will be sent to the corresponding authors.

The evaluated paper may be recommended for:

- *Acceptance without any changes - in that case the authors will be asked to send the paper electronically in the required .doc format according to authors' instructions;*
- *Acceptance with minor changes - if the authors follow the conditions imposed by referees the paper will be sent in the required .doc format;*
- *Acceptance with major changes - if the authors follow completely the conditions imposed by referees the paper will be sent in the required .doc format;*
- *Rejection - in that case the reasons for rejection will be transmitted to authors along with some suggestions for future improvements (if that will be considered necessary).*

The manuscript accepted for publication will be published in the next issue of ACTA TECHNICA CORVINIENSIS - Bulletin of Engineering after the acceptance date.

ACTA TECHNICA CORVINIENSIS - Bulletin of Engineering accept for publication unpublished manuscripts on the understanding that the same manuscript is not under simultaneous consideration of other journals. Publication of a part of the data as the abstract of conference proceedings is exempted.

All the authors and the corresponding author in particular take the responsibility to ensure that the text of the article does not contain portions copied from any other published material which amounts to plagiarism. We also request the authors to familiarize themselves with the good publication ethics principles before finalizing their manuscripts.

Manuscripts submitted (original articles, technical notes, brief communications and case studies) will be subject to peer review by the members of the Editorial Board or by qualified outside reviewers. Only papers of high scientific quality will be accepted for publication. Manuscripts are accepted for review only when they report unpublished work that is not being considered for publication elsewhere.

ACTA TECHNICA CORVINIENSIS – BULLETIN of ENGINEERING

ISSN: 2067-3809 [CD-Rom, online]

ACTA TECHNICA CORVINIENSIS – Bulletin of Engineering
Tome VI (Year 2013) – FASCICULE 4 [October–December]
ISSN 2067–3809

Regional Associate Editors & Collaborators

The Editor and editorial board members do not receive any remuneration. These positions are voluntary.
We are very pleased to inform that our journal ACTA TECHNICA CORVINIENSIS - BULLETIN of ENGINEERING is going to complete its five years of publication successfully. In a very short period it has acquired global presence and scholars from all over the world have taken it with great enthusiasm. We are extremely grateful and heartily acknowledge the kind of support and encouragement from you.
ACTA TECHNICA CORVINIENSIS - BULLETIN of ENGINEERING is seeking qualified researchers as members of the editorial team. Like our other journals, ACTA TECHNICA CORVINIENSIS - BULLETIN of ENGINEERING will serve as a great resource for researchers and students across the globe. We ask you to support this initiative by joining our editorial team. If you are interested in serving as a member of the editorial team, kindly send us your resume to redactie@fih.upt.ro.

ACTA TECHNICA CORVINIENSIS - BULLETIN of ENGINEERING

ISSN: 2067-3809 [CD-Rom, online]

ACTA TECHNICA CORVINIENSIS – Bulletin of Engineering
Tome VI (Year 2013) – FASCICULE 4 [October–December]
ISSN 2067–3809

Scientific Committee Members & Reviewers

Members from SLOVAKIA

Štefan NIZNIK
Technical University of KOŠICE, Faculty of Metallurgy, Department of Materials Science - KOŠICE
Karol VELIŠEK
Slovak University of Technology BRATISLAVA, Faculty Materials Science & Technology - TRNAVA
Peter KOŠTÁL
Slovak University of Technology - BRATISLAVA, Faculty Materials Science & Technology - TRNAVA
Juraj ŠPALEK
University of ZILINA, Faculty of Electrical Engineering - ZILINA
Vladimir MODRAK
Technical University of KOSICE, Faculty of Manufacturing Technologies - PRESOV
Michal HAVRILA
Technical University of KOSICE, Faculty of Manufacturing Technologies - PRESOV
Jozef NOVAK-MARČINCIN
Technical University of KOSICE, Faculty of Manufacturing Technologies - PRESOV
Ľubomir ŠOOŠ
Slovak University of Technology in BRATISLAVA, Faculty of Mechanical Engineering - BRATISLAVA
Miroslav BADIDA
Technical University of KOŠICE, Faculty of Mechanical Engineering - KOŠICE
Ervin LUMNITZER
Technical University of KOŠICE, Faculty of Mechanical Engineering - KOŠICE
Tibor KVAČKAJ
Technical University KOŠICE, Faculty of Metallurgy - KOŠICE
Ľudovít KOLLÁTH
Slovak University of Technology in BRATISLAVA, Manufacturing Systems Institute - BRATISLAVA
Ladislav GULAN
Slovak University of Technology, Institute of Transport Technology & Designing - BRATISLAVA
Dušan HUSKA
Slovak Agricultural University, Faculty of European studies & Regional Development - NITRA
Miroslav VEREŠ
Slovak University of Technology in BRATISLAVA, Faculty of Mechanical Engineering - BRATISLAVA
Milan SAGA
University of ŽILINA, Faculty of Mechanical Engineering - ŽILINA
Imrich KISS
Institute of Economic & Environmental Security, University of Security Management - KOŠICE
Otakav BOKŮVKA
University of ŽILINA, Faculty of Mechanical Engineering - ŽILINA
Michal CEHLÁR
Technical University KOSICE, Faculty of Mining, Ecology, Process Control & Geotechnologies - KOSICE
Pavel NEČAS
Armed Forces Academy of General Milan Rastislav Stefanik - LIPTOVSKÝ MIKULÁŠ
Milan DADO
University of ŽILINA, Faculty of Electrical Engineering - ŽILINA
Jozef PILC
University of ŽILINA, Faculty of Mechanical Engineering - ŽILINA

Members from ITALY

Alessandro GASPARETTO
University of UDINE, Faculty of Engineering - UDINE
Alessandro RUGGIERO
University of SALERNO, Department of Mechanical Engineering - SALERNO
Adolfo SENATORE
University of SALERNO, Department of Mechanical Engineering - SALERNO

ACTA TECHNICA CORVINIENSIS – Bulletin of Engineering
Tome VI (Year 2013) – FASCICULE 4 [October–December]
ISSN 2067–3809

CONTENT of FASCICULE 4 / 2013 [October–DECEMBER]

Abstract: The same application software and information systems used today on all continents, in spite of the fact that users of such systems from different national and organizational cultures. In this paper we argue that with respect and encouraging cultural diversity in the business environment can positively influence both the way of understanding, acceptance and use, and the information technology. Also it is shown the cultural heritage of a country's contemporary business culture and its impact on the development of information technology. The paper will draw attention to virtual teams and how cultural differences among them can influence the activities and the final results, as well as the possibilities of business development at the global level.

Abstract: New technologies and high quality materials are developed by manufacturers and molders of plastic to comply the emerging requirements. Applying developed technologies complex shaped plastic elements can be produced easily. The production of similar elements from steel needs more steps and more time as well. Besides these possibilities the new technologies increased the freedom of designers in the motor-car industry. This is the other important aspect of application of different type of plastics. This paper gives a brief summary about the development of application of plastic mountings in motor-cars moreover about its motivation and expectable trends. It shows the effect of international environment protection standards on design of motor-cars and construction of cars besides the plastic-industrial developments motivated by emerging demands and requirements.

Abstract: Ferrocement has the versatility that can be 'sculptured' or shaped into numerous fascinating structures and objects for very wide applications. The exposure of this technology to engineers in general is rather minimal in Romania and many are skeptical about it. The potential is not exploited for it being unconventional in nature. Its ability to compete or use as a cheaper alternative and yet a promising technology in ensuring improved living standard and environmental quality must not be neglected. The paper discusses about the applicability of ferrocement in the Romanian scene with respect to recreation and home use. The ferrocement elements can be used for outside or inside exposure, thanks to ferrocement's durability, resistence to impact and resistence to fire.

Abstract: Bridges are the vital components of each country's roads. Economic studies of the road construction show that the road bridges allocate much cost to it and due to the delicate structures of their system; they have great vulnerability as well. Therefore the detailed design of the various components of the bridge should be considered further. Erosion and transport of bed material is separated from it by a process called scouring. Occurrence of scouring around the bridge piers is one of the main reasons for the defeat and destruction of bridges and their instability. So it is important to provide methods to control and reduce this phenomenon. In the present study, the modeling of non-submerged plate's perpendicular to the water flow has been expressed in upstream of the cylindrical pier using software SSIIM. Reducing the depth of the scouring hole was observed in these pages, and has a great influence around the bridge pier.

Abstract: *This article discusses some typical disadvantages of the traditional kinematical scheme for implementing the vibratory superficially plastic deformation process, realized on manually controlled lathe machine tools and the possibilities and some difficulties in implementing that process by using 2 - axis CNC lathes and the more advanced multi-axis CNC Turn/Mill centres. Kinematical parameters of the process having an impact of the toolpath, for forming of regular reliefs from different types through the process are described, and math functions for its calculating are proposed in accordance with the diameter and length of the cylindrical surface, that will be processed. The necessity of using 4-axis turn/mill centres (with rotary C-axis) is examined. The sequence of steps for automated programming of the attributes of the operation, using FeatureCAM software system, for output the required NC code is proposed.*

Abstract: *The need to understand and predict flows that carry large loads of suspended sediments and wash loads has become acute in the Yellow River Basin, where significant erosion and siltation associated with high-concentrated floods produce significant erosion, siltation, and associated river problems. Mud flows, debris flows and slurries, which contain large concentrations of clay and/or silt particles suspended in water, often show non-Newtonian hydrodynamic properties. Non-Newtonian flows are poorly understood regarding the impact of their rheological properties on fully developed turbulent flows. In this paper, we experimentally investigated resistance and flow structure of high-concentrated sediment laden flow in an open channel using particle image velocimetry. The results showed that, compared with clear water flow, the rheological properties of sediment-laden flow significantly dissipated the turbulent flow fluctuations over the dune type bed and increased the flow resistance.*

Abstract: *Nowadays, the development of the Automated Manual Transmission (AMTs) has led to remarkable increment of their performance respect the manual ones. In fact, AMTs allow strong improvement in terms of safety, comfort, reliability, shifting quality, and driving performance, together with reduction of fuel consumption and pollutant emissions. Automated Manual Transmissions (AMTs) systems are generally constituted by a dry or wet clutch assembly and a multi-speed gearbox, both equipped with electro-mechanical or electro-hydraulic actuators, which are driven by a control unit, the transmission control unit (TCU). In this transmission type the quality of the vehicle propulsion as perceived by the driver is largely dependent on the quality of the control strategies. This paper aims at investigating the influence of the temperature on the engagement performance of an actively closed dry clutch.*

Abstract: *The traffic noise is one of the most important factors influencing the reduction of comfort life and also it can cause the increase the possibility to loss health by people. The motorcycle sports are the types of vehicles which exploitation is connected with generating noise of a higher level. In the work, the tests of influence of using different solutions of the muffler type of the exhaust system construction on the level of noise emission by the sports motorcycle are presented. One of the categories of the motorcycles on the public ways are the sports motorcycles equipped in engines with the power over 100kM and max. rotational speed more over 10000 rpm. The motorcycles use by young people are often individually modified which may cause the level increase of generated noise. In the work, the test results are presented, their aim was to estimate the emitted noise influence by sports motorcycle equipped in 4 different exhaust systems. There were conducted tests of the noise according to the norm, additionally in the place of the motorcyclists head and in the position of the pedestrian near the road.*

Abstract: *In accordance with the EU Energy Policy, developed in 2007, energy is an essential element for the development of the Union, but equally is a challenge regarding the impact of the energy sector on climate change, increasing dependence on energy imports and increasing the energy price. The paper focuses on the latest European Directive of the European Parliament and of the Council from October 25, 2012 on energy efficiency. The Directive establishes a common framework for promoting energy efficiency measures in the Member States of the Union, in order to achieve, by 2020, the main objective of 20% energy efficiency and to open up the way for further energy efficiency increase. In the paper is written a synthesis of the European Directives issued by the European Parliament on energy efficiency, specifying some of the energy-saving targets set by them.*

Abstract: Questionnaires were done for research of the local consumer evaluation aiming the topic of traditional horticultural products in the sphere of products in horticulture and food industry. We have three hypotheses: 1.The consumers are able to associate with messages bound up with characteristic, regional products. 2. In the decision-making process, in connection with the purchase and consumption of the consumer, the knowledge of the source of supply is an influential factor. 3. The product character of traditional horticultural products gives the chance to the consumer to acknowledge the excellent and individual feature of the product in a higher price, consequently, the higher price will be less influential factor in their decision-making process of the purchase. In the years 2010-2011 primary research has been conducted on agricultural and food manufacturers of traditional horticultural products. To analyse the survey data, we have used SPSS 14.0 for Windows and LISREL 8.30. Methods: Confidence-interval calculation, a variable structure test wit factor analysis, a variable structure test with cluster analysis, multi dimensional scaling and correspondence analysis. It can easily be brought to light that the consumers select product not even on the basis of its price, appearance but rather on the basis of its particular taste and the excellent quality. The consumers regard - beside the perceptible attributes - the Hungarian provenance, place of origin and the traditional feature as an important aspect. In the analysis of traditional horticultural products we can divide two independent factors can be distinguished: quality and economic factors.

Abstract: With applying of GIS information technology in decision-making processes, decision-makers were given powerful tools that enable the collection and processing of large amounts of spatial data and creating quality information in a very short time. The Geographic Information Systems (GIS) are complex five-component information systems that comprising the following components: procedures, people, data, hardware and software. This paper describes the integration of several open source GIS software for various purposes in the process of decision-making in local government. The paper presents an example of integration of various functionalities opensource GIS software to improve decision-making in local governments. It shows the synergistic possibilities of integrating various opensource GIS software to support decision-making (DSS). Special attention is paid to geoprocessing capability. Further, it is analyzed the significance of building spatial data infrastructure at the local level as basis of DSS. The research was done on the example of choosing the best options for the reconstruction of public lighting. The results of this study contribute for promote the growing trend of integration the compatibility of various GIS open source software solutions.

Abstract: The use of surface waves of the Rayleigh type enables the properties of the component materials of a layered structure, such as a pavement, to be determined. The method has the advantage that the measurements are performed dynamically, thus making an allowance for the inertial and frequency dependent response of the pavement. The velocity of the waves is not a constant, but exhibits dispersion. The manner of the variation of the wave velocity is used to determine the properties of the surface and subsurface materials of the structure. Inverse problems are involved in interpreting the results. Wave propagation in elastic plates is analogous to propagation in layered spaces and therefore the free plate system can be used to model the surface layer of a single layered pavement structure. A direct algebraic inverse technique has been developed and used to calculate the thickness of the surface layer of a pavement system employing free plate analysis. To assess the effectiveness and reliability of the proposed technique, the application of the method to a published set of experimental data obtained in the field is presented and discussed. It is shown that the experimental results and the algebraic solutions are in good agreement, indicating that the proposed method can be used to determine the thickness of the pavement surface layer without resorting to excavation and in a very quick and economic manner.

Abstract: The measurement of micro-hardness with loads between 0.09807 N and 0.9807 N has been carried out in direct mode (appraiser measured the dimensions of indentations with a measuring device fitted to the micro-hardness tester, a part of microscope) and in modified remote modes. The reference block - certified reference material with defined specified hardness and its uncertainty was used as a specimen, particular measurement involved indirect calibration of tester. The influence of applied load on the measured value of micro-hardness was evaluated by Meyer's index n and PSR method. The difference between values obtained by particular modes is statistically significant. The purpose of this paper is to evaluate the influence of load on the values of micro-hardness using Meyer's and PSR methods, to evaluate the influence of load on the uncertainty of measured micro-hardness and to compare the results obtained in direct and remote modes.

Abstract: Over the past few decades, important efforts have been made to develop and implement engineering design guidelines, construction and maintenance standards, and specifications for gas tanks used in the automotive industry, including standardized test methods. In order to provide a better understanding of the gas tank design, optimization, reliability and manufacturing feasibility, the research efforts have been focused towards new, convergent, stable and robust CAD algorithms for obtaining the optimal solution. The aim of this work is to present a method that allows the optimal design of a shrink fitted concave ended cylindrical tank for the storage of methane gas, based on the application of the Finite Element Method (FEM). This paper presents a methodology for the optimal shape design of a shrink fitted concave ended cylindrical tank for the automotive industry using the FEM and which is based on a specialized database of 3D parameterized shapes. The mechanical simulation, numerical calculations and geometrical modeling were applied for the three-dimensional complex models

Abstract: When we are testing the wear we have to measure the loss of the tested material with the same testing circumstances that cannot be easily ensured. Therefore a relative abrasion resistance is usually measured (wear of an etalon material / wear of the tested material). When somebody searches abrasive wearing properties, it is always a significant question, how to select appropriate wear testing equipment. If the chosen method is the model testing of simple specimens, lots of obtainable tribotesters will be found on the market, and there is a good chance for developing one, too. Many well-designed testing machines exist and are available. For classification my chosen main aggregate is the movement of the specimen. Here is a short summary of the advantages and disadvantages of the different kind of abrasive wear testers where the contact surfaces of the worn and the abrasive materials have relative speed difference.

Abstract: In this research, a statistical modeling is introduced in order to evaluate measuring error of diaphragm gas meters considering the effects of different ambient temperatures on the usual ($0.2Q_{max}$) and maximum (Q_{max}) consumption flow rate. In this study, a G4 diaphragm gas meter was used because of its prevalence in Iran. By considering the climate of Iran, average range of experiment's temperature was chosen between 30ºC to 60ºC and 0ºC to -30ºC. For conducting the experiments on these gas meters, a heater-cooler device and a master chamber were utilized. Proposed statistical modeling was able to evaluate the amount of using gas in the form of $0.2Q_{max}$ and Q_{max}. The obtained results may be used as a correction factor for diaphragm meter operation on different temperature conditions. In other words, the advantages of this research can be used for estimating the proper amount of using gas and calculating the proper fee for the user. According to results, in the countries that the gas consumption is done by diaphragm gas meters, national gas company will be lost for cold cities and will be profited for warm cities and the amount of fee estimation error is significant. As an example, national gas company of Iran lost about 40.7 million dollars for gas consumption measurement error for Tehran city in 2008.

Abstract: The heat transfer in the melt-mold system during die casting process is made through conduction, convection and radiation. So, during pouring of melt into the mold, interface heat transfer is through forced convection and radiation. After the melt filled the mold, the interface heat transfer depends on the contact between melt and mold. Temperature evolution in mold wall during die casting of steel was analyzed by a finite element simulation and the results were compared with experimental data. The simulation consists in solving a conduction heat transfer problem with appropriate initial and boundary conditions. In this study, the Comsol Multiphysics 4.2 software is used to simulate the conduction heat transfer in the mold wall during die casting processing. The simulation results are compared with experimental data obtained by K-type thermocouples measurements taken.

Abstract: The virtual product development is a modern approach in the product development process. Apart from the visualization itself, the virtual product development encompasses the whole range of testing in the virtual reality (VR) environment. Different testing performed in the virtual reality environment before prototype production can increase productivity and decrease development time. As an illustration of possibilities of performing different kind of testing in VR environment, this paper shows simulation in the VR environment of the process controlled by programmable logical controller (PLC) and MATLAB/SIMULINK. As an interface between VR and MATLAB/SIMULINK environment VR Toolbox library is used, and between MATLAB/SIMULINK and PLC controller that is OPC standard.

Abstract: *The ever growing interest in the utilization of solar energy as an accessible, renewable, environmentally-friendly and easily-manageable type of energy makes it a prospective branch of power engineering. The utilization of the maximum possible amount of total solar radiation reaching a certain surface depends on the azimuth angle and its inclination in relation to a horizontal plane. The empirical data about the solar radiation intensity reaching the horizontal surface under discussion within the year 2011 makes it possible to determine the solar potential at an optimum angle of an inclined surface. The paper presents data about the potential solar energy which the city of Varna receives at an optimum angle of plane inclination. The results are obtained on the basis of a methodology developed for the purposes of calculating the solar energy received. The experimental values of the total solar radiation on a horizontal plane observed within a year at a certain geographic location, namely the Technical University of Varna, serve as an output.*

Abstract: *Interaction between humans and robots was always having great attention, as robots should never hurt human beings. With technological development the totally separated operation of robots is being changed to closer cooperation. Industrial robots now can detect humans in their work-envelope and reduce their speed according to the motion of the human. This is a radical change to the previously in-fenced and no human in work-envelope concept. This paper is investigating today's policy and standards in human - robot interaction along with solutions for security of production cells. An example demo setup will also be shown, where the utilization of the newest technologies is emphasized. The paper also deals with introduction of high level control of security through simulation software.*

Abstract: *This paper gives a general overview of the EWMA statistics. In addition to already known concepts, the paper presents a comparative analysis of different smoothing schemes. The optimization possibilities of this statistics are also discussed. With intention to improve the process of exponential smoothing, the behavior of the moving trimmed mean and moving median in computer network environment was examined in relation to the most commonly used moving average. For this purpose, several different types of distribution are used to model network traffic. Using the software package "Matlab", sequences of random numbers are generated for each type of distribution, as the way to simulate network traffic. It is shown that the moving average and moving trimmed mean better follow the curve of original traffic. At the same time, comparing the situation with and without outliers, the smallest relative jump of MSE was determined for moving average and moving median. This conclusion justifies their use for the elimination of the negative impact of outliers and positively affects the general level of traffic control in computer networks.*

Abstract: *Controlling the speed of a motor is a basic functionality of modern electric drives. In order to precisely control the speed of an electric motor, it is necessary to measure the actual speed of the motor. This measurement can be done with various tools and methods. The paper introduces the basics of speed measurement with quadrature encoders. It explains the theory of the basic sensor types, and the signals of the quadrature encoder. It introduces the theory of the two main methods for speed measurement with quadrature encoders: the time based, and the frequency based method. It describes the quantization and relative errors of these two methods, and the considerations of their implementation. Finally it gives a short example of the practical implementation in LabVIEW FPGA, for the frequency based speed measurement method.*

Abstract: *The adsorption of phenol from aqueous solution using waste tyre rubber granules (WTRG) was investigated in a batch system. The effect of various factors such as initial concentration of phenol, amount of adsorbent, size of adsorbent particles, pH and temperature of solution on the adsorption capacity of WTRG and percentage removal of phenol was studied. The equilibrium time for a phenol concentration of 700mg/l was obtained to be 60 minutes indicating fast adsorption. The percentage removal of phenol and adsorption capacity of WTRG increased from 20.5 to 40% and 5 to 10.6 mg/g respectively with decrease in particle size from 2.36 to 0.30mm. The adsorption capacity of WTRG was observed to decrease from 13.4 to 9.9 mg/g with increase in solution temperature from 5 to 45°C indicating that low temperatures favoured the adsorption of phenol. Maximum adsorption was recorded at a pH of 8.5 and an adsorbent dosage of 4g. Isotherm data were analysed using Langmuir and Freundlich isotherm models. The equilibrium data for phenol adsorption on WTRG was observed to fit Langmuir isotherm best with an R^2 value of 0.995.*

Abstract: *In the city of Cluj-Napoca, the Greek-Catholic Cathedral, it is a well-known historical monument. The architecture it is baroque and it is one of the most well preserved historical buildings of its kind. As far as the plane geometry, the cathedral has a rectangular shape, with a basillical structural system in the coir section. It is a brick masonry structure, with arches, suspended domes, pilasters and a load-bearing wall with direct foundation. The Greek-Catholic Cathedral "Schimbarea la Față" it is one of the most important and well-known baroque historical monuments from the city of Cluj-Napoca, in Transylvania. From the beginning of the construction, until the end of the 90's this church had a tumultuous history and it survived in very good conditions. What the author presents are the structure with its three main historic load-bearing sub-units, the historic structural elements, where there are positioned and how they work. All this is made with an analysis based on photos, measurements and other information collected from the site. The author presents during this article, the structure with its main historic load-bearing structure subunits.*

Abstract: *The main scope of this article is to describe the structural design unmanned reconnaissance vehicle to 80kg. Apart from the design and technical and visual documentation of the work is also a detailed description of each component. This work proposes a suitable design for a simplified UAV system which promotes the autonomous movement of an UAV and includes the optimal selection of its components (avionics), such as a (Javelin Stamp) processor, GPS module, motors, gyroscopes and maneuvering equipment for an optically remote controlled drone. In the proposal, the most important part is the selection of the profile's wings, because it imparts its aerodynamic characteristics and as a result, its lift.*

ACTA TECHNICA CORVINIENSIS – Bulletin of Engineering, Fascicule 4/2013 [October-December/2013] *includes scientific papers presented in the sections of Conference on:*

- *THE 1st INTERNATIONAL SCIENTIFIC CONFERENCE - CONFERENCE on MECHANICAL ENGINEERING TECHNOLOGIES AND APPLICATIONS - COMETa 2012, organized in Jahorina, BOSNIA & HERZEGOVINA (28 - 30 November, 2012), jointly by the Faculty of Mechanical Engineering University of East Sarajevo. The new current identification number of paper is #18, in the content list.*
- *THE 11th INTERNATIONAL CONFERENCE ON ACCOMPLISHMENTS IN ELECTRICAL AND MECHANICAL ENGINEERING AND INFORMATION TECHNOLOGY - DEMI 2013, organized in Banja Luka, BOSNIA & HERZEGOVINA (30 May - 1 June, 2013), jointly by the Faculty of Mechanical Engineering, University of East Sarajevo. The new current identification number of paper is #20, in the content list.*

Also, ***ACTA TECHNICA CORVINIENSIS – Bulletin of Engineering, Fascicule 4/2013 [October-December/2013]*** *includes, also, original papers submitted to the Editorial Board, directly by authors or by the regional collaborators of the Journal [papers # 1 - 17, # 19 and # 21 - 25].*

ACTA TECHNICA CORVINIENSIS - BULLETIN of ENGINEERING

ISSN: 2067-3809 [CD-Rom, online]

ACTA TECHNICA CORVINIENSIS – Bulletin of Engineering
Tome VI (Year 2013) – FASCICULE 4 [October–December]
ISSN 2067–3809

[1.] A. LANGOVIĆ MILIĆEVIĆ, [2.] Z. LANGOVIĆ, [3.] T. CVETKOVSKI, [4.] B. PAŽUN

NECESSITY OF RESPECT THE RELATIONSHIP BETWEEN CULTURE AND INFORMATION TECHNOLOGY IN MANAGEMENT BUSINESS SYSTEMS

[1-4.] GRADUATE OF SCHOOL OF BUSINESS STUDIES, MEGATREND UNIVERSITY, SERBIA

ABSTRACT: The same application software and information systems used today on all continents, in spite of the fact that users of such systems from different national and organizational cultures. In this paper we argue that with respect and encouraging cultural diversity in the business environment can positively influence both the way of understanding, acceptance and use, and the information technology. Also it is shown the cultural heritage of a country's contemporary business culture and its impact on the development of information technology.
KEYWORDS: culture, information technology, business systems, management

INTRODUCTION

Information technology nowadays is developing rapidly. Global communications network is transformed almost every aspect of our lives. This includes the way we work, rest, entertainment, energy, education, political involvement, family experience, social structure, and communication in general.

So far, published numerous papers study the success of the project software development or information systems affect not only professional competence closely involved in the project, but by engaging experts from different cultures gives the final product that is logically acceptable for the global market. Companies who understand how the concept of multiculturalism affects business and those that have adopted this concept have the opportunity to improve their competitiveness in the market. The rapid development of information technology and its use in everyday life certainly had an impact on improving the quality of education. Both, in business and in education and the present trend is the globalization. Regardless of the choice areas of expertise in the study, it is practically inconceivable that the student does not have some kind of basis by management during the study needs to process. Since the majority of literature based on American theories that emphasize diversity as an asset, it certainly had an impact on the ability of young professionals in coping with cultural differences in everyday life. This phenomenon has certainly had an impact on the ability of experts from many countries to be the most easily cope with the difficulties that carry the cultural differences, which makes them ideal for working in a multicultural environment.

Companies today face greater challenges than ever before. A large percentage of cooperation is achieved with the countries that are remote and which are not known much. For successful cooperation besides knowing the language, it is necessary to know the culture and the national office staff. Language is no longer a barrier, as it is now mostly used English as the universal language. Today we have two extremes, globalization and the spread of mass culture on the one hand, the individual cultures of each country to the other. Despite the cancellation of today tends differences still remain remnants of national culture whose traces can not be deleted. Cultural diversity is inherent in global development. This is because team members have different national, organizational and professional culture. The very cultural diversity has a positive impact on the development of information technology It can have a positive impact on the promotion of creativity but can be barriers to communication and knowledge sharing. No matter what condition the different cultures different ways of business communication, while the use of new technologies in everyday business and personal life leads to the formation of a universal pattern of behavior. This evolutionary process allows individuals in different locations, different cultures, expectations and objectives that are part of the same virtual team. The paper will draw attention to virtual teams and how cultural differences among them can influence the activities and the final results, as well as the possibilities of business development at the global level.

CULTURAL IMPACT ON INFORMATION TECHNOLOGY

With increasing levels of multiculturalism in today's business and the necessity of information systems development and management of information systems should be considered in light of the cultural factors that affect their usefulness. Hofstede's observations, [14] and analysis provide scholars and

practitioners valuable insight into the dynamics of cross-cultural relations. However, like any scientific work can not avoid criticism. There are many more scientists who support Hofstede than those who do not. Most cites the fact Hofstede. Many people fully include their findings. Great interest has been placed on the culture of the business in the last two decades. With increased national diversity in today's business culture still gives an important dimension. Culture is important for many aspects of business life, especially in terms of design, development and management of information systems, protocols and infrastructure. Design and management choices in information systems are the result of individual values, and these values are the product of socio-cultural background. The values are the product of professional designers, social and organizational context that includes education and experience of an individual. The choice of design is strongly influenced by the socio-cultural environment. Despite the universally recognized importance, the impact of cultural factors on IT results received limited attention by researchers of information systems. When people are faced with information technology in information systems, human cultural values must be taken into consideration. Many cross-cultural researchers, including Hofstede, [14] were criticized for not providing clear guidelines. Hofstede's research has had a major impact on academics and practitioners. Hofstede's model has been instrumental in the realization of many operating systems, including: entrepreneurial behavior, conflicts, dynamics and success of the working group, innovation, leadership styles, management control systems and many other cross-cultural issues. It is necessary that the researcher overcome the many factors that are not common in typical research tasks. [14]

- ☐ *Problems of definition*
- ☐ *Methodological simplicity*
- ☐ *Equivalence - There are four dimensions: functional, conceptual equivalence of measurement instruments and*

As a result of Hof-multinational study are four dimensions of cross-cultural differences that influence the development of information systems, [14, 19]

- ☐ *power distance - Impact of power distance in information systems has been studied by many researchers. Power distance also has an influence on web design and user interface. For example, the website of the universities in Malaysia are highlighted symbols of power, and on the website of the University in the Netherlands focuses on the students and shows how they are able to improve themselves (there is the possibility of virtual college tour through the camera).*

Using information technology to interpersonal communication can be interrupted in different ways, caused by cultural differences. As the communication by electronic mail is considered the least intrusive use of information technology can promote communication between employees at different hierarchical ladder / positions in companies.

The negative social effects of using email despite individual efforts of individuals, training and other types of training and looms, can mitigate the importance of this communication "tools". Also the communication through information technology can be considered too "remote", which might be less popular.

- ☐ *individualism / collectivism - This scale measures whether people prefer to work in groups or individually. It indicates the degree of social / communication integration. The U.S. has the lowest values of the scale, ie., they prefer individual results. It stems from a cultural upbringing that people are expected to be independent at a very early age. On the other hand, in Guatemala people means the most to work in groups and performance are attributed to a cooperative achievement. Lifestyles in Guatemala would likely be based on close family ties, with strong community support.*

Promoting cooperation is one of the main goals of information systems. Tools such as the Internet and forums, shared drives and Group Support Systems are just a few of the tools that support collaboration. They provide new ways for knowledge sharing, reuse, and expansion of cooperation. These tools support the group discussion, decision making and assist in networking. Within the framework Hofstede's culture, it is possible that an individualist culture to be more resistant to these collaborative efforts support while the collectivist culture much easier to adopt. It is possible that the development of such common information systems pronounced in individualistic societies, whereas collectivist societies do not require additional support.

- ☐ *masculinity / femininity - This scale is not related to the dominance of sex. This shows the extent to which male traits such as power, assertiveness, performance, success and more preferred over female characteristics, such as personal relationships, quality of life, service and prosperity. Japan ranks lowest on the scale Hofstede and shows that they are very fatherly oriented. The other extreme of Hofstede's research as Sweden and Norway. The people in these two countries are likely to show more empathy for their colleagues.*

Interpretation of "paternal" approach to IT management could be interpreted as a controlled, centralized approach. With regard to standards, architecture, settings and processes, centralization involves top-down approach. Developers who work in the "masculinity" and the target are process-oriented, and developers who work in the "feminine" are more oriented towards long-term relationships. Some researchers suggest training as a solution to help developers with the distinctive "effeminate" characteristics, approaching developers with strong traits of "manhood." It has been proven that the good relations between people, and promote the exchange of knowledge relating to trust, which contributes to better organizational performance. Therefore, it

appears that employees with strong feature "femininity" contribute significantly to the organization.

- *Uncertainty avoidance - Cultural dimension of uncertainty avoidance is the degree to which people feel threatened by the lack of structure or uncertainty of events. It Refers to the way in Which people deal with it in the future to have full control over when events or events beyond their control. People with low levels of uncertainty avoidance will require a structure with clear rules and guidelines. Hofstede found that Greece had the lowest level of uncertainty avoidance. Therefore, the people of Greece will be willing to make decisions and they will require a very structured work routine. The Swedes on the other hand can work well without structure and have high tolerance for ambiguity. The researchers found that uncertainty avoidance plays a major role in small companies form alliances technology. Small companies face two types of uncertainty: relational uncertainty is derived from the risk of partnership and technological uncertainty is derived from the risks of new technology itself. The researchers found that the company's medium level of uncertainty is likely to access technological alliances, in order to avoid uncertainty. In a study of technology acceptance model across cultures, it was found that uncertainty avoidance is different in different cultures adopt new information technologies. This study explains how to embrace the new technological models in different cultures such as Sweden and the United States, not Japan.*

Dependence on information systems brings another dimension of uncertainty and risk. Possible threats are thieves, loss, misuse of data, destruction, and denial of service. Consequences may include unavailability, legal liability and financial losses. They can be detrimental to the survival of the organization. All of these risks can be minimized / mitigated, but also costs related to such a reduction. It is expected that companies with low tolerance of the risk to invest in mitigation of these processes. Further research on how different cultures influence these threats can provide additional research .

THE IMPACT OF TECHNOLOGY ON CULTURE

The mere application of a technique depends on logic and social needs. For example, today's computer technology is not based solely on the technical logic but also in many aspects related to the social logic and social needs. It all starts with the interaction of certain technical understanding of the social logic. It is a process of exchange and feedback between certain techniques or resources and man. It is the logic of interaction between technical and social aspects of call technology.

Information technology has a social dimension. There is a twofold process. The first is the introduction of technology in the social sphere of logic. The second is the introduction of the social logic of the technical sphere, which is at the heart of technological dynamics and its correlation with culture.

Techniques and created within a particular culture and it represents the product of the same culture as the result of some social needs. The relationship between any technique or technology and its social context is never deterministic and it is never possible to determine a single cause for any cultural or social situation. What you can look for the elements and processes that determine the joint influence of technology. Therefore, none of the techniques and the technology itself is not positive or negative, and even neutral. The impact of technology has opened up new possibilities, but does not specify the selection and implementation of specific options.

There is not only the impact of technology on culture. There are multiple relationships between people who invented, created, or use a variety of techniques in a variety of ways.

Rapid and large changes in technology influenced our daily lives, including the concept of culture. It all began the twentieth century, when the scientific process speeded up. The elements of today's culture are: the availability of information, freedom, social heritage and environment, and new pressures, the appointment of working conditions in companies, adverse impact "of new technology." Application of new technology has provided more time for training, and improve the conditions for the work. Technology can be considered as a means of culture absolve a man of some forms of oppression in their daily lives. Again, some individuals believe that today is one more "subdue" technology. Thanks to technology, man is able to encounter different cultures.

A man is placed in an appropriate social environment of a particular culture. In this important role of religion. The impact of religion on education. This is especially true for religious minorities. Language, habits, customs, traditions, climate in a specific geographical area affected both the mentality of the people, and their culture. The use and development of technology today, communication between people is facilitated. Nowadays, spatial distance is no longer a problem in the business. That's why we have more widespread distribution business outside the home country. Culture is one of the factors that has a special meaning and that today's management should pay special attention.

Development of new information technology network follows the logic that looks at the different categories of time and place. Customers around the world who use the internet do share some common values and customs. This allows them to communicate with each other and create a simpler form of "social organization". This common set of values and practices can be called technological culture. See the development of cultural forms that are not based on a particular geographic or historical-based culture has crossed over them. A potential problem may arise if the new film is not only a technological culture that is new, additional level of culture, but replaces other cultural forms and thus reduce the existing cultural diversity.

Information Technology today is determined very fast development. It may increase the effects of cultural differences between those who have access to

information technology, ie. belong to an online community, and those who do not have such access. Such a division may result in the exclusion of certain social groups. The groups remain excluded from access to information technologies remain excluded from contemporary culture. This can reduce the contemporary cultural diversity. Due to the rapid development of information technology and the strong impact it has important spot emerging problems and tries to solve them.

Increased intensity and scope of communication has resulted in two different trends. The first trend is towards unification, through two mechanisms - the domination of one culture over another. This may result in the disappearance of the weak or the emergence of new cultural mix where diversity is reduced to common elements as the original layers of culture lost. Another trend is the acceptance of cultural diversity because it allows for dialogue between members of different groups, which may again result in the emergence of several new cultural forms. How could any cultural form to survive it must continue to live and change it. Culture is alive only when it is adapted to their environment and continues to produce new cultural forms. Information technologies are mixed in the human environment and thus alter the conditions of existence of different cultures. It is logical that today's living culture to find new ways of expression and organization using information technology. Culture is necessary to try to understand as a means to integrate existing technologies into its own dynamics. As a rule, when people get used to the technology, to accept both her face, positive and negative. It is supposed to be how technology improved, and its negative consequences better managed. Many of our daily activities depend on the smooth functioning of the communication technologies.

Of particular importance is its tendency Internet time, not space. Distance does not lose importance, but we are all connected in cyberspace. A sense of community that is created on the Internet largely depends on the activity that occurs under its own terms. Internet brings us a sense of connection, but it is a random connection.

High technology has the greatest impact on the changes in communication and in general to changes in lifestyle, understanding of culture and ways of doing business. Deleted the boundaries of the area as well as the traditional boundaries between people. Now people are faster and easier to connect, but the connection at the moment can be found in different parts of the globe.

Even if the mass and virtual culture tends deleting old, traditional boundaries, people who meet at business meetings carry the characteristics of the cultures they come from. Sometimes these meetings can be very unpleasant, if encountered by people who come from very different cultures are pre-assembled. This may have an negative impact on a potential or current job. Therefore, the cultural impact can not be underestimated.

Thanks to a revolutionary improvement of computerized technology, powerful and cost-effective components, the computer has entered almost all the "pores" of human life. In many industrialized countries, more than half of all households has a personal computer. Mobile devices are also massive and fast.

The use of technology has accelerated communication, and people made more accessible to one another. It is also changed, and communication. Communication via PCs and is usually done in writing. Even if you take into account that they can use cameras with high quality, it is not the same as when communicating in person. The fact that the missing effect of non-verbal communication. It is very important to our forming an impression of the caller to recipient better understand what we want to tell him.

Besides the Internet erases the barriers of space between people, it also changes the way of life. Some believe that such people somehow makes the isolation, because people on the Internet are a variety of information, do not communicate so much with other people, because they have no need for it. Communication through an intermediary, in this case, machine / computer has become more and more prominent, ie. common. That's what happens when you communicate with other people. Very often, the communication ends with a computer, and he somehow becomes so. window to the world, which can be reviewed simultaneously isolate the person from direct communication with other people.

GLOBALIZATION AND APPRECIATION OF CULTURAL DIFFERENCES IN IT TEAMS

Software development is constantly pushing the boundaries that are set by the company, or State. Available media become more sophisticated. Advanced technology costs less. Trends in software development go more towards "virtual nature".

In this section we will focus on the development teams and how cultural differences among their members can influence the activities of the various stages of the cycle.

It will provide the evidence for the need for computerized support through effective conflict resolution, team building, dynamic role assignment, managing IT projects in a culturally diverse environment.

Demanding needs of the IT industry have led to the development of complex applications and modern virtual nature. Lack of skills, the fact that the redevelopment process costs a lot, the time of development and special requirements of the local market are some of the challenges that multinational companies are trying to overcome engaging virtual teams. Of course, there are obstacles that arise in the implementation and maintenance of virtual teams, the most common barriers are related to the characteristics of the team members. The main common factor that affects the effectiveness of virtual teams are different national cultures of their members. Individuals from different cultural backgrounds may have different beliefs, values, competencies and understanding of priorities. There are different models of national culture. Practitioners seek to understand the cultural

differences among the teams who work together or within a team.

In the majority of the members of virtual teams is often lying close to the geographically diverse locations and in different time zones. Virtual teams can involve more than one organization, which means that members of the team may belong to different organizations / companies, but to work together on a project.

Virtual teams have a network structure. They need frequent and structured communication. To work in virtual teams to be effective and to avoid delays and conflicts, the level of trust must be quite high, higher than that of traditional teams. Many companies have access to a large number of experts, in order to reduce the cost of software development project to be open 24 hours a day. This is done by engaging teams in different time zones and sourcing operations to countries with lower standards of living and lower wages. In addition to reducing costs and benefits have called. internationalization of software, creation of localized centers, construction of knowledge base and knowledge sharing. Ten most representative factors affecting the performance and sustainability of virtual teams are [19]:

cultural differences among the team members of different teams, distance between teams, 3 duration / life cycle team, 4 frequency of communication between team members and between teams, meetings held within the team, allocation of roles within the team, dependency between tasks, location of team members, technological requirements, the time differences within the team.

Also IT professionals have different views on the importance of cultural differences. Culture is a sensitive topic for discussion because it has to do with archetypes. The most effective way to deal with cultural differences is to use any of the archetype as a starting point and is constantly supplemented with new information. It should be noted that all the time dominated by individual differences in cultural differences. There are several types of cultures that exist and are responsible for the patterns of behavior of team members. Some types of cultures are stronger than others and dominate the work of all the team members and influence the quality of their interpersonal communication. These types of cultures [19]:

- ☐ *National Culture organizational / corporate culture;*
- ☐ *professional culture the operational culture within which there are several types of virtual IT team: network teams, parallel teams, project development teams, production teams, service teams, management teams;*
- ☐ *culture team*

Every man is a member of multiple culture. This can be one or more national / ethnic cultures, one or more professional cultures, functional culture, organizational culture and culture teams. For example, the Russian programmer on their characteristics more similar to the American counterpart, the developer, but the Russian marketing manager. This example provides sufficient reason for further debate about whether you cultural differences emerged to the surface in virtual IT teams despite strong professional IT culture.

Managers and team leaders of IT teams need to be aware of the impact of national cultural differences and explore what cultural impact on the formation and management of the teams. This has an impact on strategic planning and human resource management. Under the direct influence of different national cultures, team members are [19]: Team structure, Management team, Communication team members, Conflict resolution

By now it is clear that national culture influences the behavior of virtual teams. Cultural differences among team members may have an impact on conflicts within the team and end results.

CONCLUSIONS

The global development of business information systems are facing various challenges. Conducted numerous studies illustrating the impact of cross-cultural factors in the development of global information systems. The biggest causes faced by virtual teams effective communication and coordination. Virtual, global teams can be explained as teams consisting of members from different cultures and who are globally distributed. In cross-cultural management has become a common practice of introducing cross-cultural training. This is done to help employees prepare for effective relationships with colleagues who come from different cultures. Characteristic of today's society as globalization and intercultural and use of information technology. It now increasingly characterize our society. One of the most important characteristics of today's successful business leaders in the international arena is intercultural competence. On the other hand the same applications and systems used by people of different national and organizational cultures. The development of information technology faces a number of challenges, including cultural diversity and intercultural management. Cultural diversity is inherent in the global development since the team members have different national, organizational, professional culture. Cultural diversity has a positive impact on the development of information technology. Cultural differences are one of the most important factors that influence both the way of understanding, acceptance and use, and the actual development of information technology.

The globalization of business means that today's modern management is faced with the need to overcome the geographical, political, cultural and other barriers. Particular attention is drawn to the differences in national cultures. Involvement in globalization trends of today '. Globalization enables modern companies many opportunities in the form of market expansion, accessibility of material resources and cheaper labor force, availability of technological and managerial know-how. The advantages that globalization brings, it transcends geographical, political and cultural borders. Information technologies have led to changes that people and companies that are in remote locations make it easy to communicate and do business. This large number

of people provided ample opportunity to become part of the global economy, regardless of which location they live. From the survey results it follows that the potentials of information society indicate the dependence of the spread of globalization of information technology.

In today's modern society, minority groups are common. Multiculturalism is the coexistence of many cultures in a territory. The concept of multiculturalism is characteristic of the English-speaking world. This paper explains how multiculturalism affects business in the IT business. Multicultural orientation of the company and its managers is a feature of modern business. Multiculturalism is not an obstacle that can be overcome, but it is one of the major sources and maintain competitive advantage. It is concluded that the stimulation of cultural differences in business a company can improve its competitiveness in the market.

REFERENCES

[1] *Adler, N., International Dimensions of Organizational Behavior, South-Western- Thomson Learning, Canada, 2002.*

[2] *Angell, P., Rizkallah, T., Business Communication Design, McGraw-Hill, New York, 2004.*

[3] *Hofstede, G., Cultures and Organisations Software of the Mind, McGraw Hill, US, 1997.*

[4] *Jovanović-Božinov, M., Langović-Milićević, A., Interkulturni izazovi globalizacije, Megatrend univerzitet primenjenih nauka, Beograd, 2009.*

[5] *Sparrow, P., & Hiltrop, J. -M. European human resource management in transition. New York: Prentice Hall, 1994.*

[6] *Terterov, M., Doing Business in Serbia, GMB Publishing Ltd & SIEPA, 2006.*

[7] *Langović-Milićević, T. Cvetkovski, Z. Langovi cNegotiation and Globalization, Annals of Faculty Engineering Hunedoara, International Journal of Engineering, Tome IX (Year 2011) Fascicule 3 (1584-2673) pg. 131-136, 2011.*

[8] *Mića Jovanović, Langović Milićević, Tatjana Cvetkovski, "Environmental Variable and Global Competition for Talant: The Case of Serbia" East Asia: Comparative Perspective, Vol 11, No. 1, pg. 87-104 http://ineas.donga.ac.kr Printed by Sejong Printing Co. Ltd. ISSN: 1975-6135 The Institute for East Asian Studies, Dong- A University, 2012.*

[9] *Jovanović M., Milićević Langović A., Cvetkovski T. (2009) „Intercultural Management and Serbia", pg. 548-551, 4th International Conference „Innovation in Menagement: the Cutting Edge of Business Education and Practice in an Epoch of Global Collaboration", Poznan University, College of Business and Foreign Languages, Poznan, Poland, 21-22. ISBN 978-83-925092-9-5 May 2009.*

[10] *Patel, D.Lawson-Johnson, C. Patel, S, , The Effect of Cultural Differences on Software Development, Fountain Publishers, Kampala. 2009.*

[11] *Shao Qin Sun. Cultural differences in E-commerce: A comparasion between the US and China, Qiu Bin, Southeast University, China, Su-Jen Chen, *California State University, Fullerton, US, , Southeast University, China Idea group publishing, 2004.*

[12] *Halyan Huang, Elieen M. Trauth, Cultural influences on temporal separation and coordination in globally distributed software development, The Pennsylvania State University (2008) ICIS 2008 Proceedings, 2008.*

[13] *Michael Jones, , Cultural Impact of information systems - through the eyes of Hofstede - a critical journey, , University of Wollongong, Australia, Irit Alony, Central Queensland University, Rock Hampton, Australia, 2007.*

[14] *Geert Hofstede, Culture's Consequences, Sage Publications, Ltd. London, United Kingdom*

[15] *Cox H.T., Blake S. 1991, Managing cultural diversity: implications for organizational competitiveness, Academy of Management Executive, Vol.5, No.3, 2001.*

[16] *Srite, M. The Influence of National Culture on the Acceptance and Use of Information Technol ogies: An Empirical Study, dissertation, FSU, 2000.*

[17] *Straub, D., Loch, K., Evaristo, R., Karahanna, E., & Srite, M. (2002).Toward a theory-based measurement of culture. Journal of Global Information Management, 10 enkatesh, V., Morris, M.G., Davis,G.B., & Davis,F.D. (2 003). User acceptance of information technology: toward a unified view. MIS Quarterly , 27 (3) (1) 2002.*

[18] *Lucas, H.C., & Spitler, V.,. Implementation in a world of workstations and networks. Information and Management, 38, 2000.*

[19] *Zlatko Langović, Brankica Pažun, Langović Milićević A. 2012: The cultural impact of information technology, Zbornik radova sa naučnog skupa: Kulturna politika, unetničko stvaralaštvo i medijska praksa u funkciji održivog društvenog razvoja, Megatrend univerzitet, Beograd, 2012. .str. 83-90. ISBN 978-86-7747-476-8; COBISS.SR-ID 195612940 Urednik Slobodan Branković- monografski zbornik- 31. Maj 2012*

ACTA TECHNICA CORVINIENSIS - BULLETIN of ENGINEERING

ISSN: 2067-3809 [CD-Rom, online]

ACTA TECHNICA CORVINIENSIS – Bulletin of Engineering
Tome VI (Year 2013) – FASCICULE 4 [October–December]
ISSN 2067–3809

[1.] *József SOLTICZKY*, [2.] *István BÍRÓ*

MOTOR-CAR INDUSTRY AS THE MAIN MOTIVATION OF PLASTIC-INNOVATION

[1.] *TECHNICAL INSTITUTE, FACULTY OF ENGINEERING, UNIVERSITY OF SZEGED, HUNGARY*

ABSTRACT: New technologies and high quality materials are developed by manufacturers and molders of plastic to comply the emerging requirements. Applying developed technologies complex shaped plastic elements can be produced easily. The production of similar elements from steel needs more steps and more time as well. Besides these possibilities the new technologies increased the freedom of designers in the motor-car industry. This is the other important aspect of application of different type of plastics. This paper gives a brief summary about the development of application of plastic mountings in motor-cars moreover about its motivation and expectable trends. It shows the effect of international environment protection standards on design of motor-cars and construction of cars besides the plastic-industrial developments motivated by emerging demands and requirements.
KEYWORDS: CO_2 emissions, composites, fuel economy, lightweight design, organic sheets, plastics, recycling

INTRODUCTION

The ratio of plastic built in motor-cars is higher and higher year by year. The main goal is the reduction of mass of motor-cars in order to reduce the fuel consumption and CO_2 emission. There are two fields of motivation for manufacturers: thinking and habit of customers and international environment-protection standards. Steel as traditional constructional material has to be replaced by different types of plastic having the demanded mechanical properties. By application of plastics special possibilities of design and manufacturing can be utilized.

New technologies and high quality materials are developed by manufacturers and molders of plastic to comply the emerging requirements. Applying developed technologies complex shaped plastic elements can be produced easily. The production of similar elements from steel needs more steps and more time as well.

Besides these possibilities the new technologies increased the freedom of designers in the motor-car industry. This is the other important aspect of application of different type of plastics.

Nowadays the plastic-innovation is motivated by motor-car industry because the main part of plastic element needs high quality materials and manufacturing technologies. For this reason newer and newer technologies have to be carried out [1].

In the frame of this paper a short overview will be presented about the environment protection aspects of application of plastic moreover the motivation of developments and results and possibilities of different engineering developments in this field.

CONSUMPTION AND ENVIRONMENT PROTECTION ASPECTS

There is an important part in environmental protection strategy of European Union to reduce the CO_2 emission of motor-cars. The CO_2 emission of motor-cars is significantly responsible for the climate change, especially in industrialized countries. Because the CO_2 emission is proportional to the fuel consumption, the CO_2 emission and the cost can be reduced by reduction of the fuel consumption of motor-cars.

According to the EU regulation for motor-car industry the CO_2 emission has to be reached 130 g/km until 2015 and 95 g/km until 2020 what correspond to 4,5 l/100 km fuel oil consumption and 5 l/100 km petrol consumption. The average value of the CO_2 emission of motor-cars was in 2010 approximately 140 g/km [2,3,4] (Figure 1).

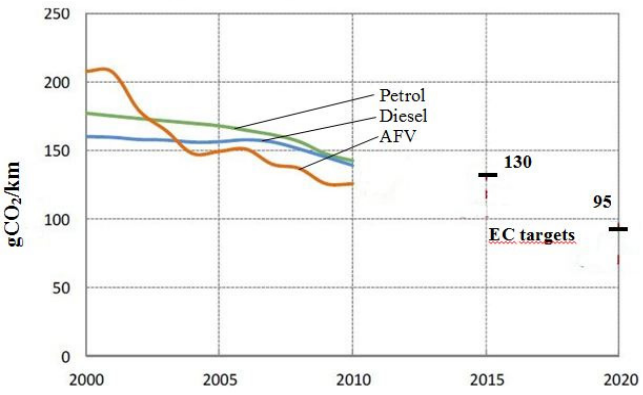

Figure 1 [5]. Evolution and EC targets CO_2 emissions from new passenger car by fuel (AFV: Alternative fuel vehicles)

The association of European, Japanese and Korean car manufacturers produced 98 percents of sold motor-cars undertook the fulfillment of emission target numbers concerning the new motor-cars. They want to reach the target numbers by different technical innovations.

TRENDS OF TECHNICAL INNOVATIONS TO MASS REDUCTION

The most important technical innovations to reduce the fuel consumption of motor-cars [6]:

- *Engine Downsizing With Power- Boosting Technologies;*
- *Hybrid & Electric Power trains;*
- *Downsize Vehicles;*
- *Lightweight Structural Materials;*
- *Fuel Cells.*

The subject of our investigation is at present the application of underweight constructional elements. The most of manufacturers have been changing the compound of material of car body to reduce the mass and the fuel consumption (Figure 2).

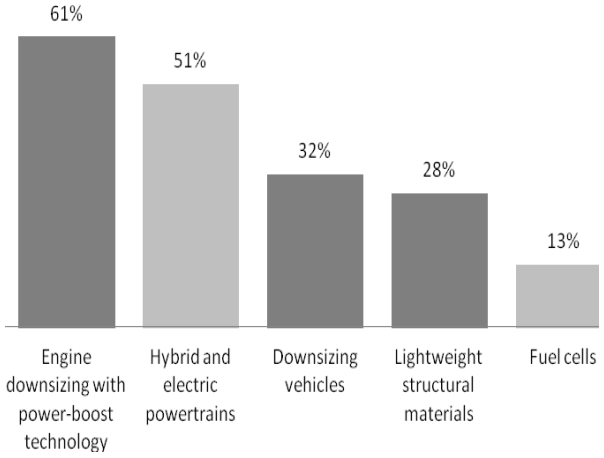

Figure 2 [6]. How will automakers meet emerging regulations

The mass reduction can be achieved by application of high-strength steel, light metal and plastic composites. The compound of materials used to motor-cars has changed considerably and this process will go on in the future (Figure 3).

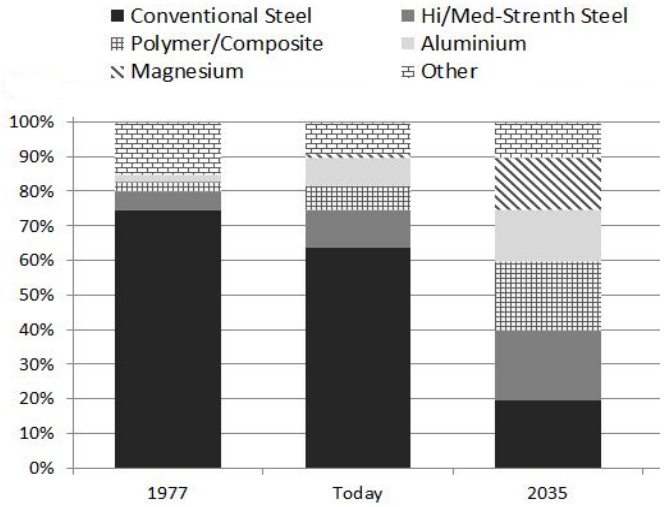

Figure 3 [7]. Typical composition of past and present cars versus a future light weight vehicle

Nowadays a medium size car contains averagely 100 kg elements made of plastic. Application of many kinds can be seen in Figure 4.

The application of thermoplastics in the motor-car industry is traditional. In spite of this fact until the last time it seemed to be suitable purely for low-load constructional elements. Due to the requirements to mass reduction the light metal alloys and reinforced-fiber plastic composites became real alternatives of steel.

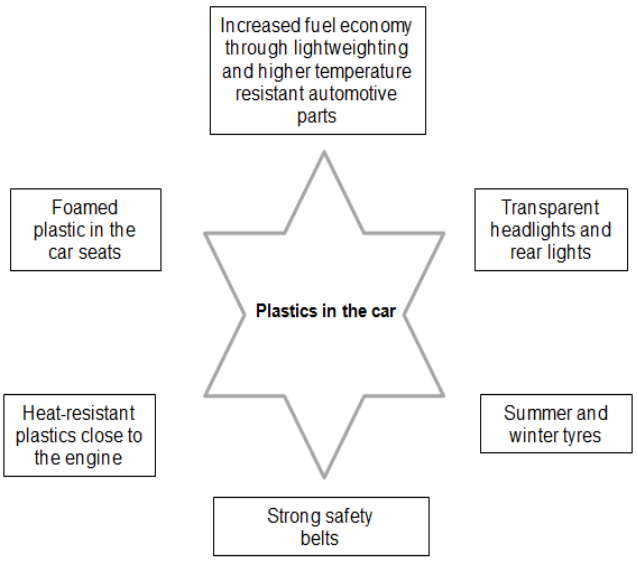

Figure 4. [13]. The use of plastics in cars

The plastic industrial innovations enable the application of plastic not only for decorating elements but also for loaded car-body elements and high heat and mechanical loaded elements in the engine space. The technical innovation will be demonstrated by several especial applications [6,8,9].

☐ ***Body structure and Components**; specific polymers: PP, ABS, PA, PC, „organic sheets"*

For manufacturers mass reduction can be reached by application of high-strength steel and light metal elements moreover complex base material including plastic as well.

- *The low beam of front part of Audi A8 is made of hybrid base material (metal/plastic). The bracing of metal can be reached by plastic plates made of thermo matrix containing reinforced-fiber plastic polymers (organic sheets).*
- *Elements having big surfaces can be produced successfully from reinforced-fiber plastic. For example the voluminous hybrid (plastic/ aluminum) plate of spare-wheel compartment of Audi A8 made from reinforced-fiber at a length of 6 mm plastic PA 6 (Durethan DP BKV60 H2.0 EF) [14, 16].*
- *The mechanical features of bumper bar can be ensured by application of ordinary kenaf hybrid KLFRT, twisted kenaf hybrid TKLFRT base material [17].*

☐ ***Under the hood***

Oil pans are exposed to many kind of loading: lubricants, high temperature, continuous and

dynamical load. The temperature of motor-oil can be reached from -40 °C until +150 °C.

- DuPont Automotive Company decided for the base material of oil pans of Mercedes C-class in 2009 the PA66 (Zytel 70G35 HSLR) reinforced-fiber plastic polymer.
- The solution of BASF Corp. was PA composite containing 35 percents reinforced-fiber plastic.
- According to Ticona Company two own products are suitable for similar application: Vectra LCP polymers and Fortron linear PPS [10].

Applied polymers in engine blocks: PPS, PBT, Long Fiber Reinforced Polymers (LFT). Mass reduction results reached by du Pont Company for 2011 applying high quality technical plastics are the followings [11, 12]:

- Rear camshaft retainer - 0.2 kg
- Manifold- 1 kg
- Charge air cooler - 1 kg
- Turbo charger duct, hose- 0.5 kg
- Oil pan - 1 kg
- Engine cooling system - 0.8 kg
- Rocker cover - 0.5 kg
- Engine cover - 1 kg
- Cylinder head - 4.5 kg
- Pumps, throttle body, small components - 0.5 kg

Other fields of application: [6, 8]

- Interior trim; specific polymers: PP, ABS, PET, POM, PVC
- Seats; specific polymers: PUR, PP, PVC, ABS, PA
- Hood; specific polymers: Nylon/PPE blend
- Door liners; specific polymers: PP, ABS, PET, POM, PVC
- Load floors; specific polymers: composites
- Fuel tanks; specific polymers: HDPE, PVDF
- Consoles; specific polymers: ABS
- Instrument panel; specific polymers: ABS, ABS/PC alloys, PC, PP, modified PPE, SMA.
- Automobile glazing: PC

CONCLUSIONS - SUMMARY

The fuel consumption and CO_2 emission depend on not only the efficient utilization of fuel but also the driving style and other no technical aspects. But yet the greatest effect on the fuel consumption is the own mass of the motor-car. For example the result of 100 kg mass reduction on a motor-car (self-mass 1500 kg) is ~0,3-0,4 l/100km reduction of fuel consumption [15].

In spite of continuous increasing of ratio of built in plastics in motor-cars there are still possibilities to reduce the self-mass of the cars in the future. At present the ratio of plastic in self-mass of small- and medium-size is ~ 15 - 17 %. According to experts there are further possibilities to replace metals in case of systematic application of light structural design.

For this purpose the most suitable material are the reinforced-fiber plastic polymers and composites but the recycling of these materials seem to be difficult. At present there is no effective technology for recycling or destruction of reinforced-fiber plastic composites. This is a quite important aspect because the manufacturers have to comply with the EU directive (End of Life Vehicle - ELV) about used cars.

The aim of this directive is to reduce the waste material coming out from used cars and to enhance the recycling of the elements of them. In order to achieve this coupled aims the EU directive prescribe new requirements for manufacturers. According to this regulation they should apply recycling or at the end of its life degradable materials [18, 19].

These coupled requirements give the motivation for manufacturers of plastic base materials to replace the generally applied artificially created reinforced-fiber by natural materials (flax, kenaf).

REFERENCES

[1.] Prof. Dr. Rudolf Stauber, Dr.Ing. Ludwig Vollrath: Plastic in Automotive Engineering, Hanser Gardner Publications, 2007

[2.] Thomas Vollmer, Nadja Cirulies: Industrielle Produktion: Automobilindustrie, Books on Demand, 2009

[3.] Regulation (EC) No 443/2009 of the European Parliament and of the Council of 23 April 2009, Official Journal of the European Union

[4.] Audun Freyr Ingvarsson, Julien Pestiaux, Francis M. Vanek: A Global Assessment of Hydrogen for Future Automotive Transportation: Projected Energy Requirements and CO_2 Emissions, International Journal of Sustainable Transportation Vol. 5, No. 2, 2011

[5.] Monitoring the CO_2 emissions from new passenger cars in the EU: summary of data for 2010, European Environment Agency, 2011

[6.] Plastics Development= Automotive Design & Production, July/August 2011

[7.] Materials Technologies: Goals, Strategiesand Top Accomplishments=Energy Efficiency & Renewable Energy, VEHICLE TECHNOLOGIES PROGRAM, August 2010

[8.] Dr. Kai Pflug, Dr. Bernhard Hartmann: Plastics in Automotives -No Longer Too Early for China, CHINA CHEMICAL REPORTER , May 6, 2011

[9.] N.L.Phadk,. Prof. K.P. Kumbhar: Plastics in automobile industry, POPULAR PLASTICS & PACKAGING April 17, 2010

[10.] Metal to Plastic Under the Hood: Plastics makers are moving into what has long been metal territory with applications that can reduce weight= Automotive Design & Production, 1/1/2009

[11.] Diane Gulyas: Fueling the DuPont Engine of Growth, du Pont Nemours and Company, May 24, 2011, phx.corporate-ir.net

[12.] High Performance Materials for Under-the-Hood Applications int he Automotive Sector, http://

[13.] tools.ticona.com/tools/documents/literature/Flyer 20UTH_english1.pdf

[14.] Plastics in cars: polymerization and recycling= Science in School, Issue 20, Autumn 2011

[15.] Matt Defosse: In automotive engineering, Lanxess sees bright future for new hybrid systems, Plastics Today, March 29, 2010

[16.] Prof. Henning Wallentowitz, Joerg Leyers, Dr. Thorsten Parr: Materials for Future Automotive Body Structures, Business Briefing: Global automotive Manufacturing & Technology, 2003

[17.] New Assembly Technologies Slash Costs= Design News, December 2010
[18.] S. Jeyanthi, J. Janci Rani: Improving Mechanical Properties by Hybrid Long Fiber Reinforced Composite for Front Beam of Automotive, European Journal of Scientific Research, Vol.60 No.2 (2011), pp. 195 -199
[19.] P. V. Joseph, G. Mathew, K. Joseph, S. Thomas, P. Pradeep: Mechanical Properties of Short Sisal Fiber-Reinforced Polypropylene Composites: Comparison of Experimental Data with Theoretical Predictions. Journal of Applied Polymer Science. 88 (2003), 602-611.
[20.] L. Jiang, G. Hinrichsen: Flax and cotton fiber reinforced biodegradable polyesteramide composites, 1. Die Angewandte Makromolekulare Chemie 268 (1999), 13-17.

ACTA TECHNICA CORVINIENSIS - BULLETIN of ENGINEERING

ISSN: 2067-3809 [CD-Rom, online]

ACTA TECHNICA CORVINIENSIS – Bulletin of Engineering
Tome VI (Year 2013) – FASCICULE 4 [October–December]
ISSN 2067–3809

[1.] L. NADASAN, [2.] T. ONET, [3.] I. PETEAN, [4.] M. SABAU

DECORATIVE FERROCEMENT ELEMENTS

[1-4.] DEPARTMENT OF STRUCTURES, FACULTY OF CIVIL ENGINEERING, TECHNICAL UNIVERSITY OF CLUJ-NAPOCA, ROMANIA

ABSTRACT: Ferrocement has the versatility that can be 'sculptured' or shaped into numerous fascinating structures and objects for very wide applications. The exposure of this technology to engineers in general is rather minimal in Romania and many are skeptical about it. The potential is not exploited for it being unconventional in nature. Its ability to compete or use as a cheaper alternative and yet a promising technology in ensuring improved living standard and environmental quality must not be neglected. The paper discusses about the applicability of ferrocement in the Romanian scene with respect to recreation and home use. The ferrocement elements can be used for outside or inside exposure, thanks to ferrocement's durability, resistence to impact and resistence to fire.
KEYWORDS: outdoor ferrocement furniture, silos, water tank, indoor ferrocement furniture

INTRODUCTION TO FERROCEMENT

Ferro-cement composite is a rich cement mortar matrix of 10 to 100 mm thickness with reinforcement volume of five to eight per cent in the form of one or more layers of very thin wire mesh and a skeleton reinforcement consisting of either welded mesh or mild steel thin bars. (Figure1) The proportions in terms of sand-cement ratio are normally 1:1,5 or 1:2. The water cement ratio may vary between 0.4 and 0.5. Admixtures can be added for achieving improved workability, reduced permeability and increased durability. The presence of small diameter steel wires closely and uniformly spaced in the volume of cement mortar improves many properties like ductility, toughness and crack resistance as compared to conventional reinforced concrete.

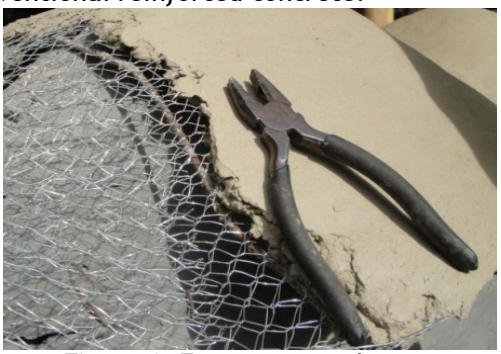

Figure 1. Ferrocement element

Joseph Monier, a gardener in Boulogne, is considered to be the first to introduce steel into concrete in 1849 to build sturdy flowerpots and garden furniture, and his version was patented in France in 1867. However two years earlier in 1847 another Frenchman, Joseph-Louis Lambot had already introduced reinforcement in cement to build boats at his estate near Brignoles. Lambot called his invention 'ferciment' and described the technique as 'construction formed of metal mesh plastered and joined together with cement'. Lambot made his invention public only in 1855 when he showed one of the boats at an International Exhibition in Paris.

According to Romauldi, "the technology of that period could not accommodate the time and effort needed to make mesh of thousands of wires. Instead, large rods were used to make what is now called standard reinforced concrete, and the concept of ferrocement was almost forgotten for a hundred years. [1] For civil buildings Pier Luigi Nervi was the first one to use the ferrocement for structural elements. Even though ferrocement has recently found a wide range of applications particularly in developing countries, unfortunately ferrocement remains generally underutilized in mainstream architecture.

FERROCEMENT NON STRUCTURAL ELEMENTS FOR EXTERNAL USE

During the opening of the second day of the International Symposium on Ferrocement FERRO 10 held between 12-17 October 2012 in Cuba, the president of the organizing committee, engineer Hugo Wainshtok Rivas presented dozens of examples of the durability of this technology after decades of application. In 1982 Baconao Park in Santiago de Cuba was opened with more than 100 large pieces (Figure 2) by sculptor Dagoberto Moreno.

Figure 2. Ferrocements sculptures in Bacanao Park Santiago de Cuba

At present all are kept in good condition. When we are talking about elements for external use we are talking about elements exposed to weather conditions, marine environments or different kind of chemicals.
Ferrocemenet's durability is the reason to be chosen for different kind of sculptures, facade elements, decorations, street furniture, drains, gutters, food and water storage. To prove it's applicability in Romania few examples are presented in this article with the hope that production of ferrocement elements will begin.

Ferrocement statues

The flexibility of meshes gives so much versatility for this material and can be molded almost in any shape. Amusement parks use it when big dimensions statues are built. Figure 3 shows the steel meshes fixed on rods taking the shape of a tree. The micro concrete is applied on the meshes having different admixtures to obtain a white concrete that can be easily painted.

Figure 3. Statue of a tree in a park

Ferrocement facade elements

Non-structural elements of a building are not part of the main load-resisting system and the design does not follow the design standards. They are considered decorative elements and the durability in time is one of the concerns. Ferrocement elements are used for balconies (Figure 4) being light weight and easy to construct and install. They need zero maintenance and are easy reparable. Meticulous building precision is crucial to the successful completion of ferrocement projects especially with respect to the cementitious composition and the way in which it is applied in and on the framework, and how or if the framework has been treated to resist corrosion. An example of facade elements is presented in Figure 5 an architectural artwork created by architect Renzo Piano for the museum Menil Collection in Houston, USA, where the ferrocement "leaves" concentrate the light only the sculptures inside.

Figure 4. Ferrocement for balconies

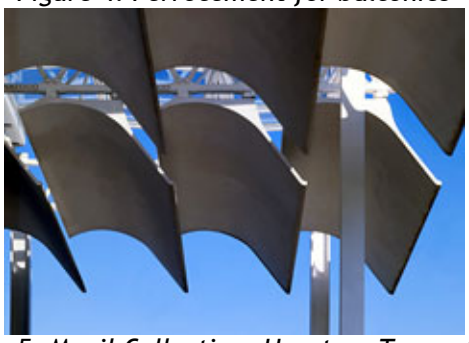

Figure 5. Menil Collection, Houston, Texas, ferro-cement leaves

Urban sculptures

Wood and steel are materials most used to build benches, bus stations, tables in cities but ferrocement is more reliable because of its resistance to impact, to fire [3] and damage can be fixed locally very easy. Figure 6-10 show this examples.

Figure 6. Ferrocement bench

Figure 7. Ferrocement bench

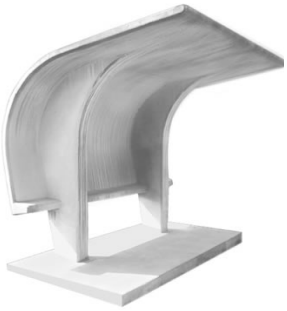

Figure 8. Ferrocement Bus Shelter

Figure 9. Ferrocement Table

Figure 10. Ferrocement Table

Food and water facilities

Ferrocement water tanks for rainwater collection in rural communities as a user-built can be an alternative to store-bought plastic tanks that can be difficult to transport for some areas or too expensive. At the moment there are many websites with all the information how to build a ferrocement water tank. (Figure 11)

Figure 11. Ferrocement Rain Water Tank

The problem of food storage in the developing countries is emerging as a major subject of attention from technical assistance organizations. Increasing supplies of food grains, such as rice, wheat, and maize, resulting from the intensive production have caused an unprecedented need for grain storage in developing countries, yet most production areas are still unprepared to store this new abundance adequately. The production is lost to inadequate harvest and inadequate storage facilities and practices. In addition to grain storage, facilities are urgently needed to protect all products sensitive to temperature, humidity, rain, wind, pest animals, bacteria, or fungi. Other typical products requiring storage are peas, beans, oil crops such as soybeans, salt and other nonfood items such as fertilizers, pesticides, and cement. Major needs are small scale silos, particularly for on farm storage. [2] Figure 12.

A particular advantage of ferrocement in building food storage facilities in developing countries is its adaptability to an almost unlimited range of curved shapes and local conditions. Ferrocement silos require little maintenance, and they offer protection against rodents, birds, insects, water, and weather. [2] Ferrocement silos could be built in a factory, but they are particularly adaptable to on-site construction, an important consideration in remote areas without vehicle access. As with other applications, silos require only simple artisan skills, performed by local labor with minimal supervision. [2]

Figure 12. Ferrocement Silo

Ferrocement gutting

Ferrocement applications are free-form and can be limited only by one's imagination. It provides easy mould ability and can take any form. To produce rain gutter a half pipe is used as a mold. (Figure 13)

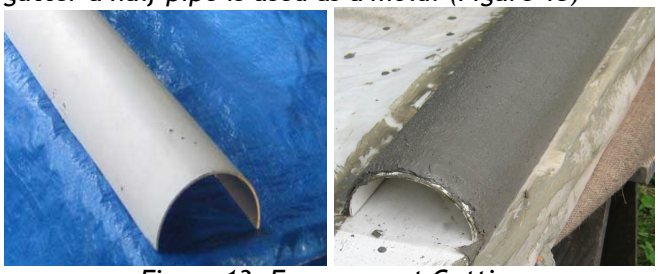

Figure 13. Ferrocement Gutting

FERROCEMENT NON STRUCTURAL ELEMENTS FOR INTERNAL USE

The versatility of ferrocement has led to its appearance in numerous non-traditional formats such as furniture, sculpture and art. Due to improved setting and molding techniques, it is now possible to create more sophisticated shaped furniture using concrete. The added durability of concrete means they can be placed indoor or outdoor, in local parks and community areas. Concrete furniture design is evolving rapidly and cement furniture is making an appearance inside the contemporary home. Cast concrete counters in the kitchen are one thing but furniture designers are bringing the material into the home in a very modern way.

Figure 14. Ferrocement Furniture

Concrete furniture has a bad reputation because most people have never seat in a well designed concrete chair. With new technologies it is possible to design pieces that conform to the body and add an amazing solution to the furniture needs.

Figure 15. Ferrocement Chair

Ferrocement applications are free-form and can be limited only by one's imagination. It provides easy mould ability and can take any form. It can be used for manufacturing precast building components that can be easily transported. Some popular uses are for making tables (Figure 16) doors, tubs (Figure 17), flower pots etc.

Figure 16. Ferrocement Table

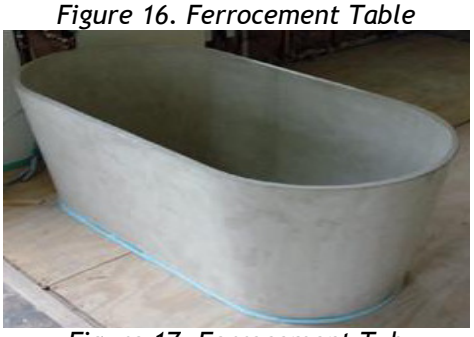

Figure 17. Ferrocement Tub

FERROCEMENT'S ADVANTAGES

- ☐ Easy to construct and install, little new training is required.
- ☐ Ferrocement may be fabricated into almost any conceivable form to meet the particular requirements of the user.
- ☐ Labor intensive technology creates more jobs for the rural community.
- ☐ Earth quake resistant design.
- ☐ The basic raw materials for the construction of ferrocement-sand, cement, and reinforcing mesh-are readily available in most countries.
- ☐ Durability.
- ☐ Zero maintenance and very easy reparability.
- ☐ Good resistance to fire [3]
- ☐ Low cost applications are lighter on the pocket.

FERROCEMENT'S DISADVANTAGES

- ☐ Labor intensive nature of it, which makes it expensive for industrial application in the western world.
- ☐ Degradation (rust) of the steel components is a possibility if air voids are left in the original construction, due to too dry a mixture of the concrete being applied.

CONCLUSIONS

In this paper were presented objectes made by ferrocement thin sections. Any person that worked with concrete before can use ferrocement with little training and by combining the fine meshes with the micro concrete any shape can be achived. This independence by comercial products can lower the prices and the use of local work and materials recomands ferrocement for a sustainable economy. Objects for the house (chairs, benches, tubs, gutting or water tanks) with a long working life can be made and all the disadvantages of steel or wood can be avoided.

Acknowledgement

This paper was supported by the project "Improvement of the doctoral studies quality in engineering science for development of the knowledge based society-QDOC" contract no. POSDRU/107/1.5/S/78534, project co-funded by the European Social Fund through the Sectorial Operational Program Human Resources 2007-2013.

REFERENCES

[1] Romualdi, James P., et. al. Ferrocement: Applications in Developing Countries. Washington DC, National Academy of Sciences, 1973.

[2] Ferrocement: Applications in Developing Countries. A Report of an Ad Hoc Panel of the Advisory Committee on Technologic; Innovation Board on Science and Technology for International Development Office of the Foreign Secretary National Academy Of Sciences Washlington. D.C. February 1973

[3] Greepala, V. and P. Nimityongskul, Structural integrity of ferrocement panels exposed to fire, Cement and Concrete Composites, 2008. 30(5): p. 419-430.

ACTA TECHNICA CORVINIENSIS - BULLETIN of ENGINEERING

ISSN: 2067-3809 [CD-Rom, online]

ACTA TECHNICA CORVINIENSIS – Bulletin of Engineering
Tome VI (Year 2013) – FASCICULE 4 [October–December]
ISSN 2067–3809

[1.] Kouros NEKOUFAR, [2.] Hafez KOUHPARI

CONTROL AND DECREASE THE SCOURING OF BRIDGE PIER BY METHOD OF NON-SUBMERGED PLATES USING SSIIM SOFTWARE

[1.] ISLAMIC AZAD UNIVERSITY, CHALOUS BRANCH, CHALOUS, IRAN
[2.] ISLAMIC AZAD UNIVERSITY, LARESTAN BRANCH, LARESTAN, IRAN

ABSTRACT: Bridges are the vital components of each country's roads. Economic studies of the road construction show that the road bridges allocate much cost to it and due to the delicate structures of their system; they have great vulnerability as well. Therefore the detailed design of the various components of the bridge should be considered further. Erosion and transport of bed material is separated from it by a process called scouring. Occurrence of scouring around the bridge piers is one of the main reasons for the defeat and destruction of bridges and their instability. So it is important to provide methods to control and reduce this phenomenon. In the present study, the modeling of non-submerged plate's perpendicular to the water flow has been expressed in upstream of the cylindrical pier using software SSIIM. Reducing the depth of the scouring hole was observed in these pages, and has a great influence around the bridge pier.
KEYWORDS: scouring, bridge pier, non-submerged plates, software SSIIM

INTRODUCTION

Bridges are the most important and widely structures in which used in long period. In most cases the bridge structure is established on the river, in which its pier is will be in contact with the water flow. Long-term experience in establishing the bridge on river has led the engineers in the past few decades to issues to consider in the design of bridges in structural geology and the location of potential traffic is not enough, but the effect of water flow should be noted too.

Destroyed or damaged hundreds of large and small bridges in different parts of Iran in recent years due to frequent flooding demonstrate along with the proper technical knowledge of Iran's engineering society in designing the structures of bridge, the hydraulic aspects did not attention in this case. Thus due to scouring it is stressed that in most cases for lack of attention to the phenomenon, the bridge's structure has lost its efficiency and destroyed many years before overdue its useful life and this problem becomes critical when we are destroying bridges just in time (For example, in the event of flooding) that we most need to have access roads to aid victims of natural disasters. The severe flooding that comes with a lot of human and financial losses, in the last century the river engineering and flood control is particularly important in the world and in Iran.

The scouring is a phenomenon that occurs due to the bed erosion through water flow and moving the bed materials by a force that the flow exerts on the bed materials. This happens in the occurrence of flood when the use of bridge felt more. Therefore the study of scouring the bridge pier and applying methods and equipments to reduce the scouring around the piers is very important.

To the economical and reliable design for the bridge pier, it is necessary to estimate the maximum depth of scouring around the piers. At present the scientific basis for the structural design of piers is well known; although there is no specific and unique theory that estimates the scouring depth at the bridge piers with high confidence. To design the bridges, their piers should be deep enough to resist against the scouring. On the other hand, it pier should not be deep enough that cause the cost to increase. The use of methods to reduce the scouring depth around the pier, we can put foundations in higher levels that it will reduce the costs. Given the above issues, understanding the phenomenon of scouring and more importantly applying the methods to reduce the scouring around bridge piers seem necessary. Various forms of scouring may threat the stability of hydraulic structures and every year a lot of bridges around the world seriously damaged or destroyed by scouring phenomenon. In general, various types of scouring around the piers can be divided into three main categories: [1]

A. General scour: while the amount of sediment arrived to the river or a part of it, is less than the exit sediment, the erosion occurs in the floor or walls of the river. In this effect, the floor of river is dished gradually that it called Kafkani. Kafkani can enumerate as the effective factors to

reduce the bed level around the bridge piers in long time period.

B. *Scouring in effect of narrowing section : This type of scouring mainly occurs in the vicinity of the piers with near distances. In the scouring in the effect of narrowing flow section, the bed level and flow rate will increased and thus the potential for sediment transport will also increased from the river bed and near the bridge piers.*

C. *Local scouring: in general, the hydraulic structures and bridge piers may change the flow pattern and create the turbulence flows near the relevant structures and finally create a hole in the place of structures. This kind of erosion is severely in the flooding conditions and is one of main factors to occur the damaged hydraulic structures and bridges.*

Numerous studies and experiments have been made by researchers to reduce scouring. To deal with this phenomenon around the bridge piers, there are three common strategies as follows: [2]

1. *Put the foundation in lower levels than the depth of erosion pit.*
2. *Reduce the vortex pier formed around the pier*
3. *Creating the secure protection of revetment and or using the crack or collar or submerged plates around the pier.*

This study examines and compares the performance of non-submerged plates to reduce scouring around the bridge pier. One of the most useful software in modeling and analysis of scouring phenomena is software SSIIM; the modeling and analysis of scouring phenomenon and also its reduction using the non-submerged plates will be discussed on the results obtained using the software and laboratory data.

The bridges at their construction site may cause to scouring in the rivers for several reasons. First to shorten the length of the bridge, the cross of the bridge is considered too narrow than the river level that it causes to increase the flow rate and cut-off tension in the bed and finally the scouring occurs (the scouring due to narrowing). Second because of pier and abutment, a three-dimensional eddy of vortex flow produces around that separates the grains from the bed and local scouring. This scouring is very important due to the complexity of formed flows. If there is a scouring in the river flow, it also added to the scouring of bridge. The bridge pier acts as a barrier against the flow of the river and affects its hydraulic properties. The geometry shape and location of pier for the flow length and also the number and distance of piers and amount of narrowing are the effective factors to change the flow location of river and its results. [2]

Many researchers due to the laboratory or field data and wide studies on the mechanism of scouring have provided many relationships to estimate and predict scouring depth. Each of these relationships is based on a number of parameters affecting the scouring. Some of the researchers consider the effect of one or two parameters in their relations and others use more parameters in their relations.

Inglis (1938) and Laursen. EM (1958) and Issard & Bradley (1959) and Hassounizadeh (1990) [3] and Dietz (1972) and Melville (1974) [4], have done numerous studies and tests to estimate the scouring. Garde & Raju (1977) [2] and Lauchlan (1999) and Chabert & Engeldinger (1956) [5] and Thomas (1967) and Ettema (1980) and Dargahi (1987) and Zaraty and Azizi (1997) [6] and Thomas (1967), Tanaka and Yanno (1967), Neill (1973) and Ettema (2001) [7] have conducted researches and experiments to control and reduce scouring. Asghar Azizian et al (2010) evaluated the scouring of bridge pier using the experimental results and using the numerical model HEC-RAS4.0 [8] and Masoumeh Rostam Abadi and Seyed Ali Akbar Neishabouri (2006) began a simulation of flow pattern around a plate over the bed of a rectangular channel using software FLUENT [9].

An extensive study has been carried to calculate the scouring using the numerical models of the actual flows on the river adjacent the channel by Lanca motta et al (2007) [11] and Tanana and also 524 bridge piers on Tanana river with respect to the proposed process HEC-18 (Richardson and Davis, 1994) in discharge condition of 100 and 500 years and the bridge of Tanana river in Parkers highway in Nenana region by Langley (2006) [13].

Using the flow field and sediment transport equations around the bridge piers, Sayadi (1996) calculated the depth of local scouring to use the finite element method. The study uses the Navier-Stokes equation as the equation that models the velocity field. Firstly the equation of Navier-Stokes to solve and the velocity field is achieved. Then the velocity in the horizontal plane uses ad the input data in the sediment transport equation [4].

Almasi (1999) using a physical model studied the scouring of rectangular piers in various modes and compared the obtained results with the results of theoretical relations. He tested the square and rectangular shaped piers and different angles to the prevailing rate in the channel [4].

Mohammad Pour and Rakhshanddeh Ru (2002) have studied the scouring around the cylindrical and non-cylindrical shaped uniform piers in the river structures. The scouring experiments have done in a flume on the basis of the surface area of a circle, square, triangle, rhombus and then the relationship between the measured data has been proposed to determine the changes of scouring depth [4].

Tayeb Zadeh et al (1384) used the SSIIM numerical model to measure the equilibrium scouring depth around bridge piers with circular cross.Their research results indicated the high accuracy of the SSIIM numerical model by calculating the scouring depth [10].

Taimaz Esmaeili (2009) with regard to the time factor was calculated the maximum scouring depth corresponding flood hydrograph using software SSIIM. The effect of changes for the geometry parameter of pier diameter as well as the change of pier shape were simulated by creating a gap in the cylindrical pier using software SSIIM. As expected, the diameter of cylindrical was correlated with the equilibrium

scouring depth but with a 2-fold increase, the pier diameter of equilibrium scouring depth around the pier increased by less than 60% [10].

MATERIALS AND METHODS - INTRODUCING A NUMERICAL MODEL [14,15]

The SSIM model is three-dimensional software for simulation of water and sediment movements and it was developed by Nilz Oulsen in the Hydraulic Engineering department and Environment of Norway Science and Technology University. The three-dimensional CFD model is based on the finite volume method and solves Navier - Stokes turbulence model based on the standard turbulence model $K-\varepsilon$.

SSIIM model is the numerical software with applications in the field of river engineering, environmental hydraulics and sediment that the primary purpose of this software structure is to simulate the movement of sediment in the river and channel geometry. Then the application of this software was developed in other hydraulic issues such as spillovers modeling, drop in tunnels, relation between depth and discharge in rivers. The main advantage of SSIIM model comparing CFD software is an ability to analyze complex geometries to model sediment transport in live bed. During the years, SSIIM software has been used to model the crossing Salmon and algae as the calculation of water quality. However, most attention has been focused on sediment transport calculations.

SSIIM software solves Navier-Stokes equations with the standard model $K-\varepsilon$ on a non- orthogonal three-dimensional grid. For detached implementation, a control volume method can be used with Power-Law scheme or Second Order Upwind algorithm. SIMPLE method also uses as a default to correct pressure. This method is invoked by the set of information K 9 in the Control File. SIMPLE method is used to relate pressure and velocity terms.Using an implicit solution, the velocity field is calculated in geometry and the velocities use when Convection-diffusion equations have been solved for various sizes of sediment. SSIIM software uses to facilitate Input file from the dialog boxes.

☐ ***Turbulence Model*** $K-\varepsilon$

Model $K-\varepsilon$ is calculated vortex viscosity as follows:

$$\mathrm{v_T} = \mathrm{C_\mu}\frac{\mathrm{k}}{\varepsilon^2} \qquad (1)$$

K is the kinetic energy of turbulence and defined as follows:

$$\mathrm{K} = \frac{1}{2}\overline{\mathrm{u_i u_i}} \qquad (2)$$

Differential equation for **k** is expressed as follows:

$$\frac{\partial \mathrm{k}}{\partial \mathrm{t}} + \mathrm{u_j}\frac{\partial \mathrm{k}}{\partial \mathrm{x_j}} = \frac{\partial}{\partial \mathrm{x_j}}\left(\frac{\mathrm{v_T}}{\sigma_\mathrm{K}}\frac{\partial \mathrm{k}}{\partial \mathrm{x_j}}\right) + \mathrm{p_k} - \varepsilon \qquad (3)$$

In the above relationship, p_k is defined in the following form:

$$p_k = v_T\frac{\partial u_j}{\partial x_i}\left(\frac{\partial u_j}{\partial x_i} + \frac{\partial u_i}{\partial x_j}\right) \qquad (4)$$

ε represents the rate of dissipation of k and is specified as follows:

$$\frac{\partial \varepsilon}{\partial t} + u_j\frac{\partial \varepsilon}{\partial x_j} = \frac{\partial}{\partial x_j}\left(\frac{v_T}{\sigma k}\frac{\partial k}{\partial x_j}\right) + C_{\varepsilon 1}\frac{\varepsilon}{k}P_k + C_{\varepsilon 2}\frac{\varepsilon^2}{k} \qquad (5)$$

In equation (1) to (5), **C** is constant coefficients that cannot be changed by the user. As described, $k-\varepsilon$ turbulence model is the default turbulence model in SSIIM.

We can summarize the equations governing the flow field in turbulent mode as the continuity equation and momentum equation. If it is assumed that the flow is constant ($\frac{\partial}{\partial_t} = 0$) and the special density fluctuations are zero ($p' = 0$), then continuity and Momentum equations are expressed as follows:

$$\frac{\partial}{\partial \mathrm{x_j}}(\mathrm{pu_j}) = 0 \qquad (6)$$

$$\frac{\partial}{\partial x_j}(pu_iu_j) = -\frac{\partial p}{\partial x_j}\delta_{ij} + \frac{\partial}{\partial x_j}\mu\left(\frac{\partial u_i}{\partial x_j} + \frac{\partial u_j}{\partial x_i}\right) + \frac{\partial}{\partial x_j}\left(-\overrightarrow{pu_i}\,\overrightarrow{u_j}\right) \qquad (7)$$

In relations (6) and (7), U is velocity component, p the fluid density and P the total pressure. $-\overrightarrow{pu_i}\,\overrightarrow{u_j}$ Term is the Reynolds stress term. According to the equations (6) and (7) , we can write three momentum equations and one continuity equations in which there are 10 unknowns (velocity in three directions of w, v, u and p pressure and six components of Reynolds stress) that means the field of equations governing the flow is not closed and Reynolds stresses are modeled by using mathematical methods. Thus, the turbulence equations will use to close the governing equation field.

☐ ***Equations Governing the Sediment Flow***

The process of calculations for SSIIM numerical model is that at first - sediment concentration is calculated by solving the Convection-diffusion equation of sediment in distance between the water level and the base level (a). The base level is considered in order to the equivalent roughness height. Sediment transport is traditionally divided into the bed load and suspended load. Suspended load can be determined using Convection-diffusion equations by calculating the sediment concentration.

$$\frac{\partial \mathrm{c}}{\partial \mathrm{t}} + \mathrm{u_j}\frac{\partial \mathrm{c}}{\partial \mathrm{x_j}} + \mathrm{w}\frac{\partial \mathrm{c}}{\partial \mathrm{z}} = \frac{\partial}{\partial \mathrm{x_j}}\left(\Gamma_\mathrm{T}\frac{\partial \mathrm{c}}{\partial \mathrm{x_j}}\right) \qquad (8)$$

In above relation, the fall velocity of particle was determined by W and Γ_T is distribution coefficient which is derived from standard equation $k-\varepsilon$.

$$\Gamma_T = \frac{u_T}{S_c} \qquad (9)$$

S_c is the Schmidt number which by default is equal to 1.

Van Rijn has offered a formula for determining sediment concentration near the bed in 1978, which is as follows:

$$C_{bed} = 0.015 \frac{d^{0.3}}{a} \frac{\left[\frac{\tau - \tau_c}{\tau_c}\right]^{1.5}}{\left[\frac{(p_s - p_w)g}{p_w u^2}\right]^{0.1}} \quad (10)$$

In the above relation, d is the sediment particle diameter, a is reference level of the roughness height, τ is bed shear stress, τ_c is critical shear stress of bed for replacing the sediment particles according to the Shields diagram, p_s, p_w are the sediment and water density, u is the viscosity of water, g is the acceleration of gravity. In SSIIM model, a reduction coefficient of critical shear stress use for sedimentation in sloping bed by Brooks (1963).

$$K = -\frac{Sin\phi Sin\alpha}{\tan\theta} + \sqrt{\left(\frac{Sin\phi Sin\alpha}{\tan\theta}\right) - Cos^2\phi\left[1 - \left(\frac{\tan\phi}{\tan\theta}\right)^2\right]} \quad (11)$$

In this relation, α is an angle between the flow and a line perpendicular to the bed, φ is the slope angle and θ is the slope parameter. K factor is calculated by multiplying the horizontal plane at critical shear stress. The SSIIM numerical model is used the following equation to calculate the bed load in distance from the bed load to baseline level.

$$\frac{q_b}{D_{50}^{1.5}\sqrt{\frac{(p_s - p_w)g}{p_w}}} = 0.053 \frac{\left[\frac{\tau - \tau_c}{\tau_c}\right]^{1.5}}{D_{50}^{0.3}\left[\left(\frac{(p_s - p_w)g}{p_w U^2}\right)\right]^{0.1}} \quad (12)$$

Experimental value of 53 0/0 is changeable in F 83 data set in the control file.

CHARACTERISTICS OF LABORATORY CHANNEL [16]

A set of long experiments using the cylindrical piers in channel have done with uniform bed under the limpid water in the hydraulic libratory of Okayama University. The tests have done in channel with 1600cm length, 60cm width and 40cm depth.

Water from a reservoir by a pipe is transmitted into the channel from a channel opening when discharge is measured by a sharp edged overflow. The flow rate in channel is set using a valve (tap water). The water depth was adjusted by a valve in downstream. Head on the sharp edged overflow and water levels were measured with a point gauge having 0.1mm sensitivity. A region with the moving bed with 100cm length and 60cm width and 57cm depth is embedded in 800cm distance in downstream of the beginning of channel and was filled with sediments having medium diameter of particles $d_{50} = 1.28mm$ and standard geometric deviation $\sigma_g = 1.29$. A vertical circular base with diameter $D = 6cm$ is inserted in the center of the moving bed that is created before the experiment. The water tap is smoothly adjusted without any turbulence in the bed materials until the expected discharge created. Steady stream is fully created under the limpid water for the required discharge. The whole process to complete the steady stream was stabilized under the limpid water in less than three minutes for each case. Experiments were stopped in a period when the scouring is created less than 1mm area or no scouring. The depths of scouring at different times were connected by a connected index. In this experiment, the water level is 200mm, cylindrical pier diameter is 6cm, average diameter of particles is $d_{50} = 1.28mm$, discharge is $Q = 0.4 m^3/s$, time of scouring is 140min and scouring depth is 78mm.

NUMERICAL MODELING

In the present study, SSIIM numerical model (2007 Olsen) was used for the purpose of networking and solution of flow and scouring around the bridge pier. As part of the field networking is seen in figure (1), the smaller network near the pier but the larger network in longer distance.

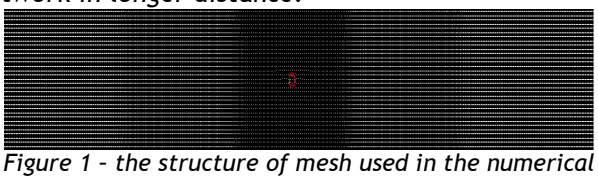

Figure 1 - the structure of mesh used in the numerical simulation and schematic view for smaller cells by approaching the pier

In order to verify the feasibility of the numerical model results from the lab results, discharge and water level of flume downstream are given to the numerical model as boundary conditions, then the numerical model or time steps 4s were calibrated with the roughness coefficient equal to 0.012.

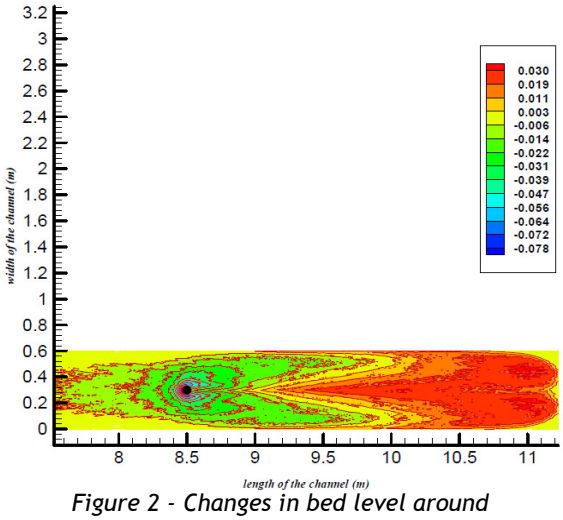

Figure 2 - Changes in bed level around the cylindrical pier

CONCLUSIONS

In the present study suggested that non-submerged plates which are designed as shear edged overflows to be used. These plates are modeled with different configurations and finally using the results obtained from the numerical model, they are selected the most optimum mode among different configurations. Then the plates are used in front of the bridge pier and the obtained results shows the reduced amount of scouring can be calculated using the plates.

In addition to create more sediments, the plates should be designed as reduce the scouring. To study

different configurations and determining the most optimum mode, various forms are modeled by the layout of plates as follows. According to the test specifications, since the diameter of the cylindrical pier is 6cm, the length of the plates' coverage in front of the pier is considered 12cm.

Figure 3 - Different configurations of plates

Now the results obtained from the above models are shown in various forms respectively.

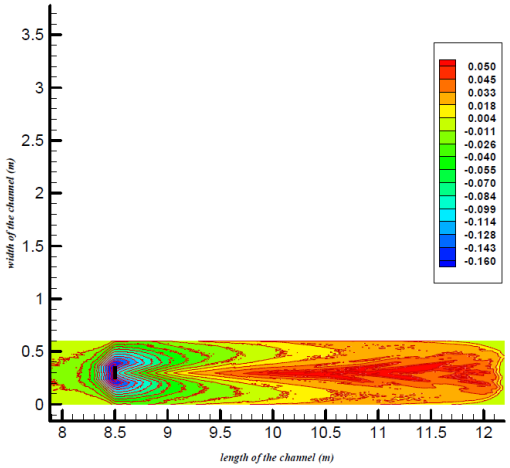

Figure 4 - Changes in bed level for a single plate model

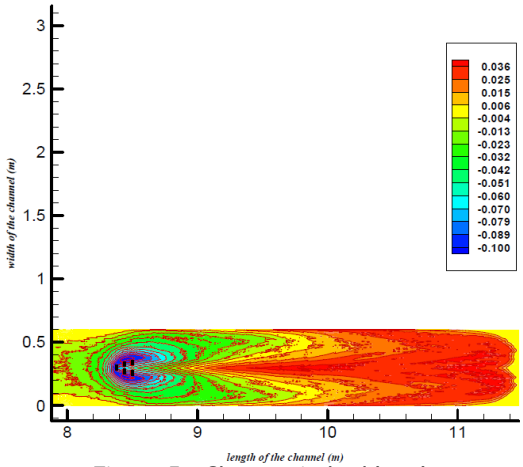

Figure 5 - Changes in bed level for the five plates model

Due to the sediment rate and scouring depth, we should consider a state that more sediment appears due to low scouring depth. According to the results obtained from the above figures, in five plates model, the scoruing depth is equal to 100.2mm and sediment rate is equal to 36mm, which is better than the other modes. As a result, the second model will use to examine the effect of sub-merged plates for reduction of scouring of cylindrical pier.

According to figure (6) observed that the area of deposited sediment is considered in range of 9m to 11.4m in channel and can determine that the range of maximum sediment is in 11m.

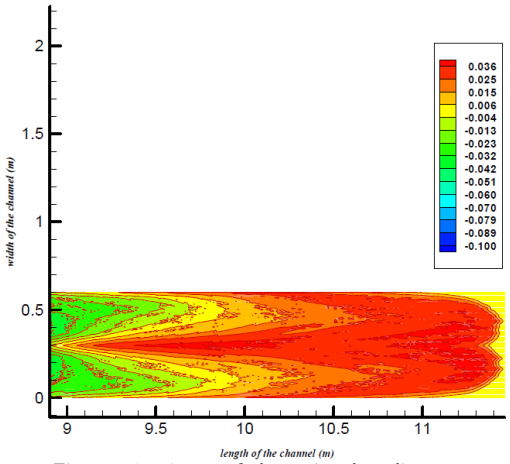

Figure 6 - Area of deposited sediment on the bed in Model 3

According to figure (6), the best points of the plates have been detected at 2.5m intervals in center of cylindrical pier and in upstream. The results of modeling, while the plates are embedded in the mentioned distances and cylindrical pier of upstream, are shown in figures (7), (8) and (9).

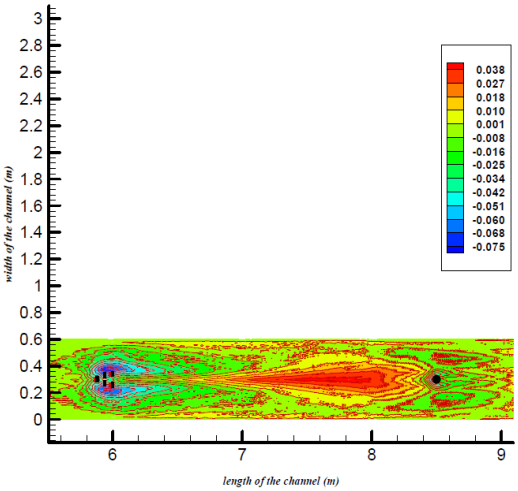

Figure 7 - Changes in the bed level if plates settled at 2.5m distance from the center of cylindrical pier and in its upstream

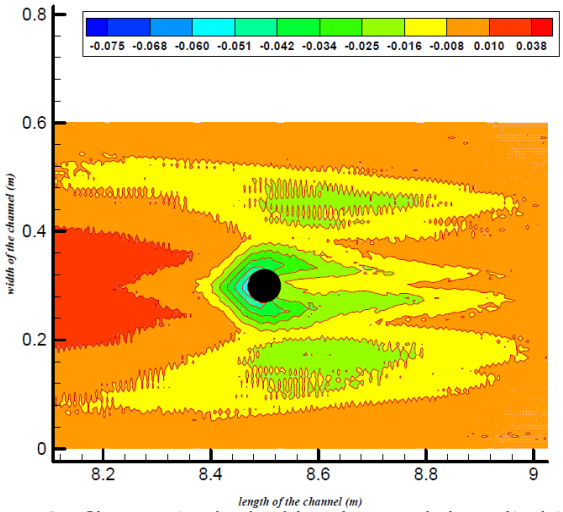

Figure 8 - Changes in the bed level around the cylindrical pier if plates settled at 2.5m distance from the center of pier and in its upstream

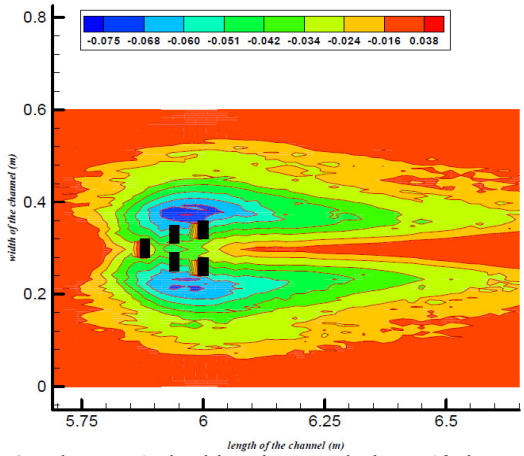

Figure 9 - changes in bed level around plates if they settled at 2.5m distance from the center of pier and in its upstream

As observed in figure (8) the maximum scouring around the cylindrical pier at 2.5m distance from the downstream of plates is equal to 0.051m and according to (9) we see that the scouring depth around the plates is equal to 0.068m. Finally the scoruing of cylindrical pier is reduced about 35% compared to the initial state.

RESULTS

1. *In this research, using a laboratory model and SSIM models, it was attempted to offer the proper procedure to confront the scouring phenomenon. According to the represented results, the use of non-submerged plates with different spatial arrangements is a proper procedure to control the scouring phenomena.*
2. *The dimensions and the place of plates on the piers are considered as the important parameters in reducing scouring, in a way that between the two conditions that were analyzed the second modle (five-plates non-submerged plates) was shown better function in regards to scouring and its sediment area.*
3. *The scouring depth reduces considerably by changing the place of cylinderical pier in the sediment area of non-submerged plates.*
4. *SSIM software is a three-dimensioanl software and can model the expand of hole depth of scouring in a mode dependent to time. The software can be a good option for calculation of sediment and scouring depth around the bridge pier.*

Parameters

K: kinetic energy of turbulence
ε : loss of kinetic energy of turbulence
U: Velocity components
p: Fluid density
P: Total pressure
$-p\overrightarrow{u_i}\overrightarrow{u_j}$: Reynolds stress term
W: Fall velocity of particle
Γ_T : Distribution Coefficient
S_c : Schmitt Number
d: diameter of sediment particles
a: Reference level due to the roughness height
τ : Shear stress of bed
τ_c : Critical shear stress of bed for replacing the sediment particles due to the Shields diagram
p_w : Water density
p_s : Sediment density
u: Viscosity of water
g: Acceleration of gravity
α : Angle between the flow direction and a line perpendicular to bed
φ : Angle of bed slope
θ : Slope Parameter

REFERENCES

[1.] *Mesbahi, M., 2009, comparing the proposed relations for maximum scouring depth of bridges piers using field data, the first regional conference of civil engineering, Khomeini Shahr, 1-2.*
[2.] *Management and Planning Organization, Technical Affairs., 2002, Publication No. 260, Manual to determine the erosion depth and methods for coping it around the bridge piers, Publication of Management and Planning Organization.*
[3.] *Tahmasebi Birgany, E., 2006, comparing the methods for calculating the scouring in bridge piers using the measured data, MS Thesis, University of Shahid Chamran.*
[4.] *Abbas Niya, A., 2005, Computer modeling of scouring around bridge pier using the precise techniques, MS Thesis, Tehran University.*
[5.] *Khoda Shenas., S., et al., 2009, reviewing the performance of gap and collar in reduction of scoruing of the bridge pier, Ferdowsi University of Mashhad, Khorasan Regional Water Company, research committee.*
[6.] *Arunqi, H, et al. 2009, determining the proper dimensions of the rectangle collat in reduction of scouring of bridge pier, Journal for knowledge of Soil and Water, Volume 19, № 1, 52-54.*
[7.] *Samimi, T. et al., 2006, laboratory view for the effect of submerged plates on the scoruing of bridge piers, National Conference on Irrigation and Drainage Networks, Shahid Chamran University, College of Water Science, 1-2.*
[8.] *Azizian, A., et al, 2010, ng of bridge piers using numerical model HEC-RAS4.0 and the experimental results, the Fifth National Congress of Civil Engineering, Ferdowsi University of Mashhad.*
[9.] *Rostamabadi, M., and Salehi Neishabouri, A., 2008 , Simulating the flow model around a submerged plate in rectangular channel, the Fourteenth National Conference on Civil Engineering students.*
[10.] *Esmaeili, T., 2009, Numerical simulation of hydraulic - Geometric scouring at the concrete bridge piers, MS Thesis, Tehran University of South.*
[11.] *Davide Motta, Ramon Pacheco, Riccardo Telò., 2007, "Advanced numerical modeling of the scouring process around the piers of a bridge".*
[12.] *Thomas A.Heinrichs, Dustin E.Langley, Robert L.Burrows, and Jeffrey S.Conaway., 2006, "Hydraulic Survey and Scour Assessment of Bridge 524, Tanana River at Big Delta, Alaska Scientific".*
[13.] *Dustin E. Langley., 2006, "Calculation of Scour Depth at the Parks Highway Bridge on the Tanana River at Nenana, Alaska, Using One-and Two-Dimensional Hydraulic Models".*
[14.] *Nils Reidar B. Olsen., 2011, "A Three-Dimensional Numerical Model for Simulation of Sediment movements In Water Intakes with Multi block Option", version 1 & 2.*
[15.] *Yonas Michael, Robel Tilaye., 2010, "Numerical Modeling for Settling Basin Design".*
[16.] *Md. Faruque Mia, Hiroshi Nago., 2003, "Design Method of Time-Dependent Local Scour at Circular Bridge Pier".*

ACTA TECHNICA CORVINIENSIS – Bulletin of Engineering
Tome VI (Year 2013) – FASCICULE 4 [October–December]
ISSN 2067–3809

[1.] Stoyan SLAVOV

OPPORTUNITIES FOR IMPLEMENTATION THE VIBRATORY SUPERFICIALLY PLASTIC DEFORMATION PROCESS FOR CYLINDRICAL SURFACES USING CNC TURN/MILL CENTERS

[1.] TECHNICAL UNIVERSITY OF VARNA, DEPARTMENT OF TECHNOLOGY OF MACHINE TOOLS AND MANUFACTURING, STUDENTSKA STR. 1, 9010 VARNA, BULGARIA

ABSTRACT: This article discusses some typical disadvantages of the traditional kinematical scheme for implementing the vibratory superficially plastic deformation process, realized on manually controlled lathe machine tools and the possibilities and some difficulties in implementing that process by using 2 - axis CNC lathes and the more advanced multi-axis CNC Turn/Mill centres. Kinematical parameters of the process having an impact of the toolpath, for forming of regular reliefs from different types through the process are described, and math functions for its calculating are proposed in accordance with the diameter and length of the cylindrical surface, that will be processed. The necessity of using 4-axis turn/mill centres (with rotary C-axis) is examined. The sequence of steps for automated programming of the attributes of the operation, using FeatureCAM software system, for output the required NC code is proposed.
KEYWORDS: vibratory superficially plastic deformation process; CNC turn/mill centres; FeatureCAM, Delcam

INTRODUCTION

Some examples from the technological practice confirms that the nature of the roughness of contact surfaces of various parts, obtained by the most common finish machining methods (e.g. grinding, lapping, polishing, etc.), do not always meet operational requirements for working conditions in the friction pairs, contact with fluids and/or different electromagnetic radiations.

Among finishing methods, the method of processing, known as "Vibratory Superficially Plastic Deformation" (VSPD) is characterized by the best better combination of complex parameters of the quality of treated surfaces [6]. This method is based on plastic deformation (without heating) of the surface layer of the workpiece by pressing the steel ball with high hardness (e.g. from ball roller bearing) with certain force, which moves along complex trajectory regarding it. The VSPD process usually performed on lathes (outfitted with special vibratory rigs) and for cylindrical surfaces of the rotating parts (e.g. plain or drive shafts).

As a result, specific overlays of traces and valleys from the ball-tool are formed onto contact surfaces of parts, which due to its high degree of repeatability are called "regular" micro-reliefs (RMR). On the Fig. 1 (a÷f) are shown the five possible types of the RMRs which can be obtained using the VSPD process. The parameters of their profile of roughness asperities and operational characteristics, which radically differ from those, obtained after implementation of other traditional finishing methods. Depending on the type of the workpiece's material (hardness) and process parameters of the VSPD operation (speed, feed, force of pressure and diameter of the ball-tool) roughness asperities with large radii of curvature, ranging from 800 to 8000 μm (at maximum height of roughness asperities from 10 to 35 μm), small angles of inclination of the roughness asperity profile from 0^0 30' to 3^0, and large horizontal distance between the peaks (from 500 to 3500 μm), the conditions of contact interaction are significantly improved [3,6]. Moreover, this finishing method increases the hardness of the surface layer, which improves resistance to wear of the parts.

Among the known kinematical schemes for processing regular reliefs around cylindrical surfaces by VSPD of the types from Fig. 1 (a ÷ f) with the most wide application has the kinematical scheme, shown in Fig. 2,a. There are some examples for successfully implementation of this scheme for VSPD (by manually operated lathes) and obtained RMRs wrapped around it. These results show, that all types of RMRs from Fig.1, a÷f can be achieved by appropriate combination of values for the regime parameters of the process (depending on the size d x L of the cylindrical part), which are follows:

- d, mm - diameter of the cylindrical surface;
- L, mm - length of the cylindrical surface;
- vf, mm/rev - feed rate;
- 2.e, mm - amplitude of the oscillations (which is influenced of the width b, mm of RMR cells);
- n_0, [min^{-1}]- speed of lathe spindle;

– *j, [osc./rev]- it is so-called "Drive Ratio" in VSPD and determines the number of oscillations of the tool per revolution of the cylindrical workpiece. This parameter basically influences of the size a,mm (see Fig. 2,b) and the type (from I to V) of the obtained valleys or cells of RMRs.*

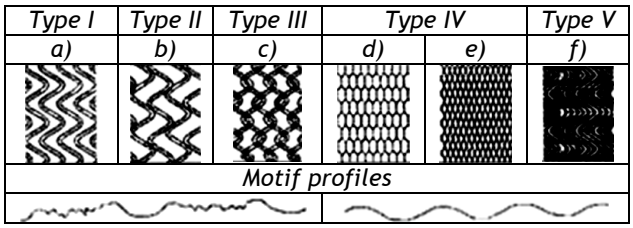

Figure 1. Types and typical motif profiles after implementation the VSPD process: a) system of not tangent ditches b) system of tangent ditches c) system of intersecting ditches d) regular relief with hexagonal cells e) regular relief with rectangular cells; f) regular relief superimposable on each other's ditches.

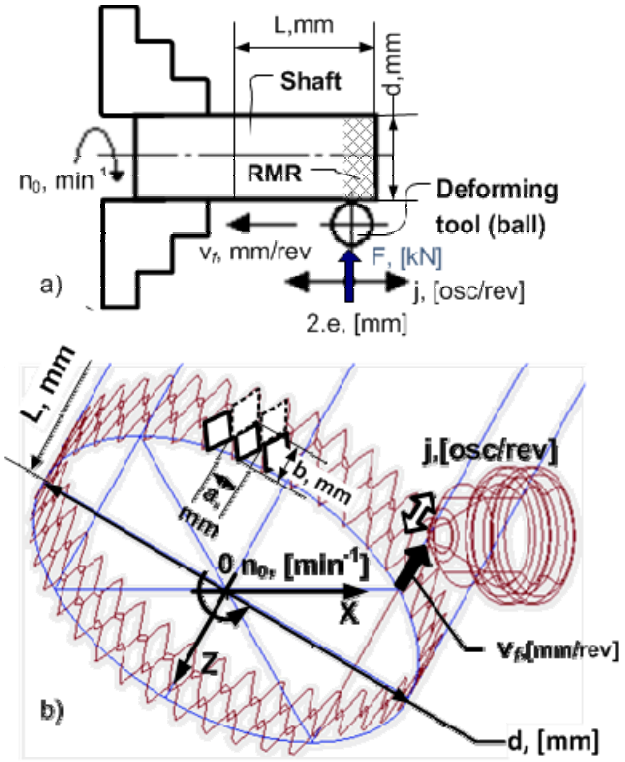

Figure 2. a) Kinematical scheme for VSPD using manually controlled lathes; (b) Toolpath and the way for obtaining the RMR cells from IV-th type, around the cylindrical surface, using VSPD process.

Using these parameters, it is possible to create appropriate mathematical model, based on periodic trigonometric functions for modelling the formation of the valleys (or cells) of RMRs wrapped around to cylindrical surface, as follows:

$$x(t) = 0.5 \cdot d \cdot \cos(n_0 \cdot t)$$
$$y(t) = 0.5 \cdot d \cdot \sin(n_0 \cdot t)$$
$$z(t) = v_f \cdot t + e \cdot \cos(2\pi \cdot j \cdot t), \qquad (1)$$

where: t ,[sec] is the time needed to processing whole length L, [mm] of the cylindrical surface.
The above system of equations (1) defines the tool path, shown graphically on Figure 2,b.

Equations (1) allows to obtaining preliminary information of the shape and size of valleys or cells of the RMR that will be formed at given combination of regime parameters.
Along with above mentioned operational advantages of RMRs, there are some technological limitations and disadvantages when the process VSPD is performed using manually operated lathes, like follows:

a) *Constructive embedded kinematics of manually controlled lathes are usually insufficient for realization of the complex trajectory of movement of the spherical indenter in VSPD, making it necessary to design and construct additional equipment devices to provide the necessary oscillations of the tool. This leads to increase the time for preparation and raises the cost of the technological equipment for implementation of this method;*
b) *Spindle rotation speeds and feedrate of manually controlled metalworking machines cannot be changed uninterruptedly, leading to restrictions in the form and dimensions of the achieved cells of RMR;*
c) *The lack of synchronization between spindle rotating and linear feed movements of manually controlled lathe machines often lead to distortion of the shape and no uniformity of the cells of the relief;*
d) *Relatively low speed feeding movements of manually operated lathe machines in comparison with CNC lathes, substantially increases cycle time and thus this method obtains low efficiency for processing of parts with large dimensions.*
e) *The necessity of using lathe machines outfitted with special equipment for implementation the VSPD operations, complicates overall processing of the cylindrical workpieces, due to the need to refixturing from one machine to another the parts, after the execution of the others turning operations. Accordingly, the duration of the cycle increases for the overall processing of the workpiece.*

Due to above reasons, the implementation of the regular reliefs, obtained by using VSPD and manually operated lathes still rarely take place in contemporary production technologies, as well as their advantages for improving performances of the contact surfaces of rotary parts are little known in the mechanical engineering industries. So their implementation most often limited to machining a specific machine parts in terms of repair (or restoration) production or in laboratory conditions.

PRECONDITIONS FOR IMPLEMENTING THE VSPD PROCESS USING CNC MACHINE TOOLS

The VSPD process productivity and accuracy can be significantly optimized by using opportunities of contemporary CNC machines, instead manually operated lathes, whereby the existing disadvantages and limitations of the method can be minimized or avoided.
Basically this is due to high accuracy, stability, cutting speeds and feeds of modern CNC machines

and ability to perform complex trajectories of movement of tools.

For example, the ability to control from simple 2 Axis (X,Z) turning to highly advanced Mill-Turn and Multi-Tasking centres, eliminates the necessity of using special and expensive additional devices to provide the necessary kinematics for VSPD process. Therefore the use of these machine tools would be particularly suitable for the implementation of the VSPD process in today industrial conditions.

The most basic combination turning or turn/mill machine uses a driven rotary cutter that is mounted in one or more tool pockets on the turning center turret. Linear axis movement of the rotary tool imitates that of the turning tool. Different attachments such as right angle heads allow longitudinal cutting along the X-axis while straight heads do the face work following the Z-axis travel. These tools generally run perpendicular to the workpiece surface being cut. On these machines, any milling off the machine's center curve is not possible because of the 2-axis limit of the CNC turning center.

Analysing the kinematical scheme from Fig. 2a is seen that it is entirely possible to implement it on CNC lathes, because the main movements (rotating of the cylindrical workpiece and linear feed movement of the tool) can be performed by all types of CNC lathes.

The main task in this case is the provision of additional reciprocating movement of the tool with an amplitude 2.e. To avoid the necessity to use additional devices to reciprocating movement of the tool it should be combined with the linear feed movement, provided by the turret of lathe machine. Therefore, the resultant movement of the tool to the linear axis (usually Z-axis for lathes) must be a combination of these two movements. Adding the rotational motion of the cylindrical workpiece (provided by rotary axis C of the spindle of the machine) the necessary tool path for VSPD operation can be obtained (i.e. the spatial sinusoidal curve from Fig. 2.b).

Entire toolpath, however, should be split into a sufficient number of elementary sections, which can be executed by CNC lathe machines (by linear interpolation in appropriate coordinate plan). Therefore it is necessary to calculate in advance the corresponding coordinates of start and end points of all elementary sections (which can be reach several tens of thousands points) of the toolpath to provide the necessary geometric accuracy of the toolpath and hence uniformity of the obtained RMR cells.

EXPLORING THE OPPORTUNITIES FOR USING CNC LATHES WHITHOUT MULTI-AXIS POSSITIONING - Defining the toolpath for 2-axis limit CNC lathes

Because considered workpiece have a cylindrical shape, the diameter d of the processed surface will be constant for the entire length L (see Fig. 2b). Therefore X-axis coordinates X_i of the points from toolpath is the same for the entire length of treatment L, i.e. X_i=d/2=const. (where $i \in 0...p-1$).

The coordinates of the points Z_i along the Z-axis are calculated as summation of both feed and reciprocating movement of the tool. The Y-axis is excluded in the system of equations (2) because the tool doesn't need to interpolate in XY or YZ coordinate plans, i.e. Y_i = 0 (where $i \in 0...p-1$).

For calculation of the toolpath for traditional CNC lathes is used a system of two equations derived from the model equations (1), as follows:

$$X_i = \frac{d}{2}$$

$$Z_i = \frac{i \cdot L}{p} + e \cdot \cos\left(\frac{2 \cdot \pi \cdot i \cdot j \cdot n_0}{p}\right), \qquad (2)$$

where:

- p - is the total number of points from the curve of the toolpath (5000≤ p ≤10 000),

- i ($i \in 0...p-1$) the index of the coordinates of the current point from the curve.

Figure 3 presents the type of resultant trajectory of movement of the tool, obtained by connecting the points whose coordinates X_i, Y_i are calculated from the system of equations (2), where curve 1 (in red) shows the evolution of the toolpath in function of time t, sec., and curve 2 (in blue) shows the arrangement of the points along the axes X and Z in the coordinate system of the CNC lathe.

From Figure 3 can be seen that as much as a larger the number of points that define the curve 2, the more precise description of toolpath will be achieved. On the other hand, the number of points p will also depend on the full (unfolded) length of the trajectory of the instrument, which itself depends on the dimensions d and L of the cylindrical surface of the workpiece. The unfolded length of the toolpath L_{uf} (see formula 6) itself depends on the dimension L, amplitude and the frequency of the reciprocating movement of the tool per one revolution of the spindle, i.e. from the parameters j and 2.e, from equations (2).

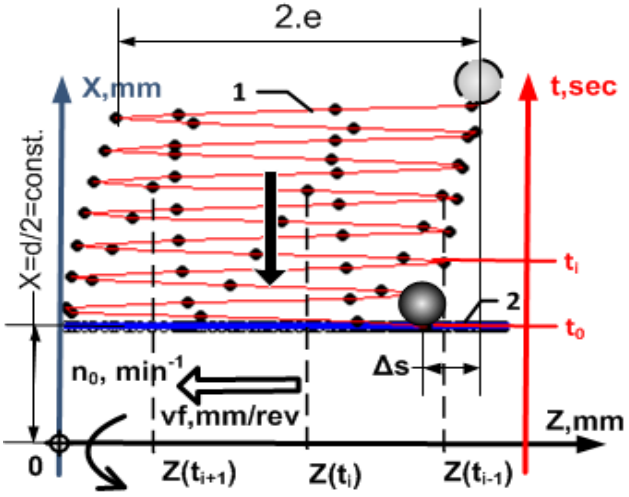

Figure 3. Graphical interpretation of the toolpath, obtained by equations (2)

Determining of the parameters participating in equations (2)

In order to obtain RMR cells with the necessary shape and size, the regime parameters must be determined. Some important dependencies that must be taken into consideration when determining the values of the regime parameters in equations (2) are described below.

The frequency j and amplitude of oscillations 2.e determines the shape and overall dimensions of RMR cells [3]. The frequency (or as also called "Drive Ratio") by its integer value j_{int} specifies the number of full reciprocating movements of the tool per revolution of the cylindrical workpiece, and it sets the value of the step a,[mm] of cells (see Fig. 2b). This parameter can also be determined based on the diameter d, [mm] and the step a, [mm] of the RMR cells using the following formula:

$$j \approx \frac{\pi \cdot d}{2 \cdot a} = j_{\text{int}} + j_{fract} \qquad (3)$$

Typically the parameter j_{int} assumes values in the range from 50 to 150 and more.

The fractional part j_{fract} from j, determines the phase shift of the sinusoidal trajectory after each revolution of the workpiece. By setting values in the range from 0 to 0.5 for j_{fract} the shape of RMR cells can be amended to achieving fourth and fifth types of reliefs, shown in Fig. 1, d,e.

The length of the cells - b, [mm] (see Fig. 2,b) in the axial direction can be determined from the displacement Δs, [mm] of the tool per revolution of the workpiece due to the feed -v_f, [mm/rev] and the amplitude - 2.e, [mm] using the following formula:

$$b = \Delta s + 2 \cdot e, [mm] \qquad (4)$$

The necessary number of complete rotations- n', for processing the entire length L, [mm] of the cylindrical surface of the workpiece can be defined as:

$$n' = \frac{L}{\Delta s} \qquad (5)$$

where Δs, [mm] is the linear displacement of the tool, along the Z-axis per revolution of the workpiece.

The unfolded length of the toolpath L_{uf} (i.e. the unfolded length of the curve 2 from Figure 3) can be calculated by summing the lengths of all elementary segments, by the following formula:

$$L_{uf} = \sum_{i=1}^{p} |Z_i - Z_{i-1}|, [mm], \qquad (6)$$

where Z_i are calculated values of the coordinates of the points in Z-axis from equations (2).

Assuming that the tool feeding speed is constant throughout the unfolded length of the trajectory L_{uf},, the feed rate v_f in [mm / rev] can be calculated by the formula:

$$v_f = \frac{L_{uf.}}{n'}, [mm/rev] \qquad (7)$$

The tool has to travel the entire length - L_{uf} for the same time that the cylindrical workpiece will be rotated of the required - n' rotations to completely process the cylindrical surface with length L.

The actual feed - v_{fm} in [mm/min] of the turret will be depending proportionally on the actual speed of the spindle and can be determined by known formula:

$$v_{fm} = v_f \cdot n_0 = \frac{L_{uf.} \cdot n_0}{n'}, [mm/\min] \qquad (8)$$

where n_0, [min^{-1}] is the actual (the lowest possible) speed of the lathe spindle.

Analysing the results for the regime parameters of the VSPD process

Because the tool actually passes the distance, equal to the length of the unfolded curve - L_{uf}, [mm] (see the curve - position 2 in Figure 3) for the same time that the spindle will make -n' turns (see equation 5), the actual feed rate must be greater than the feedrate of the traditional turning operation for the cylindrical workpiece with the same diameter d and length L. Feedrate v_{fm}, [mm/min], however, should be limited to the maximum possible feeds of the lathe turret along the Z-axis. For most of CNC lathes, the rapid feed in Z-axis cannot exceeds the upper limit of 25 ÷ 35 m/min.

Under certain combinations of values of the parameters L and Δs it is possible to be obtained lower values for n' (for example 3 ÷ 25 rpm) which spindles on two-axis limit CNC lathes cannot execute actually, due to limitations entered by manufacturers in the machine settings that protect them from overheating of driving motors at very low speeds of the spindle [4]. Therefore obtained by formula (5) values for the required numbers of turns of the workpiece -n` will not always match with lowest possible executable speed of the lathe spindle.

Using equations (5) and (6), the resultant feedrates, determined by a formula (8) for six different combinations of sizes d and L of cylindrical surfaces, and medium values for the other regime parameters, are shown in the Table 1.

Table 1. Feedrates v_{fm} obtained from equation (8)

№	j_{fract}	j_{int}	d, mm	L, mm	e, mm	Δs, mm	n',	n_0, rpm	v_{fm}, m/min
1	0.15	50	30	30	1	2	15	25	5.015
2	0.15	50	30	100	4	5	20	30	24.07
3	0.15	150	100	100	4	2	50	25	59.92
4	0.45	50	100	100	1	5	20	25	5.045
5	0.45	150	30	30	4	5	6	25	60.18
6	0.45	150	30	100	1	2	50	30	18.01

As seen from Table 1, even for relatively non large sizes for the cylindrical surface, and medium regime parameters of VSPD, some of the resultant feedrates v_{fm} in [m/min] exceeds from 1.5 to 1.9x the limits of the rapid feedrates (25 ÷ 35 m/min), even for the most highly advanced CNC lathe machines.

*Moreover, for large values for the drive ratio j, and even at low frequencies of rotation of the spindle n_0, the lathe turret should perform a large number of reciprocating movements, with amplitude **e** = 1 ÷ 4 mm. For example, if we have j= j_{int} + j_{fract} = 150.45, [osc./rev] (see Table1) and n_0=25 rpm, for the required number of reciprocating movements, which the lathe turret has to be carried out for 1 second along the Z-axis, we get:*

$$\frac{n_0 \cdot j}{60} = \frac{25 \cdot 150.45}{60} \approx 63, [osc./\sec] \approx 63, [Hz] \qquad (9)$$

The results, from Table1 and formula (9) clearly show that processing cylindrical parts by using VSPD on only 2-axis limited CNC lathes is practically inapplicable.

USING MULTI-AXIS TURNING CENTERS FOR IMLEMENTATION THE VSPD OPERATIONS - Benefits of the multi-axis machining

Multiaxis machining is a manufacturing process, where computer numerically controlled tools that move in 4 or more axis is used to manufacture parts out. Typical CNC tools support translation in 3 axes, but multiaxis machines also support rotation around one or multiple axes.

Multiaxis CNC lathe machines offer several improvements over other CNC lathes at the cost of increased complexity and price of the machine:

- ☐ Amount of work is reduced, if the piece would otherwise have to be refixturing manually during the machining.
- ☐ Better surface finish can be obtained by moving the tool tangentially about the surface.
- ☐ More complex parts can be manufactured, particularly parts with curved grooves, pockets etc.

Number of axes for multiaxis machines usually varies from 4 to 9 [2,4]. Each axis of movement is implemented either by moving the spindle (into which the workpiece is attached), or by moving the tool. The actual configuration of axes varies therefore machines with the same number of axes can differ in the movements that can be performed.

As for the rotary C-axis or spindle, it is generally an orientation-only axis on basic CNC lathe/turn machines. A coupling or other device inhibits rotation while milling, drilling or tapping operations are performed.

The next level of sophistication is to add servo-controlled actuation of the rotary C-axis. This is a common feature available on many turn/mill machine tools. Often a secondary motor is used to drive the spindle for contouring cuts. The main spindle motor would be disconnected in this case. In combination with the live tooling on the turning center turret, the C-axis adds the ability to make spiral-milling cuts, contours or other relatively complex interpolated geometries. The C-axis is widely used for the processing that more than two axis move at the same time, and the speed of rotation around Z-axis may range from 0.06 °/min to 45 rpm. Because of the lower speeds of spindles and possibility for synchronization both linear and rotational movements, would be more appropriate this type of machine tools to be used for the implementation of the process VPPD than the traditional CNC lathes (with only two-axis).

Defining the VSPD operations using CAM software systems

There are many CAM (computer aided manufacturing) software systems available to support multiaxis machining including software that can automatically convert turning or milling operations into 4-axes toolpaths.

FeatureCAM is a CAD/CAM software suite that automates machining and minimizes programming times for parts on mills, lathes, and wire EDM [1,5]. FeatureCAM generates toolpaths based on the features of the part, and automatically selects appropriate tools, determines roughing and finishing passes, and calculates feeds and speeds, based on the software's built-in machining knowledge.

The module FeatureTURN/MILL as part of FeatureCAM enables both turning and milling features to be created on a single machine in one set-up. It incorporates all the options within FeatureTURN and FeatureMILL2.5D stand-alone modules for traditional turning and 2.5D milling operations, and can be used to program CNC lathes with C-axis milling capabilities. Integrated 3D machine simulation, together with a library of over 350 fully customisable post-processors, enables visualization of exactly how to parts will be machined. During the simulation of the modelled turning and milling operations, FeatureCAM automatically output the corresponding NC code for various CNC turn/mill centers.

The main advantages of FeatureCAM, in the context of the present work, are the abilities to easily import (or define) the shape, material parameters and dimensions of the stock and part, quickly programming of turning and milling features on the outside diameter of a part with the FeatureTURN/MILL feature wizard, which in combination with the included "Curve Creation dialog" wizards, greatly facilitates the creation of the required toolpaths and the corresponding operations for processing by VSPD.

The sequence of the steps, required for defining operation for vibratory superficially plastic deformation of the cylindrical surface (using the module FeatureTURN/MIL, v.18 from FeatureCAM 2012, Delcam,UK) of the shaft with length- L=80, [mm] and diameter - d=50, [mm], will be discussed below. The required step by step sequence is shown in the flowchart in Figure 4.

☐ ***Step 1: Defining the Stock***

The Stock wizard of FeatureCAM provides step-by-step dialog boxes for specifying or modifying the general stock shape, specific stock dimensions, part program zero, and the origin of the modelling coordinate system. The stock shape is selected as Round and in the fields Length= 80, mm and OD (outside diameter) = 50, mm are filed in.

☐ ***Step 2: Defining the curve of the toolpath***

To create the curve that describes the toolpath using the Curve wizard dialog box that provides step-by-step instructions for creating curves using a variety of methods.

Because we already have the mathematical model (see Eq. 1 and Fig. 1), which describes the spatial curve of the toolpath wraped around the cylindrical surface, using the method Functions from the Other Methods section of the Curve wizard, as follow:

$$x = F(t),\ y = G(t),\ z = H(t), \qquad (10)$$

where F, G, and H are fields where the functions F(t), G(t), and H(t) must be entered separately. The

argument in all three functions - t is the same and varies from Start to End values with step given by the Increment value. When filling the functions in these fields, the other parameters (d, e, v_f, n_0 and j) participating in the model (see eq. 1) should be replaced with their numerical values. The three functions are shown below as their parameters are replaced with the appropriate indicative numerical values, for example:

*F: 25*cos(t*3), G: 25*sin(t*3),*
*H: -t+2.5*cos(2*pi*150.5*t)* (11)

Functions (11) are filled in the fields F, G, and H of the dialog box "Functions" (see Fig.4-Step 2).

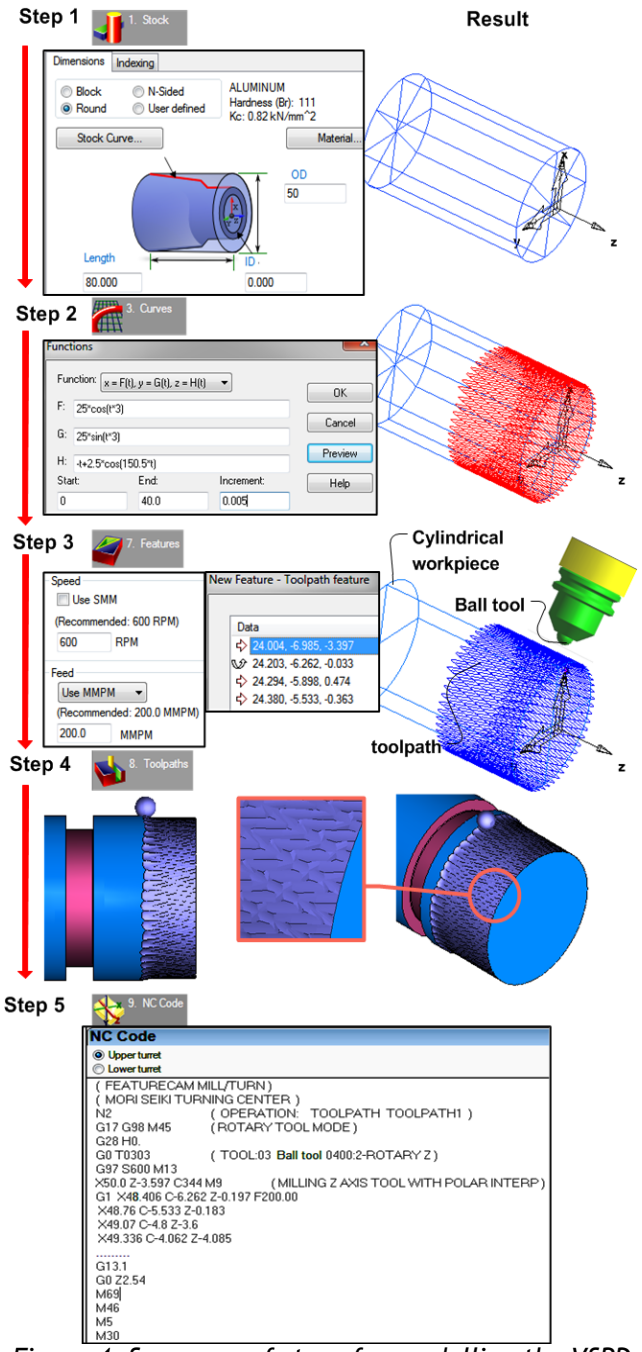

Figure 4. Sequence of steps for modelling the VSPD operation using FeatureCAM software

The Start field sets the starting point for the range over which the functions are evaluated. In this box is entered 0, which indicates that the curve of the toolpath will start from a point with coordinate Z=0. The End field sets the ending point for the range over which the functions are evaluated. In this box is entered the value 40, which indicates that the curve of the toolpath will end in a point with coordinate Z=40, mm. The Increment field sets the value added to or subtracted from the previous point evaluated for the functions to determine the next value to be run through the functions. Because the curve in our case is complex for its accurate drawing the increment value should be a smaller (for example 0.005). FeatureCAM generates the curve and apply the generated function to the drawing as geometry (see Step 2 on Fig. 4).

☐ ***Step 3: Defining the toolpath feature and setting up the VSPD operation.***

In FeatureCAM, toolpaths are generated from features, not curves; so that the part model is create using features. Features are common shop terms for describing characteristics of a part, for example, holes, pockets, slots, or step bores. These are the objects from which are create and customize toolpaths. Features provide additional information for automating the generation of toolpaths for part. FeatureCAM generates the related operations automatically. The New Feature wizard of FeatureCAM walks through the process of creation of features. This wizard guides the user through following stages:

- *Selecting the type and positioning the feature.*
- *Specifying the manufacturing strategy.*
- *Reviewing the automatically selected tools, calculated feeds and speeds.*
- *Overriding the tooling and feed/speed values and changing manufacturing attributes.*

A Toolpath feature explicitly represents a single toolpath, which create the moves of a toolpath by the curve defined in Step 2. This allows using the created curve to control the path of the tool precisely. Each Toolpath feature creates a single toolpath operation. Each toolpath operation has a Tools, Feed/Speed, and Toolpaths tabs, where filled out (or selected) the data for the type and the dimensions of the selected tool, feed and speed, and the calculated coordinates of the points of the toolpath.

Basically VPPD process doesn't require the ball-tool to perform rotations during operation, because smooth steel balls without cutting teeth are used instead of cutting tool. Because FeatureCAM not foreseen for modelling the operations such VSPD, the Toolpath operation is actually simulated as a contour milling operation with ball end endmill, that is modified such as hemisphere with a certain diameter. For that reason FeatureCAM calculates and displays in the F/S tab recommended speed of rotation for the tool. The calculated speed can be overridden to the minimum (or recommended) values specified by the manufacturer of the CNC lathe/mill center.

☐ ***Step 4: Simulating the VSPD operation and automatically generating the NC code***

FeatureCAM can provide several types of simulation. Step 4 on Fig. 4 shows the 3D Solid Simulation of the part (sometimes called Visicut) and VSPD operation. This style shows a three-dimensional shaded

rendering of the initial stock and simulates material removal in 3D. With that simulation method, video-style controls are used to pause, stop, and step through the toolpath, giving a fine control over the process. The Toolpath simulation is an important step in FeatureCAM in order to produce the NC (Numerical Control) code for the part. Prior to start simulation, it is important a suitable postprocessor to be selected, corresponding to the 4-axis CNC Turn/Mill center that will be used to perform the VSPD operation. The selected postprocessor (CNC file) could be either one that comes as standard with FeatureCAM or one that is created/modified with the XBUILD program. Using the different types of simulations that provides FeatureCAM it is possible to trace the toolpath as well as see the characteristics (shape and dimensions) of the cells from regular relief, obtained as a result of the execution of VSPD operation (see Step 4 in Fig. 4). After the simulation of VSPD operation complete the NC Code tab from Results section becomes active.

☐ ***Step 5: Reviewing and storing the NC code.***

Once the toolpath is simulated, the VSPD operation parameters are translated using a selected postprocessor into machine G-code. The NC Code dialog box of FeatureCAM in which is generated numeric control code is shown in Fig. 4 - Step 5. By clicking the Save NC button in the NC Code dialog generated NC code can be saved as a file.

CONCLUSIONS

Considered in this work possibilities for implementing the vibratory superficially plastic deformation process for making the regular reliefs on cylindrical surfaces, using traditional 2-axis lathes and 4-axis turn/mill centers (with rotary C-axis), leads to the following conclusions:

- ☐ *Despite the fact that 2-axis CNC lathes have the requisite kinematics and seemingly be able to provide the necessary movements both of the workpiece and tool to execute the VSPD operation, in practice the process cannot be implemented to them due to the lack of synchronization between the rotary motion of the workpiece and reciprocation feed movement of the tool. Even at the lowest speed of rotation of the spindle the frequency of reciprocating movement of the lathe turret would be too high (50 to 65 Hz, see eq.9) to actually execute at the lathe machine;*
- ☐ *For practical execution of the VPPD operations, however, can be used appropriate 4-axis turn/mill centers, due to their ability to perform interpolations between the rotation speed of the workpiece (around rotary axes) and linear movements of the ball-tool as well as carrying out the contour milling operations.*
- ☐ *Using the capabilities of FeatureCAM for programming live tooling operations for multi-axis machines, enables the programming of toolpaths and other parameters of the VPPD operations as well as automated generation of the NC code, required for driving the CNC machine tool.*

REFERENCES

[1] *FeatureCAM, Getting Started Guide. Thirteenth Edition, 2012, Delcam http://www.featurecam.com/.*

[2] *J.N. Lee, C.B. Huang, T.C. Chen, Tool-path generation method for four-axis NC machining of helical rotor. AMME 2008, VOLUME 31 ISSUE 2, p. 510-517;*

[3] *Slavov S. ,"Opportunities for application of advanced CAD-CAM systems and CNC machines for precise processing of regular reliefs on external planar and cylindrical surfaces of machined parts, Int. virtual journal "MTM" 2011, issue8, ISSN 1313-0226, pp.29-32;*

[4] *G. Popov, "Machine Tools", Volume 2, Issue of TU-Sofia, 2011 ISBN 978-954-438-766-2, 880 p.;*

[5] *Learning resource - FeatureCAM (2009), part I, Technologica, 332 p., ISBN: 9789549334111.*

[6] *Odintsov L. G, Hardening and finishing parts surfaces by plastic deformation, Handbook - Minsk: Engineering, 1987, 328 p.*

ACTA TECHNICA CORVINIENSIS - BULLETIN of ENGINEERING

ISSN: 2067-3809 [CD-Rom, online]

ACTA TECHNICA CORVINIENSIS - BULLETIN of ENGINEERING

ISSN: 2067-3809 [CD-Rom, online]

ACTA TECHNICA CORVINIENSIS - BULLETIN of ENGINEERING

ISSN: 2067-3809 [CD-Rom, online]

copyright © UNIVERSITY POLITEHNICA TIMISOARA,
FACULTY OF ENGINEERING HUNEDOARA,
5, REVOLUTIEI, 331128, HUNEDOARA, ROMANIA
http://acta.fih.upt.ro

ACTA TECHNICA CORVINIENSIS – Bulletin of Engineering
Tome VI (Year 2013) – FASCICULE 4 [October–December]
ISSN 2067–3809

[1.] Liany Amelia HENDRATTA, [2.] Terunori OHMOTO

RESISTANCE AND FLOW CHARACTERISTICS OF HIGH-CONCENTRATION SEDIMENT LADEN FLOW OVER DUNE TYPE BED IN AN OPEN CHANNEL

[1.] DEPARTMENT OF CIVIL AND ENVIRONMENTAL ENGINEERING, KUMAMOTO UNIVERSITY, JAPAN

ABSTRACT: The need to understand and predict flows that carry large loads of suspended sediments and wash loads has become acute in the Yellow River Basin, where significant erosion and siltation associated with high-concentrated floods produce significant erosion, siltation, and associated river problems. Mud flows, debris flows and slurries, which contain large concentrations of clay and/or silt particles suspended in water, often show non-Newtonian hydrodynamic properties. Non-Newtonian flows are poorly understood regarding the impact of their rheological properties on fully developed turbulent flows. In this paper, we experimentally investigated resistance and flow structure of high-concentrated sediment laden flow in an open channel using particle image velocimetry. The results showed that, compared with clear water flow, the rheological properties of sediment-laden flow significantly dissipated the turbulent flow fluctuations over the dune type bed and increased the flow resistance.
KEYWORDS: non-Newtonian fluid, mudflows, dune type bed, particle image velocimetry

INTRODUCTION

Waves in rivers and artificial channels are commonly caused by sand and pebbles from the base. Changes in beds and river channels occur as a result of sediment transport and that morphology influences the flow structures such as resistance law. Sand waves, which change with the characteristics of the riverbed material and water utilization conditions, have a close relationship with the flow-resistance, suspended sediment, and river bed fluctuation. Therefore, the studies of sand waves are one of the basic issues of sediment hydraulics. Various phenomena, concerning eddy of structure and sediment transport, seen in actual rivers have a strong relationship with riverbed forms. Thus, the investigation of how sand waves influence flow distribution has been the focus of strong interest among numerous researchers and engineers for years. Observing the riverbed material reach the surface of the river, Matthes (1947) predicted that a strong water spout-like rising eddy exists. From the observation of the Brahmautra river in the East Pakistan, where long term flooding occurs, Coleman (1969) pointed out that a cork boiling eddy is generated from the trough of the dune. It is difficult to grasp the organizational structure of the turbulent underwater flow in the real river. Therefore, experiments that imitate the real phenomena in the laboratory have been prevalent. Utami and Ueno (1977) conducted a visualization experiment under bed conditions that are likely to create a buoyantly rising eddy and explained the large scale characteristics of an eddy motion in an observation with a horseshoe-shaped eddy model. Ikeda and Aseada (1983) measured suspended sediment concentration of riverbed waves in the flow of the moving bed and suggested a strong relationship between suspended sediment concentration and riverbed configuration associated with the rising eddy. Yazu (1997) argued that it is possible to conduct an observation with a laser velocimeter and the hydrogen bubble method and use spatiotemporal correlational analysis to explain the eddy of structure that are formed behind the continuous sand waves with a horseshoe-shaped eddy model from the standpoint of cross sectional characteristics and three dimensionality.

Hayashi et al. (2002) conducted numerical experiment that applied the Direct Numerical Simulation (DNS) on open-channel flow with sand bank waves and demonstrated that the detection and visualization of the tubular swirling eddy can lead to the generation of reverse horseshoe-shaped eddy, a horseshoe-shaped eddy with the top and bottom of the "horseshoe" turned upside down. However, these studies used either clear water flow or low density flow. The study that focused on the relationship between high density flow such as the one observed in the Yellow River and sand waves is scarce. One of the biggest obstacles when conducting an experimental study under the high density flow conditions involves the difficulty of the measurement. It is impossible to clarify the flow structure by means of a Pitot tube current meter used in the past or the measurement of the concentration distribution.

Regarding the resistance of hyperconcentrated sediment-laden flows, it has been reported that in an experiment conducted by using silt specimens with a median grain size (d_{50}) of 0.026 mm, resistance tended to decrease as sediment concentration increased. (Yang,C.T. and X.Kong,1991), It has also been reported, however, that in an experiment conducted by Wang (1993) by using clay, resistance increased slightly at a volume concentration of about 9%.

Paying attention to non-Newtonian fluid properties of high-concentrated sediment flows, Ohmoto T. and Cui Z. (2005), conducted an experiment in which high-concentrated sediment flow was artificially generated in pipe flow by using bed material samples taken in Jinan City, China, in a lower reach of the Yellow River and commercially available clay (kaolin) and investigated their resistance properties. Both in the Yellow River sediment case and in the kaolin case, the friction loss coefficient increased as sediment concentration increased. At the volume concentration of 10%, the friction loss coefficients of the Yellow River sediment and kaolin were greater than the friction loss coefficient of clear water flow by factors of 1.30 and 1.28, respectively, indicating a slightly greater value for the Yellow River sediment

In the present study we took advantage of the sodium polyacrylate (PSA) solution that resembles high-concentration sediment in viscosity characteristics to thoroughly consider the impact of sediment concentration on resistance characteristics of the dune-type beds and flow structures in the drug-reducing flow. Particle image velocimetry (PIV) was applied to current meters to compare clear water flow with the flow field over a fixed wavy bed that mimicked a dune-type bed. This study deals only with wash loads when considering high-concentrated sediment-laden flows and assumes that fine-grained sediment is not deposited on the channel bed, and spatial changes in concentration distribution are small. To investigate resistance characteristics, artificial flow was created with the PSA solution through fixed wavy bed in open channels that mimicked dune. We examined flow mechanism of the high-concentrated sediment laden flow over dune-type beds of open channels with the PSA solution as stimulant fluid.

EXPERIMENTAL APPARATUS AND METHODS

For the measurement of viscosity, Brookfield's DV-II +PRO digital viscometer was used. The DV-II viscometer is a coaxial cylinder type rotational viscometer that excels in low-viscosity and low-shear-rate measurement. Temperature control can be adjusted by connecting a well-insulated tube from the circulation-type temperature-controlled water tank capable of controlling water temperature at accuracy of ±0.3°C to the viscometer.

The materials used for viscosity measurement are suspensions of the Yellow River sediment, suspensions of kaolin and sodium polyacrylate (PSA) solutions used as polymer solutions. The Yellow River sediment used is bed material sampled at the Kuokou hydrometric station (278 km upstream from the river mouth) in Jinan City located in a lower reach of the Yellow River. The Yellow River sediment had a median grain size of d_{50} = 16.4 μm and a density of ρ_s = 2.68 g/cm^3, while the kaolin had a median grain size of d_{50} = 5.3 μm and a density of ρ_s = 2.7 g/cm^3.

The kaolin suspensions and PSA solutions used in the viscosity experiment were made to flow in a circulating variable-slope flume made of acrylic resin measuring 10 m in length, 0.4 m in width and 0.2 m in height. The experiment conditions are shown in Table 1. Resistance was calculated by measuring water depth of a uniform flow field with gauges point. In order to simulate a continuous dune bed, we installed 80 waves in the direction of downward flow between the space of 6.4m from the upper reach of the channel. Although each wave length and each wave-height of the dune may seem varied, on average both wave length and wave-height demonstrate strong correlations with depth. The wave length is about five times the value of the depth while wave-height ranges between 1/4 to 1/3 of the depth. In this experiment the wave length and wave height were established at λ = 8 cm and h_s = 1 cm, respectively. The dimensionless wave height h_s /H and dimensionless wave length λ/H relative to the water depth H are about 1/3 and 3, respectively. Thus, wave length is somewhat short. The dune is more or less two dimensional in planar form and has transversely uniform ridges and valleys.

Table 1. Experimental conditions

	Clear water	PSA solution (800mg/l)
Flow rate Q(l/s)	1.7	1.7
Flow depth H(cm)	2.5	3.5
Mean flow velocity U_m(cm/s)	17.0	12.1
Maximum velocity U_0(cm/s)	20.8	18.0
Gradient of channel i0	1/2000	1/2000
Froude number Fr	0.34	0.21
Reynolds number Re	4250	

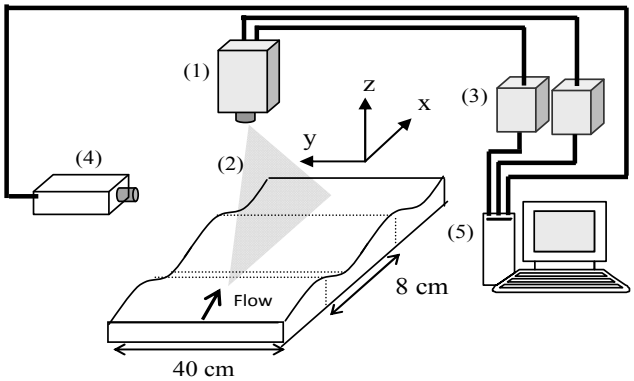

(1) Double-pulsed LASER Illumination System
(2) Laser sheet
(3) YAG - Laser Main unit
(4) CCD- Camera Kodak Megaplus ES1.0
(5) P.C.with Visi flow-software (Timing control and analyze)

Figure 1. Particle image velocimetry (PIV) measurement system

Figure 1 illustrates the measuring system used in the present study. The origin of the coordinate system was located at the midpoint of a dune ridge 2 m downstream from the upstream end of the flume. The x, y and z axes were defined as the streamwise direction, the transverse direction and the vertical

direction, respectively, and their velocity fluctuation components were defined as u, v and w. We used air-cooled double pulsed YAG laser as a light source for PIV. The sheet light was adjusted to 1mm in thickness, 10cm in width, and 1000μsec in pulse interval. We transmitted the light vertically downward from the upper channel to the bottom. We captured the two visualized images of the particle passing through the laser sheet with the CCD camera (Kodak Megaplus ES1.0 : 1008×1008 pixel) installed at the side of the channel. The particle image velocimetry (PIV) was measured between the interval of one wavelength at the point 2m from the upper reach of the channel. Sampling frequency for flow velocity was 15Hz. Statistical analysis was conducted with the 1000 samples of image data per one measurement site. The present experiment investigated the effects of changes in PSA concentration on resistance characteristics and the resistance laws of the flow at fixed concentration. Nylon particles 5 μm in diameter and having a specific gravity of 1.02 were used as tracers.

EXPERIMENTAL RESULTS - Viscous properties

Figures 2 and 3 show the shear rate dependence of shear stress and the apparent viscosity of high-concentrated sediment suspensions and PSA solutions. Shear stress and the apparent viscosity of a PSA solution is linearly related to the shear rate on log-log paper. This indicates that a PSA solution and a hyper-concentrated sediment suspension have similar viscous properties.

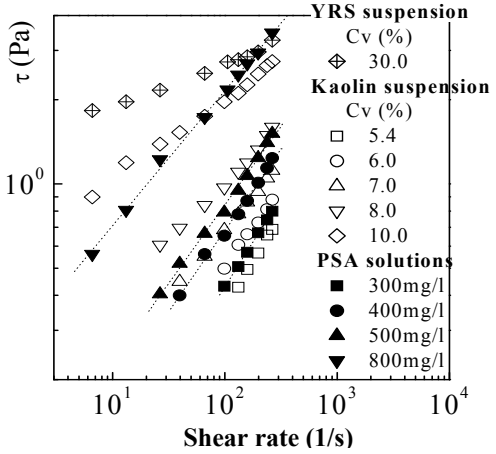

Figure 2. Relation between shear stress and shear rate

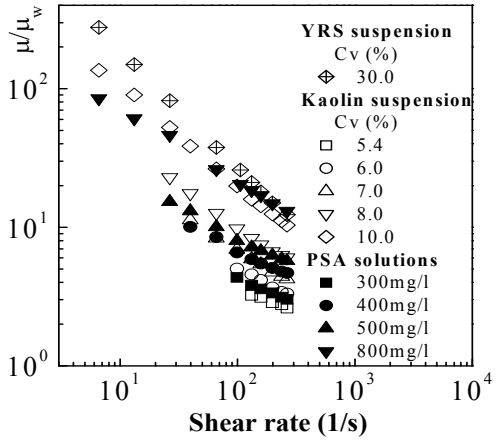

Figure 3. Relation between viscosity and shear rate

Figure 4 shows the shear rate dependence of the kinematic viscosity of kaolin suspensions and the kinematic viscosity of PSA solutions. As shown, the kinematic viscosities of the PSA solutions at concentrations of 300 mg/l, 400 mg/l, 500 mg/l and 800 mg/l are close to the kinematic viscosities of the kaolin suspensions at volumetric concentrations (C_v) of 6%, 7%, 8% and 10%, respectively. This indicates that the PSA solutions have non-Newtonian fluid properties affects the apparent viscosity.

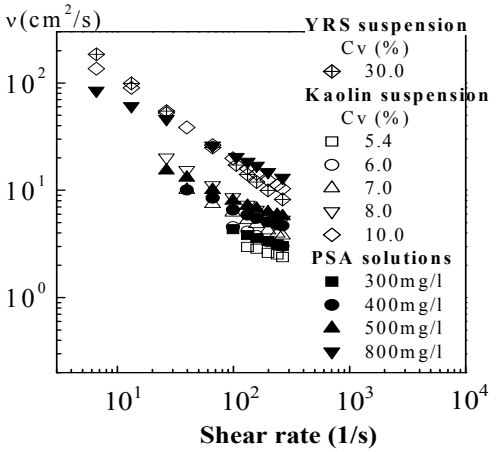

Figure 4. Relation between kinematic viscosity and shear rate

Resistance properties

Figure 5 shows the relationship between the total resistance coefficient and PSA solution concentration.

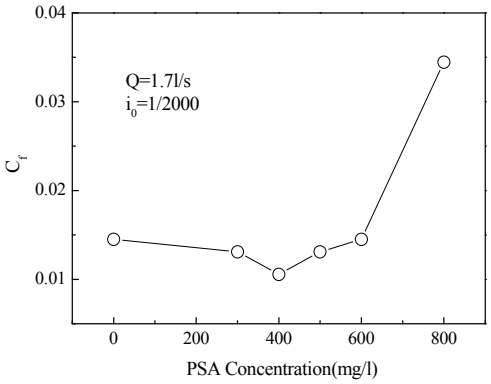

Figure 5. Relationship between the total resistance coefficient and PSA solution

The total resistance coefficient, which is defined as the ratio between the inertia force of a fluid and the total resistance calculated as the sum of friction resistance and form resistance, can be expressed as

$$C_f = 2\left(\frac{U}{U_M}\right)^2 \qquad (1)$$

where $U_* = (g\, h_m\, i_0)^{1/2}$; g, gravitational acceleration; i_0, the slope of the flume; U_m, section-averaged flow velocity. The total resistance coefficient C_f decreases to PSA400mg/l (7% sediment concentration) with the thickness in the PSA concentration, up to 27% compared to that of the clear water and tends to increase again from that point. In the PSA800mg/l solution case (10% sediment concentration) the resistance can increase about 146% of that of the clear water. This tendency for resistance to decrease with the increase in the thickness of the concentration to a certain point until it starts to increase has been observed in a smooth open channel

by Ohmoto et al. (2012). In contrast to the simplicity of the flow over the smooth open channels, this is one of the characteristics of the high density flow that exists under the complicated boundary condition.

Average flow characteristics

Figure 6 shows isolines of a stream function Ψ defined by Eq. (2).

$$\psi(x,z) = \int_0^z U(x,\zeta)d\zeta \qquad (2)$$

where U represents a time-averaged flow velocity. As demonstrated in the Figure reattachment point in the in the clear water case was at x/hs=3.5. Furthermore, circulating flow was detected near the substratum of the separation line. However, in the PSA800mg/l case the circulating zone with Ψ smaller than 0 was identified in the vicinity of the base behind the ridge. The location of the reattachment point was not clearly acknowledged due to the extremely small size of the region.

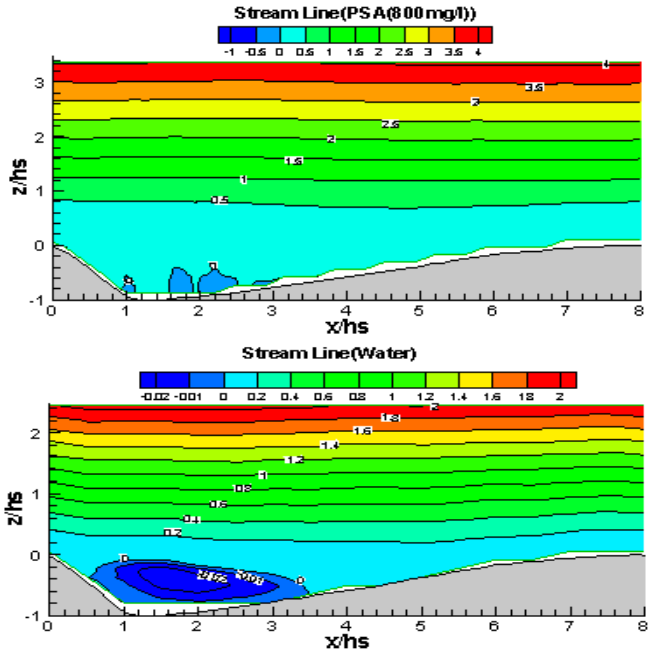

Figure 6. Isolines of a stream function

Figure 7 shows the vertical distribution of main flow velocity changes in the flow direction over a dune-type bed in the clear water case and the PSA solution case. The vertical and horizontal axes were made dimensionless by dune wave height h_s. The flow velocity scale was made dimensionless by the maximum over-ridge flow velocity U_0. The vertical axis is shown at intervals of x/hs = 0.5 in the flow direction. In the PSA 800mg/l solution case, the range in which the rate of change for main flow velocity in the vertical direction is high, has been approximated with a straight line. The vertical distribution of main flow velocity shows characteristics of a free mixing layer behind a ridge, suggesting the growth of an internal boundary layer along the bed surface further downstream and the influence of flow acceleration due to the forward pressure gradient. Compared to the clear water case, flow separation and the resultant development of circulation flows are not pronounced in the PSA solution case. It is interesting to note that in the PSA solution case, unlike in the clear water case, there are two clearly-discernible high-shear-rate areas. The solid line in the clear water case indicates the flow separation line.

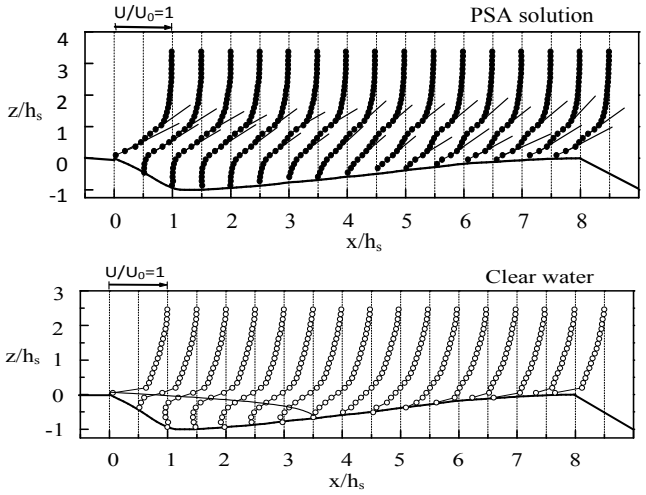

Figure 7. Vertical distribution of main flow velocity

Turbulence characteristics

Figure 8 demonstrates how downward flow and vertical flow directions influence the vertical distribution of turbulence intensity and changes in the streamwise direction.

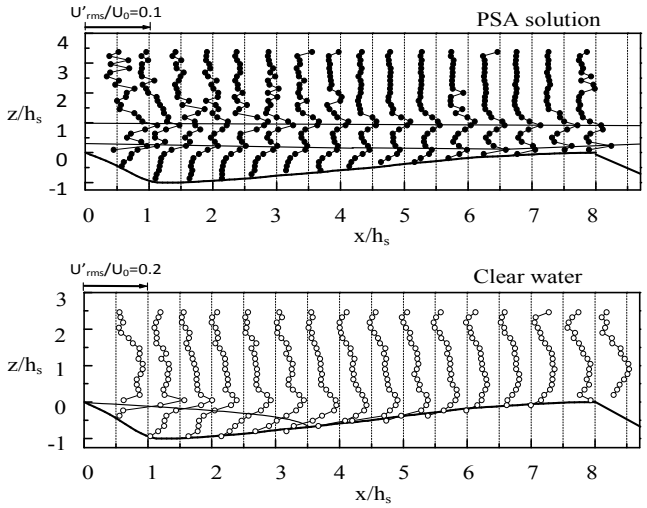

Figure 8. Vertical distribution of turbulence intensity

The solid lines in the figures were drawn to connect the maximum values of turbulence intensity at different flow distances. In the PSA solution case, the maximum values of turbulence intensity are identified at two height levels, namely, z/h_s = 1 and z/h_s = 0.2 to 0.3, both in the streamwise direction and in the vertical direction. In the clear water case, turbulence intensity tended to increase in the deceleration region from the upstream ridge to the reattachment point and decreased considerably near the bed surface in the acceleration region from z/h_s = 4 to the downstream ridge. Compared to the clear water case, in the PSA 800mg/l solution case, turbulence intensity decreased to about 50% in the streamwise direction and about 30% in the vertical direction relative to the clear water case. In the vertical distribution of turbulence intensity in the PSA solution case, the maximum values occurred at two locations under the influence of flow separation and shear deformation of the internal boundary layer

of the bed. This greatly differs from what was observed in the clear water case.

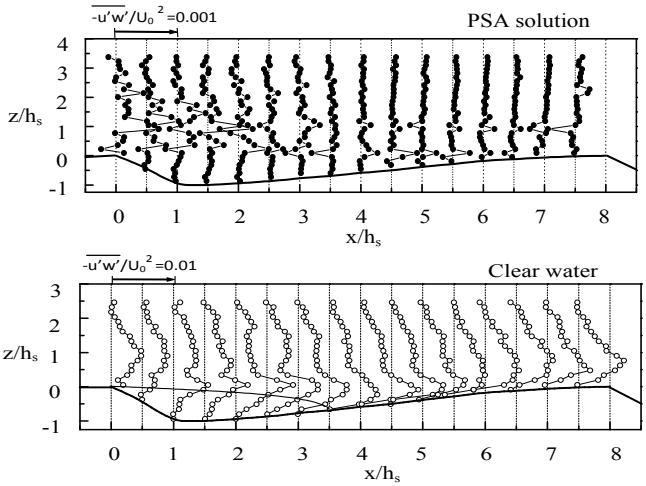

Figure 9. Vertical distribution of Reynolds stress

Figure 9 shows spatial changes in Reynolds shear stress. Overall, the maximum value for Reynolds in the PSA800mg/l case it is approximately less than 10% of that of the clear water. This corresponds to the decrease in turbulence intensity. In the clear water case, large values were shown near the point of inflection of main flow velocity and in the region downstream of the reattachment point, near the bed surface. PSA solution in both viscosity levels demonstrated close to 0 value near the reattachment point at x/hs=3.5~4.5. In the deceleration region between the ridge to the point of x/hs=3.5, the positive maximum value was attained. In the acceleration region from x/hs=5 to the downstream ridge, the negative maximum value was reported. This suggest that turbulence caused by flow separation from the crest was reduced in the flow direction, and momentum transport and energy losses due to turbulence decreased as the viscosity of the PSA solution increased. In particular, turbulence intensity and energy losses due to turbulence were very small in the PSA 800 mg/l solution case in which the resistance coefficient reached the maximum value.

Shear rate and shear stress

Figure 10 illustrates the rate of change for the vertical distribution of the main flow velocity in the vertical direction.

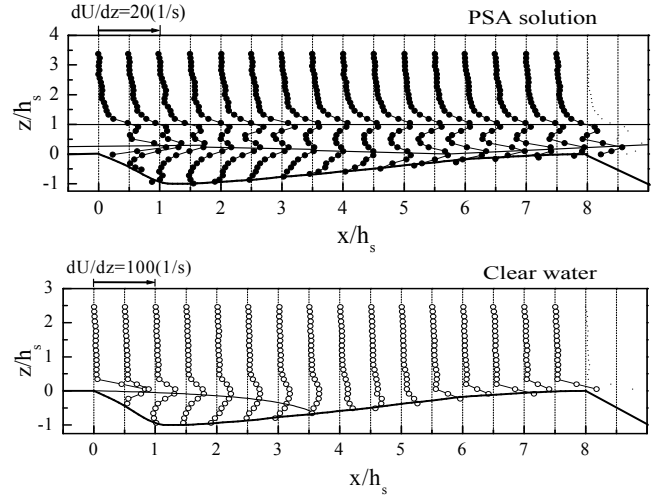

Figure 10. Vertical distribution of shear rate

The rate of change for main flow velocity in the vertical direction was in the range of: 0-20(1/s) in the PSA 800mg/l case and 0-100(1/s) in the clear water case. Compared to the clear water case, the rate of change for main flow velocity was lower in the PSA solution cases due to the effects of viscosity. In the PSA800mg/l solution case, the maximum value for turbulence intensity was identified at two points: z/ h_s=1 and z/h_s=0.2¤0.3, respectively.

Figure 11 shows the spatial distribution of viscous stress in PSA solutions (C_w=800 mg/l). Based on the power-law model, viscous stress is determined by Eqs. (3) and (4):

$$\tau_\mu = \mu\left(\frac{dU}{dy}\right) \quad (3)$$

$$\mu = \eta_0\left(\frac{du}{dz}\right)^{n-1} \quad (4)$$

The apparent viscosity coefficient is represented by μ, and the experimental values of η_0 and the exponent n were determined by least-squares approximation of the experimental data. Viscous stress demonstrated similar trends as those for spatial distribution of turbulence intensity and shear rate.

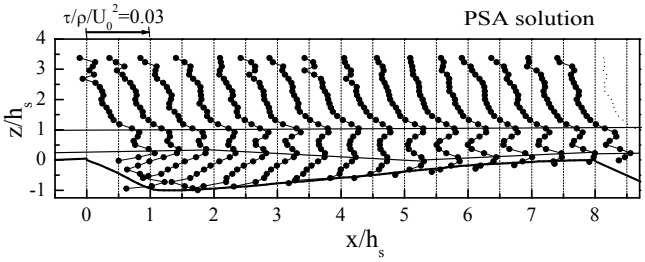

Figure 11. Vertical distribution of viscous stress

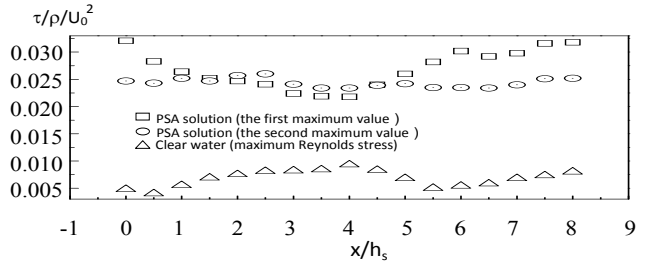

Figure 12. Streamwise distribution of maximum shear stress

Figure 12 describes the distribution of shear stress. Shear stress can be calculated from Eq.(5):

$$\tau = -\rho\overline{u'w'} + \mu\left(\frac{du}{dz}\right) \quad (5)$$

Change in vertical distribution of the shear stress in the flow direction demonstrated the intermittency similar to the one observed in spatial distribution of the turbulence intensity in the vertical direction. In the PSA 800mg/l solution case, the maximum value occurring near z/hs = 0.2 to 0.3 is referred to as the first maximum value, and the maximum value occurring near z/hs=1 is referred to as the second maximum value.

In the PSA800mg/l solution case, the first maximum value of shear stress becomes small near the reattachment point, and the second maximum value does show notable change throughout the wave

length section. In addition, the values are about 2.2 to 7 times as large in the PSA 800mg/l solution case than in the clear water case. Resistance to fluid constitutes: (1) viscosity shear stress caused by viscosity and (2) Reynolds shear stress caused by turbulence. The reasons why the total resistance coefficient decreased up to 27% compared to the clear water case in the PSA 400 mg/l case (7% sediment concentration) with the increase in the concentration of the PSA solution, a non-Newtonian fluid, might be attributed to: (1) the increase in the concentration associated with the viscosity was reduced in the flow direction by the turbulence caused by flow separation from the crest and (2) the decrease in momentum transport and energy losses due to turbulence. The total resistance coefficient tended to increase again in the solution with the concentration level higher than the PSA 400mg/l. Another reason for why the total resistance coefficient increased about 146% of the clear water case in the PSA 800mg/l (10% sediment concentration) case might be that despite the decrease in momentum transport, energy losses caused by viscosity became prominent.

CONCLUSIONS

In this study, sodium polyacrylate (PSA) solution that is similar in viscosity characteristics to high-concentrated sediment flows was used to clarify the resistance characteristics and flow mechanism of high-concentrated sediment flows over a dune type bed. Specifically, we applied the Particle Image Velocimetry measurement system to compare the high-concentrated sediment flows to the clear water flows. The results are summarized in the following six points.

1. The kinematic viscosities of PSA solutions having concentrations of 300 mg/l, 400 mg/l, 500 mg/l and 800 mg/l show non-Newtonian fluid properties similar to the kinematic viscosities of kaolin suspensions having volumetric concentrations (C_v) of 6%, 7%, 8% and 10%, respectively.
2. The total resistance coefficient Cf decreased to PSA400mg/l (7% sediment concentration) with the increase in the PSA solution concentration, up to 27% compared to that of clear water and tended to increase again from that point. In the PSA800mg/l case (10% sediment concentration) the resistance increased about 146% of that of the clear water.
3. Unlike in the clear water flow, flow separation and the circulating flow formed by flow separation were not noteworthy in the high viscosity PSA solution case, and the two regions with high levels of shear rate were identified at z/h_s=1and z/h_s=0.2 ~0.3.
4. Compared to the clear water case, in the PSA 800mg/l solution case, turbulence intensity decreased to about 50% in the streamwise direction and about 30% in the vertical direction. The location of the maximum value of turbulence intensity in the PSA solution showed close agreement with the location of the maximum value of the shear rate, but the spatial distribution differed considerably from that in the clear water. The maximum value for Reynolds stress corresponds to the decrease in the maximum value for turbulence intensity. In the PSA800mg/l case, it is approximately less than 10% of that in the clear water.
5. The spatial distribution of viscous stress in the PSA solution showed a tendency similar to the tendencies of the spatial distributions of turbulence intensity and the shear rate. In the PSA800mg/l solution case, the first maximum value of shear stress became small near the reattachment point, and the second maximum value did not show notable change throughout the wave length section. In addition, the values of shear stress were about 2.2 to 7 times as large in the PSA 800mg/l solution case as in the clear water case.
6. One of the reasons for why the total resistance coefficient increased about 146% of the clear water case in the PSA 800mg/l (10% sediment concentration) case might be attributed to the fact that: despite the decrease in momentum transport, energy losses caused by viscosity was prominent.

REFERENCES

[1.] Bradley, J. B. and McCutcheon, S.C: The effect of high sediment concentration on transport processes and flow Phenomena, proc.Conf. Erosion, Debris prevention, Japan,1985

[2.] Coussot, P.: Rheology of debris flow-Study of concentrated suspensions. Ph.D.thesis, INPG, Grenoble, France, 1992

[3.] Dodge, D.W., and Metzner, A.B.: Turbulent Flow of Non-Newtonian System, A.I.Ch.E.J., Vol. 5, No.2, 1959

[4.] Hershey, H.C., and Zakin, J.L.: Existence of Two Type of Drag-reduction in Pipe Flow of Dilute Polymer Solutions, Ind.Eng.Chem.Fundamentals, Vol.6, No.23, p.381, 1967.

[5.] Egashira S.,Ashida K., Tanonaka S. And Sato T.: Studies on Mud Flow-Stress Structure-, Annuals, Disas. Prev.Res. Inst., Kyoto Univ. No.35, B-2, pp79-88,1992.

[6.] Metzner, A.B., and M.G. Park: Turbulent Flow Characteristics of Viscoelastic Fluid, J. Fluid. Mech., Vol.20, p.291, 1964.

[7.] Oldroyd, J.G.: A Suggested Method of Detecting Wall Effects in Turbulent Flow Thorough Pipes, in Proc. First Intern.Congr.on Rheol., pp.130-134, Vol.II, North Holland, Amsterdam, 1948.

[8.] Ohmoto T., Cui Z. and Kakihara Y.: On Rheology of Hyperconcentrated Sediment-laden Flow, Journal of Applied Mechanics, JSCE, Vol.7, pp979-986, 2004.

[9.] Wang H. and X. Fei,: The fluctuation of Bingham shear stress on hyperconcentrated flow in flowing conditions, Proc. of 4th Intern. Symp. on River Sedimetation,pp.198-205,(1989).

[10.] Yang, C.T. and X.Kong.: Energy Dissipation Rate and Sediment Transport, Journal of Hydraulic Reasearch, Vol.29, no.4, pp.457-474, 1991.

[11.] Yang, C.T.: Sediment Transport in the Yellow River , Journal of Hydraulic Engineering , Vol.122, 2004, pp237-244, 1996.

[12.] Z.Y.Wang: A study on debris flow surges, Hydraulic Engineering'93, Vol.2, American Society of Civil Engneers, New York,pp. 1616-1621, 1993.

ACTA TECHNICA CORVINIENSIS – Bulletin of Engineering
Tome VI (Year 2013) – FASCICULE 4 [October–December]
ISSN 2067–3809

[1.] Adolfo SENATORE, [2.] Alessandro RUGGIERO, [3.] Mario PISATURO

MODELS FOR PRESSURE CONTROL OF AUTOMATED DRY CLUTCHES: TEMPERATURE INFLUENCE ON FRICTIONAL AND ELASTIC BEHAVIOUR

[1.] DEPARTMENT OF INDUSTRIAL ENGINEERING, UNIVERSITY OF SALERNO, I-84084 FISCIANO-SALERNO, ITALY

ABSTRACT: Automated Manual Transmissions (AMTs) systems are generally constituted by a dry or wet clutch assembly and a multi-speed gearbox, both equipped with electro-mechanical or electro-hydraulic actuators, which are driven by a control unit, the transmission control unit (TCU). In this transmission type the quality of the vehicle propulsion as perceived by the driver is largely dependent on the quality of the control strategies. This paper aims at investigating the influence of the temperature on the engagement performance of an actively closed dry clutch.
KEYWORDS: Automated manual transmissions, Dry clutch transmissibility, Frictional coefficient map, Temperature effect.

INTRODUCTION

Nowadays, the development of the Automated Manual Transmission (AMTs) has led to remarkable increment of their performance respect the manual ones. In fact, AMTs allow strong improvement in terms of safety, comfort, reliability, shifting quality, and driving performance, together with reduction of fuel consumption and pollutant emissions [1-6]. In automotive drivelines, the goal of the clutch is to smoothly connect two rotating masses, the flywheel and the transmission shaft, which rotate at different speeds, to allow the torque transfer generated by the engine to the driveline [7]. In the Figure 1, an actively closed dry clutch system suitable for pressure-controlled engagement is shown.

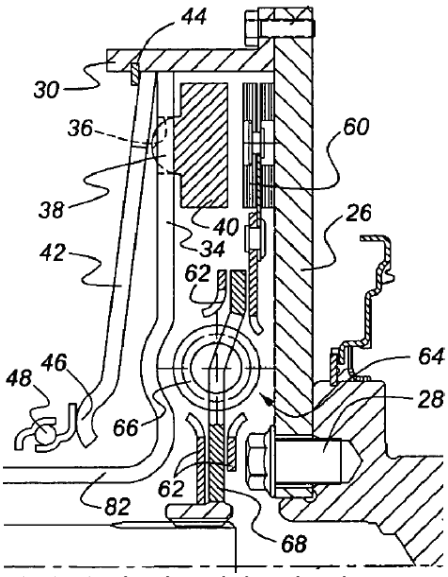

Figure 1: Actively closed dry clutch system (open position) [3]: 48, throwout bearing; 42, lever spring; 40, pressure plate; 60, clutch disc; 26, flywheel.

In AMTs the clutch engagement during gearshift is managed by an actuator which is driven by a control unit, the transmission control unit (TCU). Consequently, high importance is assumed by the control scheme implemented in the TCU. In fact, to reach high performances is fundamental implement a dependable control scheme in order to obtain reduction of fuel consumption, short gearshift time, reduction of facing wear and comfort.

In order to achieve these objectives on clutch engagement, several models of control strategies for dry clutches in AMTs have been recently proposed in the literature, e.g., classical controller [1], optimal control [8, 9], predictive control [10, 11], decoupling control [7], and robust control [12, 13]. However, effective AMTs controllers are difficult to be designed without having a physical model of the clutch-torque transmissibility characteristic [6].

A model of dry clutch torque transmissibility is given by equation (1). It explains the relationship between the torque transmitted by the clutch T_{fc} and the pressure plate clamping load F_{pp}.

$$T_{fc}(F_{to}) = n\mu_d R_m F_{pp}(F_{to}) \qquad (1)$$

In (1): n is the number of clutch disc frictional sides; μ_d is the dynamic coefficient of friction, R_m the mean radius, F_{to} the force applied by the actuator to the throwout bearing.

It is well known the importance to evaluate how both the friction coefficient and the cushion spring characteristic affect the performance of the dry clutch assembly during operation, along with their sensitivity to the clutch working temperature [11-15].

For this purpose, this paper aims at investigating the engagement performance of an actuated dry clutch by taking into account the inference of the contact

pressure and the sliding speed on the friction coefficient.

Firstly, the inference of the temperature, of the contact pressure and of the sliding speed on the friction coefficient have been analyzed in order to obtain useful information on the behavior of the clutch facing material during the working conditions. Secondly, the inference of the temperature on the cushion spring characteristic has been analyzed in order to obtain information on the pressure values which operate on the clutch facing material during the engagement phases. Thirdly, it has been analyzed the relationship between $F_{pp}(F_{to})$ at various temperature, by assigning a bilinear relationship between $x_{pp}(x_{to})$.

TEMPERATURE EFFECT

Temperature plays an important role on the engagement phase in a dry clutch system. In fact, repeated gear shifting induce a rise of the temperature due to the friction between the flywheel and a clutch facing on one side and between the push plate and the second clutch facing on the other side. This thermal effect has a strong influence on the behavior of the main components of the dry clutch assembly. Therefore, if they have not taken into account accurately, they could lead to a poor engagement. For example, after repeated clutch engagement the temperature on the clutch facing could attain very high values, around 300-350 °C and, above 350-400 °C the friction system starts to suffer permanent damage [15].

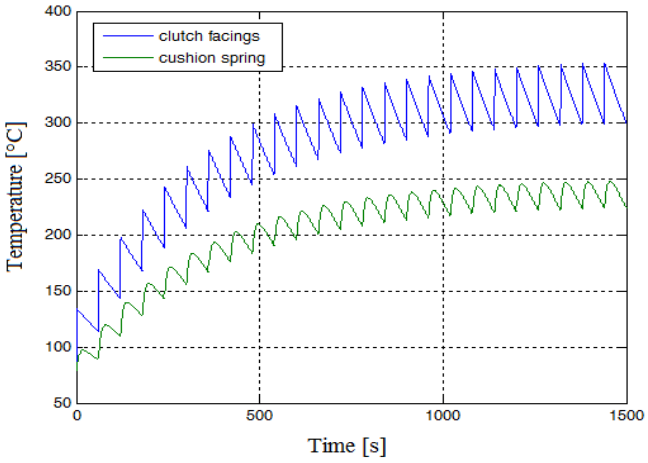

Figure 2: Clutch facings and paddles temperature after repeated starts

A simplified heat transfer model has been assumed in order to calculate the average temperature of the cushion spring. The two clutch facings on flywheel side and pressure plate side have been assumed at the same temperature levels. Say the thermal capacity of the cushion spring, the heat transfer mechanism through the facing materials is mainly given by conductive flux; the heat transfer can be modeled as the conductance times the temperature difference. A more detailed model should take into account the actual heat patterns through the rivets or other metal joints between the facings and the cushion spring. Furthermore, a convective radial heat flux toward an ambient at room temperature is modeled by way of the transfer coefficients. On the base of these hypotheses a simplified thermal dynamics of the cushion spring is provided by a 1st order differential equation [4]. The temperature of the facing material has been simulated through this differential model aiming at reproducing literature results [15, 16], by considering repeated clutch engagements with 60 seconds period (Fig. 2).

FRICTION COEFFICIENT

The friction coefficient has a strong effect on the clutch torque characteristic as shown in the equation (1). For this reason a deep analysis on its variation during the engagement phase is fundamental to improve the performance of an actuated dry clutch. In fact, effective controllers are difficult to be designed without having a dependable frictional map of the clutch-torque transmissibility characteristic [5].

The modeling of friction variation during the clutch engagement process has been studied by numerous authors. The relationship between the static and/or dynamic friction coefficient and the sliding speed has been extensively studied in [17-19]. Raghavan and Jayachandran [20] considered that the coefficient of friction varies with the sliding speed as well as with the generated contact pressure and the number of clutch engagements due to the thermal effect. The thermal effect was also approached through FE analysis for ceramic clutch in [16]. In [14], instead, tests on automotive clutch facings have been carried out in order to analyze the temperature effect. Poser et al. [21] investigated the dependence of friction coefficient of clutch conventional and innovative facings on the sliding speed. In order to ascertain the rise up of the judder phenomenon during the engagement process, Centea et al. [22] and Maucher [23] investigated the gradients of the friction coefficient with slip speed.

FRICTION COEFFICIENT VS. TEMPERATURE

In this section it has been analyzed the thermal impact on the frictional behavior of the clutch disc facings. In fact, during the engagement phase the friction between the clutch facings and the flywheel on one side and the push plate on the other side brings about a rise of the temperature, especially after repeated engagements, see Figure 2. In [14] tests on automotive clutch facings have been carried out in order to analyze the temperature effect. In these tests the friction coefficient exhibits a smooth variation within the temperature range from 25 °C to 250°C, whereas it begins to decline at 250 °C, more sharply after 340 °C [14].

This effect is due to the decomposition of the phenol resin of the clutch facings at high temperature. In fact, when the temperature is higher than 330 °C, a severe thermal decomposition produces fluids and gas emissions. This effect induces not expected phenomena transition from dry friction to lubricated friction. For this reason the friction coefficient drops [14].

FRICTION COEFFICIENT VS. SLIDING SPEED

In this section the influence of the sliding speed, at different contact pressure, on the friction coefficient has been analyzed. In [5] tests on commercial clutch facings have been carried out in order to investigate how these parameters affect the friction coefficient.

The results as function of the sliding speed and for two contact pressure levels are shown in Figure 4. It is evident that for both contact pressure level the friction coefficient tends to an asymptotic value at higher sliding speeds. The friction coefficient asymptotic value is higher for higher contact pressure. Moreover, the contact pressure has a nearly linear influence on the friction coefficient [5]. The relationship between the friction coefficient μ_d, the temperature θ_{cm} and the contact pressure p is given by the equation:

$$\mu_d\left(p,\theta_{cm}\right)=\alpha\left(p-p_0\right)+\mu_0\left(p_0,\theta_{cm}\right) \quad (2)$$

a has been identified and the corresponding value is: $a=0.333\ MPa^{-1}$, $p_0=0.50$ MPa and μ_0 (p_0,θ_{cm}) is derived [14].

Based on the experimental results in Fig. 3, the function that better fits the experimental data, for strictly positive slip speed, is given by the equation:

$$\mu(v)=\mu_s+\Delta\tanh(\gamma v) \quad (3)$$

$$\Delta=\mu_d-\mu_s \quad (4)$$

$$\mu_s\left(p,\theta_{cm}\right)=\mu_d\left(p,\theta_{cm}\right)-\Delta \quad (5)$$

where v is the local sliding speed, Δ and γ have been identified and the corresponding value are 0.09 and 2 s m^{-1}, respectively.

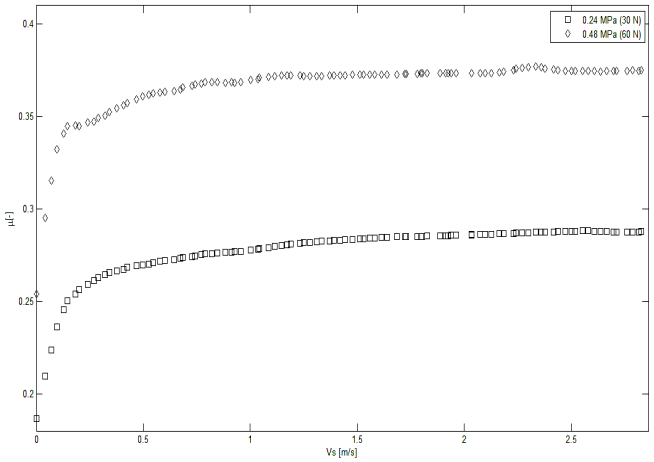

Figure 3: Friction coefficient vs. sliding speed at different contact pressures [5]

INFERENCE ON ELASTIC CHARACTERISTICS

***Cushion Spring**. The cushion spring is a thin steel disc placed between the clutch friction pads and is designed with different radial stiffness in order to ensure the desired smoothness of engagement [2]. When the cushion spring is completely compressed by the pressure plate we say that the clutch is closed, whereas when the pressure plate position is such that the cushion spring is not compressed we say that the clutch is open. We say that the clutch is in the engagement phase when is going form open to locked-up. The temperature influences the local stiffness in the cushion spring load-deflection characteristic [4]: it results in a modification of the function $F_{pp}(F_{to})$ in the equation (1). Thus, the frictional torque transmissibility curve is influenced. In order to evaluate the influence of the temperature on the cushion spring characteristic a finite element analysis has been carried out by using commercial software. The temperature yields also the axial thermal expansion of the cushion spring leading to a variation of the first contact point ("kiss point") between pressure plate and clutch disc.*

***Lever Spring**. The lever spring is the component driven by the electro-hydraulic actuated throwout bearing in order to engage/disengage the clutch (element No. 42 in the Fig. 1). The FEA model allowed exploring the temperature influence on the relationship between the throwout bearing force F_{to} and the pressure plate force F_{pp}. In Figure 4, the results of this analysis are shown.*

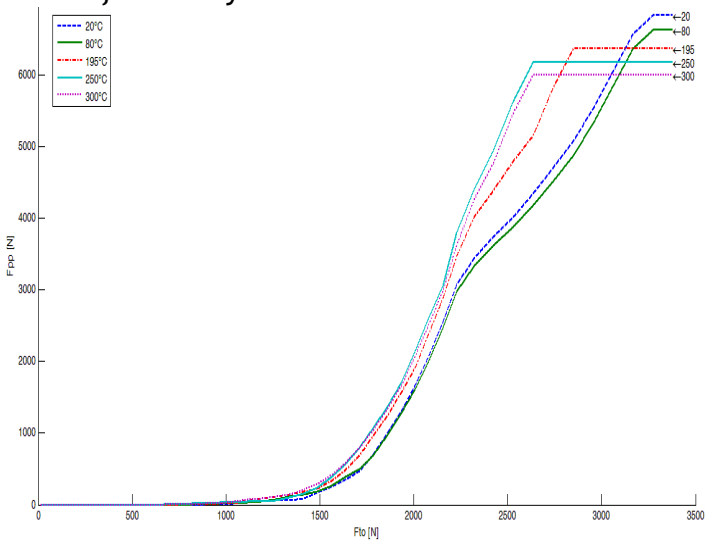

Figure 4: Pressure plate clamping load F_{pp} vs. throwout bearing force F_{to} at different temperatures

CONCLUSIONS

In this paper the multi-variable frictional map and the thermal effect on the cushion spring load-deflection curve have been analyzed in order to find out how they influence the relationship between the pressure plate clamping load and the friction torque uncertainty in a actively closed dry clutch for automated manual transmission (AMT).

After repeated engagements the temperature of the facings rises and this influences the friction coefficient behaviour. In fact, the friction coefficient exhibits a smooth variation within the temperature range from 25°C to 250°C, whereas it begins to decline at 250°C, more sharply after 340°C. This effect is due to the decomposition of the phenol resin of the clutch facings at high temperature. In fact, when the temperature is higher than 330°C and this mechanism leads to friction coefficient drop.

The sliding speed and the contact pressure also influence the friction coefficient. In particular the friction coefficient tends to an asymptotic value at higher sliding speed, and this value is higher for higher contact pressure level. This means that the contact pressure has a nearly linear influence on the friction coefficient.

The temperature affects in two ways the cushion spring load deflection curve. In fact, by increasing the temperature level, the material stiffness changes and this results in point-to-point modification of the load-deflection characteristic slope. Conversely, the thermal load induces a thermal expansion with axial size increasing. These effects result in a modification of the relationship between the pressure plate force and the throwout bearing force.

REFERENCES

[1] G. Lucente, M. Montanari, C. Rossi. Modelling of an Automated Manual Transmission System. Mechatronics, vol. 17, pp. 73-91, 2007.

[2] F. Vasca, L. Iannelli, A. Senatore, M. Taglialatela Scafati. Modeling Torque Transmissibility for Automotive Dry Clutch Engagement. American Control Conference 2008, 306-311, 2008.

[3] A. Senatore, Advances in the automotive systems: An overview of dual clutch transmissions, Recent Patents on Mech. Eng., vol. 2, no. 2, pp. 93-101, 2009; Figure 1: adapted from drawing in: D. Janson - Pat. No. US 6,997,298 B2, 2006.

[4] N. Cappetti, M. Pisaturo, A. Senatore. Modelling the Cushion Spring Characteristic to Enhance the Automated Dry-Clutch Performance: the Temperature Effect. Proc IMech Part D: J Autom. Eng., DOI: 10.1177/0954407012445967, 2012.

[5] A. Senatore, V. D'Agostino, R. Di Giuda, V. Petrone. Experimental investigation and neural network prediction of brakes and clutch material frictional behaviour considering the sliding acceleration influence. Tribology International, Vol. 44, pp. 1199-1207, 2011.

[6] F. Vasca, L. Iannelli, A. Senatore, G. Reale. Torque Transmissibility Assessment for Automotive Dry-Clutch Engagement. IEEE/ASME Transaction on Mechatronics, vol. 16, n. 3, pp. 564-573, June 2011.

[7] L. Glielmo, L. Iannelli, V. Vacca, F. Vasca. Gearshift control for automated manual transmissions. IEEE/ASME Trans. Mechatronics, vol. 11, no. 1, pp. 17-26, Feb. 2006.

[8] L. Glielmo, F. Vasca. Optimal Control of Dry Clutch Engagement. SAE 2000 World Congr, Detroit, MI, SAE Technical Paper 2000-01-0837, 2000.

[9] P. Dolcini, C. Canudas de Wit, H. Bechart. Lurch Avoidance Strategy and its Implementation in AMT Vehicles. Mechatronics, vol. 18, pp. 289-300, 2008.

[10] A. Bemporad, F. Borrelli, L. Glielmo, F. Vasca. Hybrid Control of Dry Clutch Engagement. Presented at the Eur. Control Conf., Porto, Portugal, 2001.

[11] R. Amari, M. Alamir, P. Tona. Unified MPC Strategy for Idle Speed Control, Vehicle Start-up and Gearing Applied to an Automated Manual Transmission. Presented at the 17th IFAC World Congr., Seoul, South Korea, 2008.

[12] L. Glielmo, P. O. Gutman, L. Iannelli, F. Vasca. Robust Smooth Engagement of an Automotive Dry Clutch. in Proc. 4th IFAC Symp. Mechatronics Syst., Heidelberg, Germany, pp. 632-637, 2006.

[13] G. J. L. Naus, M. Beenakkers, R. Huisman, M. J. G. van de Molengraft, M. Steinbuch. Robust Control to Suppress Clutch Judder. Presented at the 8th Int. Symp. Adv. Veh. Control, Kobe, Japan, 2008.

[14] Huang Feng, Mo Yimin, Lv Juncheng, Study on Heat Fading of Phenolic Resin Friction Material for Micro-automobile Clutch. 2010 International Conference on Measuring Technology and Mechatronics Automation, pp. 596-599, 2010.

[15] K.-L.Kimming, I. Agner. Double Clutch - Wet or Dry, this is the question, LuK Symposium, 2006.

[16] B. Czel, K. Varadi, A. Albers, M. Mitariu. Fe thermal analysis of a ceramic clutch. Tribol. Int., 42:714-23, 2009.

[17] B. Armstrong-Helouvry. Stick slip and control in low speed motion. IEEE Trans. Autom. Control; 38:1483-96, 1993.

[18] JC. Heap. Application of variable coefficient of friction and wear to block brakes and clutches. J Mech Eng Sci; 8:406-18, 1996.

[19] S. Herscovici. Determining the static and dynamic coefficient of friction and its causes for variation. SAE Paper 690570; 1969.

[20] MR. Raghavan, R. Jayachandran. Analysis of the performance characteristics of a two-inertia power transmission system with a plate clutch. J Mech Mach Theory; 24:499-503, 1989.

[21] K. Poser, KH. Zum Gahr, J. Schneider. Development of Al2O3 based ceramics for dry friction systems. Wear, 259:529-38, 2005.

[22] D. Centea, H. Rahnejat, MT. Menday. The influence of the interface coefficient of friction upon the propensity to judder in automotive clutches. Proc IMechE Part D: J Autom Eng, 245:58, 1999.

[23] P. Maucher. Clutch chatter. In: Proceedings of the 4th international symposium on torsional vibrations in the drive train, Baden-Baden, 1990.

[24] HS Qi, AJ Day. Investigation of disc/pad interface temperatures in friction braking. Wear; 262:505-13, 2007.

[25] A. Khamlichi, M. Bezzazi, A. Jabbouri, P. Reis, JP. Davim. Optimizing friction behaviour of clutch facings using pin-on-disk test, Int J Phys Sci;3:65-70, 2008.

[26] H. So. Characteristics of wear results tested by pin-on-disc at moderate to high speeds. Tribol Int 29:415-23, 1996.

[27] A. Gaard, N. Hallback, P. Krakhmale, J. Bergstrom. Temperature effects on adhesive wear in dry sliding contacts. Wear, 268:968-75, 2010.

[28] F. Garofalo, L. Glielmo, L. Iannelli, F. Vasca, Smooth Engagement for Automotive Dry Clutch. Proc. 40th IEEE Conference on Decision and Control, Orlando, Florida, 529-34, 2001.

ACTA TECHNICA CORVINIENSIS - BULLETIN of ENGINEERING

ISSN: 2067-3809 [CD-Rom, online]

ACTA TECHNICA CORVINIENSIS – Bulletin of Engineering
Tome VI (Year 2013) – FASCICULE 4 [October–December]
ISSN 2067–3809

[1.] Tomasz FIGLUS, [2.] Andrzej WILK, [3.] Štefan LIŠČÁK, [4.] Mateusz KALAFARSKI

THE INFLUENCE OF MUFFLER TYPE OF THE EXHAUST SYSTEM IN THE SPORTS MOTORCYCLE ON THE LEVEL OF THE EMITTED NOISE

[1,2,4.] DEPARTMENT OF AUTOMOTIVE VEHICLE CONSTRUCTION, FACULTY OF TRANSPORT, THE SILESIAN UNIVERSITY OF TECHNOLOGY, 8 KRASINSKIEGO STREET, KATOWICE, POLAND
[3] UNIVERSITY OF ŽILINA, FACULTY OF OPERATION AND ECONOMICS OF TRANSPORT AND COMMUNICATIONS, DEPARTMENT OF ROAD AND URBAN TRANSPORT, 1 UNIVERZITNÁ STREET, ŽILINA, SLOVAKIA

ABSTRACT: The traffic noise is one of the most important factors influencing the reduction of comfort life and also it can cause the increase the possibility to loss health by people. The sports motorcycle are the types of vehicles which exploitation is connected with generating noise of a higher level. In the work, the tests of influence of using different solutions of the muffler type of the exhaust system construction on the level of noise emission by the sports motorcycle are presented.
KEYWORDS: Traffic noise, sports motorcycle, exhaust system

INTRODUCTION

The traffic noise has a significant effect on reducing the life comfort in the habitats [1]. The communication development [2], the number of vehicles increase on 1000 of inhabitants and the density in the communication infrastructure cause that the traffic noise increases [3-9]. This phenomenon has a great importance in this parts of the world which develop quickly and experience system and political changes. One of the development aspects of the communication market is the increase of the sale of single-track vehicle especially motorcycles.

The motorcycles belong to a group of vehicles which characterizes with significant indicator power on unit displacement volume of engine. It causes that their producers have to face important requirements in the construction of exhaust system but the noise decrease generated by the motorcycles is a more difficult task than in case of cars [10-11]. The crucial cause is the smaller size of the vehicle. The norm compliance of the noise level emission can require reduction of the engine power and the loss of some individual acoustic features required by their users [11-16].

One of the categories of the motorcycles on the public ways are the sports motorcycles equipped in engines with the power over 100kM and max. rotational speed more over 10000 rpm. The motorcycles use by young people are often individually modified which may cause the level increase of generated noise.

In the work, the test results are presented, their aim was to estimate the emitted noise influence by sports motorcycle equipped in 4 different exhaust systems. There were conducted tests of the noise according to the norm, additionally in the place of the motorcyclists head and in the position of the pedestrian near the road.

THE OBJECT AND METHODS OF TESTS

For conducting the tests, used sports motorcycle was applied, which was equipped in four-cylinder engine with cylinders in the V configuration set laterally, with engine displacement 781 cm^3, which power is 110KM reached by the rotating speed 10500 rpm and the torque 82 Nm reached when the speed is 8500 rpm. The exhaust system of the engine is manufactured equipped in catalyst and the repressive muffler.

In figure 1 there is engine view used in the tests.

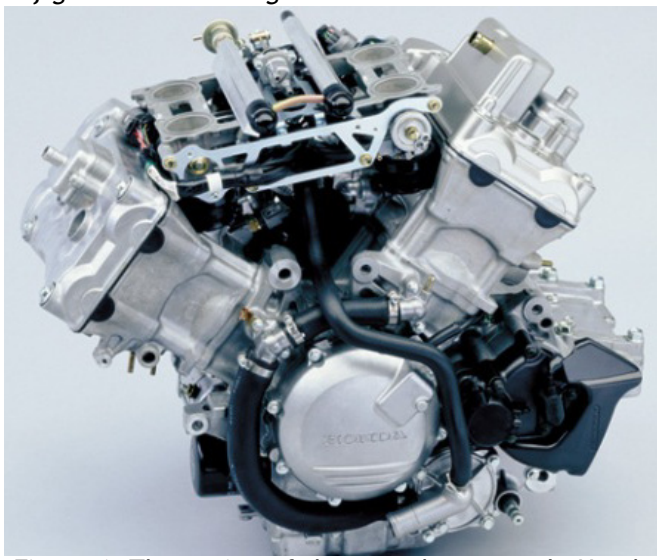

Figure 1. The engine of the tested motorcycle Honda VFR 800 - left side [17]

For the tests, 4 different solutions of the exhaust sytem are used they represent different technical solutions which can be bought on the market of the motor parts as original and accessory models:

- *solution 1 (marked R1) - mass exhaust system possessing homologation, which fulfills Polish noise norm for the motorcycles at stopping-place, equipped in muffler of the repressive type,*
- *solution 2 (marked R2) - accessory exhaust system inside which there is a perforated tube and the suppressive cotton wool, the muffler does not have road homologation,*
- *solution 3 (marked R3) - similar to muffler 2 but in a short variation the muffler does not have road homologation,*
- *solution 4 (marked R4) - accessory exhaust system, this solution is used in extreme sports and instead of classic muffler of the exhaust system a short exhaust system was used which directs the exhaust gases from the engine, the system does not have road homologation.*

The noise measure was carried out with digital sound analyser I class Sonopan DSA-50, according to corrective filter A and the time constant F. The analyser view is presented in figure 2.

The measures were carried out in the open air without any acoustic obstacles nearby. In the initial tests the measures of the acoustic background pressure level were carried out. The recorded values of the level equaled about 55 dB(A) so they did not have a significant influence on the level of values recorded in the fundamental measures.

According to the Polish Norm PN-92S-04051 the general measure conditions were maintained in the atmospheric conditions. During the measures the protection against the wind for the microphone was used owing to the fact that the recorded wind speed was between 3 and 5 m/s.

Figure 2. Sonopan DSA-50

In the tests it was assumed that the measures would be carried out according to the following schedule:

Trial 1. *The measure of the equivalent sound level in the distance of 0,5m from the end of the exhaust train:*

- *at the constant rotating engine speed amounting 5250 rpm (according to the PN-92S-04051),*
- *at the moment of acceleration by the engine in the scope of rotating speed from 1500 to 12500 rpm.*

Trial 2. *The measure of the equivalent sound level in the place of position the motorcyclist's head, at the rotating speed like in trial 1.*

Trial 3. *The measure of the equivalent sound level of the motorcycle moving at the constant speed in relation to the microphone which was set at the height of 167cm and in the distance from the moving motorcycle about 200cm. The trial was conducted at the speed 50, 70 and 90 km/h, respectively II and IV gear.*

The tests conducted in trials number 1 were to compare the level of the sound emitted with the values given in the Norm and the estimation of change of the level at accelerating the speed by the engine, the measures in the 2nd trial were to estimate the influence of the sound level on the motorcyclist and the measures in 3rd trial were to check the influence of the moving motorcycle on the noise received by the pedestrian near the road.

The measure position used in the 1st and 2nd trial are presented in the figure 3.

a)

b)

Figure 3. The measure position during 1st trial (a) and 2nd trial (b)

THE TESTS RESULTS AND THEIR ANALYSIS

In figure 4 there are the results of the measures of the equivalent sound level at 1st trial. The recorded values of the sound level prove that only solution 1 and 2 of the exhaust system fulfill the requirements of PN-92S-04051. The other two solutions do not fulfill the requirements of the acceptable level 96 dB(A) given in the Norm. The values of sound level L_{Aeq} present during accelerating the speed by the engine exceed 100 dB which at a longer time of being present near such a motorcycle can be harmful for our health. The tests results confirm that there are significant differences in the sound level recorded during the measure compatible with the Norm (at the constant rotating speed) and measuring the engine

working in the full scope of rotating speed. From the measures it is seen that the difference of these values can amount even 16 dB(A) and even for the solution of the exhaust system having homologation it exceeds the acceptable values.

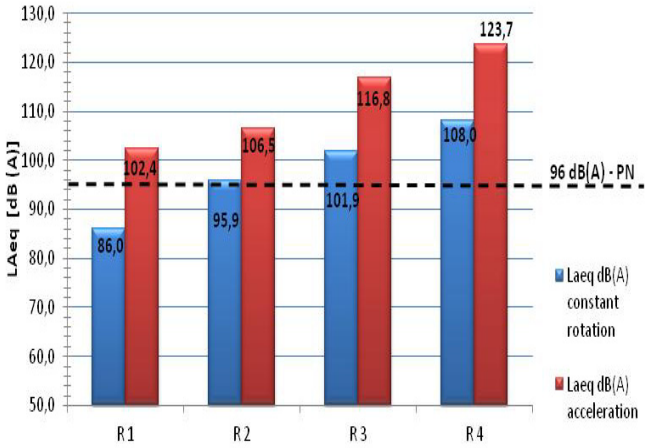

Figure 4. Values of the sound level - trial 1

The carried out measures of the sound level at the position of the motorcyclist's head (trial 2) showed similar dependences but the sound level was lower (figure 5). It can be noticed that the level at the constant rotating speed of the engine exceeds the values 80 dB(A) and at accelerating the speed - the level 98 dB(A). The measure results show that despite isolating the motorcyclist from the surrounding with the helmet the recorded values of the sound level can be still too high and harmful for their health.

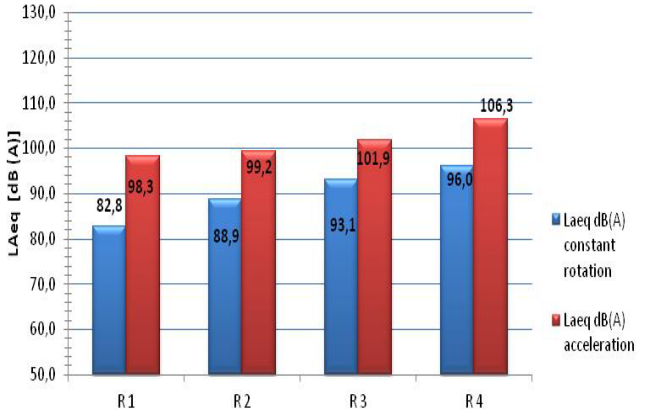

Figure 5. Values of the sound level - trial 2

The tests of influencing the emitted noise by the passing motorcycle on the pedestrian standing near the road were carried in case of solution of the exhaust system 1 and 4. The results at the speed of 50, 70 and 90 km/h with II and IV gear of the motorcycle are present in figures 6 and 7.

As it is seen from the measures even the exhaust system having the homologation causes noise reaching to the pedestrian with the equivalent level above 69 dB(A). The values can be onerous for the people present in the closest neighbourhood of the road and may cause general irritation and deterioration of mood. In case of using professional exhaust system (4) the recorded values of the sound level are higher for above 14 dB(A) and may cause deterioration of mood and health of the pedestrians. In the cases the received values of the sound level exceed also the established values acceptable in the build-up area.

The measures were conducted at different gears (II and IV) so at different rotating speed of engine they show the beneficial influence of using the same speed of the gear with lower transmission so at lower rotating speed of engine. The difference of level of emitted sound by moving motorcycle at II and IV gear at the same speed was about 4 dB(A).

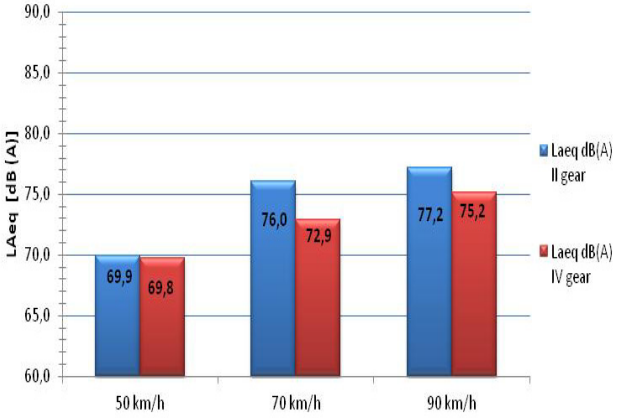

Figure 6. Values of sound level - 3rd trial - exhaust system solution 1

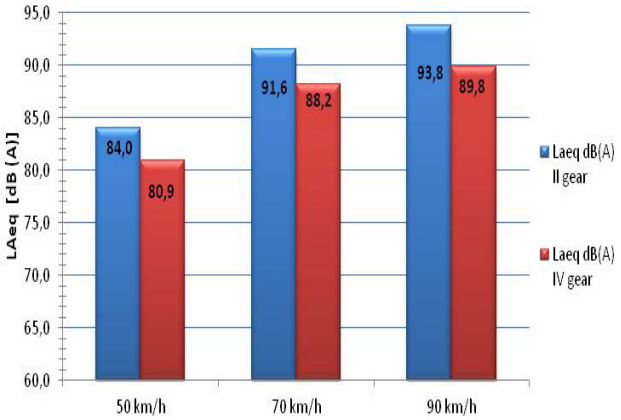

Figure 7. Values of sound level - 3rd trial - exhaust system solution 4

CONCLUSIONS

In the work, the measure of level of emitted noise by sports motorcycle equipped in different technical solutions of exhaust system were carried out. The results showed that noise generated by the engine of motorcycle is significant problem of road traffic. The possible solutions of the exhaust system only in two cases fulfilled the requirements of Polish Norm dealing with acceptable noise level generated by motorcycle. The conducted measures of all exhaust system according to experiments more similar to the real use of motorcycles allow to draw a conclusion that the generated sound level is high and can influence the health both of the motorcyclist and of the people who are close to them.

REFERENCES

[1] *Sadowski J.1982. Podstawy akustyki urbanistycznej, Wydawnictwo Arkady, Warszawa.*

[2] *Bartłomiejczyk M., Połom M. Eksploatacja i rozwój infrastruktury oraz taboru*

przedsiębiorstwa komunikacji trolejbusowej w Gdyni. Technika Transportu Szynowego, nr 7-8/2010, s. 18-21, ISSN 1232-3829.

[3] Engela Z. W., Sadowskiego J. 2005. Ochrona środowiska przed hałasem w Polsce w świetle przepisów europejskich. Centralny Instytut Ochrony Pracy - Państwowy Instytut Badawczy, Warszawa.

[4] Makarewicz R., Kokowski P. Prediction of noise changes due to traffic speed control, Journal of the Acoustical Society of America 122 (4), pp. 2074-2081.

[5] Ross B.M., Wolde T. Noise from traffic as a worldwide policy problem, Noise Control Engineering Journal 49 (4) , pp. 159-161.

[6] Salomons E.M., Berghauser Pont, M. Urban traffic noise and the relation to urban density, form, and traffic elasticity, Landscape and Urban Planning 108 (1) , pp. 2-16.

[7] Paslawski J. 2008. Highway noise management using advisory system, International Journal of Environment and Pollution, Volume 35, Issue 2-4, Pages 275-295.

[8] Figlus T., Wilk A., Liščák Š., Gozdek Ł. 2012. The influence of acoustic baffles of noise barriers on the noise level of traffic. Doprava a spoje -elektronický časopis Fakulty prevádzky a ekonomiky dopravy a spojov Žilinskej univerzity v Žiline, Number of pages 8 (473-480).

[9] Figlus T., Wilk A., Liščák Š., Gozdek Ł. 2012. The influence of acoustic baffles of noise barriers on the noise level of traffic. Doprava a spoje -elektronický časopis Fakulty prevádzky a ekonomiky dopravy a spojov Žilinskej univerzity v Žiline, Number of pages 8 (465-472).

[10] Burdzik R., Konieczny Ł. 2011. Research into noise emissions by a car combustion engine exhaust system, Zeszyty Naukowe Akademii Marynarki Wojennej rok LII NR 1 (184).

[11] Lu M.-H., Jen M.U. Source identification and reduction of engine noise, Noise Control Engineering Journal 58 (3) , pp. 251-258

[12] Hu G., P. Xia, W. Lu. 2011. The Testing and Improving of Acoustic Performance on Muffler. Advanced Materials Research. Vol. 291-294.

[13] Hu G. Y., P. Q. Xia, X. X. Wang, W. F. Lu. 2012. The Vibration Analyses of Motorcycle Exhaust System and Suspension-Point Improvement. Applied Mechanics and Materials. Vol. 105-107.

[14] Liang S. -M. C. -J Wang. 2011. Experimental and Numerical Study on a Straight Exhaust Pipe. Journal of Mechanics 27 (4): 597-605.

[15] Rodrigues F., Nassi C. D., Kahn S. 2012. Simulations of Different Configuration of Modal Split: Impacts on Traffic Noise in Urban Centers.

[16] Vogiatzis K., Paviotti M. 2012. Noise and Annoyance from Motorbikes, Scooters and Mopeds in Urban Areas.

[17] http://www.bikescatalog.com/wp-content/uploads/2013/02/engine.jpg 20.02.2013.

ISSN: 2067-3809 [CD-Rom, online]

ACTA TECHNICA CORVINIENSIS – Bulletin of Engineering
Tome VI (Year 2013) – FASCICULE 4 [October–December]
ISSN 2067–3809

[1.] Alma-Gabriela VARGA

THE NEW DIRECTIVE 2012/27/EU AND AMENDMENTS IMPOSED BY IT ON ENERGY EFFICIENCY

[1.] DEPARTMENT OF CIVIL BUILDINGS & MANAGEMENT, FACULTY OF CIVIL ENGINEERING,
TECHNICAL UNIVERSITY OF CLUJ-NAPOCA, ROMANIA

ABSTRACT: In accordance with the EU Energy Policy, developed in 2007, energy is an essential element for the development of the Union, but equally is a challenge regarding the impact of the energy sector on climate change, increasing dependence on energy imports and increasing the energy price. The paper focuses on the latest European Directive of the European Parliament and of the Council from October 25, 2012 on energy efficiency. The Directive establishes a common framework for promoting energy efficiency measures in the Member States of the Union, in order to achieve, by 2020, the main objective of 20% energy efficiency and to open up the way for further energy efficiency increase. In the paper is written a synthesis of the European Directives issued by the European Parliament on energy efficiency, specifying some of the energy-saving targets set by them.
KEYWORDS: energy efficiency; energy consumption; energy audit; building renovation; European Directive

INTRODUCTION

The context of current orientation on European and global energy saving in buildings requires the development and implementation of energy efficient and comfortable buildings. For this purpose it is important to consider the whole lifetime of a building, when assessing "sustainability", who aims to create living conditions that are ecologically compatible, economically supported and have the user's needs as a priority.

At REGIONS20 Conference/Vienna, President of the European Commission Jose Manuel Barroso said in his speech entitled: "Sustainable energy: The European Union and the global agenda" the following phrases: "A global consensus is essential among governments on all levels, but also, and above all, among peoples. I firmly believe that it is possible to achieve sustainability without shutting people out of development. Energy plays an essential role in this and must be the heart of all our policies in the years to come."[1]

Given the large share of total energy consumption of buildings and especially the large share in heat consumption, it was considered necessary that the related legislation to be supplemented by a series of laws that concern directly the construction sector. The first normative acts took into account the regulations regarding the design and execution of new construction, in order not to increase building fund with poor thermophysical characteristics. Subsequently, in accordance with EU requirements of aligment with the standards in the field, there has been developed a package of legislations to support the work of thermal rehabilitaton of the buildings.

The main documents aiming energy consumption in buildings can be classified into framework regulations that establish the course of action and specific regulations that allow achieving the objectives.[2]

In accordance with the EU Energy Policy, developed in 2007, energy is an essential element for the development of the Union, but equally is a challenge regarding the impact of the energy sector on climate change, increasing dependence on energy imports and increasing the energy price. To overcome these challenges, the European Commission (EC) considers absolutely necessary for the EU to promote a common energy policy based on energy security, sustainable development and competitiveness.[3]

The European Commission proposes in the set of documents that are the new EU Energy Policy the following objectives:

- ☐ reducing emissions of greenhouse gases by 20% until 2020 compared to 1990;
- ☐ increasing the share of renewables in the total energy mix from less than 7% in 2006, to 20% of total EU energy consumption by 2020;
- ☐ reduction of global primary energy consumption by 20% until 2020.[3]

Romania is considered to be a country in transition to a market economy, so after the Kyoto Conference, from December 11, 1997 and the Protocol signed at this conference the quantitative limitation percentage reduction in the period between 2008÷2012 (percentage compared to 1990) is 92%.

The accession of Romania to the European Union on January 1, 2007 determined the adoption of solutions for solving a long list of problems in various areas of social life, political, economic etc.[4]

STATE OF ART REGARDING EUROPEAN DIRECTIVES ON ENERGY EFFICIENCY

The first energy efficiency requirements for buildings were related to inadequate insulation which could lead to health problems due to moisture and it's infiltration into structural elements of buildings.[5]

Specific requirements for thermal characteristics of building's elements occur in the period between the two World Wars, when some countries have regulated the introduction of a simple insulation as an air layer in the walls or slabs of wooden beams arranged in double layer.[5]

Although most energy efficiency requirements in building codes have followed the tradition to be national, in the last decade there has been a trend in cooperation between countries to develop international energy efficiency requirements or standards. Examples are based on US standards for energy efficiency (IECC 2004 and ASHRAE 2004) that is used in the USA and Canada and the EU Energy Performance in Buildings Directive (EPBD), which requires Member States to establish requirements for energy efficiency in new buildings, starting from January 2006.

To complete the EPBD, the European Union aims to establish a model building code for the European region and to develop CEN standards for calculating energy performance. These CEN standards are about to be modified and adopted as ISO standards. Most countries have started with a common standard for energy efficiency, but along the way they developed separate standards for small and simple residential buildings and large buildings, complex or non-residential.[5]

Energy Performance Buildings Directives (EPBD)

Buildings account for 40% of total energy consumption in the Union. Therefore, the reduction of energy consumption and the use of energy from renewable sources in the buildings sector constitute important measures needed to reduce the Union's energy dependency and greenhouse gas emissions. The EU has taken several actions to honour both its long term commitment to maintain the global temperature rise below 2°C, and its commitment to reduce, by 2020, overall greenhouse gas emissions by at least 20% below 1990 levels, and by 30% in the event of an international agreement being reached. One of the most important is the Energy Performance Buildings Directive (EPBD), which was developed and will be implemented with the following milestones:

- ☐ *Dec 2002: EU adopts Energy Performance Buildings Directive EPBD 2002;*
- ☐ *Jan 2006: Deadline for transposing directive into national law;*
- ☐ *Nov 2008: Commission proposes revision of EPBD (EurActiv 14/11/08);*
- ☐ *Apr 2009: Parliament adopts first-reading position (EurActiv 24/04/09);*
- ☐ *Nov 2009: EU reaches political agreement on directive (EurActiv 18/11/09);*
- ☐ *May 2010: Parliament approves the EPBD Directive 2010/31/EU on the energy performance of buildings;*
- ☐ *October 2012: EU adopts a new EPBD Directive 2012/27/EU;*
- ☐ *End 2018: Public buildings to have to be nearly zero energy standards;*
- ☐ *End 2020: All new buildings to be nearly zero energy.[6]*

The Energy Performance of Buildings Directive adopted in 2002 (2002/91/CE) includes a methodology for calculating the energy performance of buildings, minimum standards for the energy performance of new buildings and those undergoing renovation, building energy certification systems and requirements for regular inspection of boilers and air conditioning system.[7]

In early 2006, the European Commission adopted the Directive of Final Energy Consumption and Energetic Services 2006/32/CE. The Directive incorporates an objective for energy saving for the member states of 1% per year and a requirement for member states to draw up a plan for how they will achieve this goal.[8, 9]

Directive 2006/32/EC on energy efficiency to end users, which is mandatory for Romania since 2008, provides that EU Member States commit to reducing final energy consumption by at least 9% in a period of 9 (nine) years between 2008-2016 compared to the average consumption of the last five years for which data is available (2001-2005). In this regard, there has been adopted the following energy efficiency measures:

a) *using financial instruments for energy savings, including energy performance contracts that stipulate the delivery of measurable energy savings;*
b) *purchasing equipment and technology specifications taking into account the priority on energy efficiency;*
c) *acceleration of rigorous energy audits execution at industrial consumers, public and residential buildings, certified audits, followed by measures to reduce energy consumption.[3, 8]*

Later in 2006, the EU adopted the Energy Efficiency Action Plan (2007-2012)-COM(2006)545. A mid-term review of the Action Plan was held in 2009. The Commission presented an Action Plan for Energy Efficiency in 2011. The action plan includes improvements in the application of energy efficiency standards, of labeling requirements and expands the scope of the Directive on energy performance of buildings. It also calls for the banking sector to offer funding to help increase energy efficiency, invites the European public investment institutions to facilitate public-private partnerships and sets a target for the European Commission to remove national legal obstacles of the common economies. Finally, the Action Plan includes a number of measures to strengthen education and awareness regarding energy efficiency. [9]

In its current from, Directive 2009/28/EC on renewable energy is designed to ensure the achievement of the targets on energy from renewable sources by 2020. The Directive provides the adoption in 2018 of a roadmap for the period after 2020. [10, 11]

Directive 2010/31/UE is concerned with promoting energy efficiency in buildings across Europe using cost effective measures, while at the same time harmonising standards across Europe to those of the more ambitious Member States.
The directive centres around four key strands:

- ☐ *Providing a methodology framework for calculating the energy performance of buildings, taking into account local climatic conditions.*
- ☐ *Applying energy performance requirements to both new buildings and existing building stock.*
- ☐ *Providing a certification scheme for all buildings.*
- ☐ *Regular assessments of any heating and cooling equipment installed.[12, 13]*

All new buildings must comply with high energy performance standards as well as generating a significant proportion of their own energy through renewables after 2020. The intention is that the public sector will lead the way through using buildings with "nearly zero" energy standards two years earlier, from January 2018. However the definition of "nearly zero" was left vague, and this will allow member states to define their own standards.
Buildings with a useful floor area > 500 m^2 that are occupied by public authorities and frequently visited by the public will be required to display the energy performance certificate in a proeminent place, where one has been issued.
Directive 2010/30/EU is a recast of the original Energy Labelling Directive (92/75/EEC-applicable to household appliances). The Directive 2010/30/UE aims to improve the overall environmental performance of products and to help consumers buy more eco-friendly products, through its application to "energy related products", including construction products, that have a significant direct or indirect impact on the consumption of energy.[12, 13]
Many EU Member States have failed to implement the EPBD in time, therefore the European Commission proposed a recast of the Directive in 2008. The restatement was approved by the European Parliament in May 2010 (2010/31/EU). This Directive reduces EU total energy consumption by 5-6% and creates from 280000 to 450000 new jobs through cost-effective measures by 2020. The governmental buildings of the member countries are obliged to consume "nearly zero" energy by the end of 2018 and the same is required for new buildings from the private sector after 2020. Energy performance certificates will also become mandatory for all rental and sale properties. The proposed standards not beeing mandatory to increase the energy performance of existing buildings have determined the Member States to develop national plans and programs to encourage owners to improve the energy efficiency of existing buildings.[9, 14]

EU Proposals on Reducing Consumption through Energy Efficiency

The European Union tried to explain to the citizen the EU proposals for cutting energy consumption through greater efficiency, through answering some frequently asked questions:

1. What's the issue?

- ☐ *Current estimates show the EU is not on track to achieve its target of reducing its estimated energy consumption for 2020 by 20%.*
- ☐ *As a result, new measures on energy efficiency are now being proposed for implementation throughout the economy to bring the EU back on track to achieve its objective by 2020.*

2. What exactly would change?

- ☐ ***Public bodies** would need to buy energy-efficient buildings, products and services, and refurbish 3% of their buildings each year to drastically reduce their energy consumption.*
- ☐ ***Energy utilities** would have to encourage end users to cut their energy consumption through efficiency improvements such as the replacement of old boilers or insulation of their homes.*
- ☐ ***Industry** would be expected to become more aware of energy-saving possibilities, with large companies required to undertake energy audits every 3 years.*
- ☐ ***Consumers** would be better able to manage their energy consumption thanks to better information provided on their meters and bills.*
- ☐ ***Energy transformation** would be monitored for efficiency, with the EU proposing measures to improve performance if necessary, and promoting cogeneration of heat and electricity.*
- ☐ ***National energy regulatory authorities** would have to take energy efficiency into account when deciding how and at what costs energy is distributed to end users.*
- ☐ ***Certification schemes** would be introduced for providers of energy services to ensure a high level of technical competence.*

3. Who would benefit and how?

- ☐ ***Consumers** would benefit from having better information available to control their energy consumption and influence their energy bills.*
- ☐ ***The environment** would benefit from reduced greenhouse gas emissions.*
- ☐ ***Public bodies** could reduce their spending for energy consumption by using more efficient buildings, products and services.*
- ☐ *The **EU economy** would benefit from a more secure energy supply and economic growth through the creation of new jobs, particularly in building renovation.*

4. What happens next?

- ☐ *Once the proposal is adopted by the European Parliament and the Council, EU countries will have to transpose the rules into national law within one year.*
- ☐ *Progress made in achieving EU's 20% energy saving target in 2020 will be reviewed in 2014. If it is insufficient, mandatory national energy efficiency targets will be proposed.[15]*

THE NEW EUROPEAN DIRECTIVE 2012/27/EU

Directive 2012/27/EU amends Directive 2009/125/EC on ecodesign requirements for energy-related products and Directive 2010/30/EU on energy efficiency labelling of energy-related products, and repeals Directive 2004/8/EC on the promotion of

cogeneration and Directive 2006/32/EC on energy end-use efficiency and energy services.

The Directive 2012/27/EU entered into force on 5 December 2012 and Member States have until 5 June 2014 to transpose the Directive into national legislation. Each Member State shall set an indicative national energy efficiency target based on the parameters set in the Directive and shall notify those targets to the Commission. From 30 April 2013 onwards, Member States shall report each year on the progress achieved towards their national 2020 energy efficiency targets. By 30 April 2014, and every three years thereafter, Member States shall submit National Energy Efficiency Action Plans.[16, 17]

The Directive lays down rules designed to remove barriers in the energy market and overcome market failures that impede efficiency in the supply and use of energy and provides national indicative targets for energy efficiency in 2020. [16, 18]

The requirements laid down in the Directive are minimum requirements and do not prevent any Member State from maintaining or introducing more stringent measures.

Among the Directive's provisions included in specific articles are:

*1. Regarding **EFFICIENCY IN ENERGY USE***

- ☐ *Energy efficiency targets*
- ☐ *Building renovation*
- ☐ *The exemplary role of public buildings*
- ☐ *Energy efficiency obligation schemes*
- ☐ *Energy audits and energy management systems*
- ☐ *Metering and Billing information and access to these*
- ☐ *Consumer information and empowerment*

*2. Regarding **EFFICIENCY IN ENERGY SUPPLY***

- ☐ *Promotion of efficiency in heating and cooling*
- ☐ *Energy transformation, transmission and distribution*

*3. Regarding **HORIZONTAL PROVISIONS***

- ☐ *Availability of qualification, accreditation and certification schemes*
- ☐ *Information and training*
- ☐ *Energy services*
- ☐ *Other measures to promote energy efficiency*
- ☐ *Energy Efficiency National Fund, Financing and Technical Support*

Implementation foresees that by 30 April each year as from 2013, Member States shall report on the progress achieved towards national energy efficiency targets. By 30 April 2014, and every three years thereafter, Member States shall submit National Energy Efficiency Action Plans, covering significant energy efficiency improvement measures and expected and/or achieved energy savings, including those in the supply, transmission and distribution of energy as well as energy end-use, in view of achieving the national energy efficiency targets. The National Energy Efficiency Action Plans shall be complemented with updated estimates of expected overall primary energy consumption in 2020, as well as estimated levels of primary energy consumption in specific sectors. [16, 19]

Directive 2012/27/EU proposes measures targeting energy saving, including renovation of public buildings, saving programs for public services sector and energy audits for companies in order to decrease energy consumption by 20% in the European Union by 2020.

The Directive requires Member States to establish a long-term strategy for mobilizing investments in renovating residential and commercial building stock, both public and private, available nationwide. Given the high cost of heating for houses, thermal rehabilitation or improving the energy performance of buildings has a positive impact on consumer's utility bills and contributes in improving their quality of life. Investments to improve energy efficiency will lead, in the short and medium term, to reduce energy bills.[16, 20]

CONCLUSIONS

In conclusion regarding the Directive 2012/27/EU member states shall set up measures in order to use energy more efficiently at all stages of energy chain, from the transformation of energy and its distribution to its final consumption. These measures include energy efficiency obligations schemes, the exemplary role to be played by the public sector and consumers' right to have exact information on their energy consumption. Some of these measures are listed as follows:

- ☐ *Setting up of an energy efficiency obligation scheme ensuring that energy distributors and/or retail energy sales companies that are designated as obligated parties achieve a cumulative end-use energy savings*
- ☐ *Renovation of the national stock of residential and commercial buildings, both public and private*
- ☐ *Purchasing by public bodies of products, services, buildings with high energy-efficiency performance*
- ☐ *Obligation for energy distributors and retail energy sales companies to reduce annual energy sales to final customers*
- ☐ *Promotion of availability of cost-effective energy audits for final customers*
- ☐ *Provision of individual meters reflecting the final customer's actual total energy consumption*
- ☐ *Give consumers access to clear and precise information on metering and billing*
- ☐ *Promotion of efficiency in heating and cooling*
- ☐ *Guarantee highly efficient energy transformation, transmission and distribution.[16, 17]*

Until June 5 2014, Romania, along with other EU Member States will have to transpose the European Directive on energy efficiency in national legislation.[20]

Building only eco-efficient or green buildings will be the next step for the European Union. These buildings besides being energy efficient will fit into the landscape, will have forms inspired from nature, will be built from environmentally friendly materials and will use renewable energy sources (solar energy, geothermal energy and wind power). Therefore they will be built to reduce pollution, minimize the amount of waste and reduce the negative impact on human health.

ACKNOWLEDGEMENT

This paper was supported by the project "Improvement of the doctoral studies quality in engineering science for development of the knowledge based society-QDOC" contract no. POSDRU/107/1.5/S/78534, project co-funded by the European Social Fund through the Sectorial Operational Program Human Resources 2007-2013.

REFERENCES

[1] *Speech by President of the European Commission Jose Manuel Barosso: Sustainable energy: The European Union and the global agenda, REGIONS20 Conference Vienna, 31 January 2013.*
[2] *O. Cocora, Dan Berbecaru (2004), Efficient use of energy in buildings (Utilizarea eficientă a energiei în clădiri), Alma Mater Publishing House, Sibiu.*
[3] *Romanian Energy Strategy (Strategia energetică a României) for 2007-2020, (September 2007).*
[4] *The Kyoto Protocol to the United Nations Framework Convention on Climate Change (11 December 1997).*
[5] *International Energy Agency (2008), Energy Efficiency Requirements in Building Codes, Energy Efficiency Policies for New Buildings, IEA Information Paper, Jens Laustsen, March.*
[6] *www.rehva.eu*
[7] *Directive 2002/91/EC of the European Parliament and of the Council of 16 December 2002 on energy performance of buildings.*
[8] *Directive 2006/32/EC of the European Parliament and of the Council of 5 April 2006 on energy end-use efficiency and energy services.*
[9] *Climate Strategy and Partners (2010), Financing Energy Efficiency Building Retrofits, International Policy and Business Model Review and Regulatory Alternatives for Spain, Peter Sweatman, Katrina Managan, Madrid, Spain.*
[10] *Directive 2009/28/EC of the European Parliament and of the Council of 23 April 2006 on the promotion of the use of energy from renewable sources.*
[11] *COM(2012), 271 (06.06.2012), Brussels, Communication from the Commision to the European Parliament, the European Economic and Social Committee and the Committee of the Regions, Renewable energy: a major player in the European energy market.*
[12] *Directive 2010/30/EU of the European Parliament and of the Council of 19 May 2010 on the indication by labelling and standard product information of the consumption of energy and other resources by energy-related products.*
[13] *www.ec.europa.eu/environment/gpp/pdf/windows_GPP_background_report.pdf-Accesat 01.02.2013 sau Green Public Procurement-Windows Technical Background Report-Windows, Glazed Doors and Skylights, Report for the European Commission, DG Environment by AEA, Harwell, Brussels, June 2010*
[14] *Directive 2010/31/EU of the European Parliament and of the Council of 19 May 2010 on the energy performance of buildings.*
[15] *www.ec.europa.eu/energy/efficiency/eed/eed_en.htm, Accessed 01.02.2013, Energy efficiency Directive-Citizen Summary.*
[16] *Directive 2012/27/EU of the European Parliament and of the Council of 25 October 2012 on energy efficiency.*
[17] *www.bureauveritas.com/wps/wcm/connect/bv_com/group/home/about-us/our-business/our-business-consumer-products/news+and+events/regulatory+bulletins/eu_directive_energy_efficiency*
[18] *www.ec.europa.eu/energy/efficiency/eed/eed_en.htm*
[19] *www.buildup.eu/publications/32236*
[20] *www.devonenergy.ro/articole/facturi-mai-mici-la-intretinere-si-energie--directiva-ue-privind-eficienta-energetica-intra-in-vigoare.html*

ACTA TECHNICA CORVINIENSIS - BULLETIN of ENGINEERING

ISSN: 2067-3809 [CD-Rom, online]

ACTA TECHNICA CORVINIENSIS - BULLETIN of ENGINEERING

ISSN: 2067-3809 [CD-Rom, online]

ACTA TECHNICA CORVINIENSIS - BULLETIN of ENGINEERING

ISSN: 2067-3809 [CD-Rom, online]

copyright © UNIVERSITY POLITEHNICA TIMISOARA,
FACULTY OF ENGINEERING HUNEDOARA,
5, REVOLUTIEI, 331128, HUNEDOARA, ROMANIA
http://acta.fih.upt.ro

ACTA TECHNICA CORVINIENSIS – Bulletin of Engineering
Tome VI (Year 2013) – FASCICULE 4 [October–December]
ISSN 2067–3809

[1.] Márta NÓTÁRI, [2.] Árpád FERENCZ

ASSESSMENT OF THE IMPORTANCE OF TRADITIONAL PRODUCTS IN HUNGARY

[1-2.] COLLEGE OF KECSKEMÉT, 6000 KECSKEMÉT ERDEI FERENC SQUARE 1-3, HUNGARY

ABSTRACT: Questionnaires were done for research of the local consumer evaluation aiming the topic of traditional horticultural products in the sphere of products in horticulture and food industry. We have three hypotheses: 1.The consumers are able to associate with messages bound up with characteristic, regional products. 2. In the decision-making process, in connection with the purchase and consumption of the consumer, the knowledge of the source of supply is an influential factor. 3. The product character of traditional horticultural products gives the chance to the consumer to acknowledge the excellent and individual feature of the product in a higher price, consequently, the higher price will be less influential factor in their decision-making process of the purchase. In the years 2010-2011 primary research has been conducted on agricultural and food manufacturers of traditional horticultural products. To analyse the survey data, we have used SPSS 14.0 for Windows and LISREL 8.30. Methods: Confidence-interval calculation, a variable structure test wit factor analysis, a variable structure test with cluster analysis, multi dimensional scaling and correspondence analysis. It can easily be brought to light that the consumers select product not even on the basis of its price, appearance but rather on the basis of its particular taste and the excellent quality. The consumers regard - beside the perceptible attributes - the Hungarian provenance, place of origin and the traditional feature as an important aspect. In the analysis of traditional horticultural products we can divide two independent factors can be distinguished: quality and economic factors.
KEYWORDS: Hungarian agriculture, production, prise, quality, country image

INTRODUCTION

A new tendency of consumer attitude has been emerging with a shift from the simplistic perception of foodstuff as mere agricultural products towards a more complex perception where foodstuff also has a cultural dimension. According to Sini (2000), the associability of a product with a special purpose, tradition or place of origin gives rise to the adoption of this attitude. Products that can be easily associated with a particular culture or place of origin have the potential to create market gaps, thus a reverse tendency to consumer standardization emerges (Szakály et al, 2008, 2010).

In the case of foodstuff, the country image is of utmost importance due to the fact that consumers, besides building a specific mental image of a particular product, also tend to assign products positive or negative images of the country of origin.

The favorable geographical location of Hungary allows the production of foodstuff of high added-value and outstanding quality.

Hungarian agricultural production areas generally enjoy wide international recognition; however, building a strong international image of Hungarian agricultural production areas needs product restructuring and technological innovation as well as a variety of other factors, such as the atmosphere of a particular agricultural production area, production related know-how or the history and traditions of the given region, can benevolently contribute to this image building.

MATERIAL AND METHOD - Market research

The opinion survey refers to information collection, whereby a small section of a group of numerous individuals or institutions is selected via professional sampling and this selected section is then interviewed (Baglyas et al, 2013).

The primary market research consists of the gathering of original, previously uncollected information and data, whereby the collection is undertaken with a specific purpose. I sought the answer to various questions during recording; therefore each answer can be registered as a variable as they can take varying values within a certain number interval. These are the dependent variables because, depending on the respondents, the result will be different, too. The questions (variables) remain the same throughout the questionnaire and the interviewees (respondents) are referred to as cases (Kőszegi et al, 2013).

Paired t-test analysis

For paired t-tests, the same respondents are tested repeatedly, thus test series are conducted on the same respondents and the paired t-test is used to examine the differences.

A variable for the differences observable in the pair is created (marked as D) and then the average and variance of this variable is calculated.

Subsequently, the t-statistics is established. The degree of freedom is "n-1", where "n" stands for the even number of the examinations (Pallóné, 2007).

Pearson's Chi-squared test

The exact significance test is based on two hypotheses; one is referred to as null hypothesis and the other is as alternative hypothesis, respectively (Deák et al, 2010, 2011). The Chi-squared test uses the following formula:

$$X^2 = \sum_{i=1}^{2}\sum_{j=1}^{2}\frac{\left(f_{ij} - e_{ij}\right)^2}{e_{ij}}$$

Confidence interval calculation

During the evaluation of questionnaires, representing the results simply in percentages is often insufficient or even misleading, given that the resulting differences do not reflect reliably whether the variation is significant or not.

The answers to the particular questions in the examined population helped me identify both the percentage of the positive answers and their confidence-intervals, the latter values revealing the real differences. The calculation of the confidence-intervals is inevitable for the establishment of a reliable conclusion on our hypotheses, especially in cases where the number of sample elements significantly differs.

RESULTS - Assessment of the importance of taste

Quality has various components which can be communicated in a variety of messages. Taste, ingredients, high quality and traditional production methods are all related to the attitudes associated with Hungarian foodstuff. Our research examines the importance of taste for making decisions on the purchase of traditional products.

The respondents have been segmented on the basis of their sex, age and educational attainment in order to examine whether these factors influence the outcome of the purchase decision making process. No significant difference can be identified; the respondents obviously find taste either important or very important.

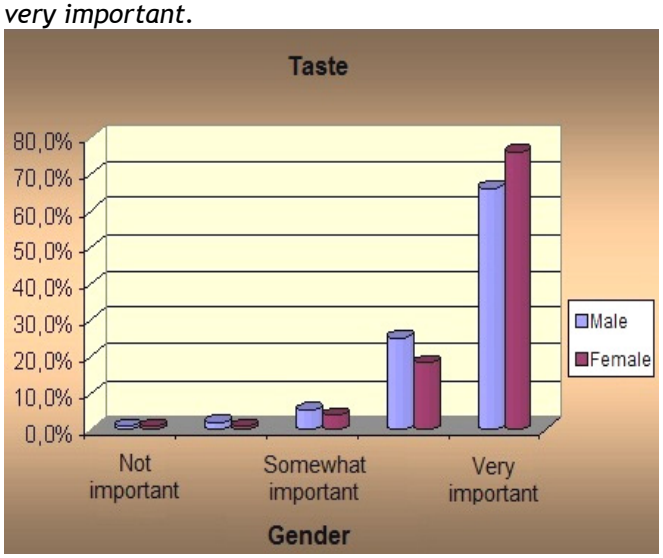

Figure 1: Assessment of the importance of taste by gender

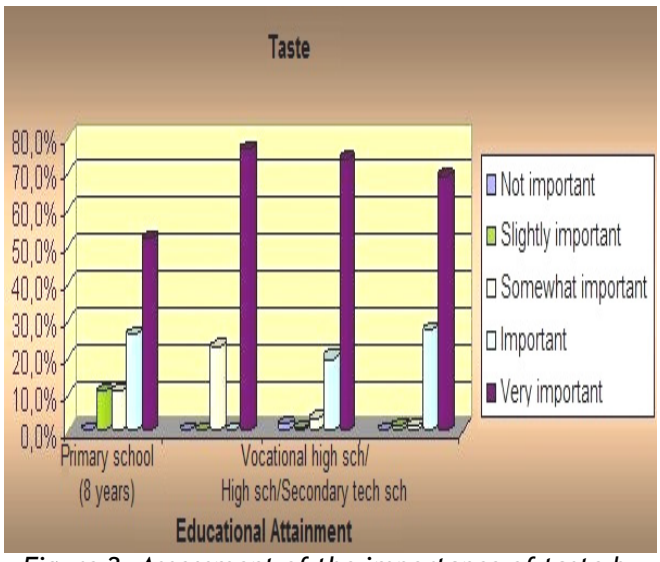

Figure 2: Assessment of the importance of taste by educational attainment

Assessment of the importance of tradition

The added value of unique, high quality, region-specific foodstuff is partly owing to their traditional nature.

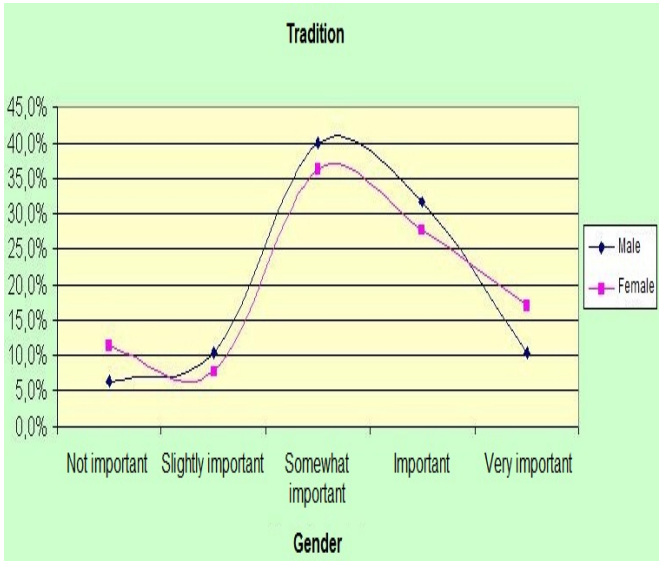

Figure 3: Assessment of the importance of tradition by gender

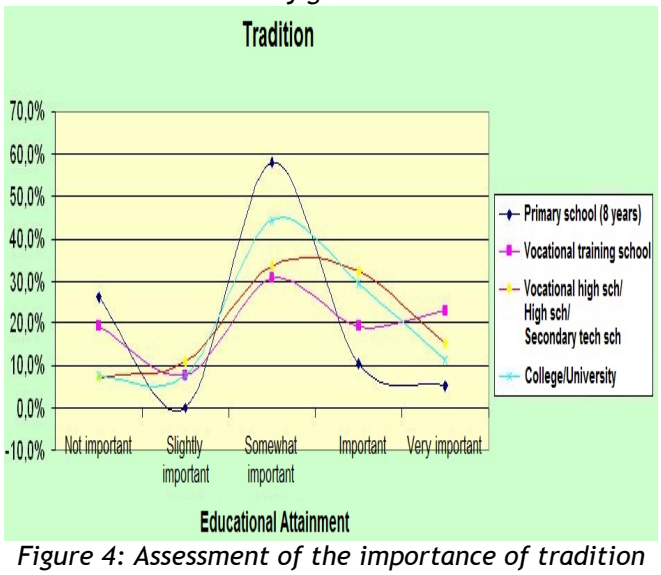

Figure 4: Assessment of the importance of tradition by educational attainment

As the specificity of a product does never originate only from a single component, the traditional nature also gains its significance in a specific component context.

All respondent segments evaluated this quality dimension as important or somewhat important. In a broader context, the traditional nature is a cultural asset and a certain consumer segment expects purchasables to have this added value.

Assessment of importance of the place of origin

The European Commission sets two criteria to differentiate regional products from other products. One such criterion is quality or fame attributable to the place of origin, the other is the identifiability of the product name with the place of origin.

The importance of the place of origin incorporates traditions and region-specific production technology. As shown above, the place of origin is a more important decision making factor for female consumers (59 percent) than for their male counterparts.

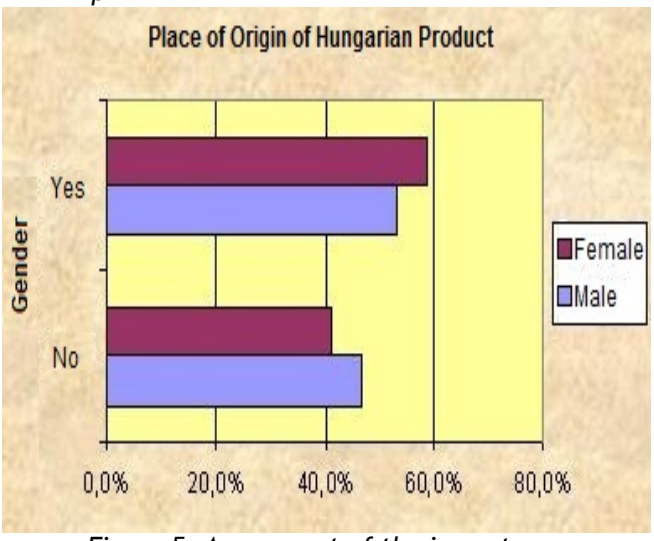

Figure 5: Assessment of the importance of the place of origin by gender

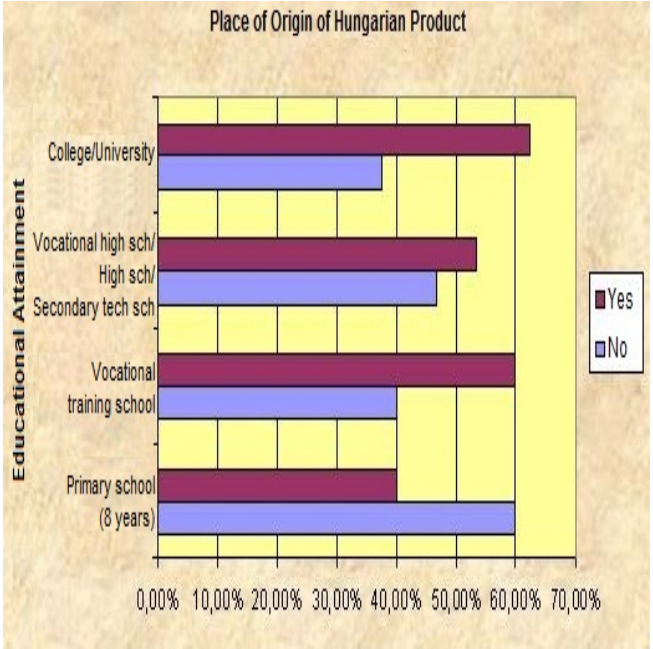

Figure 5: Assessment of the importance of the place of origin by age group

The assessment by age group points out that the place of origin plays an important role for seniors (over 60) in their purchase decisions. Figure 9 reveals that 60 percent of the respondents with low educational attainment do not take the place of origin into consideration for their purchase decisions.

CONCLUSION AND RECOMMENDATION

- ☐ *The significant changes in the attitude towards food consumption in the developed industrialized countries over the past decades have resulted in the modification of consumer habits as well; the purpose of foodstuff is no more primarily to cover our material needs but it is equally a source of pleasure (Deák et al, 2011). Succeeding on the overbought globalised market becomes more challenging, survival on the market requires novel methods, thus searching for new market gaps where products of special qualities can target special groups can be an alternative way of this succeeding.*
- ☐ *Beyond the perceivable characteristics, consumers also find the place of origin (the source region) and the traditional character of products important. "Traditional" means that the product looks back to least a ten-year-old history, which emphasises the importance of the time aspect. Analytical methods help little to assess the special characteristics of traditional and region-specific products but the consumer survey reveals that these factors play a significant role in the consumers' judgement on value. The communication of these special values towards the consumers for the purpose of enhancing the profile and competitiveness of the products is of utmost importance. Special, traditional foodstuff has a lot to offer to the ever growing consumer segment which craves for products with embedded emotional messages. These emotional messages are to be conceived region-specifically and communicated in plain language.*

REFERENCES

[1] *Baglyas F - Dobos N. I. Kőszegi (2013): Dry flower consumer behaviour in Hungary, Review on Agriculture and Rural Development 2013. vol. 2. (1) pp. 126-130.*

[2] *Deák Zs.-Hajdu I-né (2011): Az élelmiszer-ipari vállalkozások környezeti teljesítménye és a pénzügyi eredmények. Gazdálkodás Vol. 5. No.7. pp. 662-667.*

[3] *Deák Zs.-Hajdu I-né (2010): Fenntartható fejlődés és a fogyasztói társadalom. Agrár- és Vidékfejlesztési Szemle. Vol.5. pp. 516-521.*

[4] *Kőszegi I.- Baglyas F. (2013): Trade-off analysis in a wine market research in Hungary, F.*

[5] *Pallóné Kisrédi I. (2007): Hagyományos és tájjellegű termékeink európai szintű hasznosítási stratégiája. EOQ MNB, 4-20.p.*

[6] Sini M.P. (2000): Typical local products and their zone of origin: The importance of their reevaluation emphasizing the links which connectthem. Dolphins research

[7] Szakály et al. (2008): Fogyasztói szokások és attitűdök elemzése a hagyományos élelmiszerek piacán, kutatás jelentés.

[8] Szakály Z. – Pallóné Kisérdi I.- Nábrádi T. (2010): Marketing a hagyományos és tájjellegű élelmiszerek piacán. Kaposvári Egyetem Gazdaságtudományi kar, 31.p.

ISSN: 2067-3809 [CD-Rom, online]

ACTA TECHNICA CORVINIENSIS – Bulletin of Engineering
Tome VI (Year 2013) – FASCICULE 4 [October–December]
ISSN 2067–3809

[1.] Dejan JANKOVIC, [2.] Radmila MILIDRAGOVIC

INTEGRATION OPENSOURCE GIS SOFTWARE FOR IMPROVING DECISION-MAKING IN LOCAL COMMUNITY

[1.] THE CITY OF TREBINJE, BOSNIA AND HERZEGOVINA
[2.] "NEIMARSTVO" AD, BOSNIA AND HERZEGOVINA

ABSTRACT: The paper presents an example of integration of various functionalities opensource GIS software to improve decision-making in local governments. It shows the synergistic possibilities of integrating various opensource GIS software to support decision-making (DSS). Special attention is paid to geoprocessing capability. Further, it is analyzed the significance of building spatial data infrastructure at the local level as basis of DSS. The research was done on the example of choosing the best options for the reconstruction of public lighting. The results of this study contribute for promote the growing trend of integration the compatibility of various GIS open source software solutions.
KEYWORDS: GIS, geoproccessing, opensource software, local government, DSS, SDI

INTRODUCTION

Collection and processing of spatial information is a fundamental process of decision making. If we do not have high-quality and forehand information, and we do not have the necessary tools for their high quality and fast processing treatment, we will get the results that neither forehand nor appropriate to make prompt and quality decisions. About this would be paid attentions in decision-making in local governments. Decisions have made at this level significantly affect the development or stagnation of local communities, such as rational or irrational use its limited resources.

With applying of GIS information technology in decision-making processes, decision-makers were given powerful tools that enable the collection and processing of large amounts of spatial data and creating quality information in a very short time. The Geographic Information Systems (GIS) are complex five-component information systems that comprising the following components: procedures, people, data, hardware and software. This paper describes the integration of several open source GIS software for various purposes in the process of decision-making in local government.

The first part of papers namely the first three chapters present basic information about opensource GIS software and spatial data infrastructure. The second part describes underlying problem and research methodology. At the end of the study presents the results and conclusions.

OPENSOURCE GIS SOFTWARE

Open source software (OSS) is computer software with its source code made available and licensed with an open source license in which the copyright holder provides the rights to study, change and distribute the software to anyone and for any purpose. Open source software is very often developed in a public, collaborative manner. [1]

GIS software encompasses a broad range of applications which involve the use of a combination of digital maps and georeferenced data. GIS software can be sorted into different categories [2]:

- Desktop GIS usually serve all GIS tasks and are sometimes classified into three functionality categories: GIS Viewer, GIS Editor, and GIS Analyst.
- Spatial Database Management Systems (DBMS) are mainly used to store the data, but often also provide (limited) analysis and data manipulation functionality.
- Web Map Servers (WMS), Web Feature Servers (WFS) are used to distribute maps and data over the internet.
- WebGIS Clients are used for data display and to access analysis and query functionality from Server GIS over the internet or intranet.
- Libraries and Extensions provide additional (analysis) functionality that is not part of the basic GIS software, for instance functions for network and terrain analysis, or functions to read specific data formats.
- Mobile GIS are often used for field data collection.

Large number of open source projects is active today. A significant number of them have reached a remarkable level of maturity. That is one of reason why increase number of government institutions which use open source GIS software. However, there are still a significant number of customers are choosing a commercial GIS software. Causes for this are numerous, but it is undoubtedly one of the most important is that the open source GIS projects are specialized.

While commercial vendors usually offer products for all of software categories (e.g. ESRI Inc), open software projects often concentrate on a single category, e.g. desktop GIS or WebMap server.

In this paper are explored possibilities of integrating various opensource GIS software in order to create unique integrated Decision Support System (DSS). The survey was conducted on example of solving problems in local governance. Solution has been showed is integrated functionality: Desktop GIS software (gvSIG), spatial DBMS (PostGIS), server applications (GeoServer) and geoprocessing framework spatial data analysis library (Sextante).

SPATIAL DATA INFRASTRUCTURE

The term "Spatial Data Infrastructure" (SDI) is often used to denote the relevant base collection of technologies, policies and institutional arrangements that facilitate the availability of and access to spatial data. The SDI provides a basis for spatial data discovery, evaluation, and application for users and providers within all levels of government, the commercial sector, the non-profit sector, academia and by citizens in general [3].

Establishing SDI creates the preconditions for rational spatial data collection, their standardization and marketing and its put to develop of any local community. All stakeholders who interesting for development specific community (investors, researchers, entrepreneurs and others.) will be able data which necessary for conduct complex searches and analysis as the basis of them decision-making processes [3], [4].

In this example was shown applied three-tier architecture of information system. (Figure.1). [5]

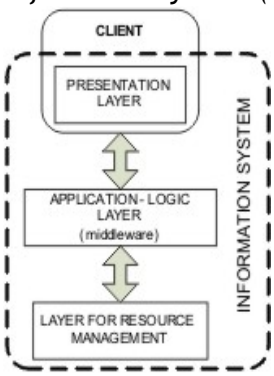

Figure 1. Tree-layer arhitecure of infomation system

Resource management layer is a base layer of the architecture, and includes data sources, most often databases (e.g. PostGIS DBMS).

Presentation layer provides communication between information system and external users who may be a person or another computer for example web browser (e.g. gvSIG, Sextant).

Application-logic layer namely middleware, includes a collection of programs that accept data from multiple data sources and transform it into a form that corresponds to the presentation layer (Web mapping service (WMS), Web Feature Service (WFS), Web Processing Service (WPS)).

Applying service-oriented SDIs compared to the traditional approach are achieved by the following advantages [4], [6]:

1. *reduce costs,*
2. *reduce development costs by not developing all the components,*
3. *services allow avoiding incompatibility of software,*
4. *the cost of applying of services is less than the cost of construction.*

Specifications of these services are defined by the standards of the Open Geospatial Consortium (OGC). OGC Web Services standards are defined frames which are provided by the dealer an independent, interoperable framework for web-based discovery, access, integration, analysis, exploitation and visualization of multiple online sources of spatial data and their processing capacity [8], [9].

During of this research it is executed simulation using of spatial data that was obtained through Geoserver's web services. In this way it is possible to analyze data which are stored in different locations. For example, spatial plans by the database of local government, water supply infrastructure by the database companies for management of water supply system or electrical network plans by the database of power supply company. Thus, we always have available update spatial data that is very important in decision making.

THE RESEARCHE PROBLEM

Integration differently oriented opensource GIS software, in order to develop GIS-based decision support system of local government, was made on the example of solving the problem of energy efficiency in poor lighting system. For instance, in Trebinje (Bosnia and Herzegovina) almost 4% of the city budget goes to the cost of electricity lighting. The main causes of this inefficiency are defined: inefficient lighting modules, a large number of lamps and the lack of an effective system of managing public lighting. Therefore, it was decided to choose the best variant of reconstruction of public lighting.

If we want to choose the best solution, we will define amount of saving electrical energy by existing lighting modules with mercury bulbs are being replaced with new energy efficient lighting modules with LEDs diodes or high pressure sodium lamps.

In addition, it was necessary to take into account assessment of fulfill the standards that define the nominal brightness of certain public areas. Furthermore, it is necessary to change deployment of available light module to illuminate so far darkened public space. The results of the analysis it was necessary to show in the form of maps that would clearly be identified which public space are satisfactory illuminated and which not, such as are presented that in numerical form.

METHODOLOGY

To create a DSS for selecting the best options for increasing the energy efficiency of lighting were used the following opensource GIS software:

- *gvSIG was developed by the European GIS community offering multiple language user interfaces. gvSIG has nice vector data editing functions. gvSIG is well known for its flexible GIS data input format. You can use various GIS data formats (both vector and raster) and online resources (such as WMS, WCS and WFS). Some GIS professionals believe that gvSIG is becoming close to replacing ESRI ArcMap software. [10]*

- *Sexstante is a spatial data analysis library written in Java and a powerful geoprocessing framework. It currently contains more than three hundred algorithms for raster and vector data processing, as well as tabular data analysis tools. Sextante integrates seamlessly with open source Java GIS (such as gvSIG) , proprietary GIS (such as ArcGIS) and non-GIS tools (such as the 52N WPS server). The SEXTANTE for gvSIG extension makes it possible to use Sextante tools directly in gvSIG, using module Model Builder. [11]*
- *Geoserver is an open source software server written in Java that allows users to share and edit geospatial data. Designed for interoperability, it publishes data from any major spatial data source using open standards. GeoServer is the reference implementation of the Open Geospatial Consortium (OGC) Web Feature Service (WFS) and Web Coverage Service (WCS) standards, as well as a high performance certified compliant Web Map Service (WMS). GeoServer forms a core component of the Geospatial Web. [12]*
- *PostGIS is a spatial database extension for PostgreSQL object-relational database. It adds support for geographic objects allowing location queries to be run in SQL. The database can then be used to store and query spatial data (points, lines and polygons). [13]*

The first is upgraded a software gvSIG with Sextant data analysis library. After that, spatial data are prepared by gvSIG software. On the base of aerial photographs have been made vector maps of streets of Trebinje, currently deployment of lamps lighting and currently deployment of lamps lighting with isolux diagrams. For each of the analyzed variants of public lighting reconstruction it has been prepared vector map that included isolux diagrams of new lamps with appropriate new spatial deployment. These vectors files and related raster file have been loaded in the spatial database and WMS and WFS Geoserver services. On this way, the data necessary to perform the analysis were provided.

The next step is being made algorithm of analysis. Namely, the steps of spatial and attribute analysis that needs to be done on the available spatial and attribute data would be defined in order to obtain the desired result.

For comparison of the current state of illumination of public areas with expected brightness is being used with the new energy efficient light bulbs is defined by the following algorithm:

- *load vector maps backgrounds (the streets - line, the isolux of lights modules diagrams - polygon, the boundaries of analyzed area - polygon);*
- *overlapping vector map - streets and vectors map - isolux diagram over vector file in which borders are defined in the study area and is being copped (algorithm-Clip);*
- *depending on the width of streets, which is listed as attributive data the buffer function is executed. Results would be vector maps of polygon street view, depending on their width;*
- *to define public surfaces that are illuminated it would be done algorithm - intersection of vector layer street - polygon and vector layer of isolux light diagram on specific the analyzed surface;*
- *finally, it would be got a vector polygon layer that display illuminated public areas and presented their statistics, the most important figure is the total amount is illuminated public surface in the analyzed area.*

In addition is done algorithm that computes expected energy consumption of public lighting in the analyzed area. This algorithm had the following steps:

- *load vector files (position lights - point, analyzed area - polygon) and attribute data (average daily working hours of public lighting - hours, time analysis - days);*
- *overlay vector files to define the area to be analyzed;*
- *using an algorithm that summarizes all the power lights that are located in the project area in one layer with the polygon will have this information as an attribute;*
- *do calculations under certain defined formula;*
- *present the expected total energy consumption for the whole period of time and analyzed area in KWh.*

The above algorithms are implemented by combining and linking Sextant algorithms within their GUI Modeler (Figure 2).

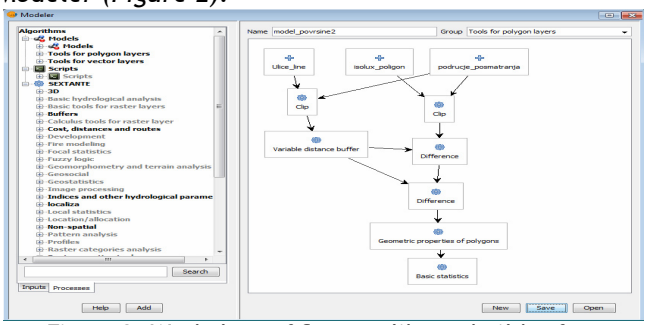

Figure 2. Workplace of Sextant library builder for geoproccessing

The graphical modeler allows to create complex models using a simple and easy-to-use interface. Using the graphical modeler, that chain of processes can be wrapped into a single process, so it is easier and more convenient to execute than a single process later on a different set on inputs. No matter how many steps and different algorithms it involves, a model is executed as a single algorithm, thus saving time and effort, specially for larger models.

In this example, the Sextant GUI modeler is started within an integrated environment with gvSIG software. GUI modeler interface are consist of a desktop where is dragged and associated algorithms from the list that is on the left side. Besides there is the possibility that offered to the user to combine all of algorithms have been offered by vendor or user-making. This allows to user creating algorithms which are performed really complex analysis.Algorithms are listed previously, can be activated in two ways:

- *directly employed through gvSIG environment (Figure 3)*
- *executive through batch file (Figure 4)*

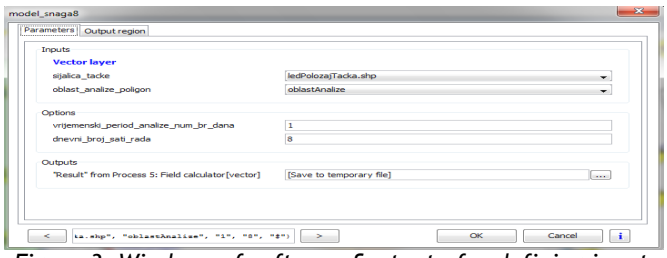

Figure 3. Windows of software Sextante for defining input of parameters in gvSIG workplace

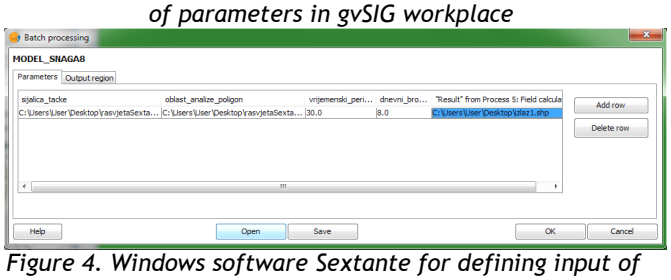

Figure 4. Windows software Sextante for defining input of parameters in batch mode

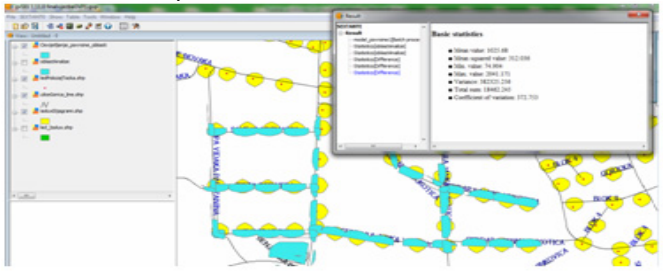

Figure 5. Windows of gvSIG software with result of spatial analysis with Sextante library

Input parameters can be loaded from the local disk, database or through WMS, WFS service. The following figure (Figure 5.) shows the result of the processing algorithm created for representing illumination of public areas by applying the appropriate model lamps.

RESULTS

The main results of this research can point out the successful integration of more functionality opensource GIS software into a single decision support system for the local government.

Applying service of Geoservers is highlighted the importance of establishing a spatial data infrastructure at the local level. The SDI at the local level should provide the necessary spatial data for the analysis as support of decision-making processes. In beforehand examples are defined algorithms through which are successfully integrated spatial data from different locations. Moreover, using Sextant GUI modeler for development of algorithms for data processing with aim to solve complex problems, it is shown that for implementation of complex spatial analysis is not necessary to have a complex programming knowledge. The examples of complex geoprocessing algorithms it is showed possibilities that beginners GIS users with a basic introduction of geoprocessing might have done complex spatial analysis. The end result shows capability and benefits of applying geoprocessing to solve everyday problems faced up not the only in local government but also in any other organizations.

CONCLUSIONS

Looking separately, currently opensouce GIS software can be concluded that none of them offers a complete solution for use in solving complex spatial problems. The only if we integrate their functionality and with increasing their compatibility it will be possible to create one that system.

The paper research and its results clearly are showed that is achievable. The current trends of integration of existing opensource geoproccessing tools with desktop or web applications by are being taking advantage of service-oriented SDIs lead on there. In the future, with improvement of the existing capabilities of the opensource GIS software will be able to increase accessibility these technology to ordinary GIS users. Given methodology can be successfully are applied to a wide range of problems they encounter every day. In this way it will increase using these integrated systems by local authorities, state institutions, and other organizations.

REFERENCES

[1] *Verts, William T. 2008. Open source software, World Book Online Reference Center, Available from: http://en.wikipedia.org/wiki/Open_source_software Last accessed: 01 June 2011.*

[2] *Steiniger S. and Weibel R., 2009. GIS Software - A description in 1000 words, Available from http://ignum.dl.sourceforge.net/project/jump-pilot/w_other_freegis_documents/articles/gissoftware_steiniger2008.pdf, Last accessed: 01 March 2012.*

[3] *Nebert D.D. (ed.), 2004. Developing spatial data infrastructures: the SDI cookbook ver. 2.0., Global Spatial Data Infrastructure Technical Working Group, GSDI*

[4] *Obradovic Ž., 2011. Spatial Data Infrastructure in the Federation of Bosnia and Herzegovina, II. Congress on Cadastre in Bosnia with international participation, Centar, Sarajevo, 28-30.09., Available from: http://www.gdhb.ba/Radovi_II_Kongres_o_katastru/03-nacionalna_infrastruktura_prostornih_podataka-izazov_za_buducnost/obradovic/ipp_u_fbih_tekst.pdf , Last accessed: 01 October 2011.*

[5] *Alonso G., Casati F., Kuno H., and V. Machiraju. 2004. Web services: concepts, architectures and applications, Springer*

[6] *Yuliadi T., Aditya T., and W. Vries, 2011. A local spatial data infrastructure to support the merapi volcanic risk managment: A case study at Selman regency, Indonezia, Indonesian Journal of Geography, Vol. 43, No. 1, June, p.25-48.*

[7] *Aditya T., and M.-J. Kraak. 2009. Geoportal and the GDI Accessibility, Handbook of Research on Geinfomatics, Information Science Publishing: Hershey, PA., p.42-50*

[8] *Web page - Open Geospatial Consortium (OGC), Open geospatial consortium, [online]. Available from: http://www.opengeospatial.org/. Last accessed: 01 March 2011.*

[9] *Doyle A., and C. Reed, 2011. Introduction to OGC Web Services, OGCWhite paper, Available from: http://www.opengeospatial.org/domain/gov_and_sdi #resources Last accessed: 01 February 2013.*

[10] *Web page - Opensource project "gvSig" - http://www.gvsig.org/web/ Last accessed: 01 March 2013.*

[11] *Web page - Opensource project "Sextante" - http://www.sextantegis.com/index.html Last accessed: 01 March 2013.*

[12] *Web page - Opensource project "Geoserver" - http://geoserver.org/display/GEOS/Welcome Last accessed: 01 March 2013.*

[13] *Web page - Opensource project "Postgis" - http://postgis.net/ Last accessed : 01 March 2013.*

ACTA TECHNICA CORVINIENSIS – Bulletin of Engineering
Tome VI (Year 2013) – FASCICULE 4 [October–December]
ISSN 2067–3809

[1.] Tohid AKHLAGHI, [2.] Ali NIKKAR

APPLICATION OF ALGEBRAIC INVERSE METHOD TO SURFACE WAVE TESTING OF PAVEMENTS USING FREE PLATE SOLUTION

[1-2.] FACULTY OF CIVIL ENGINEERING, UNIVERSITY OF TABRIZ, TABRIZ, IRAN

ABSTRACT: The use of surface waves of the Rayleigh type enables the properties of the component materials of a layered structure, such as a pavement, to be determined. The method has the advantage that the measurements are performed dynamically, thus making an allowance for the inertial and frequency dependent response of the pavement. The velocity of the waves is not a constant, but exhibits dispersion. The manner of the variation of the wave velocity is used to determine the properties of the surface and subsurface materials of the structure. Inverse problems are involved in interpreting the results. Wave propagation in elastic plates is analogous to propagation in layered spaces and therefore the free plate system can be used to model the surface layer of a single layered pavement structure. A direct algebraic inverse technique has been developed and used to calculate the thickness of the surface layer of a pavement system employing free plate analysis. To assess the effectiveness and reliability of the proposed technique, the application of the method to a published set of experimental data obtained in the field is presented and discussed. It is shown that the experimental results and the algebraic solutions are in good agreement, indicating that the proposed method can be used to determine the thickness of the pavement surface layer without resorting to excavation and in a very quick and economic manner.
KEYWORDS: Algebraic inverse, Free plate, Pavement, Surface wave testing

INTRODUCTION

The determination of in-situ elastic properties of pavement materials along with layers thicknesses is of great importance in pavement management system. The information is needed in order to (1) design the constructed layers in such a manner that the imported materials are strained only to within acceptable limits, and (2) locate and to characterize zones of weakness. The use of surface waves of the Rayleigh type enables this information to be determined, with the advantage that the measurements are conducted dynamically, thus making an allowance for the inertial and frequency dependent response of the pavement. The use of Rayleigh wave enables an estimate to be formed of the thickness of the surface layer of a pavement. The precision of the estimate depends upon the contrast between the elastic properties of the materials in the surface and the underlying layers. The greater the contrast, the more precise is the estimate. The measurement of the deflections at the surface of a pavement, in the neighborhood of a known load, can also be used to estimate the elastic moduli of the subsurface materials. It is preferable, although not essential, to make separate measurements of the thicknesses, and to supply the thicknesses of the component media as data. The measurement of surface deflections is widely used as a means of pavement investigation. The interpretation of the results yields information on the elastic moduli of the component materials.

WAVE METHODS

Waves of the Rayleigh type are generated by applying an impulsive load, a hammer blow, at right angles to the surface of the pavement. SH-waves are generated by applying an oscillatory torque to the free surface: the axis of the torque is normal to the free surface. Sensors are placed at suitable distances from the source of the vibration. It is sufficient to perform measurements at two sensors. The velocity of the generated wave is determined as a function of the frequency, enabling a frequency-dispersion curve to be plotted. This curve shows the phase velocity of a wave at the surface of the structure. The frequency-dispersion data can be used to determine the properties of the media of which the structure is composed. Graphical methods sometimes suffice for approximate results, although most systems must be analyzed with the aid of relevant solutions of the wave equation of the particular system studied.

FREE PLATE SOLUTION

The simplest assumption is that the structure consists of a free plate. Free plate solutions for the propagation of plane stress waves can be used to determine the engineering properties of the surface layer of a layered medium from the frequency-dispersion data of the system obtained in the field. A number of different types of vibrations can exist in a solid plate (or layer) with free boundaries. In a free isotropic elastic plate of thickness 2H, three types of particle motions can occur. These types of particle motions are often called wave modes and depend on

the characteristics and stiffness of the transmission medium, existing boundary conditions and the frequency of the wave. Figure 1 shows these different wave modes in a free isotropic plate.

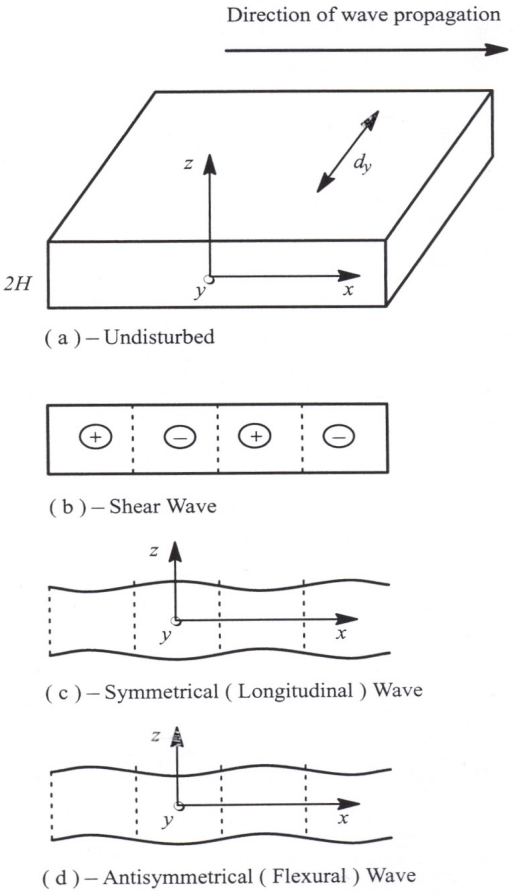

Figure 1. Wave modes in free isotropic elastic plate

Plane waves in plates can be described as symmetrical (longitudinal) and antisymmetrical (flexural) waves depending upon the symmetry with respect to the median plane of the plate. The antisymmetrical wave corresponds approximately with the Rayleigh waves [4]. For symmetrical and antisymmetrical modes, the wavelength (or phase velocity) and frequency of the wave are related by the corresponding characteristic equations. The characteristic equation for the antisymmetrical mode is as follows [2]:

$$\frac{\tanh q\,H}{\tanh s\,H} = \frac{4k^2\,q\,s}{(s^2+k^2)} \qquad (1)$$

where

$$q^2 = \omega^2\left(\frac{1}{c^2} - \frac{1}{V_P{}^2}\right) \qquad (2\text{-a})$$

$$s^2 = \omega^2\left(\frac{1}{c^2} - \frac{1}{V_S{}^2}\right) \qquad (2\text{-b})$$

$$k = \frac{\omega}{c}; \quad k_P = \frac{\omega}{V_P}; \quad k_S = \frac{\omega}{V_S} \qquad (2\text{-c})$$

INVERSE PROBLEM

The problem is to determine the unknown parameters of the component materials of the surface layer of a pavement structure, based on the wave propagation theory in the free plate. The unknown parameters are the elastic modulus (whether Young's or shear modulus) and thickness of the uppermost layer in a given pavement system.

Most of the inverse techniques developed thus far are based on the numerical methods, which have been used as a criterion for back calculation of the shear wave velocities or shear moduli and thicknesses of the pavement layers. With the numerical inverse method, an initial layered model is assumed for the system, and the theoretical dispersion curve is obtained by employing the theory of wave propagation in elastic layered media. Then the necessary structural changes are iteratively made until the experimental and theoretical dispersion curves are matched adequately. Thus the user must be familiar with surface wave dispersion theory in order to know what structural parameters to adjust, whether to decrease or increase the magnitudes and if so by how much. Therefore this process is time consuming and considerably dependent on the experience of the user. Also it requires engineering judgment and finally the solution is not a unique one. Other possible solutions must be sought and developed.

Graphical methods of interpretation can be applied to the results of measurements obtained from field measurements conducted on a layered structure [1]. The reciprocal of the wavelength is plotted against the frequency, from which the elastic parameters of the surface layer can be derived. The plot of reciprocal of wavelength against the frequency consists of data points which fall on a straight line and the reciprocal of the slope of line gives the shear wave velocity. By employing the graphical inverse method for determining the elastic shear modulus of the surface layer, the thickness of the layer is the only unknown parameter which can be calculated directly from the characteristic equation of the system.

ALGEBRAIC INVERSE

With algebraic inverse method, the characteristic equation of the system is expanded as a polynomial and is solved for the unknown parameters of the system. The characteristic equation which corresponds with Rayleigh waves can be represented by power series. By making power series, the equation is expanded symbolically in terms of the layer thickness parameter. Thickness of the layer, as illustrated in Fig. 1, is 2H.

The following file shows the necessary input to Mathematica [5]:

```
(* Expansion of the free plate equation, Mathematica file *)
k = w / c ;    kP = w / VP ;    kS = w / VS
q = Sqrt [ k ^ 2 - kP ^ 2 ]
s = Sqrt [ k ^ 2 - kS ^ 2 ]
Do [ fH [ i ] := Series [ Tanh [ q H ] / Tanh [ s H ] , {H , 0 , i } ] , { i , 2 , I , 1 } ]
Do [ gH [ i ] := fH [ i ] - q / s , { i , 2 , I , 1 } ]
h := 4 k^ 2 q s / ( s ^ 2 + k^ 2 ) ^ 2 - q / s
Do [ aH [ i ] := Normal [ InverseSeries [ gH [ i ] , H ] ] , { i , 2 , I , 1 } ]
Do [ bH [ i ] := aH [ i ] / . H -> h , { i , 2 , I , 1 } ]
Do [ H [ i ] := bH [ i ] / . { VP -> VP , VS -> VS , c -> c , w-> ω } , { i , 2 , I , 1 } ]
```

This input yields a series of the power series expansion for the left hand side of the characteristic equation about the point H = 0 to the order H^i, where the variable I successively takes on the values 2 through 15 in steps of 1. The value of I equating to 15 is found by trial and error. The value of I is increased at each step by one and the calculation is repeated until the difference between the two successive results become negligible. Inverse Series performs reversion of the series, which gives a series for the inverse of the function represented by gH [i]. The inverse can only be calculated when the first term in the gH [i] is of order H. The normal expression aH [i] now is a polynomial representing H in terms of the velocities of longitudinal and shear waves in the surface layer and of measured values of the frequency and the corresponding surface phase velocity. The frequency and the surface phase velocity are obtained from the results of the measurements made in the field on the ground surface of the system, and are data pairs ω and c. The limiting velocity of waves of the Rayleigh type in the component material of the surface layer can be read directly from the results of the field measurements. If a value of Poisson's ratio is assumed, the parameters V_P and V_S can be estimated. The resulting explicit function representing the thickness of the layer can be directly used to calculate the layer thickness 2H.

APPLICATION TO EXPERIMENTAL RESULTS

As an application, the data shown below on Fig. 2 are based on the experimental results given by Jones [3]. His investigation was on a pavement section and the results were obtained from experiments on a concrete slab with ν = 0.25 for Poisson's ratio and 9.5 inches in thickness, laid on a thick ground base.

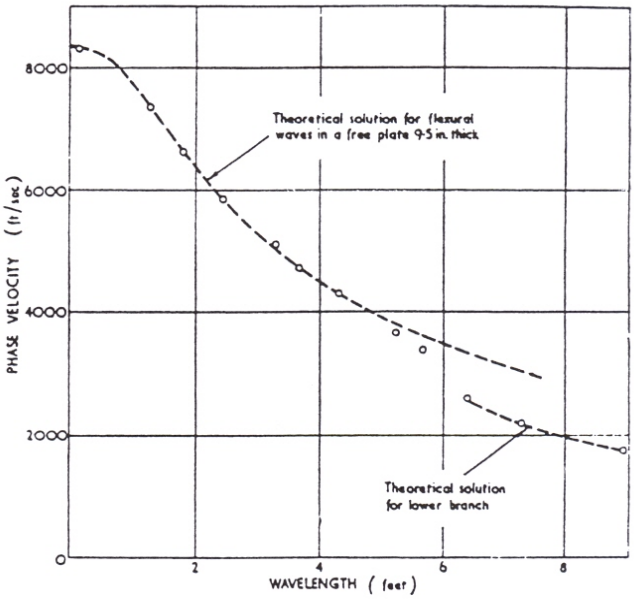

Figure 2. Results from concrete slab laid on well-compacted hoggin [3]

This example shows the results of the measurements of the phase velocities of waves of the Rayleigh type as a function of the wavelength on a practical construction of the single layered surface. The value of Rayleigh wave velocity was 8350 feet per second, from which the shear and longitudinal wave velocities are calculated to be 9100 ft/sec and 15760 ft/sec, respectively.

Table 1. Experimental results

Frequency ω (rad/sec)	Phase Velocity c (ft/sec)	$k=\frac{\omega}{c}$	$k_P=\frac{\omega}{V_P}$	$k_S=\frac{\omega}{V_S}$
37196	7400	5.03	2.36	4.09
23650	6700	3.53	1.50	2.60
15315	5850	2.62	0.97	1.68
9860	5100	1.93	0.63	1.08
8203	4700	1.75	0.52	0.90
6225	4260	1.46	0.39	0.68
4261	3650	1.20	0.27	0.47
3759	3350	1.21	0.24	0.41

Numerical values of the phase velocity and the frequency are supplied as data. These data have been summarized and shown in Tab. I. The calculated surface layer thickness for different values of expansion order, applied to the characteristic equation of the free plate for making power series in terms of H, are plotted in Fig. 3.

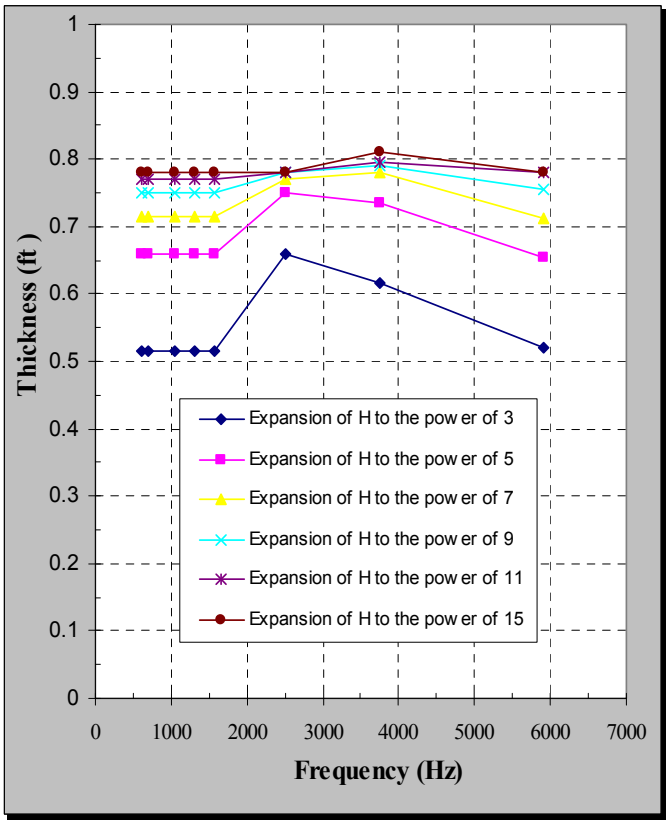

Figure 3. Variation of free plate thickness at different expansion powers

Figure 3 shows the calculated depth as a function of the frequency. It can be seen that as the expansion order increases, the calculated thickness becomes convergent towards the measured value. The average layer thickness obtained from the thicknesses calculated for each pair of dispersion data is also shown in Fig. 4. This figure shows that the average thickness increasingly becomes convergent as expansion order increases. In other words, if the average thickness approaches the real existing value, it does not change with increase in the expansion order. It is evident from Fig. 4 that the average H remains constant at expansion order equal to and/or

greater than 13. According to the calculated results shown in Fig. 4, the solution of the thickness at I = 13 is equal to 0.79 ft which is comparable to measured depth of 0.80 ft. It can be concluded that the experimental results and the algebraic inverse solutions are in best agreement.

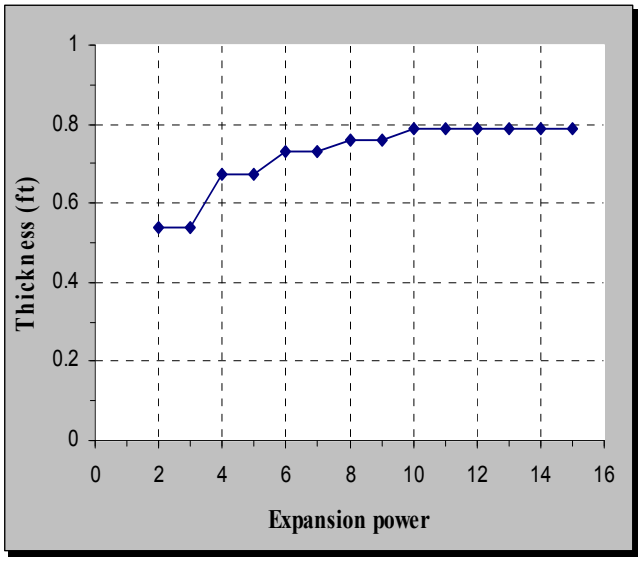

Figure 4. Variation of free plate average thickness against expansion power

SUMMARY AND CONCLUSIONS

Surface waves can be used to determine the mechanical and physical properties of the materials of a layered structure such as soil sites, highway pavements and airport runways. The elastic properties and thicknesses of the component materials are derived from measurements of the wavelength and the phase velocity of vibrations generated along the surface of the ground. The dispersion curve of Rayleigh waves can be determined in the field with the aid of measurements of ground motions induced by a hand hammer using transducers placed on the ground surface. The surface wave method has been successfully used to construct the dispersion curve of the waves of the Rayleigh type. The phase velocity is not constant, but varies with the frequency. The manner of the variation is used to determine the required parameters of the system (the velocity of wave propagation in each medium).

For many years, the numerical inverse procedure has been extensively employed for the determination of the layers moduli and thicknesses of a layered structure. However, this technique is complex time consuming and requires experienced person and engineering judgment. Ideally, the inverse should be obtained by means of a true mathematical inverse. The frequency equation for the system is expanded as a polynomial, and is solved for the unknown parameters of the system. A direct symbolic solution for the determination of the thickness of the free plate model, using mathematical software, has been developed. It is used to calculate the thickness of the uniform free plate corresponding with pairs of the values of phase velocity and frequency as data. The wave propagation in elastic plates is analogous to propagation in layered spaces and therefore this system can be used to model the surface layer of a single layered pavement structure. To assess the effectiveness and reliability of the proposed technique, the application of the method to a published set of data obtained in the field is presented and discussed. The comparison between the experimental results and the developed algebraic solutions show very good agreement, indicating that the proposed method can be used as an economic and effective technique to determine the thickness of the pavement surface layer.

REFERENCES

[1] *T. B. Akhlaghi, & W. H. Cogill, "Application of the free plate analogy to a single-layered pavement system," Insight, The Journal of the British Institute of Non-Destructive Testing, 36(7), 1994, pp. 514-518.*

[2] *W. M. Ewing, W. S. Jardetzky, and F. Press. Elastic waves in layered media. New York: McGraw-hill, 1957.*

[3] *R. Jones, "Surface wave technique for measuring the elastic properties and thickness of roads: theoretical development," Brit. J. appl. Phys. 13, 1962, pp. 21-29.*

[4] *M. Redwood, Mechanical waveguides. Pergamon Press, New York, 1960.*

[5] *S. Wolfram, Mathematica: A system for doing mathematics by computer. Redwood City, California: Addison-Wesley, 1990.*

ACTA TECHNICA CORVINIENSIS - BULLETIN of ENGINEERING

ISSN: 2067-3809 [CD-Rom, online]

ACTA TECHNICA CORVINIENSIS – Bulletin of Engineering
Tome VI (Year 2013) – FASCICULE 4 [October–December]
ISSN 2067–3809

[1.] Jozef PETRÍK, [2.] Pavol PALFY, [3.] Vojtech MIKLOŠ, [4.] Milan HAVLÍK

THE REMOTE LABORATORY AND MICROHARDNESS MEASUREMENT

[1.] TECHNICAL UNIVERSITY OF KOŠICE, FACULTY OF METALLURGY, DEPT. OF INTEGRATED MANAGEMENT, SLOVAKIA

ABSTRACT: The measurement of micro-hardness with loads between 0.09807 N and 0.9807 N has been carried out in direct mode (appraiser measured the dimensions of indentations with a measuring device fitted to the micro-hardness tester, a part of microscope) and in modified remote modes. The reference block - certified reference material with defined specified hardness and its uncertainty was used as a specimen, particular measurement involved indirect calibration of tester. The influence of applied load on the measured value of micro-hardness was evaluated by Meyer's index n and PSR method. The difference between values obtained by particular modes is statistically significant.
KEYWORDS: Hardness test, micro-indentation, metal, CRM, remote laboratory

INTRODUCTION

Measurement of micro-hardness is frequently used for determination of hardness of small items or thin layers, and identification of individual phases in metallography. It can be carried out in a similar manner to the Vickers macro-indentation tests with diamond pyramid, except for considerably smaller loads. However, the most important and intractable problem associated with low loads (the deep of indentation is less than 10 μm deep as a rule [1]), is that concerned with change in indentation size [2]. The micro-hardness of solids depends on the applied load. The study of relationship between micro-hardness and load has been carried out not only for metallic materials, but also for semiconductors, glass, slag, ceramics and organic crystals [3-5].

"NORMAL" AND "REVERSE" ISE

When a very low load is used, the measured hardness is usually high; with an increase in test load, the measured hardness decreases. Such a phenomenon is referred to as "normal" indentation size effect (ISE). Using a load dependent hardness in material characterization may result in some unreliable conclusions [6]. The ISE may be caused by the testing equipment. The experimental errors resulting from the measurement of indentation diagonals as a result of the limitations of the resolution of the objective lens and determination of the applied load belongs in this group [6-8]. Another source of ISE is intrinsic properties of the tested material (work hardening during indentation, load to initiate plastic deformation, indentation elastic recovery, elastic resistance of the materials) [7-9]. The effect of machining-induced residually stressed surface (grinding, polishing) of specimen and indenter/ specimen friction are also explanations of the ISE [6, 8-10]. In contrast to "normal" ISE, a reverse type of ISE (inverse ISE, RISE), where the apparent micro-hardness increases with increasing test load, is also known. It essentially takes place in materials in which plastic deformation is predominant. Reverse ISE can be explained in terms of the existence of a distorted zone near the crystal-medium interface, effects of vibration and bluntness of indenter, the applied energy loss as a result of specimen chipping around the indentation and the generation of the cracks [9].In the literature, there are many examples, which reveal that, the "normal" ISE occurs in brittle materials while the reverse ISE has been reported mainly for materials undergoing plastic deformation [7].

A perfect measurement would obtain the true value of a quantity. True values are, by nature, indeterminable because a perfect measurement cannot be performed. Difference between the true value and the value obtained by a measurement is the error of measurement. The final result is an estimate of the true value. The measurement uncertainty is a parameter that characterizes the dispersion of the values that could reasonably be attributed to the result of measurement. The uncertainty is inversely proportional to the quality of measurement [11, 12].

The purpose of this paper is to evaluate the influence of load on the values of micro-hardness using Meyer's and PSR methods, to evaluate the influence of load on the uncertainty of measured micro-hardness and to compare the results obtained in direct and remote modes.

MODE OF LABORATORY

In engineering education, a key-activity to improve the learning process is hands-on experimentation, carried out by simulation tools or laboratory facilities [13].

Laboratory studies provide experience, try-and-error type of learning, building connections among other concepts and previously learned subjects. However, for many educational organizations it is not always

possible to provide such an experience for their learners, since the establishment and maintenance cost especially for the fields that need high level equipment in such laboratories. In such cases, several educational organizations are using some technologies for supporting their students remotely or virtually [14].

In a traditional proximal laboratory, the user interacts directly with the equipment by performing physical actions (e.g. manipulating manually, pressing buttons, turning knobs) and receiving sensory feedback [15].

Online laboratories (Labs) became a very useful support for practical aspects of teaching methods since the time their technical basis got available world wide. A lot of online Labs are available via the internet. They support for example live experiments during lectures, distance learning courses (students work at home) or ed-to-ed scenarios (students work at an institute and access an online Lab at another institute to save costs for expensive equipment). As mentioned in many papers, online Labs can open possibilities for an experimental approach to a wide audience and are independent of opening hours. We can distinguish them by location and experimental equipment, as can be seen in tab. 1 [16].

Virtual Lab allows students around the world to log into a computer equipped with the suitable interface circuits, such as data acquisition systems connected to various sensors or communication modules, and perform real-time experiments [17].

Table 1. Concepts of Labs [16]

		Access to Laboratory	
		Local	Remote
Experimental equipment	Virtual	Local simulation	Virtual laboratory
	Real	Traditional (proximal) laboratory	Remote laboratory

Remote Lab (remote mode) can be defined as a laboratory (apparatus, rigs) that can be accessed and controlled via the internet (actual laboratory experiments that are run remotely via a web interface) [15]. Most of such Labs require complicated hardware and software for communication with human and specially to create a feeling of remote presence [18]. Users of remote Lab are able to interact with the apparatus, from any computer connected to the internet through interface applications that allow them to manipulate the equipment, monitor the process and receive the results of the experiment for analysis. In many cases, remote Labs can be made available 24/7 with minimal requirements for maintenance or staff intervention [19]. Remote Labs are intended to complement the hands-on laboratory experience by providing access to a greater number of laboratories, and more opportunity to run and re-run experiments at a time and from a location that is convenient for the student. Remote Lab conception requires technical, pedagogical and computer science competencies. Due to these requirements, it appears to be more complex than other e-learning contexts such as on-line courses, virtual classrooms, e-projects, role-playing, etc. however, this kind of training is essential for scientific and technical disciplines and fits a real need [13]. Motivations for remote laboratories development are:

- sharing heavy, highly specialized and expensive instruments and equipments between institutions,
- anytime and anywhere Lab access, the students can login and carry out experiments from any place of the world,
- putting students in front of real situations and allowing them: to discover system behavior, to train by using instruments, to verify scientific theories, etc.,
- remote Labs give students the opportunity to work in the remote mode,which will eventually become important in engineering jobs,
- unlike simulations remote Labs provide real experience,
- remote Labs improve safety and security,
- complex experimental systems, including specific media addition such as cooling, inert gas maintained by specialist staff at a specific location, can be directly controlled,
- team members, working at different locations can take advantage of the same test-run results without extra travelling,
- long-term trials (reliability, failure performance) can be comfortably supervised from home, e.g. on weekends [13, 20].

In broader sense, the process of remote measurement contains also objective explanation of remote measurement - conceptual solution to wider understanding of measurement. Conceptual solutions depend on measurement possibilities, monitoring and control in a real Lab (the equipment side), on knowledge, informational, technical, personal, organization but also financial situation of individual joined participants. Following situations may be counted in:

- Concept A: Measurement systems and processes can be monitored and/or controlled locally - requires a physical presence in the laboratory.
- Concept B: Measurement systems and processes can be monitored and/or controlled remotely (virtually) - based on thin www client with connection to selected www server. In some situations, there will be a possibility of live stream from Lab - by webcams or virtual simulation [18].

In accordance with aforementioned definition presented model of remote Lab is not a full-value (more or less corresponds with concept A) model of a remote Lab. The equipment (micro-hardness tester) is not operated from the user's side and the appraiser operating the tester is required on the equipment side.

The remote Lab allows dividing an appraiser hand-operating tester from evaluating process in the described experiment. The evaluation can be carried out by students during the lessons. The direct contact between the tester and the student (unless is required by his/her field of study) without a required competence and experience is excluded (the risk of the defect of expensive and sensitive equipment).

The appraiser carries out the indentations according to operating instructions (number of trials, load,

identification of indentations) in remote mode. He/she controls the place of indentation, the distance between them, the load duration time and the loading rate. He/she is not distracted by measuring of the dimensions of indentations and by recording of measured values.

The indentations are photographed one at a time or in groups (cluster or its part according to size, the indentations could be scanned on-line and transferred into PC in a remote Lab, if appropriate. The appraiser scans the gauge (calibration line standard) for calculation of actual magnification, calibration of the dimensions measuring part of software and for calculation of the uncertainty of the gauge calibration.

The user (appraiser or student) measures the dimensions of diagonals of indentations comfortably in a remote Lab and calculates the values of micro-hardness. The quality of the user can be evaluated by type of error (bias, random) using Youden plot, Z-score, Mandela's statistics, analysis of uncertainty or measurement systems analysis (MSA) [21].

EXPERIMENTAL MATERIALS AND PROCEDURES

The tester Hanemann (Mod D32) fitted to microscope Neophot-32 and reference block - certified reference material (CRM) for indirect calibration with specified hardness H_c = 242 HV0.05 and standard uncertainty u_{CRM} = 5.4 HV0.05 were used. The applying loads P were between 0.09807 N (10 g) and 0.9807 N (100 g) with a 0.09807 N step size. An appraiser performed five indentations at each load in a row.

The result was a cluster of 50 indentations in 10 rows. The load duration time was 15 seconds, the loading rate was 0.042 $N.s^{-1}$ and the ambient temperature was 19.2 °C.

Table 2. The normality (p - value), average micro-hardness value of all 50 indentation HV, micro-hardness HV0.05, "true hardness" H_{PSRc2} and relative expanded uncertainty of calibration U_{rel} (%) for direct and remote mode

Mode	Normality (p)	HV	HV0.05	H_{PSRc2}	$U_{rel\ HV0.05}$
Direct	0.2788	258	258	184	13.0
Remote 1	0.4875	248	272	150	7.3
Remote 2	0.3407	242	266	151	19.4
Remote 3	0.0626	292	306	96	36.2

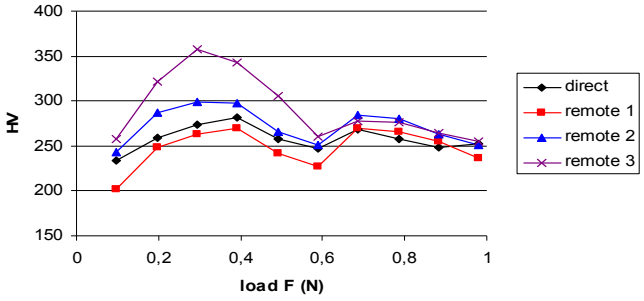

Figure 1. The values of micro-hardness

The length of two diagonals of the square-shaped Vickers indentation is measured by the appraiser immediately after each indentation with a calibrated micrometer attached to the eyepiece of microscope (magnification 480×) in direct mode. The cluster of indentations was thereafter photographed (scanned) for remote Lab (remote mode).

Computerized methods used software ImageJ in mode "remote 1" for measuring the indentation area and software TechDig. 1.1.b in mode "remote 2" for measuring of the diagonals. The diagonals on the hard copy of indentations were measured by slide caliper (scale division 0.01 mm) in mode "remote 3".

The normality (p - value), average micro-hardness value of all 50 indentation HV, micro-hardness HV0.05 and relative expanded uncertainty of calibration U_{rel} (in %, k = 2) for direct and remote mode are in tab. 1. The values of micro-hardness, measured at particular loads are in Fig 1 and the box-plots in Fig. 2. The results of calibration were used for calculation of relative expanded (k = 2) uncertainty U of the hardness values (in %), Fig. 3. The maximum value of U_{rel} is 10 % according to standard [22], only the mode "remote 1" match this requirement. The uncertainty depends on the mode and dencreases with increasing load. The ambiguity in the measurement of small indentation areas, particularly with pile-up or sink-in effects, results in over- or underestimation of the indentation area [23]. The remote mode simplifies the measurement of such indentations. The value of uncertainty obtained in remote mode is nevertheless higher in comparison with direct mode (except for "remote 1").

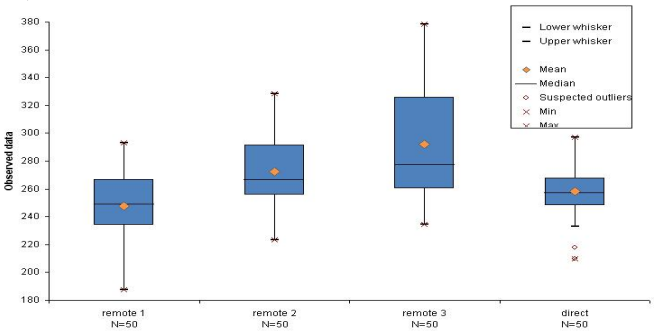

Figure 2. The box plot

It is necessary to remember that indirect calibration of micro-hardness testers is not routinely practiced process, unlike the (macro)hardness testers. Small dimensions of indentations diagonals and indentations with irregular shape are measured with difficulty. Small difference in reading of diagonals has a significant effect on the obtained (measured) value of micro-hardness and is a source of possible influence of appraiser's individuality and skill [24]. It is possible that high value of uncertainty of calibration is a result of low capability (high value of index %GRR, obtained by MSA analysis) [25].

Grubbs' test (significance level a = 0.05) was used for detection of statistical outliers. Their presence would indicate measurement process suffering from special disturbances and out of statistical control. The normality was determined by Freeware Process Capability Calculator software (Anderson - Darling test). The normality and the outliers were determined for particular clusters (50 indentations obtained in particular modes). As it can be seen in tab. 2, the normality was confirmed for all files. Absence of outliers suggests that the measurement process has avoided the gross errors.

According to the two factor ANOVA (Analysis of Variance) without replication the mode ($p = 2.79.10^{-6}$) and the load ($p = 1.06.10^{-5}$) have statistically

significant effect on the value of measured micro-hardness.

The values of p of unpaired t-test, comparing the means of two groups (a = 95%) are in tab. 3. By conventional criteria, this difference is considered statistically significant between all modes. According to one sample t test the difference between the mean micro-hardness measured in particular modes (HV in tab. 1) and an expected value - standard hardness of CRM (H_c = 242 HV0.05) is statistically significant for all modes except for "remote 1".

Table 3. The values p of unpaired t-test.

	direct	remote 1	remote 2
remote 3	0.0001	0.0001	0.0032
remote 2	0.0009	0.0001	-
remote 1	0.0222	-	-

EVALUATION OF THE INFLUENCE OF THE LOAD ON THE MICRO- HARDNESS - Meyer's Power Law

The simplest way to describe the ISE is Meyer's Law:

$$P = Ad^n \qquad (1)$$

The parameters n and A_{ln} are determined from a straight line graph of ln d (mm) versus ln P (N). Meyer's index n (work hardening coefficient) is the slope and A_{ln} is the y-intercept of the straight line, tab. 3.

When n=2, the micro-hardness is independent of the applied load and is given by Kick's Law. However, n<2 indicated "normal" ISE behavior, the measured micro-hardness decreases with applied load. When n>2, there is the reverse ISE behavior, measured micro-hardness increases with increasing of the load.

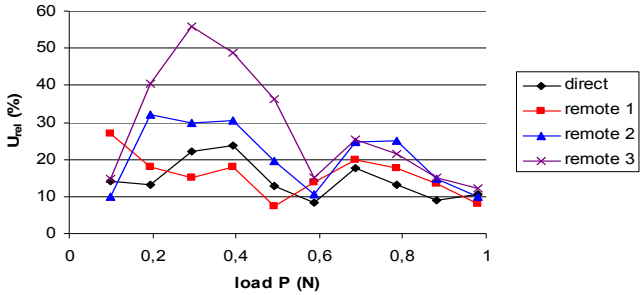

Figure 3. The values of expanded uncertainty u for particular loads and measurements

Table 3. The values of Meyer's index n and indices A_{ln}, c_0, c_1, c_2 for direct and remote mode.

mode	n	A_{ln}	c_0	c_1	c_2	c_1/c_2
direct	2.0209	7.3000	-0.9220	12.859	974.08	0.013
remote 1	2.1151	7.6304	-0.1620	19.435	792.50	0.025
remote 2	1.9846	7.2053	-0.1354	19.996	796.83	0.025
remote 3	1.8589	6.7591	-0.1645	28.576	506.83	0.056

The curves load vs. micro-hardness shows that the micro-hardness increases with load nonlinearly up tol about 0.5 N for the all modes and then remains practically constant (Fig. 1). The values of n, calculated in direct mode (n = 2.0209) and "remote 2" (n = 1.9846) practically confirm independence of the micro-hardness on load.

PSR (Proportional Specimen Resistance model) and modified PSR

Several authors [6, 8, 13] have proposed that ISE behavior may be described by the Eq. (2):

$$P = c_1 d + c_2 d^2 \qquad (2)$$

Gong et al. [2, 6] used an energy balance approach to examine the ISE and rearanged Eq. (2) into modified form of the PSR:

$$P = c_0 + c_1 d + c_2 d^2 \qquad (3)$$

The values of constants c_0 (N), c_1 (N mm^{-1}) and c_2 (N mm^{-2}) of Eq. (3), obtained from the quadratic polynomial regressions of P/d (N mm^{-1}) against d (mm) are given in tab. 3. The parameter c_1 characterises the load dependence of micro-hardness (elastic properties). It consists of the elastic resistance of the test specimen and the friction resistance developed at the indenter facet/specimen interface [12, 13, 26].

The parameter c_2 may be a measure of the load-independent micro-hardness (plastic properties) sometimes referred to as "true hardness" H_{PSR} = 0.1891c_2. As can be seen in tab. 2, the "true hardness" is signifficantly less the measured hardness (HV 0.05 and HV) for all modes. The ratio c_1/c_2 may be treated approximately as a measure of the residual stresses due to machining and polishing [6, 27].

CONCLUSIONS

The differencies between direct and remote mode are statistically significant as far as measured values of micro-hardness but also uncertainty and indices, obtained by Meyer's and PSR methods. However, the differences are also beween particular remote modes. The influence of the load expressed by value of Meyer's index n was different for individual modes despite the identical specimen and equipment.

The relationship between differencies would be optimal, of course. It is possible, that observed difference is the result of raising uncertainty of measured values of the micro-hardness at low loads which partly obscures the occurrence and type of ISE.

Further research will be focused on preparation of factual and generalized knowledge about creative laboratory teaching at Higher Education Institution technical faculties especially in the field of Production Quality, especially: design, realization and work methods in Creative Laboratory Tuition at Technical Faculties (CRELABTE).

It is necessary to analyze the influence of repeatability, reproducibility, individual appraisers, methods of indentations diagonals measuring and other factors on the differences between modes at the same time. The results will be used for the improvement of analyzed system of Lab.

ACKNOWLEDGEMENTS

This work was supported by the Slovak Grant Agency for Science KEGA 009TnUAD-4/2011.

REFERENCES

[1] Cai, X. Yang, X., Zhou, P.: Journal of Materials Science Letters, Vol. 16, 1997, p. 741-742.
[2] Sargent, P.M.: Use of Indentation Size Effect on Microhardness for Material Characterization, first ed., ASTM, Philadelphia, 1985.
[3] Golan, G. et al: Journal of Optoelectronics and Advanced Materials. Vol. 2, 2000, No. 4, p. 317-325.
[4] Layar, S., Selvarajan.: Recent Research in Science and Technology, Vol. 2, 2010, No. 10, p. 77-81.
[5] Kumar, A. R. Kalainathan, S.: Journal of Physics and Chemistry of Solids., Vol. 71, 2010, p. 1411-1415.

[6] Gong, J., Wu, J., Zh. Guan, , Zh.: Journal of the European Ceramic Society, Vol. 19, 1999, No. 15, p. 2625-2631.
[7] Sangwal, K., Surowska, B., Błaziak, P.: Materials Chemistry and Physics, Vol. 77, 2002, No. 2, p. 511-520.
[8] Ren, X. J., Hooper, R. M., Griffiths, C.: Journal of Materials Science Letters, Vol. 22, 2003, No. 15, 1105-6.
[9] Sangwal, K.: Materials Chemistry and Physics, Vol. 63, 2000, No. 2, p. 145-152.
[10] Navrátil, V., Novotná, J.: Journal of Applied Mathematics. Vol. 2, 2009, No. 3, 241-244.
[11] ISO10012:2003 Measurement management systems - Requirements for measurement processes and measuring equipment.
[12] International Vocabulary of Basic and General Terms in Metrology, ISO, Geneva, 1993.
[13] Benmohamed, H., Leleve, A., Prevot, P.: Remote Laboratories: New Technology and Standard Based Architecture. [online]. [cited 29 November 2012]. Available from: http://arxiv.org/ftp/arxiv/papers/0706/0706.2974.pdf
[14] [online]. [cited 28 January 2013]. Available from: http://editlib.org/noaccess/38402.
[15] A. Ferrero, A., Piuri, V.: A Simulation Tool for Virtual Laboratory Experiments in A WWW Environment, IEEE Instrumentation and Measurement Technology Conference, St. Paul, Minnesota, USA, May 18-21,1998.
[16] [16] Wuttke, H.D., Henke, K., Ludwig, N.: Remote Labs versus Virtual Labs for Teaching Digital System. [online]. [cited 28 January 2013]. Available from: http://ecet.ecs.ru.acad.bg/cst05/Docs/cp/sIV/IV.2.pdf
[17] Abu-aisheh, A. A.: Implementation of Virtual and Remote Laboratiries to improve the Quality of Engineering Education in the Palestinian Universities and Community Colleges. [online].[cited 28 January 2013]. Available from: http://www.paleng.org/cons/papers/implementation%20of%20virtual%20and%20remote%20laboratories%20to%20improve%20the%20quality%20of%20engineering%20eduaction%20in%20the%20pala.pdf
[18] Zgodavová, K., Zolotova, I., Roznik, J.: Creative Laboratory Engineering Education at Technical Faculties. The 14th International Conference on Interactive Collaborative learning (ICL 2011), 21-23. 9. 2011 Piešťany, p. 632-636.
[19] [online]. [cited 3 October 2012]. Available from: http://www.rmit.edu.au/browse/Staff%2FLearning%20and%20Teaching%2FSupport%20and%20resouces%2FTeaching%20technologies%2FRemote%20laboratories/
[20] Auer, M. E.: Virtual Lab versus Remote Lab. [online]. [cited 28 January 2013]. Available from: http://www.eu-lab.net/rel/documents/auer_icde.pdf
[21] Petrík, J. et al.: Acta Metallurgica Slovaca, Vol. 16, 2010, No. 1, p. 50-57.
[22] EN ISO 6507-2:2005 Metallic materials. Vickers hardness test. Part 2: Verification and calibration of testing machines.
[23] Chanya, Ch., Pojjanut, B., Paitoon, D.: Materials Research, Vol. 12, 2009, No. 4, 473-476.
[24] Tobolski, E., Advanced materials & processes, Vol. 161, 2003, No. 5, p. 25-27.
[25] Measurement systems analysis (MSA). Reference manual. 2010.
[26] Kim, H., Kim, T.: Journal of the European Ceramic Society, Vol. 22 2002, No. 9-10, p. 1437-1445.
[27] Machaka, R. et al.: Analysis of the indentation size effect in the microhardness measurements in B_6O. [online]. [cited 29 November 2012]. Available from: http://www.hindawi.com/journals/amse/2011/539252

ACTA TECHNICA CORVINIENSIS - BULLETIN of ENGINEERING

ISSN: 2067-3809 [CD-Rom, online]

ACTA TECHNICA CORVINIENSIS - BULLETIN of ENGINEERING

ISSN: 2067-3809 [CD-Rom, online]

ACTA TECHNICA CORVINIENSIS - BULLETIN of ENGINEERING

ISSN: 2067-3809 [CD-Rom, online]

copyright © UNIVERSITY POLITEHNICA TIMISOARA,
FACULTY OF ENGINEERING HUNEDOARA,
5, REVOLUTIEI, 331128, HUNEDOARA, ROMANIA
http://acta.fih.upt.ro

ACTA TECHNICA CORVINIENSIS – Bulletin of Engineering
Tome VI (Year 2013) – FASCICULE 4 [October–December]
ISSN 2067–3809

[1.] Mirela C. GHIȚĂ, [2.] Constantin A. MICU, [3.] Mihai D.L. ȚĂLU, [4.] Ștefan D.L. ȚĂLU

3D MODELLING OF A SHRINK FITTED CONCAVE ENDED CYLINDRICAL TANK FOR AUTOMOTIVE INDUSTRY

[1.] "Spiru Haret" University Of Craiova, Faculty Of Management, ROMANIA
[2.] University Politehnica Of Bucharest, Faculty Of Mechanical Engineering And Mechatronics, ROMANIA
[3.] University Of Craiova, Faculty Of Mechanical Engineering, Department Of Applied Mechanics, ROMANIA
[4.] Technical University Of Cluj-Napoca, Faculty Of Mechanical Engineering, Department Of Automotive Engineering And Transports, ROMANIA

Abstract: The aim of this work is to present a method that allows the optimal design of a shrink fitted concave ended cylindrical tank for the storage of methane gas, based on the application of the Finite Element Method (FEM). This paper presents a methodology for the optimal shape design of a shrink fitted concave ended cylindrical tank for the automotive industry using the FEM and which is based on a specialized database of 3D parameterized shapes. The mechanical simulation, numerical calculations and geometrical modeling were applied for the three-dimensional complex models
Keywords: engineering design, methane gas tank, optimization, Finite Element Method

INTRODUCTION

Over the past few decades, important efforts have been made to develop and implement engineering design guidelines, construction and maintenance standards, and specifications for gas tanks used in the automotive industry, including standardized test methods [1-6].

In order to provide a better understanding of the gas tank design, optimization, reliability and manufacturing feasibility, the research efforts have been focused towards new, convergent, stable and robust CAD algorithms for obtaining the optimal solution [1-6].

THE OPTIMIZATION METHOD

This paper presents a methodology for the optimal shape design of a shrink fitted concave ended cylindrical tank for the automotive industry using the FEM and which is based on a specialized database of 3D parameterized shapes. The mechanical simulation, numerical calculations and geometrical modeling were applied for the three-dimensional complex models [7-21].

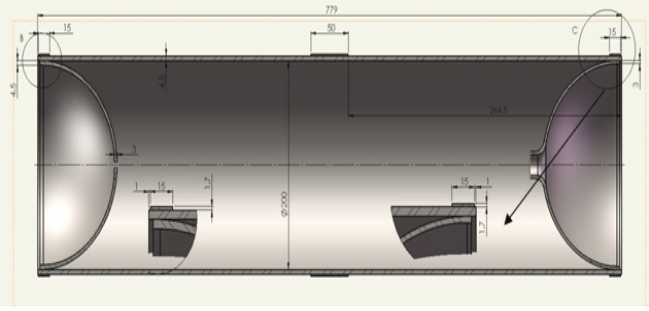

Figure 1. Constructive shape of a shrink fitted concave ended cylindrical tank

A gas tank for the automotive industry is made of three elements: a lateral one, an end up and a bottom one (Fig. 1). The elements are assembled afterwards to get the final form of the gas tank cover. A new analysis of the efforts and deformation states is done afterwards and the surety coefficient value is calculated and compared to the admissible value.

Further to consecutive optimizations, a shrink fitted cylinder with 3 rings (at the ends and around the middle of the tank) was chosen (Fig. 1). The volume of the gas tank is about 20 l.

THE FINITE ELEMENT ANALYSIS OF A SHRINK FITTED CONCAVE ENDED CYLINDRICAL TANK

The Finite Element Analysis is a practical application of the finite element method (FEM), and can be used by engineers to mathematically model and numerically solve the complex structural problems of the gas tank [22].

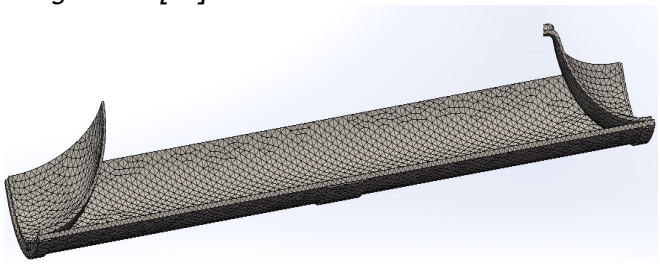

Figure 2. The finite element discretization of the model

The Finite element discretization of the 3D model is shown in Fig. 2. The pressure (distributed on all inner surfaces of the tank) and constraints (symmetry and roller slider) used in the finite element analysis are shown in Fig. 3.

For mathematical calculations, we use the following input data:
- maximum test pressure: p_h = 30 N/mm^2;
- normal range of working temperature: T= -40 ^{0}C,..., +60 ^{0}C;
- type of gas tank cover material: AISI 4340;
- value of gas tank cover diameter: ϕ = 200 mm.

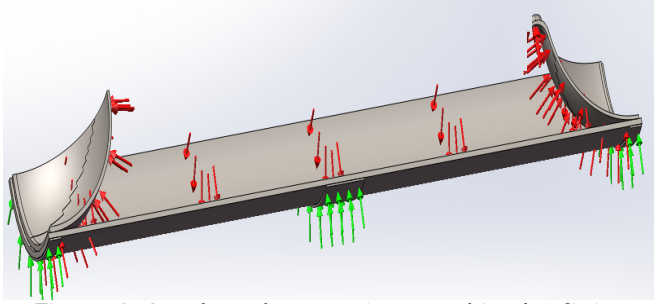

Figure 3. Loads and constraints used in the finite element analysis

Applying the finite element analysis to the 3D model, with the SolidWorks 2011 software [23], the results which are shown in Figs. 4-23 were obtained.

Analysis of the unpenetrated lid end tank

For the unpenetrated lid, the curves are symbolized by A - B and B - C. "e" index is used to define the curve on the exterior of the body, while "i" index is used to define the curve on the interior of the body. Effort variation on the inner and outer surfaces of the unpenetrated lid is shown in Figs 4-5.

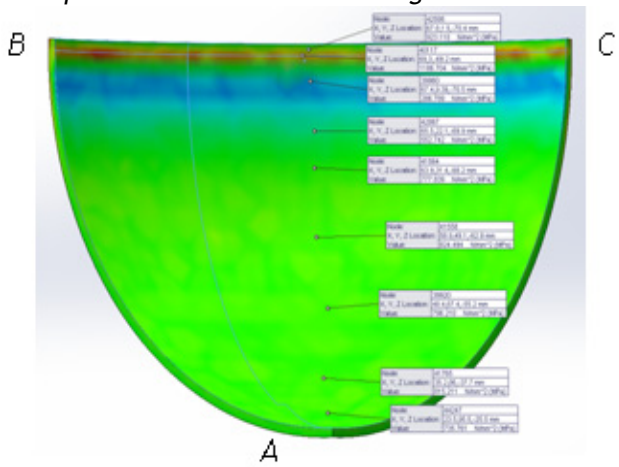

Figure 4. Effort variation on the inner surface of the unpenetrated lid

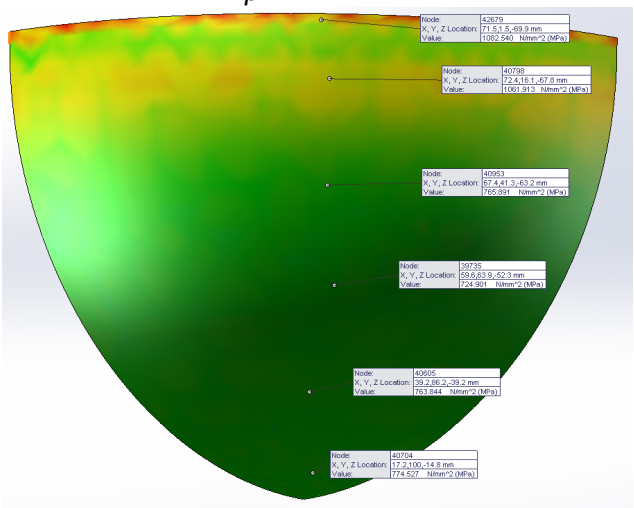

Figure 5. Effort variation on outer surface of the unpenetrated lid

The distribution of the efforts along the A - B curves is given in Figs. 6-7.

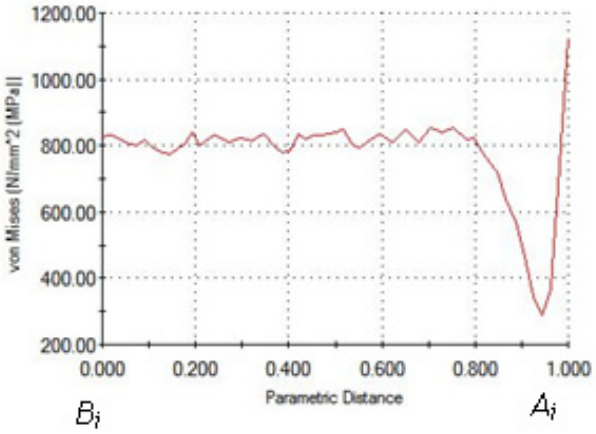

Figure 6. Graphical representation of efforts along the A_i - B_i curve for the unpenetrated lid

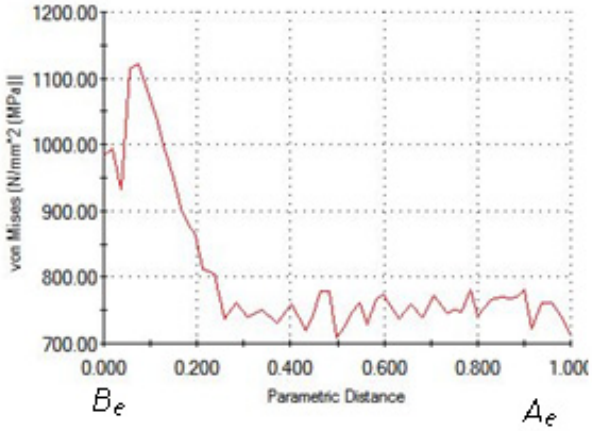

Figure 7. Graphical representation of efforts along the A_e - B_e curve for the unpenetrated lid

Based on the distribution of efforts on the external side (Fig. 7), a maximum value of effort is obtained at about 3.5 mm distance from the unpenetrated lid. Let us note this curve with D - E, keeping the same indexes "e" and "i" (Fig. 8) and let us trace the graphical variation of efforts (Figs. 9-10).

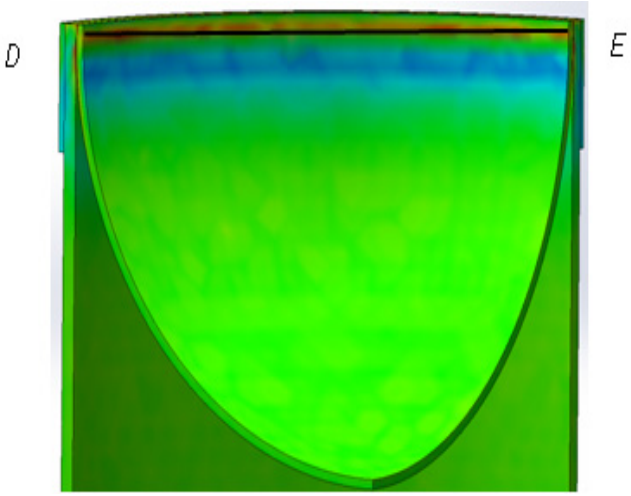

Figure 8. D - E curve, used to analyze the effort variation for the unpenetrated lid

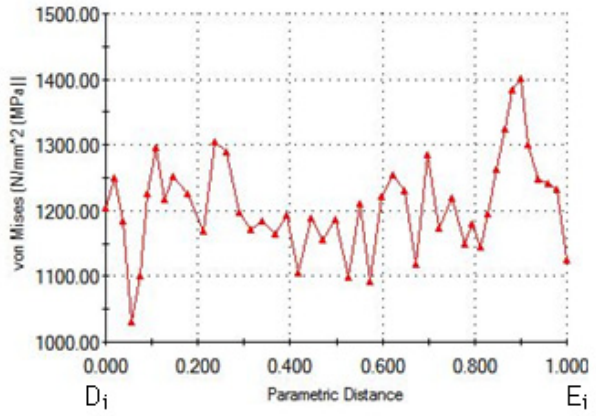

Figure 9. Graphical representation of the efforts along the D_i - E_i curve for the unpenetrated lid

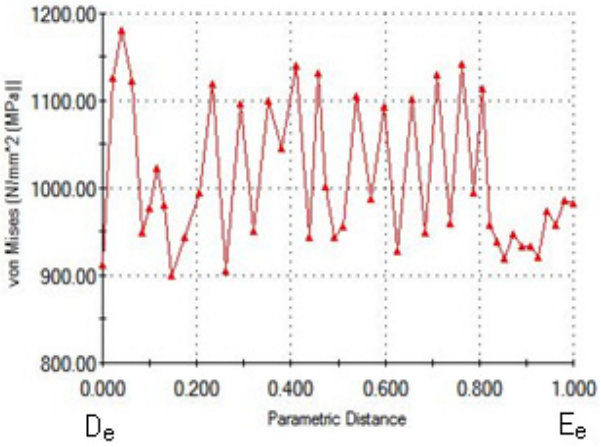

Figure 10. Graphical representation of the efforts along the D_e - E_e curve for the unpenetrated lid

Analysis of the penetrated lid end tank

For the penetrated lid, the curves are symbolized with A - B and B - C. "e" index is used to define a curve on the exterior of the body, while "i" index is used to define a curve on the interior of the body. Effort variation on the inner and outer surfaces of the penetrated lid is shown in Figs. 11-12.

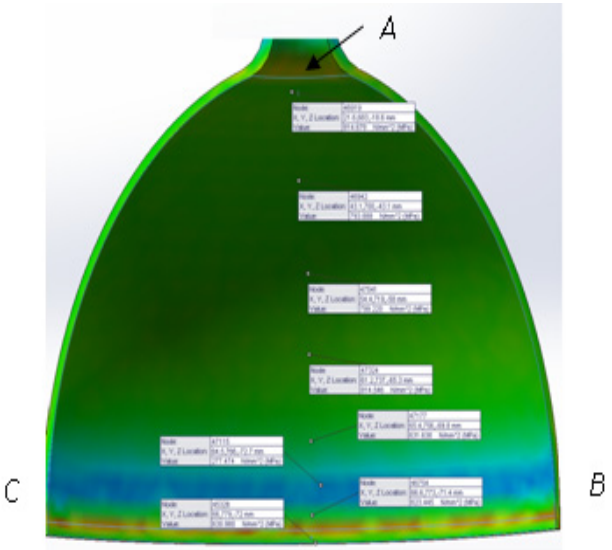

Figure 11. Effort variation on the inner surface of the penetrated lid

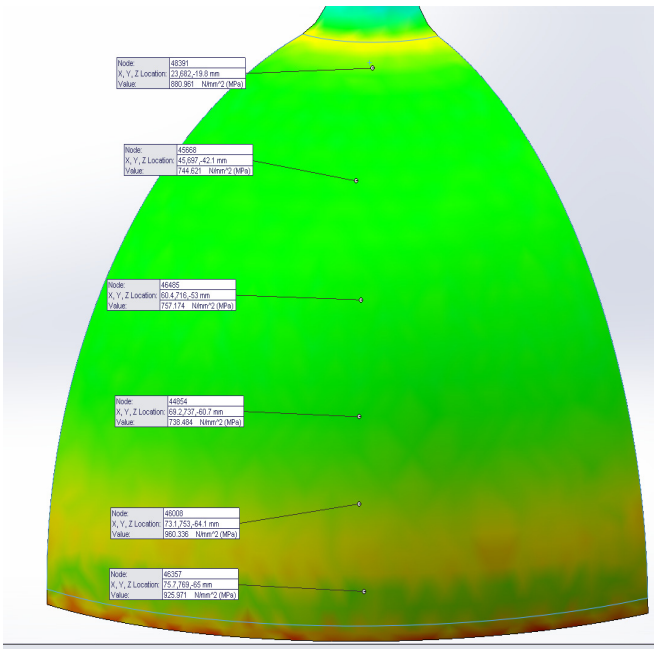

Figure 12. Effort variation on the outer surface of the penetrated lid

The effort distribution along the A - B curves is shown in Figs. 13-14.

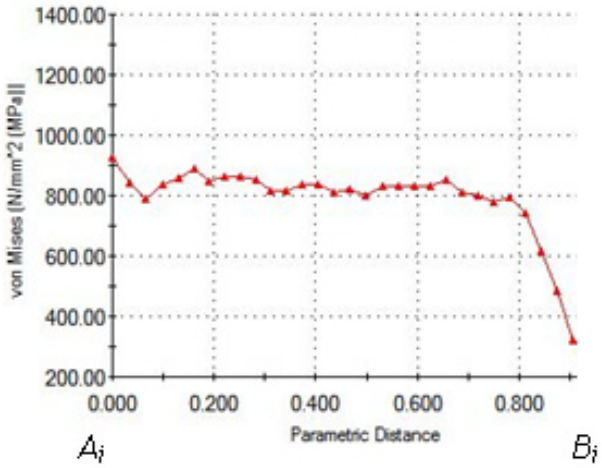

Figure 13. Graphical representation of efforts along the A_i - B_i curve for the penetrated lid

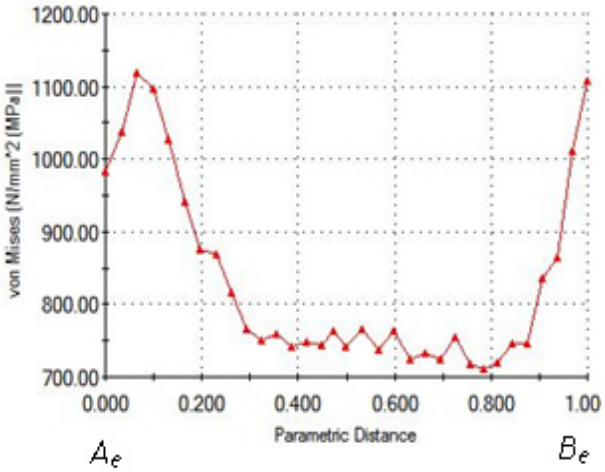

Figure 14. Graphical representation of efforts along the A_e - B_e curve for the penetrated lid

The effort distribution along the B - C curves is shown in Figs. 15-16.

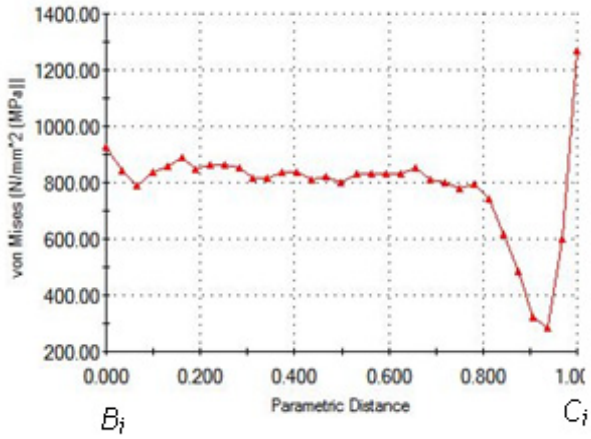

Figure 15. Graphical representation of efforts along the B_i - C_i curve for the penetrated lid

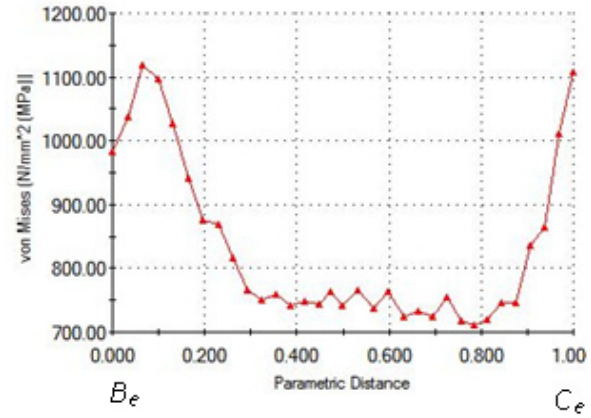

Figure 16. Graphical representation of efforts along the B_e - C_e curve for the penetrated lid

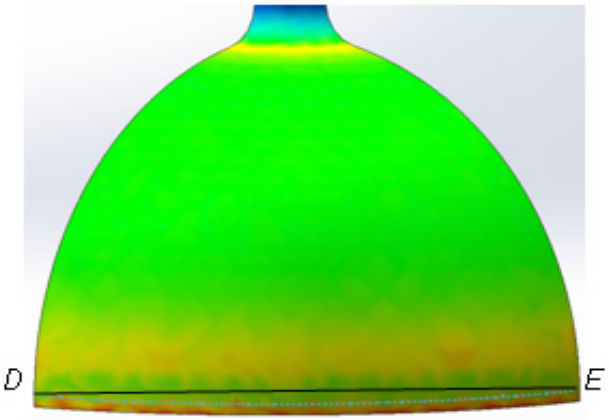

Figure 17. D - E curve, used to analyze the effort variation for the penetrated lid

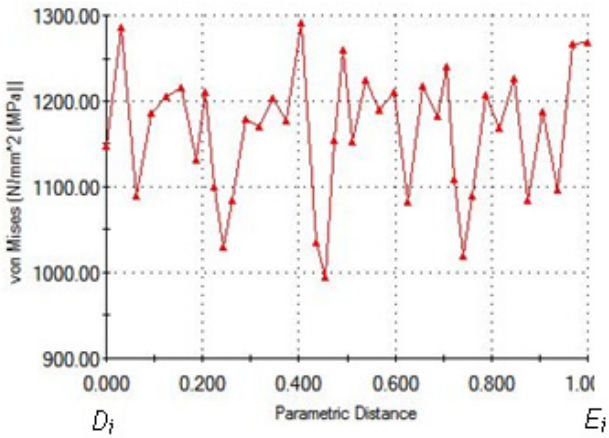

Figure 18. Graphical representation of efforts along the D_i - E_i curve for the penetrated lid

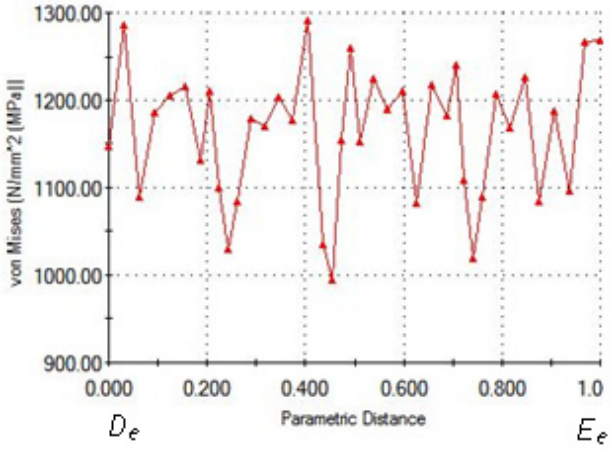

Figure 19. Graphical representation of the efforts along the D_e - E_e curve for the penetrated lid

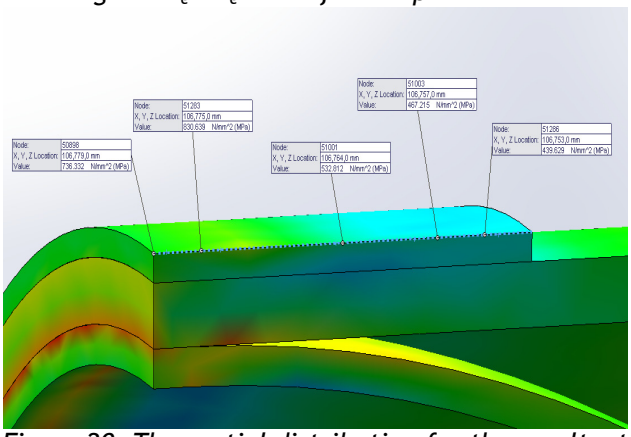

Figure 20. The spatial distribution for the resultant efforts on the shrink end ring

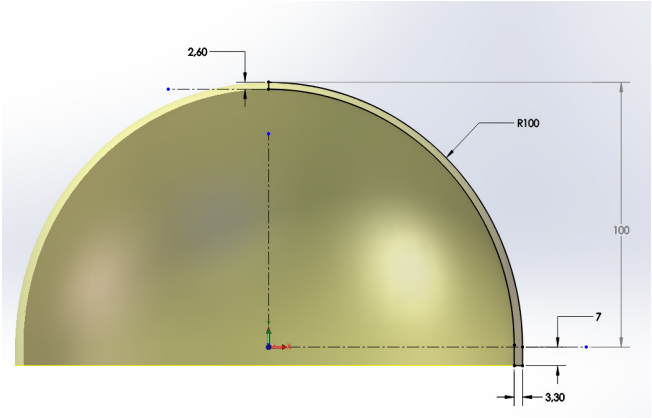

Figure 21. Constructive shape for the unpenetrated lid

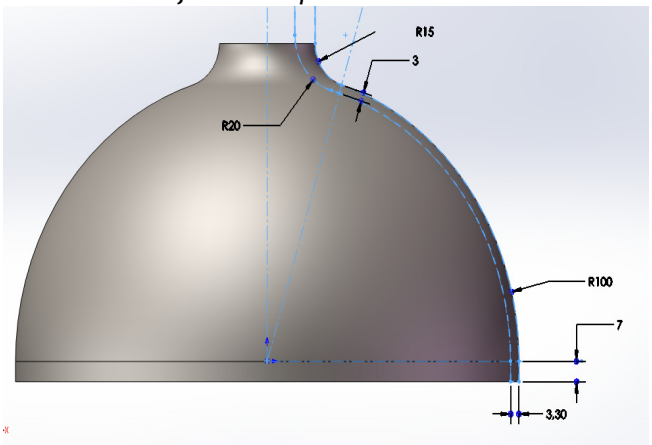

Figure 22. Constructive shape for the penetrated lid

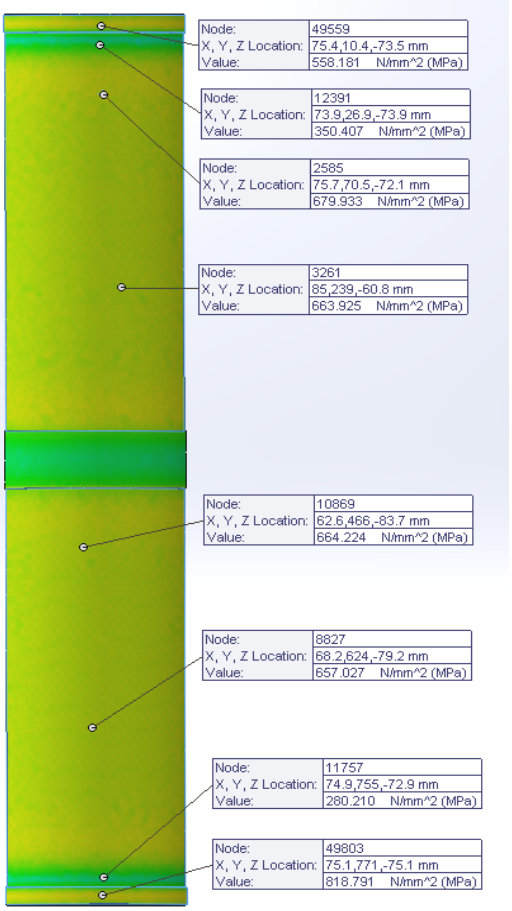

a)

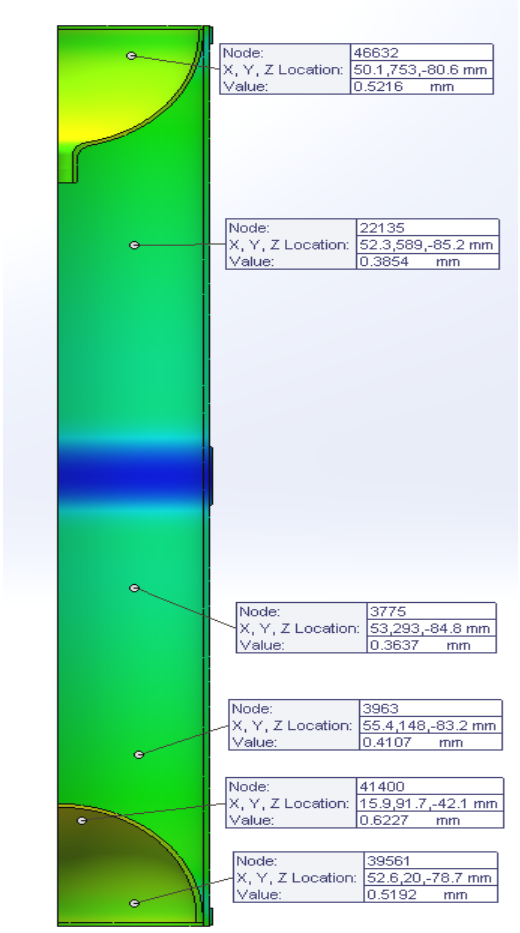

b)

Figure 23. The spatial distribution for T = 65 ^{0}C and p_h = 35.2 N/mm^2: a) the resultant efforts state von Mises; b) the linear resultant deformations

CONCLUSIONS

The resultant efforts state von Mises and the linear resultant deformations agree well with those derived from the experimental measurements. To validate the theoretical results, a reduced scale gas tank was built and tested with full pressure on a special test stand.

REFERENCES

[1] *Shr-Hung, C., Master's Thesis: Novel design and optimization of vehicle's natural gas fuel tank, Ohio University, USA, 1997.*

[2] *Cavaropol, D.V., Elemente de dinamica gazelor: Instalatii de GPL sI GNL, Ed. Ministerului Internelor si Reformei Administrative, Bucuresti, 2008.*

[3] *Lisowski, E., Czyzycki, W., Transport and storage of LNG in container tanks, Journal of KONES Powertrain and Transport, vol. 18, no. 3, 2011, pp. 193-201.*

[4] *Ghiță, M.C., Micu, A.C., Țălu, M., Țălu, Ș., Shape optimization of vehicle's methane gas tank, ANNALS of Faculty of Engineering Hunedoara - International Journal of Engineering, Hunedoara, Tome X, Fasc. 3, 2012, pp. 259-266.*

[5] *Ghiță, M.C., Micu, A.C., Țălu, M., Țălu, Ș., Shape optimization of a thoroidal methane gas tank for automotive industry. ANNALS of Faculty of Engineering Hunedoara - International Journal of Engineering, Hunedoara, Tome X, Fasc. 3, 2012, p. 295-297.*

[6] *Benton, J., Ballinger, I., Ferretti, A., Ierardo, N., Design and manufacture of a high performance, high mass efficient gas tank for the VEGA AVUM, AIAA-2007-5500, pp. 1-14.*

[7] *Bîrleanu, C., Țălu, Ș., Organe de mașini. Proiectare și reprezentare grafică asistată de calculator, Editura Victor Melenti, Cluj-Napoca, 2001.*

[8] *Nițulescu, T., Țălu, Ș., Aplicații ale geometriei descriptive și graficii asistate de calculator în desenul industrial, Editura Risoprint, Cluj-Napoca, 2001.*

[9] *Dumitru, N., Margine, A., Organe de mașini. Asamblări. Elemente elastice. Proiectare asistată de calculator. Editura Universitaria, Craiova, 2002.*

[10] *Dumitru, N., Margine, A., Bazele modelării în ingineria mecanică, Editura Universitaria, Craiova, 2002.*

[11] *Florescu-Gligore, A., Țălu, Ș., Noveanu, D., Reprezentarea și vizualizarea formelor geometrice în desenul industrial, Editura U. T. Pres, Cluj-Napoca, 2006.*

[12] *Țălu, Ș., AutoCAD 2005, Editura Risoprint, Cluj-Napoca, 2005.*

[13] *Țălu, Ș., Țălu, M., AutoCAD 2006. Proiectare tridimensională, Editura MEGA, Cluj-Napoca, 2007.*

[14] *Țălu, Ș., Racocea, C., Reprezentări axonometrice cu aplicații în tehnică, Editura MEGA, Cluj-Napoca, 2007.*

[15] *Țălu, Ș., Geometrie descriptivă, Editura Risoprint, Cluj-Napoca, 2010.*

[16] *Ţălu, Ş., Ţălu, M., A CAD study on generating of 2D supershapes in different coordinate systems, ANNALS of Faculty of Engineering Hunedoara - International Journal of Engineering, Hunedoara, Tome VIII, Fasc. 3, 2010, pp. 201-203.*

[17] *Ţălu, Ş., Ţălu, M., CAD generating of 3D supershapes in different coordinate systems., ANNALS of Faculty of Engineering Hunedoara - International Journal of Engineering, Hunedoara, Tome VIII, Fasc. 3, 2010, pp. 215-219.*

[18] *Racocea, C., Ţălu, Ş., Reprezentarea formelor geometrice tehnice în axonometrie, Editura Napoca Star, Cluj-Napoca, 2011.*

[19] *Ţălu, Ş., Study on the construction of complex 3D shapes with superellipsoids and supertoroids, ANNALS of Faculty of Engineering Hunedoara - International Journal of Engineering, Hunedoara, Tome IX, Fasc. 3, 2011, pp. 299-302.*

[20] *Ţălu, Ş., CAD representations of 3D shapes with superellipsoids and convex polyhedrons, ANNALS of Faculty of Engineering Hunedoara - International Journal of Engineering, Hunedoara, Tome IX, Fasc. 3, 2011, pp. 349-352.*

[21] *Ţălu, Ş., Complex 3D shapes with superellipsoids, supertoroids and convex polyhedrons, Journal of Engineering Studies and Research, Bacău, vol. 17, no. 4, 2011, pp. 96-100.*

[22] *Fenner, R.., Finite Element Methods For Engineers, Imperial College Press, 2nd Edition, UK, 2012*

[23] *SolidWorks 3D CAD Design, User Guide, SolidWorks Corporation, 2011.*

ACTA TECHNICA CORVINIENSIS - BULLETIN of ENGINEERING

ISSN: 2067-3809 [CD-Rom, online]

ACTA TECHNICA CORVINIENSIS – Bulletin of Engineering
Tome VI (Year 2013) – FASCICULE 4 [October–December]
ISSN 2067–3809

[1.] Péter SZUCHY

DELINEATION OF ABRASIVE WEAR TESTING EQUIPMENTS

[1.] TECHNICAL INSTITUTE, FACULTY OF ENGINEERING, UNIVERSITY OF SZEGED, HUNGARY

ABSTRACT: When we are testing the wear we have to measure the loss of the tested material with the same testing circumstances that cannot be easily ensured. Therefore a relative abrasion resistance is usually measured (wear of an etalon material / wear of the tested material). When somebody searches abrasive wearing properties, it is always a significant question, how to select appropriate wear testing equipment. If the chosen method is the model testing of simple specimens, lots of obtainable tribotesters will be found on the market, and there is a good chance for developing one, too. Many well-designed testing machines exist and are available. For classification my chosen main aggregate is the movement of the specimen. Here is a short summary of the advantages and disadvantages of the different kind of abrasive wear testers where the contact surfaces of the worn and the abrasive materials have relative speed difference.
KEYWORDS: Wear, wearing test, tribotester

INTRODUCTION - ABRASIVE WEAR

What is wear? Material particles are separating step by step from the interacting, frictioning surfaces as a result of the mechanical, thermal and chemical stresses. Several wearing types are named: abrasive wear, fatigue wear, tribochemical wear, cavitation wear, etc., but abrasive wear is the most common wearing type in the technical practice. In the course of abrasive wear between the surfaces moving on each other the peaks of the harder material gouges grooves into the softer material, peeling some material, so it is a groove-proceeding process (appearances: craters, scores, scratches, scrape traces). Typical occurring area: active tools of agricultural machines (e.g. plough). [1]

When we are testing the wear we have to measure the loss of the tested material with the same testing circumstances that cannot be easily ensured. Therefore a relative abrasion resistance is usually measured (wear of an etalon material / wear of the tested material).

The abrasion resistance (AR) hangs on many factors and circumstances but two material-features have to be highlighted [3.]:

- AR is related linearly to the hardness of the material. AR can be increased significantly better by alloying softened metals than hardening by heat treatment.
- AR is influenced by the modulus of elasticity (Young-modul). The tougher material the more resistant.

Influence of the wearing material [2]

- Hardness: If the hardness of the abrasion grain is at least twice of the worn material's than occurs mainly abrasion wear. As it decreases, the abrasion wearing effect decreases too. From experience: the rate of the wear is not influenced if the hardness of the grain is more than 50% harder than the worn material.
- Brittle grain: when the grain breaks easily that decreases the wear on one hand because of the smaller grain size, on the other hand increases the wear due to the sharp ledges of the fresh break of grain.
- Grain size: the smaller then 10μm grains' abrasion effect is minor, as the size grows, the wear increases, degressive heading to a limited value.
- Shape: the influence of the shape is hardly traceable.

ABRASIVE WEAR TESTING EQUIPMENTS

Many well-designed testing machines exist and are available. For classification my chosen main aggregate is the movement of the specimen.

Moving specimens: „sand-slurry" equipments

These are rather real-life than scale models and these rigs are mostly self-designed constructions. It gives opportunity to test the real abrasive material (e.g. agricultural use). Successful tests rely on close control of the abrasive material's features (particle size, shape, toughness and their fracture) and the contact temperature.[5]

The main difference is the driven path of the specimen:

1. Rotating movement: barrel / drum design. Simple, space-saving construction, where the specimen is rotated around a fixed, vertical shaft, in a standing cylinder-shaped vessel filled with abrasive material.

2. *Rectilinear movement: trough design. The specimen is driven straight in a long trough filled with abrasive material. It needs more place and cost than the previous design but the movement resembles more to the real circumstances (e.g. plough). It is not introduced through an example below.*

Fixed specimens

These machines are widely used because they are cost-effective. In each case the specimen geometry is simple and relatively easy and cheap to manufacture. Their principal advantage is that it is easy to cover wide load and speed ranges. Former there were rather three-body abrasion testers, where the stationary specimen was loaded against a rotating body with non- or recirculated abrasive particles introduced into the contact. Nowadays the two-body testers come to the front, where the abrasive particles are mounted on a carrying surface (e.g. abrasive paper). Here the main problem is how to ensure the stationary conditions of the abrasion (contact temperature, abrasive particles).[5]

The classification is driven by the principle of the contact:

1. *Ball-plane contact:*
   a. *fixed-ball,*
   b. *rolling ball,*
   c. *rambling ball tribotesters*
2. *Cylinder-plane contact*
3. *Plane-plane contact: Pin-on-disk equipment*
4. *Cylinder-cylinder contact*

The advantages and disadvantages are introduced by the following samples.

Modified sand-slurry tribotester

The following equipment was developed by SZIE Gépipari Technológia Intézet for testing hot-dip galvanized elements. [2]

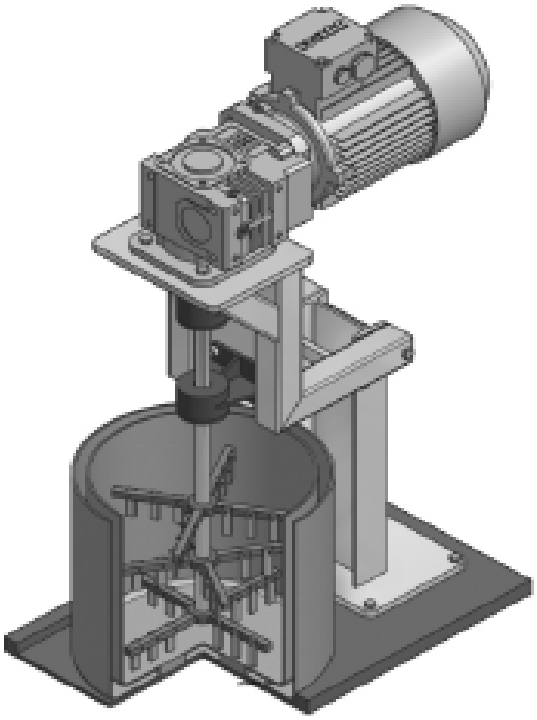

Figure 1. Modified san-slurry tribotester [2]

Advantages:

- *Fast comparing tests for simple specimens.*
- *Testing by different speed and pressure circumstances.*
- *In this model there is a double wall drum filled with cooling liquid, so the heat circumstances can be influenced.*

Problems:

- *Heat cumulating due to friction - cooling of the system is tough. Only low speed can be used or only a few specimens can be tested side by side.*
- *The abrasive medium is susceptible to stratification that leads higher drag in the lower stratum.*
- *The system is sensible to the applied abrasive medium (mould can burn on the worn surface, grain size influence the heat).*
- *The steady conditions are hard to be ensured during the test (grain break, making even the former way's trace, pressure conditions).*

Fixed-ball tribotester

The abrasive ball is fixed in a holder and loaded onto the rotating disk's surface. An increasingly deeper and wider crater comes into existence on the surface of the disk. By a steady load as the crater becomes deeper, the contact pressure increases, so the surface pressure decreases. During the wearing process the shape and roughness of the ball changes significantly. The fixed-ball tribotester is used rather for short time experiment and needs practice to evaluate right the wear picture. [4]

I have not found an example for adding plus abrasive medium to the system.

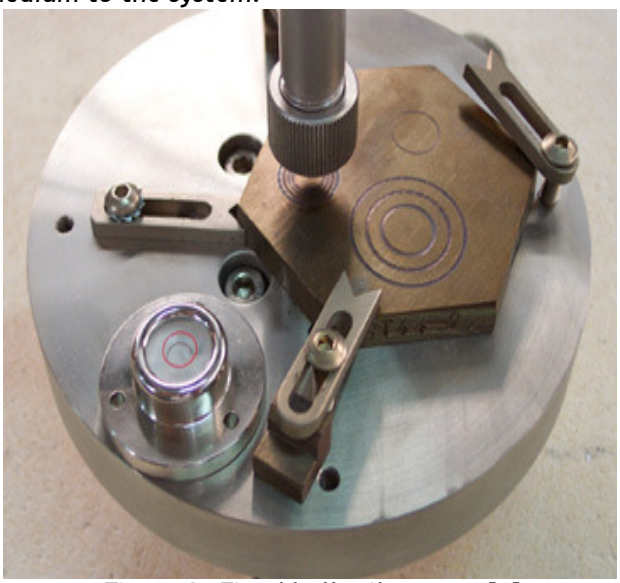

Figure 2. Fixed ball tribotester [6]

Rolling-ball tribometer

The specimen is fixed and loaded to the rotating ball. The ball is fixed on a driving shaft, and abrasive medium is poured between the contacting surfaces. If the abrasive medium is non-recirculated that ensures steadier conditions in the contact.

As the wear progresses it causes higher touching surfaces that decreases the force per unit of surface. [1, 6]

We have to count with the change of the ball's shape too, since the contact is localized on a narrow strip of the ball, so the contact line becomes wider as time passes.

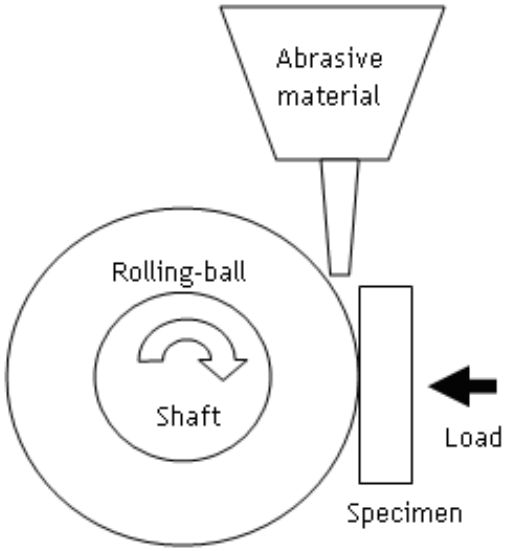

Figure 3. Rolling ball tribotester

Rambling-ball tribometer (free-ball)

The rambling ball is driven by a shaft by friction, so the speed of the ball is not steady. The normal power of the surface comes only from the weight of the ball, so this equipment is not able to test heavy loads. Even this smaller load is also not steady, since the ball can jump off from the surface. [6]
The ball moves on a rambling way, it touches the specimen with its whole surface, so it doesn't changes its shape significantly.

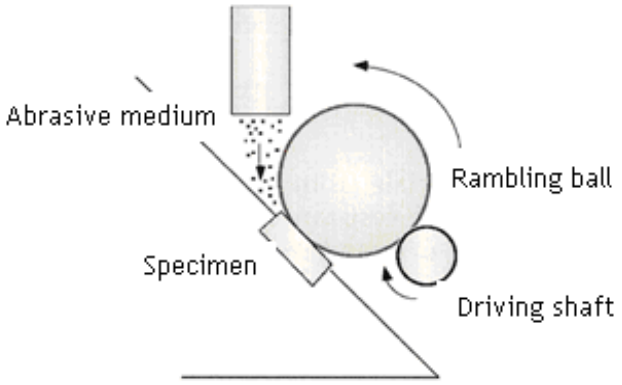

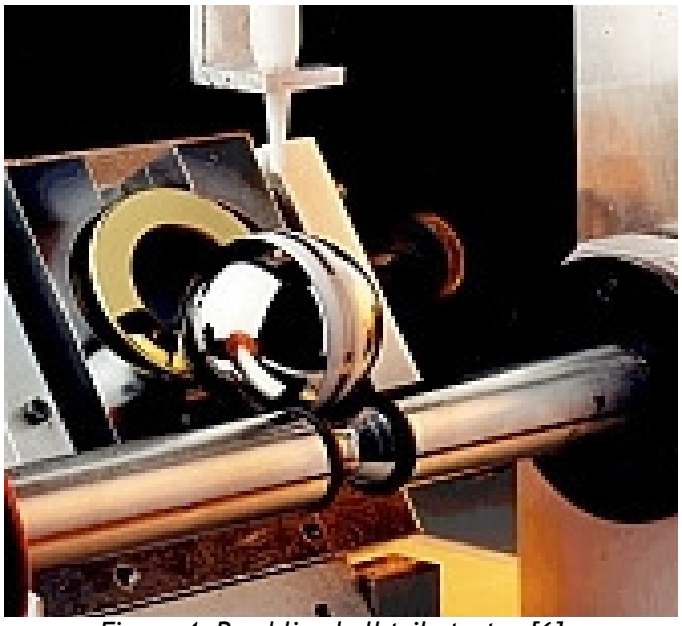

Figure 4. Rambling ball tribotester [6]

Cylinder-plane tribometer

Several arrangements of cylinder-specimen (horizontal, vertical) of this tribotester type are available on the market.
As the wearing process progresses and the trace increases the force per unit of surface decreases as well, but there is no significant change in the shape of the cylinder that would influence the wearing picture on the specimen.
There is an ASTM Standard G65-04 (2010) is for using the dry sand / rubber wheel apparatus. [7]

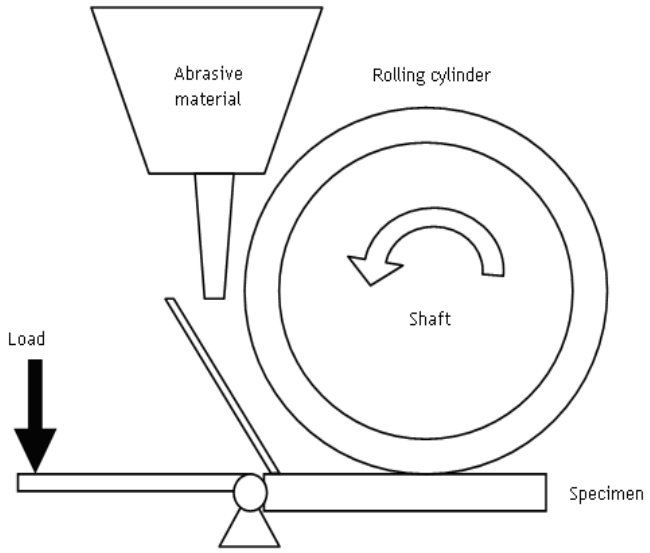

Figure 5. Cylinder-plane tribotester

Pin-on-disk construction

The specimen is a pin pushed by load on an abrasive disk. The linear loss of the pin shows directly the wear and the wear-resistance of the tested material. As the test progresses the abrasive paper degrades and becomes clogged so the loss of the worn material per time-unit reduces too.

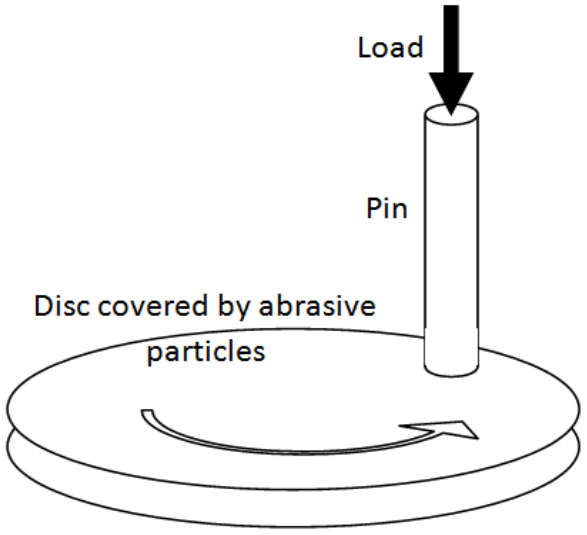

Figure 6. Pin-on-disk tribotester

There are some recommendations of standards for this type: ASTM G99 and DIN 50324. [5]

Cylinder-cylinder construction

There is a wear scar occurring by using this type of wearing test. The vertical dimension and the depth of scar can be measured.

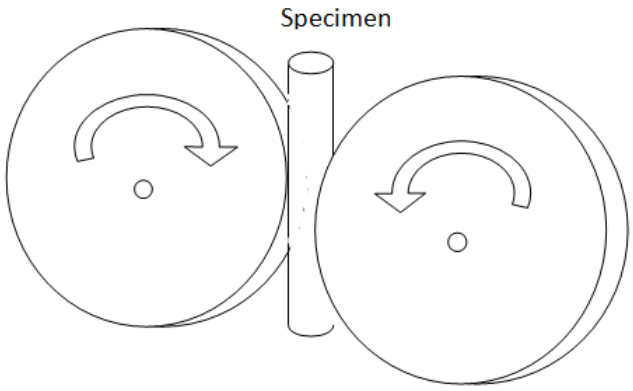

Figure 7. Cylinder-cylinder type

CONCLUSIONS

In technical practice it is more and more important to develop and use abrasive resistance materials. Therefore the modeling of wear is inevitable. Ensuring the adequate method and circumstances is the key for the success of testing.

REFERENCES

[1.] *Kalácska Gábor: Műszaki polimerek és kompozitok a gépészmérnöki gyakorlatban. Gödöllő, 2007.*

[2.] *Szabadi László: Többrétegű tüzihorgany bevonatok abráziós kopása. Ph.D értekezés, Gödöllő SZIE, 2011.*

[3.] *Valasek István - Törös Mihályné: Tribológia, Képzőművészeti Kiadó, Bp. 2006.*

[4.] *Czél György - Kollár Mariann: Anyagvizsgálati praktikum. Sunplant, Mickolc, 2008.*

[5.] *George Plint: Choice of Test Machines. Phoenix Tribology Ltd., 2003. http://www.phoenix-tribology.com/cat/at2/index/choice%20of%20machine.pdf*

[6.] *Kovács Tünde Anna: Acélok szövetszerkezetének hatása a lokális kopásra. Ph.D értekezés, Budapest BME, 2007.*

[7.] *ASTM International: Corrosion standards and wear standards, Abrasive wear. http://www.astm.org/Standards/corrosion-and-wear-standards.html*

ACTA TECHNICA CORVINIENSIS - BULLETIN of ENGINEERING

ISSN: 2067-3809 [CD-Rom, online]

ACTA TECHNICA CORVINIENSIS – Bulletin of Engineering
Tome VI (Year 2013) – FASCICULE 4 [October–December]
ISSN 2067–3809

[1.] J. MASSAH, [2.] K. Asefpour VAKILIAN

STATISTICAL MODELLING OF ERROR MEASUREMENT FOR DIAPHRAGM GAS METERS AT DIFFERENT AMBIENT TEMPERATURES

[1-2.] DEPARTMENT OF AGROTECHNOLOGY, COLLEGE OF ABOURAIHAN, UNIVERSITY OF TEHRAN, TEHRAN, IRAN

ABSTRACT: In this research, a statistical modeling is introduced in order to evaluate measuring error of diaphragm gas meters considering the effects of different ambient temperatures on the usual ($0.2Q_{max}$) and maximum (Q_{max}) consumption flow rate. In this study, a G4 diaphragm gas meter was used because of its prevalence in Iran. By considering the climate of Iran, average range of experiment's temperature was chosen between 30ºC to 60ºC and 0ºC to -30ºC. For conducting the experiments on these gas meters, a heater-cooler device and a master chamber were utilized. Proposed statistical modeling was able to evaluate the amount of using gas in the form of $0.2Q_{max}$ and Q_{max}. The obtained results may be used as a correction factor for diaphragm meter operation on different temperature conditions. In other words, the advantages of this research can be used for estimating the proper amount of using gas and calculating the proper fee for the user. According to results, in the countries that the gas consumption is done by diaphragm gas meters, national gas company will be lost for cold cities and will be profited for warm cities and the amount of fee estimation error is significant. As an example, national gas company of Iran lost about 40.7 million dollars for gas consumption measurement error for Tehran city in 2008.
KEYWORDS: Error of gas measurement, Gas consumption, Fee of gas, Diaphragm gas meter

INTRODUCTION

Iran, locating between latitudes 24° and 40° N and longitudes 44° and 64° E has various climates in different regions. Most of these climates have a hot summer and cold winter. It is obvious that the warmth and coldness of the weather have some undesirable influences on working elements of gas meters during the year. Thus, the gas consumption measuring would not be the same in different temperatures. In Iran, depending on the amount of needed flow rate, diaphragm gas meters are used in one of G2.5, G4, G10, G25, G40, G65, and G100 categories.

Some of the parameters that can have effects on the measuring devices are already studied. Nath and Dietrich (1997) analysed the effect of temperature on the measuring accuracy of turbine gas meters. Nilsson (1998) invested the accuracy of gas meters in the weather conditions on Lound city. Kolpatzik et al. (1998) considered the effects of temperature sensor positions in the pipe flows for determining the mean gas temperature.

Petunin (2008) presented an algorithm for indirect measurement of difficult-to-measure GTE parameters on the basis of its mathematical model. In his research, different principles of constructing GTE gas temperature meters based on indirect measurements were considered and simulation results were presented. Douglas (1977) invented a gas meter temperature compensating tangents. The tangent device was able to provide improved accurate deflection due to temperature changes as a result of built-in radial rigidity of the tangent wrist relative to the tangent arm. Cardelius and Skoglund (2004) invented an acoustic gas meter with a temperature probe having an elongated sensor region. In this manner, a temperature measurement can be made which more accurately reflects the temperature of the actual gas through which the emitted acoustic energy propagates. Vanderkamp (1988) studied high pressure test facilities for industrial gas meters in the Netherlands. The calibration procedures and systems were presented in his article. He showed that the gas compressibility effects on calibration and test facility accuracy.

Based on International Organization of Legal Metrology (OIML), for a mechanical gas meter with built-in mechanical temperature conversion device, maximum permissible error is 0.5% in a temperature range of 30°C extending symmetrically around the temperature specified by the manufacturer. The equation that converts the measured volume to a corresponding volume at the base gas temperature is presented as below (MID, 2004).

$$V_b = \frac{T_b}{T} V \qquad (1)$$

where V is the volume at metering conditions, V_b is the volume at base gas temperature, T is the absolute gas temperature at metering conditions and T_b is the base gas temperature specified by the

manufacturer. Equation 1 discussed ambient temperature affects on gas and not on the gas meter. Both of Iranian Gas Standard (IGS) and the Gas Meters-Diaphragm Gas Meters-DIN EN 1359 have not considered the effects of temperature on gas flow measuring accuracy in diaphragm gas meters (IGS, 1998; DIN EN 1359, 1993). Massah et al. (2010) studied the effects of ambient temperature on flow rate meters on the medium ($0.2Q_{max}$) and maximum (Q_{max}) flow rate consumption.

The objective of this research was to present statistical models for determining the error of flow rate measurement for diaphragm gas meters considering the effect of ambient temperature at the maximum (Q_{max}) and the medium ($0.2Q_{max}$) flow rate.

MATERIALS AND METHODS

To determine the effects of different ambient temperatures on the accuracy of diaphragm gas meters, the influences of warmth and coldness of the weather on the $0.2Q_{max}$ and Q_{max} were studied. $0.2Q_{max}$ is an index to measure the accuracy of a gas meter in 0.2 of maximum working flow rate (medium flow rate). Q_{max} is an index to measure the accuracy of a gas meter in maximum working flow rate. These two indexes are important parameters in measuring the accuracy of gas meters (IGS, 1998; DIN EN 1359, 1993).

In Iran, temperature of most cities rises up to 45ºC in summer and for some colder cities does fall to -25ºC in winter. When a gas meter is located directly in the sunlight, its temperature may increase up to 60ºC. Thus, the temperature range of experiments was considered 30º to 60ºC and 0º to -30ºC to determine the accuracy of flow rate measuring for a diaphragm gas meter (IGS, 1998).

The experiments were conducted using a G4 diaphragm gas meter. A heater-cooler and a master chamber (CA12-2232, Camos, Iran) were used to change the temperature of gas meters from -30ºC ±0.1ºC to 70ºC ±0.1ºC. Gas meters were located in these chambers. The master chamber had the ability of controlling the temperature at a standard range (19-23ºC ±0.1ºC) (IGS, 1998). A gas meter was placed in the master chamber as a master gas meter and another gas meter in heater-cooler chamber that its temperature changed at each stage of the experiment. Both chambers were kept next to each other in a way that the outlet gate of master meter was connected to the inlet gate of experimental gas meter, so the amount of passage air from both gas meters would be equal. A blower was used to produce the inlet air with 18 m-bar pressure (Figure 1). To avoid the influence of inlet air temperature on the experiments, both chambers were kept at room temperature (19-23ºC ±0.1ºC). Therefore, the inlet air to the chambers had standard temperature.

It was necessary to measure the rate of pressure drop, which was caused by the passage of air through the master chamber, concerning that the air first passed through the master chamber and then entered the heater-cooler chamber. Hence, the master chamber was connected to the gas meter in the heater-cooler chamber in series. Then, a volume of 100 Lit of air was passed (IRM3, instrument, Netherlands) through the master and experimental gas meters, which the difference of the value indicated by mechanical counter in the master chamber and experimental gas meters showed the rate of the pressure drop in the master gas meter (Figure 2).

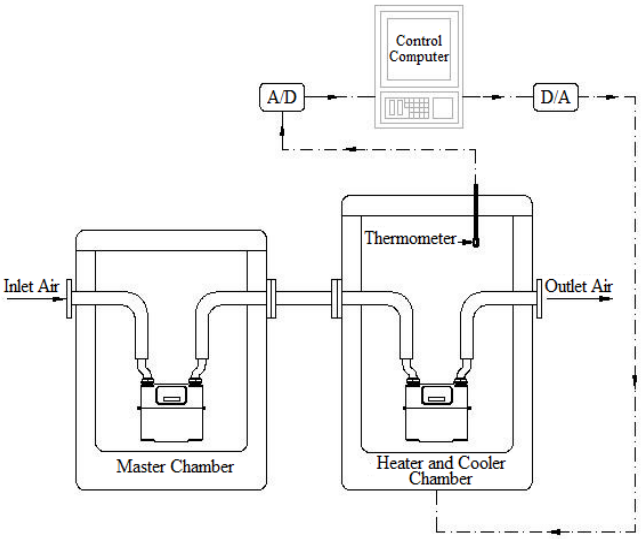

Figure 1. Schematic view of the test chambers

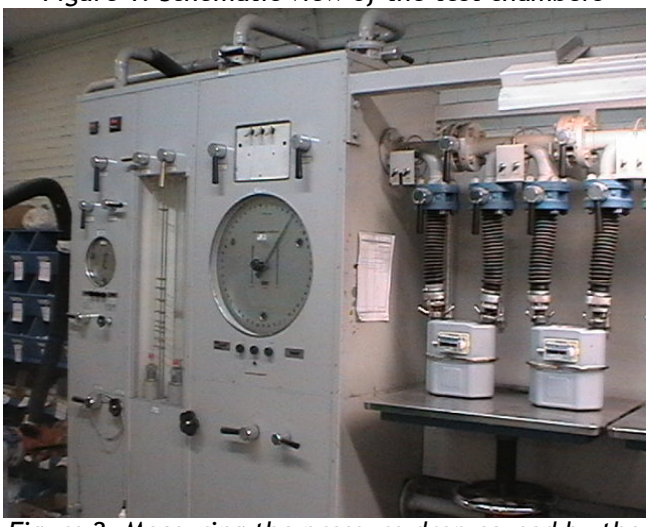

Figure 2. Measuring the pressure drop caused by the air passage from master gas meter

For measuring the effect of warmth and coldness in the form of $0.2Q_{max}$, a 1200 l/h rate of air and in the form of Q_{max}, a 6000 l/h rate of air were passed from master and experimental gas meters. Then, the temperature of passing air from gas meter, which was placed in the heater-cooler chamber, was changed from -30ºC to 20ºC and from 25ºC to 60ºC and recorded every 5ºC to investigate the effects of warmth and coldness, respectively. The experiment was done with five iterations. Considering obtained results, the linear regression method was used to present the best fit to the data. Then, the percentage of measurement error (E) was calculated as The percentage of measurement error is expressed by equation (2).

$$E\% = \frac{|Q\_Q_m|}{Q_m}.100 \qquad (2)$$

where Q is the measured flow rate of meters in each temperature, and Q_m is the measured flow rate of master meter.

RESULTS AND DISCUSSION

As is illustrated in Figure 3, based on the results of the experiments in form of normal working flow rate ($0.2Q_{max}$) the reduction of temperature from 20ºC to -25ºC caused the reduction of approximately linear in the measurement error of the gas meter. Nevertheless, the measurement error of meters remained constant between -25ºC to -30ºC. At temperatures above 25ºC to 55ºC, the measurement error of gas meters were remained approximately constant, but between 55ºC to 60ºC this error was risen. As shown in Figure 3, a part of the diagram had more slope and a part of this diagram had less slope. The value of $Q_{0.2Qmax}$ was the same for 20ºC to 25ºC. Therefore, two equations were determined to measure the gas consumption to determine $Q_{0.2Qmax}$ at different temperatures appropriately by statistical models:

$$Q_{0.2Q_{\max}} = 1089 + 4.95t \qquad -30 \le t \le 20 \qquad (3)$$

$$Q_{0.2Q_{\max}} = 1168.5 + 1.18t \qquad 25 \le t \le 60 \qquad (4)$$

Where t is the ambient temperature (ºC), $Q_{0.2Qmax}$ was estimated value of the flow rate in the form of $0.2Q_{max}$ (l/h). Equations 3 and 4 were able to evaluate the gas consumption measurement in the form of $0.2Q_{max}$ between -30ºC to 20ºC and 25ºC to 60ºC with a coefficient of determination 0.98 (R=0. 99) and 0.69 (R=0.83), respectively.

Statistical models for estimating the measurement error of gas meters in the form of $0.2Q_{max}$, are presented as below.

$$E_{0.2Q_{\max}} = (1200 - (1089 + 4.95t))/1200 \qquad -30 \le t \le 20 \qquad (5)$$

$$E_{0.2Q_{\max}} = (1200 - (1168.5 + 1.18t))/1200 \qquad 25 \le t \le 60 \qquad (6)$$

where $E_{0.2Qmax}$ represents the measurement error in the form of $0.2Q_{max}$ in l/h. As shown in Figure 3, the stretch line belongs to the obtained data during the experiments and slash line belongs to the fitted line with equations (3) and (4).

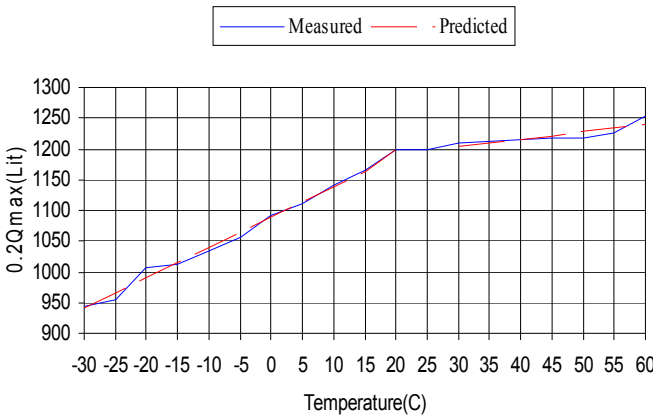

Figure 3. Effect of warm and cold temperature in the form of $0.2Q_{max}$

As is illustrated in Figure 4, based on the results of the experiments in form of maximum working flow rate (Q_{max}) linear reduction of temperature caused the linear reduction of measurement error in gas meter. Thus, it is possible to present the measurement error by a fitted linear equation to determine Q_{max} at temperatures between -30ºC to 20ºC and 25ºC to 60ºC. The temperature that used to determine the equations was considered above 25ºC and under 20ºC because the measured values with the master and experimental gas meters were the same between 20ºC to 25ºC.

$$Q_{Q_{\max}} = 5844.3 + 9.9t \qquad -30 \le t \le 20 \; and \; -25 \le t \le 60 \qquad (7)$$

Where t is the ambient temperature (ºC), Q_{Qmax} was estimated value of the flow rate in the form of Q_{max} (l/h). Equation 6 was able to evaluate the amount of using gas in the form of Q_{max} between -30ºC to 20ºC and 25ºC to 60ºC with a coefficient of determination 0.98 (R=0. 99). A statistical model for estimating the measurement error of gas meters in the form of Q_{max}, is presented as below.

$$E_{Q_{\max}} = (6000 - (5844.3 + 9.9t))/6000 \qquad -30 \le t \le 20 \quad and \quad 25 \le t \le 60 \qquad (8)$$

where E_{Qmax} represents the measurement error in the form of Q_{max} in l/h. As shown in Figure 4, the stretch line belongs to the obtained data during the experiments and slash line belongs to the fitted line with equation 7.

In this research, the effects of ambient temperature on the measured flow rate of meters in $0.2Q_{max}$ and Q_{max} forms and also measurement errors between them have been considered, but Nath and Dietrich (1997) considered the temperature behavior of diaphragm gas meters.

Errors below and above room temperature condition are named positive and negative errors, respectively. Cold temperature caused the meter's measurement show less amount (positive errors), and warm temperature caused the meter's measurement show more amount (negative errors).

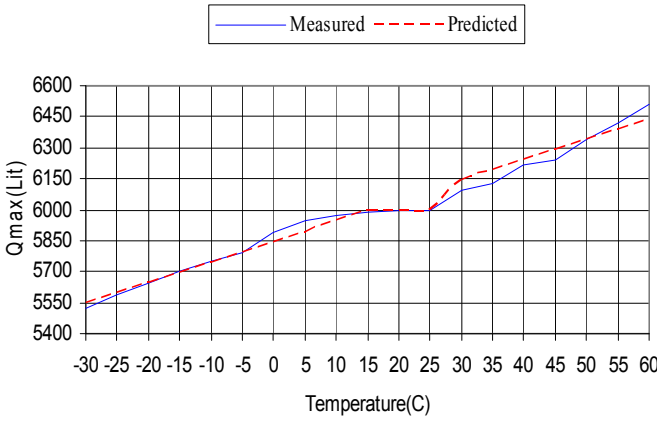

Figure 4. Effect of warm and cold temperature in the form of Q_{max}

To clarify the importance of results that are obtained above, the consumed gas amount of Tehran (The largest city of Iran with a population over 9,000,000 people) is analyzed. This amount in 2008 is presented in table 1. In this table, the average temperature for each month is also shown. The value of $E_{0.2Qmax}$ for each month was calculated using equations (5) and (6) (shown in Figure 5). Considering the gas consumption and the gas measurement error of diaphragm gas meters in each month and considering that each m^3 of gas costs about 0.05$ in Iran, fee estimation error (done by national gas company) was calculated and shown in Figure 6. As it is seen in this

figure, national gas company of Iran had a large error and lost about 40.7 million dollars in gas consumption of Tehran in 2008.

Table 1. Consumed gas amount of Tehran during the year 2008

Month	Gas consumption (×1000, 000 m^3)	Average temperature (°C)
January	2877	-1
February	1821	6
March	1543	10
April	997	15
May	886	21
June	896	31
July	835	27
August	874	22
September	837	16
October	1067	13
November	1294	7
December	1921	2
Total	15848	-

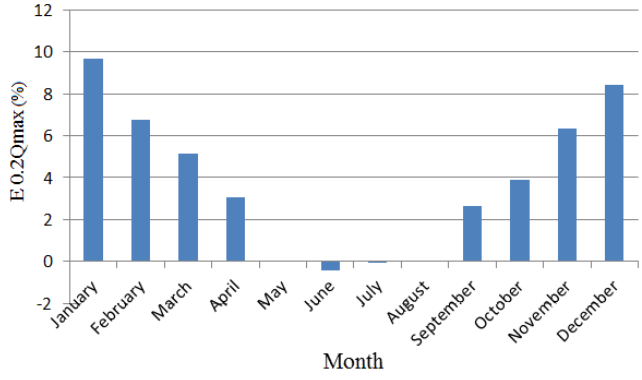

Figure 5. The value of $E_{0.2Qmax}$ (%) for each month

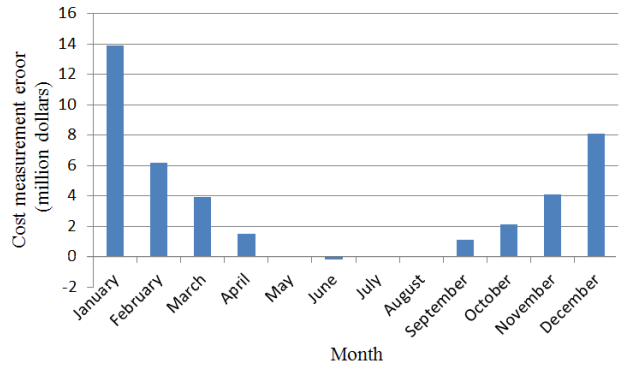

Figure 6. Cost measurement error (done by National Gas Company) for each month

CONCLUSIONS

The following conclusions can be drawn from this study:

1. Presented statistical models were able to evaluate the amount of using gas in the form of $0.2Q_{max}$ between -30ºC to 20ºC and 25ºC to 60ºC with a coefficient of determination 0.98 (R=0. 99) and 0.69 (R=0.83), respectively.
2. This model was able to evaluate the amount of using gas in the form of Q_{max} between -30ºC to 20ºC and 25ºC to 60ºC with a coefficient of determination 0.98 (R=0. 99).
3. Increasing and decreasing the ambient temperature cause to increase the positive and negative measure error of gas meters, respectively.
4. In the countries that the gas consumption is done by diaphragm gas meters, National Gas Company will be lost for cold cities and will be profited for warm cities and the amount of fee estimation error is significant.

REFERENCES

[1.] Cardelius, E., Skoglund, L.: U.S. Pat. No. 6817250, 2004.
[2.] Douglas, R.R.: U.S. Pat. No. 4040296, 1977.
[3.] Gas Meters - Diaphragm Gas Meters- English Version of DIN EN 1359; 1993.
[4.] IGS-MS-IN, 101(3), 1998.
[5.] Kolpatzik, S.J., Hilgenstock, A., Dietrich, H., Nath, B.: The location of temperature sensores in pipe flows for determinig the mean gas temperature in flow metering applications, Flow Measurement and Instrumentation, 9, 43-57, 1998.
[6.] Massah, J., Mohammadifar, H., Khazaei, J.: Consideration of Effects of Ambient Temperature On Measuring Accuracy of Diaphragm Gas Meters, Modelling and Optimization in the Machines Building fields, 16(1), 70-75, 2010.
[7.] Measurement Instrument Directive (MID), 2004/22/EC
[8.] Nath, B., Dietrich, H.: Analysis of the recovery-effect on the accuracy in gas metering, XIV IMEKO world Congress, Tampere , Finnland, 1997.
[9.] Nilsson, U.R.C.: A new method for finding inaccurate gas flow meters using billing data: finding faulty meters using billing data, Flow Measurement and Instrumentation, 9, 237-242, 1998.
[10.] Petunin, V.I.: GTE gas temperature determination with the use of indirect measurements, Russian Aeronautics (Iz.VUZ), 51(1), 67-74, 2008.
[11.] Vanderkamp, P.: Accuracy of high pressure gas meter calibration in the Netherlands, Conference of problems of large gas flow measurements at high and low pressures, Germany, 117-144, 1985.

ACTA TECHNICA CORVINIENSIS - BULLETIN of ENGINEERING

ISSN: 2067-3809 [CD-Rom, online]

ACTA TECHNICA CORVINIENSIS – Bulletin of Engineering
Tome VI (Year 2013) – FASCICULE 4 [October–December]
ISSN 2067–3809

[1.] Mihaela FLORI, [2.] Daniela MILOSTEAN

HEAT TRANSFER SIMULATION IN MOLD DURING DIE CASTING OF STEEL

[1-2.] "POLITEHNICA" UNIVERSITY OF TIMISOARA, FACULTY OF ENGINEERING HUNEDOARA, ROMANIA

ABSTRACT: The heat transfer in the melt-mold system during die casting process is made through conduction, convection and radiation. So, during pouring of melt into the mold, interface heat transfer is through forced convection and radiation. After the melt filled the mold, the interface heat transfer depends on the contact between melt and mold. Temperature evolution in mold wall during die casting of steel was analyzed by a finite element simulation and the results were compared with experimental data. The simulation consists in solving a conduction heat transfer problem with appropriate initial and boundary conditions.
KEYWORDS: die tool steel, die casting, K-type thermocouple, finite element analysis

INTRODUCTION

The die casting process consists in pouring a molten material (metal or alloy) into the mold cavity and pressing it under high pressure. The cavity mold is filled in a few seconds. After the melt has solidified, the casting is removed [1].

The heat transfer in the melt-mold system during die casting process is made through conduction, convection and radiation [1-5]. So, during pouring of melt into the mold, interface heat transfer is through forced convection and radiation. After the melt filled the mold, the interface heat transfer depends on the contact between melt and mold.

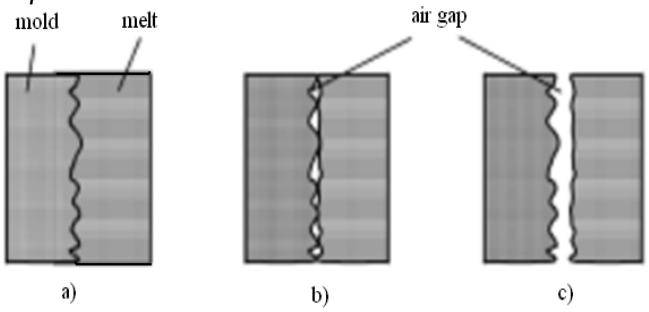

Figure 1. Possible contacts at the melt-mold interface:
full (a), partial (b) and no (c) contact [1]

The melt-mold contact is expected to be formed during three stages, which are summarized in figure 1 [1]:

- In stage I, at the beginning of solidification, the contact between molten metal and mold can be assumed good (figure 1a). Heat transfer is made through conduction from molten metal to mold wall;
- As a solid layer forms, the metal will shrink away from the mold and a discontinuous air gap will result (stage II). So, the mold and solid metal will have partial contact (figure 1b). Heat transfer is made now through solid metal/mold conduction at the contact surface and through radiation at the air gap.
- In stage III the solidified metal will pull away completely from the mold wall and the heat transfer will be made only through the gap (figure 1c).

Also, heat transfer by free convection and radiation at the mold exterior surface in contact with the environmental air, have a profound influence on temperature gradient inside the mold [4]. Figure 2 shows the expected temperature distribution during die casting process [1].

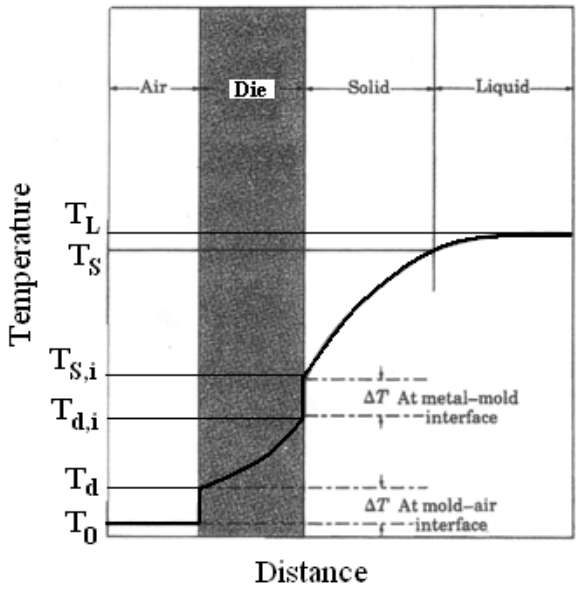

Figure 2. Temperature gradient during die casting process in the melt-mold system [1]

The temperature subscripts used in figure 2 are: L - liquidus, S - solidus,
i - interface, d - die, 0 - ambient.

Both analytical and numerical models were developed to treat the heat transfer during solidification process, mainly based on the finite difference method [2, 4, 6, 7] and Beck's nonlinear estimation method [8, 9].
Also, several commercial software packages, based on finite element analysis, were used to simulate this process, such as: ProCAST [5], Ansys [10] or Abaqus [11].
In this study, the Comsol Multiphysics 4.2 software is used to simulate the conduction heat transfer in the mold wall during die casting processing. The simulation results are compared with experimental data obtained by K-type thermocouples measurements taken from [12].

MATERIALS AND EXPERIMENTAL METHOD

The experimental details were described widely elsewhere [12].
The mold material is 55MoCrNi16 die tool steel grade (corresponding to AFNOR 55NCDV7 or EN 1.2714), with the following chemical composition: 0.5-0.6 %C, 0.1-0.4 %Si, 0.5-0.8 %Mn, 1.4-1.8 %Ni, 0.5-0.8 %Cr, 0.15-0.3 %Mo, max. 0.03 %S, max. 0.03 %P.

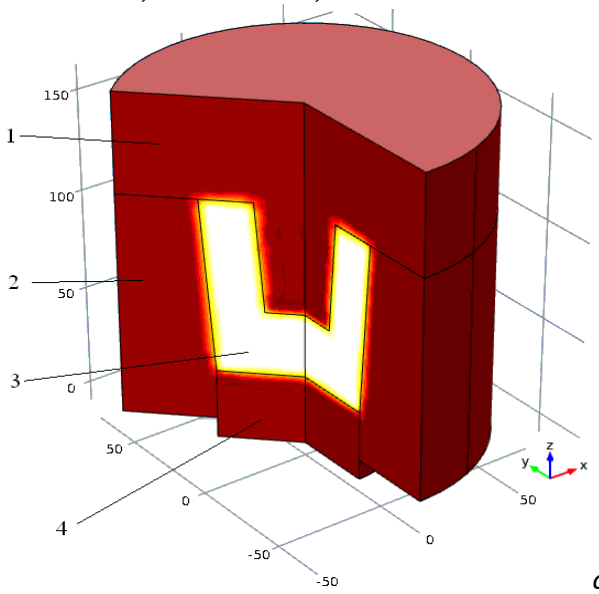

a)

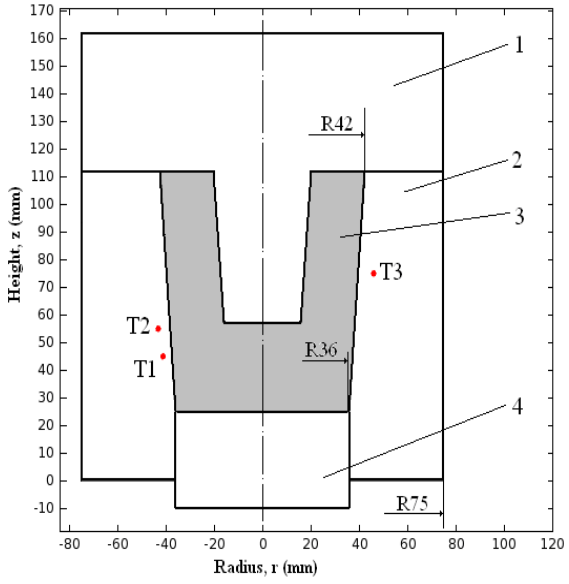

b)

Figure 3. Mold assembly (a) and T1-T3 thermocouples position (b): 1-upper die, 2-mold, 3-melt, 4-lower die

In order to evaluate the temperature changes in the mold wall, three K-type thermocouples were inserted in holes drilled to different depths around the mold diameter. The whole assembly is 162 mm height and 150 mm diameter. The mold has a glass shape with a height of 112 mm and wall thickness of 39 mm at the bottom and 33 mm at top.
Figure 3 shows the geometric shape of mold assembly (a) and the thermocouple position in the mold wall (b).
The thermocouples position coordinates are given in table 1.

Table 1. Thermocouple position coordinates

Thermocouple	Radius, r (mm)	Height, z (mm)
T1	41	45
T2	43	55
T3	46	75

Experimental measurements with the three temperature sensors were recorded simultaneous with a computer aided data acquisition system [12].

MODEL FORMULATION

To simulate the temperature evolution in mold wall during die casting of steel, the Comsol Multiphysics 4.2 software is used. In the Heat transfer module of the program, the space dimension was selected as 2D axisymmetric and the study was selected as time dependent. The time step was fixed at 10 seconds, for a total period of 90 seconds. This period coincides with the total experimental processing time (purring the melt into de mold and die casting [12]).

Heat conduction in mold wall

The program determines the temperature changes in the mold wall, in function of processing time, as a conventional heat conduction problem governed by the Fourier law.

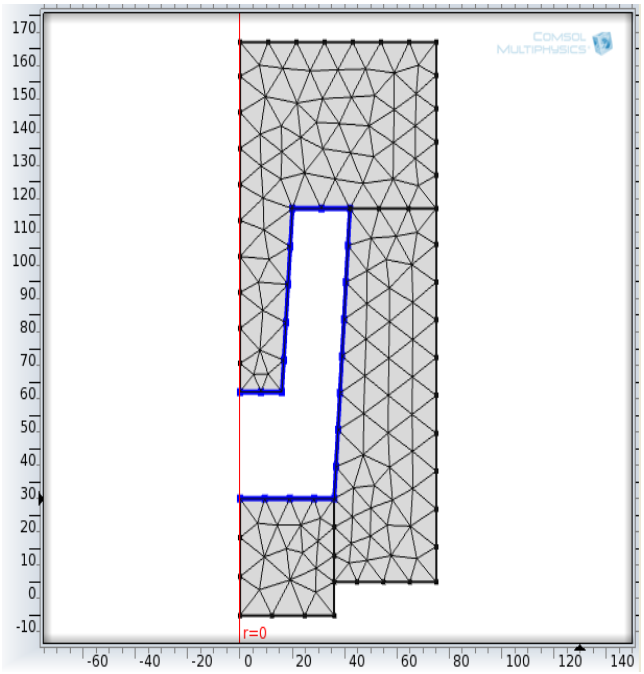

Figure 4. Mesh of the mold assembly consisting of 265 elements

The upper die, mold and lower die were modeled together as one piece because they are made of the same steel grade. The complete assembly mesh consists of 265 elements and is presented in figure 4.

The input parameters for the heat conduction problem were the thermo-physical properties of the die tool steel (thermal conductivity $\lambda = 50\ W/m \cdot K$; density $\rho = 7833\ kg/m^3$; heat capacity at constant pressure $c_p = 465\ J/kg \cdot K$ [3]) and mold initial temperature experimentally determined ($T1_i = 125°C$, $T2_i = 117°C$ and $T3_i = 126°C$).

By the simulation were obtained values of the temperature in the same points in the mold wall where thermocouples were mounted (see table 1).

Heat flux transmitted at melt/mold interface

The heat flux coming from the melt through the mold wall area is calculated with the following formula:

$$q_0 = \alpha(T_{ext.} - T_i)\left[W/m^2\right] \qquad (1)$$

The program input parameters are: the heat transfer coefficient $\alpha\left[W/m^2 \cdot K\right]$ and the melt temperature, which was experimentally measured by an infrared thermometer after purring the melt in the mold $T_{ext} = 1541\ °C$ [12].

The most important factor affecting the rate of heat transfer at melt/mold interface is the heat transfer coefficient $\alpha\left[W/m^2 \cdot K\right]$. Its value depends on the thickness of the air gap at the interface. Once the air gap forms, the heat transfer across the interface decrease rapidly and a relatively constant value of α is attended [2].

In the simulation the value of α was changed until the temperature values were overlapping the experimental ones.

Mold exterior surface to ambient radiation

The input parameters are: mold surface emissivity $\varepsilon = 0.9$ and the ambient temperature $T_{amb.} = 20°C$.

Also, the following major assumptions were considered in the simulation:

- the heat flow is unidirectional;
- the thermo-physical properties of the mould material are uniform (throughout the bulk) and remain constant over the processing time;
- the melt is in complete contact with the mould surface (no air gap is formed);
- the melt/mould interface temperature remains constant from the start to
- end of die casting processing.

RESULTS AND DISCUSSIONS

The temperature values of the heat conduction simulation were verified by comparison with the experimental measurements. The results are given in figure 5a-c).

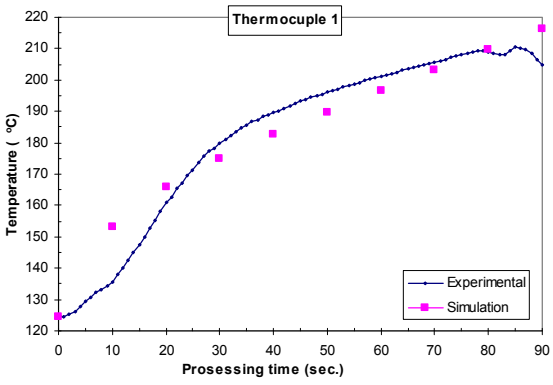

a)

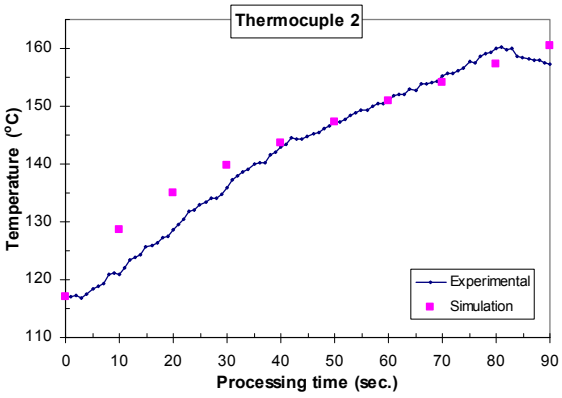

b)

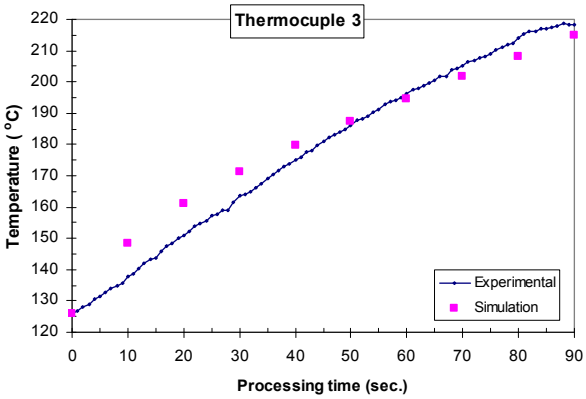

c)

Figure 5. Experimental and simulation temperature values

For matching the experimental and simulated temperature values, the following values of the heat transfer coefficients were used: α_1 and $\alpha_3 = 130\ W/m^2 \cdot K$, $\alpha_2 = 60\ W/m^2 \cdot K$.

CONCLUSIONS

The Comsol Multiphisycs 4.2 software package was used to simulate the heat transfer through the mold wall during die casting of steel.

The simulation by the finite element method was done to solve the conduction heat transfer problem inside the mold body. Boundary conditions and initial values were set before starting.

Among initial temperatures of the melt and mold, the heat flux at melt/mold interface and the radiation heat transfer at the external mold surface, were taken into account. The most important parameter was the heat transfer coefficient $\alpha\ [W/m^2 \cdot K]$ used to find the match between the simulation results and the experimental ones.

REFERENCES

[1] D.M. Stefanescu, Science and engineering of casting solidification, Second edition, Springer Science and Bussiness media, New York, ISBN 978-0-387-74609-8, 2009.

[2] C.A. Santos, J.M.V. Quaresma, A. Garcia, Determination of transient interfacial heat transfer coefficients in chill mold castings, Journal of Alloys and Compounds 319 (2001) 174-186.

[3] John H. Lienhard IV, John H. Lienhard V, A heat transfer textbook. Third edition, Phologiston Press, Cambridge, 2005.

[4] W. Gong, L. Chen, R. Liu, J. Hao, Derivation and application of time step model in

solidification process simulation, Research & Development, Vol.4 No.3 (2007) 206- 209.

[5] L. Q. Zhang, R. J. Wang, Estimation of heat flux at metal-mold interface during solidification of cylindrical casting, Int. J. Mater. Form, DOI 10.1007/s12289-012-1098-3.

[6] A. Fardi Ilkhchy, N. Varahraam, P. Davami, Evaluation of pressure effect on heat transfer coefficient at the metal- mold interface for casting of A356 Al alloy, Iranian Journal of Materials Science & Engineering 9/1(2012)11-20.

[7] K.V. Sreenivas Rao, P. Usha, N.S. Archana, Application of Mathematical Model for Assessment of Interface Heat Flux of the Mold during Gravity DieCasting, International Journal of Engineering and Innovative Technology (IJEIT) 2/6 (2012) 357-361.

[8] Z. Guo, S. Xiong, M. Murakami, Study of interfacial heat transfer coefficient at metal/die interface during high pressure die casting process of AZ91D alloy, China Fondry 4/1 (2007) 5-9.

[9] K. Narayan Prabhu, A. A. Ashish, Inverse modeling of heat transfer with application to solidification and quenching, Materials and manufacturing processes 17/4 (2002) 469-481.

[10] M. M. Pariona, A. C. Mossi, Numerical Simulation of Heat Transfer During the Solidification of Pure Iron in Sand and Mullite Molds, J. of the Braz. Soc. of Mech. Sci. & Eng. Vol. XXVII, No. 4 (2005) 399- 406.

[11] B. Santillana, L. Hibbeler, B. Thomas, Heat transfer in funnel-mold casting: effect of plate thickness, ISIJ International 48/10 (2008) 1380-1388.

[12] D. Milostean, M. Flori, Experimental investigations of temperature evolution in steel die during die casting, Annals of Faculty Engineering Hunedoara – International Journal of Engineering, 2012, accepted paper.

ACTA TECHNICA CORVINIENSIS - BULLETIN of ENGINEERING

ISSN: 2067-3809 [CD-Rom, online]

ACTA TECHNICA CORVINIENSIS – Bulletin of Engineering
Tome VI (Year 2013) – FASCICULE 4 [October–December]
ISSN 2067–3809

[1.] Aleksandar KOŠARAC, [2.] Saša PRODANOVIĆ, [3.] Milan ZELJKOVIĆ

POSSIBILITIES FOR INTERACTIVE CONTROL OF MACHINE TOOLS IN THE VIRTUAL REALITY ENVIRONMENT

[1-2.] UNIVERSITY OF EAST SARAJEVO, FACULTY OF MECHANICAL ENGINEERING, BOSNIA AND HERZEGOVINA
[3.] UNIVERSITY OF NOVI SAD, FACULTY OF TECHNICAL SCIENCES, SERBIA

ABSTRACT: The virtual product development is a modern approach in the product development process. Apart from the visualization itself, the virtual product development encompasses the whole range of testing in the virtual reality (VR) environment. Different testing performed in the virtual reality environment before prototype production can increase productivity and decrease development time. As an illustration of possibilities of performing different kind of testing in VR environment, this paper shows simulation in the VR environment of the process controlled by programmable logical controller (PLC) and MATLAB/SIMULINK. As an interface between VR and MATLAB/SIMULINK environment VR Toolbox library is used, and between MATLAB/SIMULINK and PLC controller that is OPC standard.
KEYWORDS: Virtual Reality, PLC controller, OPC standard, MATLAB/SIMULINK

INTRODUCTION

Simultaneously with development of information technology, advanced approach to product development is also being improved. All of this is in order to shorten the product development process and minimize the number of physical prototypes. One of these approaches is the development of virtual products which, except for visualization, provides a wide range of testing of the product in the virtual reality environment [2].

The main idea of this paper is the simulation of process control that are realized on the machine tools in the 3D virtual environment. In this case, the virtual model of the machine tool (partially automated pillar drilling machine) is connected with a real PLC (programmable logic controller) using OPC server. This model does not include dynamic simulation. State of the system is changed by the appearance of discrete events. The result of the simulation are movements, which tools perform in 3D virtual environment depending on values of input variables. In this case, the input variable are logical (Boolean) variable representing the state of sensors, buttons, switches that are activated by user in the VR environment.

The simulation can be used in a demonstration of the machine tool functioning and for testing the control algorithm on interactive realistic models of machine tools in the VR environment, where the process is controlled by the real programmable logic controller.

DEFINING THE PROBLEM

The example that is discussed in this paper is pillar drill, shown in Figure 1. We need to create a virtual model of a scene that includes drilling machines, sensors, buttons, switches and other elements of the information lap, so that users can manage the main, auxiliary and additional movements. Also, it is useful to provide possible solution for, partly automatized, drilling proces on this machine, which means defining the required number of inputs, actuator, and a program written for the PLC controller. It is necessary to develop a model in Matlab / Simulink environment, that manage with virtual models, in accordance with the defined initial conditions, together with PLC controller.

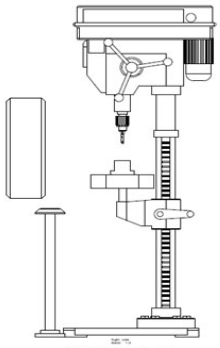

Figure 1. Pillar drill

A brief description of the drilling cycle on the considered machine tools is given below [8]. Workpiece is placed in clamping device, when the sensor LSPP (Limit Switch Part in Place) is activated. After the operator presses two buttons at the same time, the tool begins the main movement (rotation of drills) and simultaneously support motion (linear movement of drill, i.e. drilling machines spindle along the z axis downward). Drive of support movement is automated by kinematic pair of gear - rack. Rack is connected to the double-acting cylinder, that is controlled by the electrically activating monostable directional control valve 5/2. When the tool reaches its lower finite position, which corresponds to the completion of drilling, the sensor,

i.e. limit switch is being activated. LSDD (Limit Switch Drill Down). At that point, we have stop power electromagnet that activates monostable piston direction control valve 5/2, so that the spring returns direction control valve in its start position. Then begins the return movement, i.e. tool moves upward. After tool reach its upper limit position, appropriate limit switch is activated and entire system is being turned off. If the workpiece isn't in the clamping device, i.e. appropriate sensor doesn't detect its presence, process can't start. In order to increase operator safety, security doors close automatically after workpiece was placed and before movement of the tool. Safety door opens when drilling process is completed. Pressing the stop button, rotation of the tool is stopped and linear moving upward is started. After that the door is being open.

PLC CONTROLLER OMRON

Here we use programmable logic controller manufacturers OMRON, Series CJ1, which belongs to the class of microcontrollers [5]. This type of PLC are used in many industries, on the CNC machine tools for the control of individual modules, machines for different purposes, the packaging, the operations with various materials, in automated plants, etc. Product Group CJ series is intended for the use from simple sequential control to the powerful and fast models that can manage the system with a large number of input / output units. Complete modularity in composing this PLC provides the ability to apply a wide range of central processor units (CPU), which are fully compatible and can be quickly and easily combined with any other module of PLC. Central processor unit CPU11, which is used in this device, is designed for smaller systems, such as automatic machines, control devices, etc. The controller has a digital input unit with 16 points of connection, and a digital relay output unit with 16 points of connection.

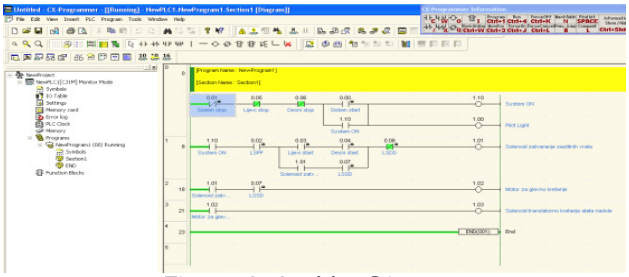

Figure 2. Ladder Diagram

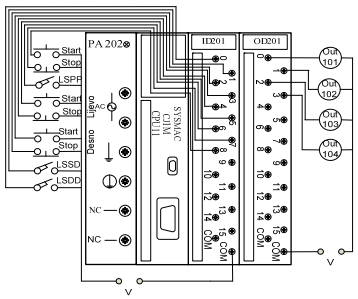

Figure 3. Wiring the input and output modules in case of physical model

Standard interface RS 232 is used for its connection with computer. Programming of PLC is performed using a graphical programming language called Ladder Diagram (LD) CX Programmer, figure 2, as a common platform for programming CS/CJ/C/CV serie OMRON controllers [4]. Figure 3 shows the wiring of I / O modules for the example under consideration.

APPLICATION OF OPC STANDARD FOR THE DATA EXCHANGE BETWEEN MATLAB SOFTWARE AND PLC

In order to exchange data between programmable logic controllers and virtual reality environments a suitable interface is required. As a solution, it is possible to apply the OPC standard, (abbreviation OLE for Process Control), which means Microsoft technology OLE Object Linking and Embedding [1], [7]. In this case, we use the CX OPC server that provides the ability to connect and exchange data between OMRON's PLC series CS/CJ/C/CV and CP, and applications operating in the Microsoft environment and have the support for the OPC standard. CX-Server OPC supports all Omron communication protocols. It should be noted that it is possible to use other software, such as MATRIKON OPC, which supports communications with OMRON PLCs. On the other hand, Matlab / Simulink has library of OPC Toolbox, which enables access to the OPC server in real time. In other words, utilization of this library enables reading of data in real time, that OPC server takes from controller or sending of data from Matlab to the PLC. Figure 4 shows the way of data exchange between the PLC and Matlab.

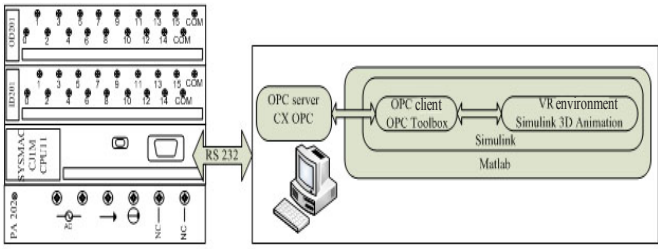

Figure 4. Data exchange between the PLC & Matlab[3]

CREATING MODELS OF DRILLS IN CATIA SOFTWARE AND VIRTUAL SCENE USING VRML LANGUAGE

Having in mind the complexity of virtual scenes, CATIA software for general purposes had been used to create 3D models, figure 5, recognizing that the same could be done by using any other CAD software system, which allows recording files in .wrl format.

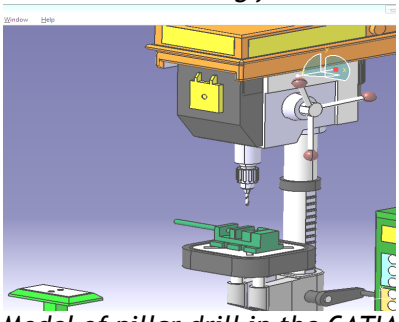

Figure 5. Model of pillar drill in the CATIA software

In developing the model it is necessary to plan in advance all movements that are performed by individual components or sub-assemblies in the VR environment, in order to properly set up a parent-child relationship, as well as take into account the orientation of the coordinate system in Matlab.

To create a virtual scene, VRML (Virtual Reality Modeling Language) is used , which is suitable for easy conversion with other 3D formats [6]. VRML is an

ISO standard for interactive, three-dimensional web graphics, or create virtual worlds on the Web. Virtual scene does not imply only objects that are visible in the scene, there are still lighting, background, camera position, the command to define the paths between nodes, the script nodes, which are easy to define the behavior of nodes, and many more, all to enable different interaction for user, as well as object control in the VR environment. Previous considerations [2], [3] have explained the application of different nodes to define geometric shapes, description of properties, as well as the nodes for grouping and their fields.

Without repeating of the foregoing, the paper contains a brief explanation of the specific mechanisms for communicating between nodes, important for this paper.

Since VRML has a specific purpose - to describe three-dimensional scenes and objects, it requires many features of generalized programming languages. The language itself is not object-oriented, but using Prototype mechanisms it can be derived object-oriented model, i.e. encapsulation and "reusability". This means, using prototype (PROTO node), allowing the definition of new nodes by the user. Using the prototype enables defining the objects in the scene that are "repetitive", such as sensors of object's presence, security door, buttons and switches for handling machinery, etc. Some nodes generate events in relation to the changing environment or user actions. These nodes are called sensors (Anchor, Collision, CylinderSensor, PlaneSensor, ProximitySensor, SphereSensor, TimeSensor, TouchSensor, VisibilitySensor) and represented essential elements that provide interaction with user. This approach uses a Touch Sensor that detects the mouse interaction with geometry. Event management is carried out using the ROUTE command, i.e. by writing a special script. Once the user completes an event (a mouse click in this case) to a geometric shape, ROUTE command defines paths between nodes, which generate events and those who receive them. At that time, the given geometric shape, sensor and ROUTE command are in the same node for grouping.

VRML files are displayed in a VRML browsers that can be a standalone application or VRML plugin html browser. The most popular VRML browsers are: Cortona VRML Client, Blaxxun Contact, Cosmo Player and others. For the purposes of this paper, the virtual scene is displayed in the application called Simulink 3D Animation Viewer, which is part of the library of Simulink 3D Animation.

MATLAB SIMULINK MODEL

Movement of kinematics modules as the basic kinematic entity, is being controlled from Simulink environment, figure 6. In that way, the VR Sink and VR Source blocks of libraries Simulink 3D Animation are used for the connection between Simulink and virtual scene (Figure 8). The blocks: OPC Configuration, OPC Read and OPC Write from the OPC Toolbox library are used for connecting with PLC.

VR Sink block "enters" the value of its ports into virtual world through the fields defined in the dialog box called Block Parameters, figure 9.

VR Sink block is responsible for the display of virtual scene in the application Simulink 3D Animation Viewer. The application is run after the user double-clicks the left mouse button on the VR Sink block. Inputs of VR Sink block directly change the characteristics of objects in the virtual scene.

Defining characteristics of virtual objects, which are changing, enables selection of the option "Simulation > Block Parameters ..." from the menu into application Simulink 3D Animation Viewer. On the right side of the window is a tree for a given virtual scene that is defined in the VRML file, whose name is shown in the left side of the window. This tree shows the structure of the VRML file. Blocks with names are marked with red arrow and available from the Matlab environment. Blocks without name, but whose children have the names are also marked with a red arrow. Fields of blocks that can be changed, have a square next to the name. Selecting a square enables changing of field values from Simulink (simultaneously, input with corresponding name is generated on the VR Sink s-block). If it is need to make changes in the VRML file, the option "File> Open in Editor" from application Simulink 3D Animation Viewer should be chosen. Then the .wrl file is opened in V-Realm Builder VRML editor, which is distributed with MATLAB, figure 7.

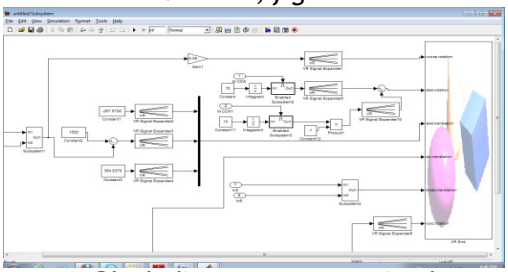

Figure 6. Block diagram - connection between Matlab/SIMULINK and VR environment

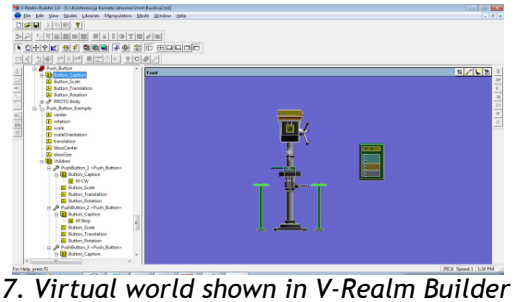

Figure 7. Virtual world shown in V-Realm Builder editor

Figure 8. Virtual scene

Particular changes to VRML files can be manually performed, due to .wrl is text file, but it is necessary to know the syntax of VRML. Application of VRML editor is definitely more comfortable and easier way, but not always sufficient.

It has already been said that the Simulink model does not involve dynamic simulation, and system state is being changes with the occurrence of discrete events.

But simulation is changing in time, which is called a continuous simulation. The reason for this is in the fact that the position of the tool is determined by the output of the block Integrator, whose values is changed continuously in time, figure 10.

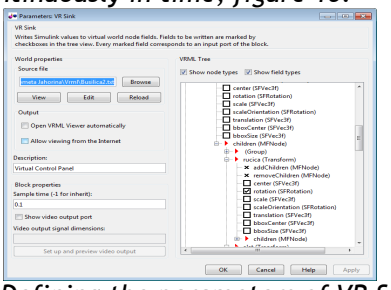

Figure 9. Defining the parameters of VR Sink block

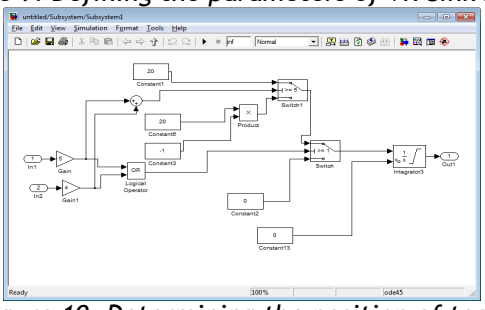

Figure 10. Determining the position of tools

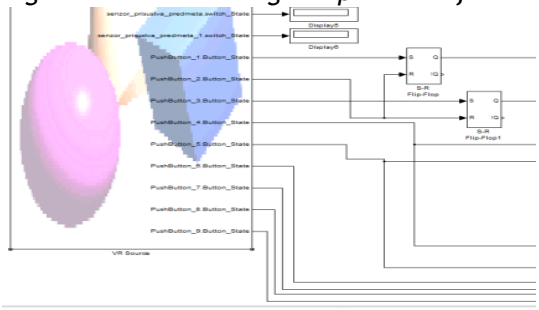

Figure 11. VR Source block

VR Source block is very similar to the VR Sink block. Using this block, we can run applications Simulink 3D Animation Viewer, and edit .wrl files. Also, the defining characteristics of virtual objects can be performed as previously described. The difference is that this block reads different values from the virtual world and forwards them to the Simulink model. Figure 11 shows VR Source block, where the outputs contain values of logical variables, that represent the state of sensors, switches and buttons in the virtual scene. Blocks OPC Read and OPC Write communicate with OPC server and OPC server with PLC. Figure 12 displays the address (called tags) input and output terminals on the PLC that are defined on the OPC server.

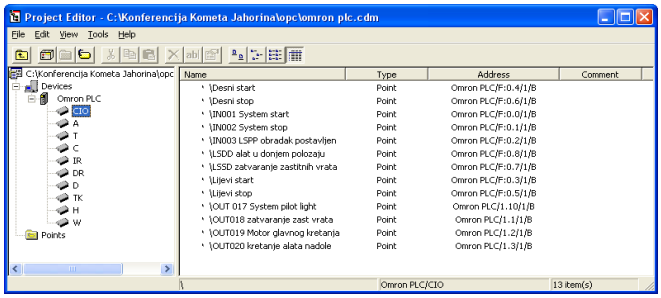

Figure 12. Addresses of input and output terminals

OPC Write block sets the (forced) state of bits at the input terminals, depending on the initial conditions (sensor state), while the OPC Read block takes the value of the output terminals of the controller, that represent a control signals for kinematic modules of machine tools in a virtual environment.

CONCLUSIONS

The paper presents the possibilities of using connection between Matlab and PLC, where OPC server has utilized as interface for data exchange. In the virtual reality environment, in addition to the visualization, various tests of products can be performed. One of the approaches involves the management with 3D virtual models using real programmable logic controllers. This concept can be used for different purposes like testing of the developed control algorithm, shortening product development time and increasing productivity, as well as for educational purposes.

Realization requires a standard PC platform, which is an advantage because of the low cost.

The disadvantage is quite a complex process of creating such a scene since it is required the knowledge of a CAD tool (which can export geometry into .wrl file format), VRML language, JavaScript i.e. Java programming language, Matlab, and the knowledge of working with PLC, i.e. programming of PLC.

REFERENCES

[1] *Guzina, M., Stupar, M., Naumović, M.: Possibilities of communication between MATLAB/Simulink environment and processes controlled by programmable logic controllers using OPC concept, Infoteh-Jahorina Vol. 8, Ref. A-15, p. 66-70, March 2009. (in Serbian).*

[2] *Košarac, A.: Design automation and visualization of flexible technology structures running, Master thesis, Faculty of Technical Sciences, Novi Sad, 2010. (in Serbian).*

[3] *Košarac, A., Zeljković, M.: Simulation of process controlled by Programmable Logic Controller PLC in the Virtual Reality Environment, Procedings - CD rom, 11th INTERNATIONAL SCIENTIFIC CONFERENCE MMA 2012 - Advanced Production Technologies, Faculty of Technical Sciences, Novi Sad, 2012, pp. 239-242, ISBN 978-86-7892-419-4*

[4] *Matić N.: Introduction to industrial PLC controllers, mikroElektronika, Beograd, 2001. (in Serbian).*

[5] *OMRON, Technical Library, Multilanguage edition, 2005.*

[6] *Pașc, I., Țarcă, R., Popențiu-Vlădicescu, Florin.: The VRML model and VR simulation for a SCARA robot, Annals of the Oradea University, Fascicle of Management and Technological Engineering, Volume VI (XVI), 2007.*

[7] *Persin, S., Tovornik, B., Muskinja, N.: OPC-driven Data Exchange between MATLAB and PLC-controlled System, Int. J. Engng Ed. Vol. 19, No. 4, pp. 586-592, 2003 TEMPUS Publications.*

[8] *Webb, W. J., Reis, A. R.: Programmable Logic Controllers, Principles and Applications, Fifth Edition, Pearson Education, Inc., Upper Saddle River, New Jersey 07458, 2003*

ACTA TECHNICA CORVINIENSIS – Bulletin of Engineering
Tome VI (Year 2013) – FASCICULE 4 [October–December]
ISSN 2067–3809

[1.] Irina PETROVA PAVLOVA

SOLAR POTENTIAL AT AN OPTIMUM ANGLE OF PLANE INCLINATION FOR THE CITY OF VARNA

[1.] DEPARTMENT OF HEAT ENGINEERING TU-VARNA, 9010, №1 STUDENTSKA STR., BULGARIA

ABSTRACT: The ever growing interest in the utilization of solar energy as an accessible, renewable, environmentally-friendly and easily-manageable type of energy makes it a prospective branch of power engineering. The paper presents data about the potential solar energy which the city of Varna receives at an optimum angle of plane inclination. The results are obtained on the basis of a methodology developed for the purposes of calculating the solar energy received. The experimental values of the total solar radiation on a horizontal plane observed within a year at a certain geographic location, namely the Technical University of Varna, serve as an output.
KEYWORDS: solar radiation, solar panel optimum inclination

INTRODUCTION

The ever growing interest in the utilization of solar energy as an accessible, renewable, environmentally-friendly and easily-manageable type of energy makes it a prospective branch of power engineering.

The utilization of the maximum possible amount of total solar radiation reaching a certain surface depends on the azimuth angle and its inclination in relation to a horizontal plane. The empirical data about the solar radiation intensity reaching the horizontal surface under discussion within the year 2011 makes it possible to determine the solar potential at an optimum angle of an inclined surface. The empirical data concern the region of the Technical University of Varna with geographical coordinates 43°13.3858'N, 27°56.3065'E registered with a LI-COR 200 pyranometer mounted on an NRG Now System 34 m meteorological mast.

The maximum solar energy utilized at the inclined surface in the region under discussion is determined by the constituents obtained by means of the methodology developed in [1] in the following steps:

- ☐ Calculation of direct solar radiation on a horizontal and an inclined surface;

$$I_b = I - I_d, \quad (1)$$

$$I_{b,\beta} = R_b * I_b. \quad (2)$$

- ☐ Calculation of the solar radiation emitted on a horizontal and an inclined surface;

The diffuse solar radiation on a horizontal surface (I_d) is defined through the method of Reindl et al – 2 [2].

$$I_d = k_t * I, \quad (3)$$

$$I_{d,\beta} = R_d * I_d. \quad (4)$$

- ☐ Calculation of the reflecting solar radiation;

$$I_{ref} = I * R_r. \quad (5)$$

- ☐ Determination of the total solar radiation on an inclined surface.

$$I_\beta = I_{b,\beta} + I_{d,\beta} + I_r, \quad (6)$$

where:

I - the intensity of global radiation on a horizontal surface, W/m^2;

I_b - the intensity of direct solar radiation on a horizontal surface, W/m^2;

I_d - the intensity of diffuse radiation on a horizontal surface, W/m^2;

k_t - clearness index,

$$k_t = \frac{I}{I_{oH}};$$

I_{oH} - extraterrestrial radiation on a horizontal surface, W/m^2;

$I_{b,\beta}$ - the intensity of the beam radiation on an inclined surface, W/m^2;

R_b - ratio of the beam radiation on an inclined surface and the beam radiation on a horizontal surface,

$$R_b = \frac{\cos(\theta)}{\cos(\theta_z)},$$

θ - the incidence angle of the sun rays on the horisontal surface, deg;

θ_z - the zenith angle, deg;

$I_{d,\beta}$ - the intensity of diffuse radiation on an inclined surface, W/m^2;

I_r - the intensity of reflected radiation on a horizontal surface, W/m^2;

R_r - ratio of reflected radiation on an inclined surface and the reflected radiation on a horizontal surface,

$R_r = 0.5*(1-\cos(B))*\rho$,

β - the inclination angle, deg;

ρ - the ground surface (albedo).

The calculations of the total solar radiation are carried out at a different angle of the surface varying from 10^o to 90^o within the period from 1st January to 31st December, 2011.

RESULTS - MONTHLY OPTIMUM ANGLE OF AN INCLINED SURFACE

Figure 1, as well as Table 1, illustrates the results of the monthly optimum angle on an inclined surface obtained in the city of Varna. The graphs are based on the total monthly value of the solar potential received. The table also shows the average daily value of the solar energy per month.

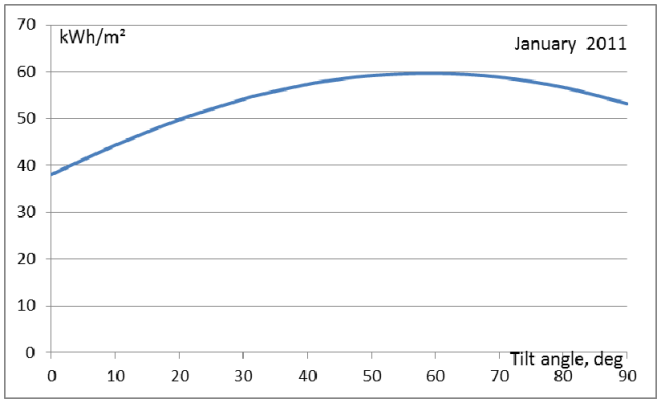

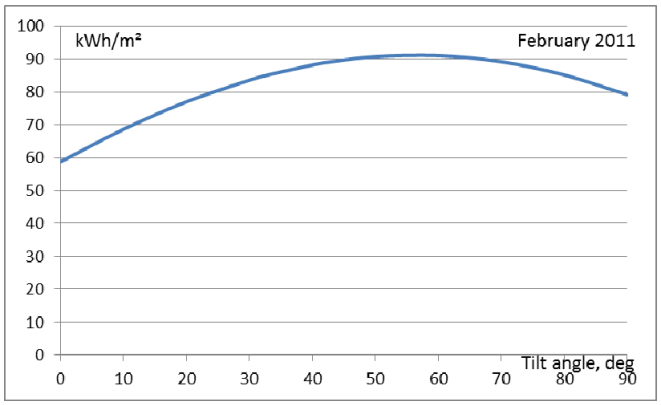

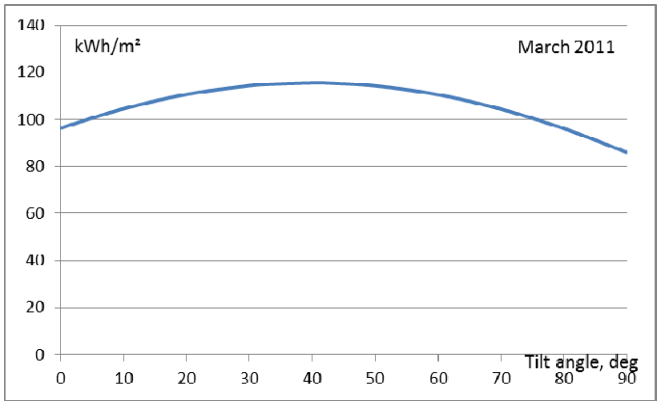

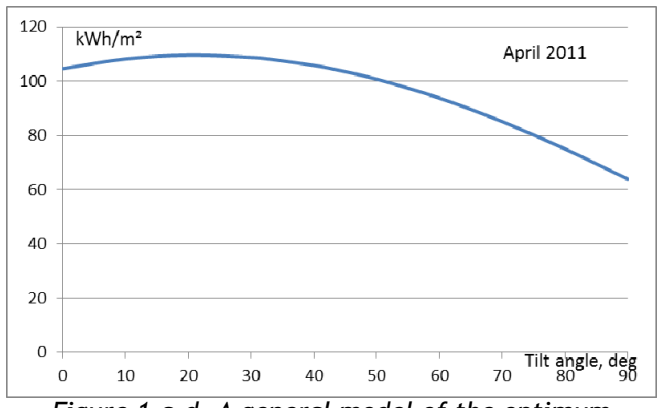

Figure 1.a-d. A general model of the optimum monthly angle on an inclined surface on the basis of the total monthly value of the solar radiation for 2011

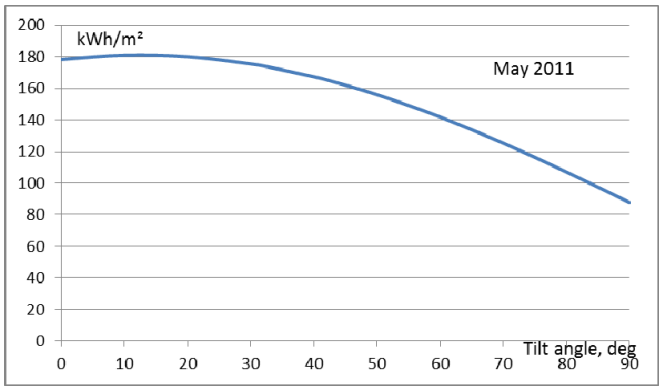

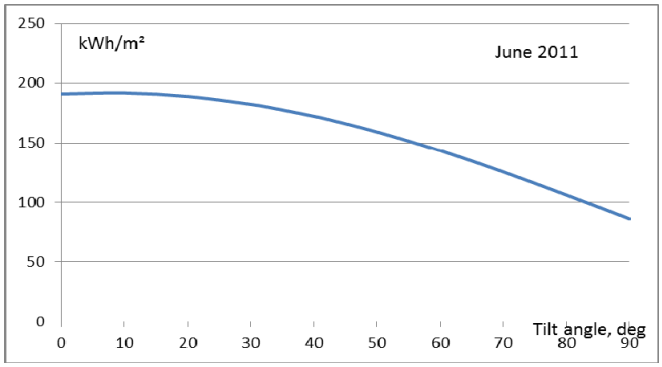

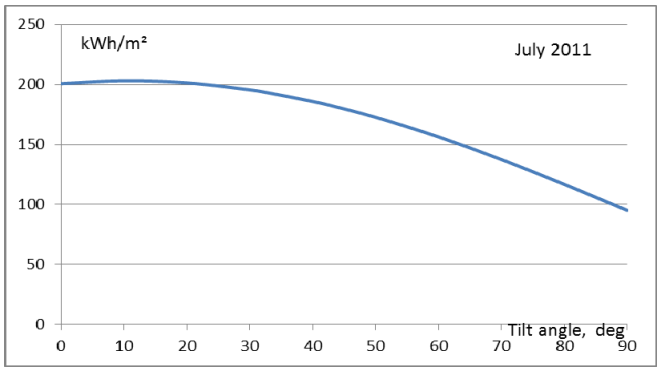

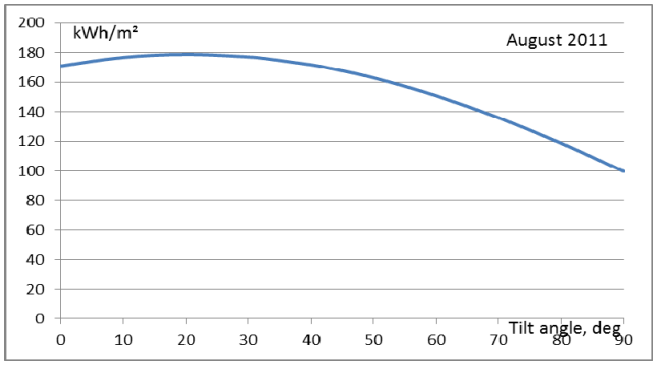

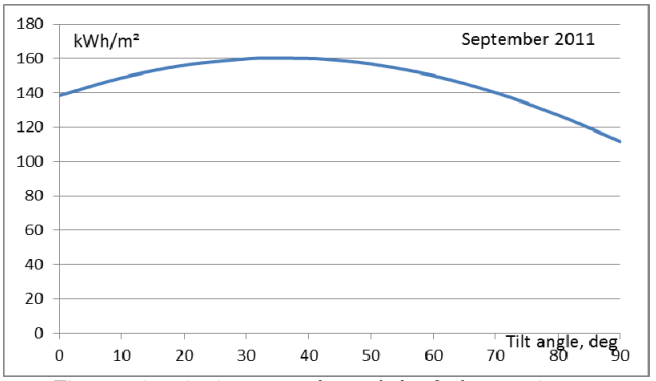

Figure 1.e-i. A general model of the optimum monthly angle on an inclined surface on the basis of the total monthly value of the solar radiation for 2011

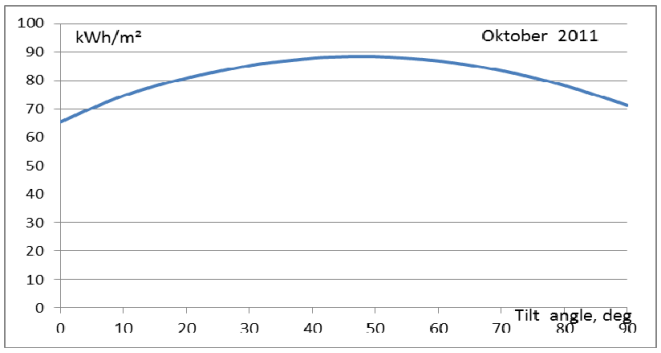

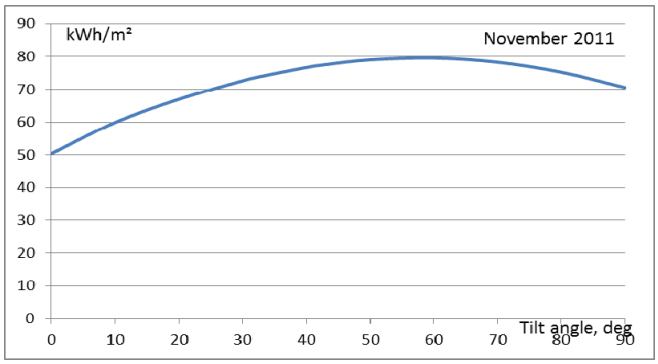

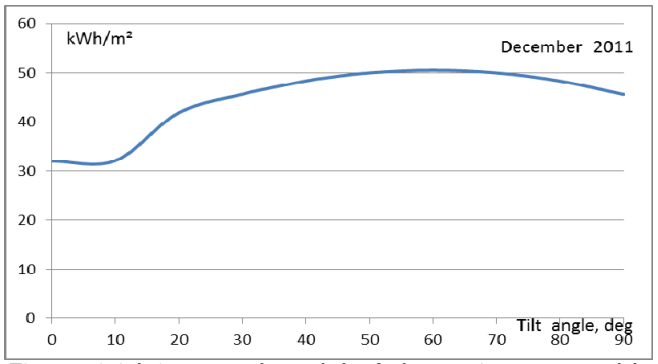

Figure 1.j-l A general model of the optimum monthly angle on an inclined surface on the basis of the total monthly value of the solar radiation for 2011

Table 1. Monthly optimum angle of the inclined surface of Varna

Month	Opt. angle	I_{max}, kWh/m²	I_{srm}, kWh/(m².day)
1	2	3	4
I	60°	59.70	1. 9
II	60°	91. 02	3 .25
III	40° 43°	115.54 115. 41	3. 73 3. 72
IV	20°	109 .581	3 .78
V	10°	181. 08	5. 84
VI	10°	191. 60	6. 39
VII	10°	203. 03	6 .55
VIII	20°	178.78	5. 77
IX	33°	160. 20	5. 34
X	50°	88 .23	2.85
XI	60°	79. 54	2. 65
XII	60°	50 .58	1. 63

Figure 2 shows the changes in the optimum angle on an inclined surface by month. As can be seen, during winter months (January, February, November and December) the optimum angle is 60° and during the summer months (May, June, July) it is 10°.
All results obtained for the total solar radiation on an inclined surface for 2011 are shown in Table 2.

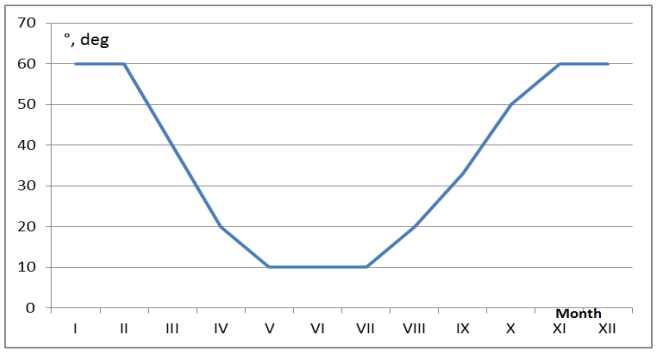

Figure 2. Variation of the optimum angle on an inclined surface by month

Table 2. Total monthly solar radiation on an inclined surface, kWh/m²

Angle/ Month	0°	10°	20°	30°
I	38.05	44.34	49.77	54.14
II	58.79	68.66	77.00	83.58
III	96.38	104.59	110.63	114.31
IV	104.62	108.19	109.58	108.77
V	178.29	181.08	180.08	175.45
VI	190.70	191.60	188.70	182.14
VII	200.67	203.03	201.27	195.46
VIII	171.01	176.78	178.78	177.09
IX	138.35	148.76	155.97	159.76
X	65.52	74.65	80.79	85.19
XI	50.39	59.91	66.98	72.62
XII	32.04	32.13	41.91	45.62
I-XII	**1324.8**	**1393.7**	**1441.5**	**1454.1**
IV-IX	983.7	1009.4	1014.4	998.7
X-III	341.2	384.3	427.1	455.5

Angle/ Month	33°	40°	50°	60°
I	55.22	57.31	59.18	59.70
II	85.17	88.19	90.70	91.02
III	114.94	115.54	114.26	110.52
IV	108.10	105.79	100.74	93.76
V	173.36	167.31	155.99	141.86
VI	179.50	172.19	159.14	143.42
VII	192.91	185.82	172.61	156.31
VIII	175.82	171.75	162.90	150.84
IX	160.20	160.00	156.72	149.99
X	86.14	87.69	88.23	86.78
XI	74.00	76.67	79.00	79.54
XII	46.55	48.35	50.03	50.58
I-XII	**1451.9**	**1436.6**	**1389.5**	**1314.3**
IV-IX	989.9	962.9	908.1	836.2
X-III	462.0	473.8	481.4	478.2

Angle/ Month	70°	80°	90°
I	58.85	56.65	53.18
II	89.16	85.16	79.15
III	104.43	96.17	86.01
IV	85.10	75.03	63.88
V	125.36	107.10	87.82
VI	125.58	106.31	86.49
VII	137.48	116.79	95.16
VIII	135.95	118.73	99.77
IX	140.01	127.09	111.65
X	83.40	78.19	71.29
XI	78.29	75.25	70.55
XII	50.02	48.34	45.60
I-XII	**1213.6**	**1090.8**	**950.6**
IV-IX	749.5	651.0	544.8
X-III	464.1	439.8	405.8

OPTIMUM AMOUNT OF SOLAR ENERGY ON AN INCLINED SURFACE

The optimum amount of solar energy for the one-year period of study, as Figure 3 shows, is obtained at an optimum angle of an inclined surface of 30° having a value of 1454.12 kWh/m².

Table 2 shows that the values of the solar energy at 20° and 33° are similar – 1441.5 kWh/m² and 1451.9 kWh/m² respectively.

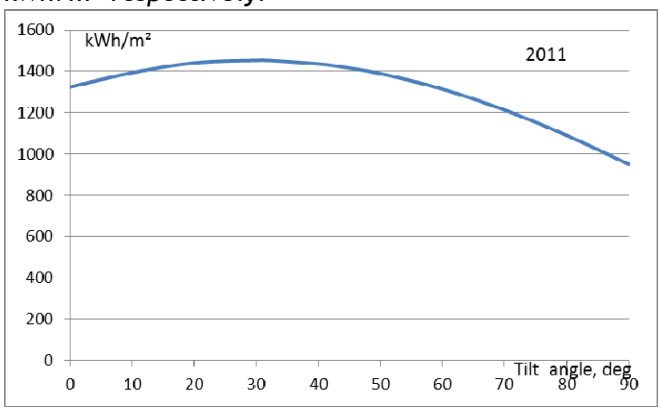

Figure 3. Optimum annual angle on an inclined surface

Figure 4 presents the line graph of the solar energy which the region under study receives during the summer and the winter months.

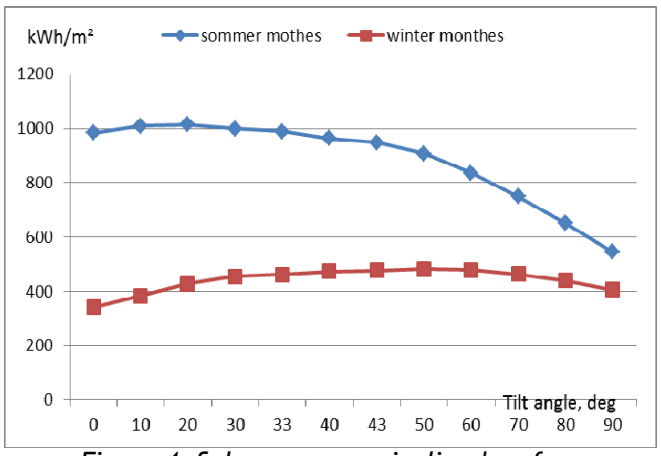

Figure 4. Solar energy on inclined surface in summer and winter

CONCLUSIONS

The results obtained are intended to be preliminary data for the purposes of a solar system design. The selection of the type of a certain solar system in advance will reduce the time necessary for its design and construction in the region studied.

The following conclusions can be made from the obtained results:

1. *The optimal annual angle of an inclined surface for the city of Varna as per experimental data (2011) is 30°.*
2. *The obtained data for the solar radiation of an inclined surface show that the city of Varna has a sufficient solar potential (1454.12 kWh/m²), which can be used for heating and energy production.*
3. *The results obtained serve as preliminary information and can be used by technologists, designers and architects when designing a solar system.*

The preliminary selection of the type of the respective solar system (heating or energy transformation/power conversioning), will decrease the time for its design and construction in the respective studied region.

REFERENCES

[1.] *Pavlova, I. Dissertation (in Bulgarian) Павлова И. Дисертация на тема „Теоретична и експериментална оценка на слънчевия потенциал за град Варна", 2012 г., Технически университет – Варна.*

[2.] *Batlles F.J., M.A. Rubio , J. Tovar, F.J. Olmo, L. Alados-Arboledas; Empirical modeling of hourly direct irradiance by means of hourly global irradiance, Energy 25 (2000) 675-688.*

[3.] *Ahmad M. Jamil, G.N. Tiwari; Optimization of Tilt Angle for Solar Collector to Receive Maximum Radiation, Renewable Energy Journal, 2009, 2, 19-24.*

[4.] *Ulgen K., Optimum Tilt Angle for Solar Collectors, Energy Sources, Part A, 28:1171-1180, 2006, ISSN:1556-7036.*

[5.] *Radosavljević Jasmina, Amelija Đorđević; Defining of the intensity of solar radiation on horizontal and oblique surfaces on earth, UDC 551.521.1:504.06, Facta Universitatis Series: Working and Living Environmental ProtectionVol. 2, No 1, 2001, pp. 77 - 86.*

[6.] *Wlodarczyk D., H. Nowak, Statistical analysis of solar radiation models onto inclined planes for climatic conditions of Lower Silesia in Poland, ARCHIVES OF CIVIL AND MECHANICAL ENNNNNGINEERING Vol. IX, 2009.*

ACTA TECHNICA CORVINIENSIS - BULLETIN of ENGINEERING

ISSN: 2067-3809 [CD-Rom, online]

ACTA TECHNICA CORVINIENSIS – Bulletin of Engineering
Tome VI (Year 2013) – FASCICULE 4 [October–December]
ISSN 2067–3809

[1.] Tanja KEREZOVIĆ, [2.] Gabor SZIEBIG, [3.] Bjørn SOLVANG, [4.] Tihomir LATINOVIC

HUMAN SAFETY IN ROBOT APPLICATIONS – REVIEW OF SAFETY TRENDS

[1-4.] FACULTY OF MECHANICAL ENGINEERING, BANJA LUKA, BOSNIA & HERZEGOVINA
[2-3.] NARVIK UNIVERSITY COLLEGE, NARVIK, NORWAY

ABSTRACT: Interaction between humans and robots was always having great attention, as robots should never hurt human beings. With technological development the totally separated operation of robots is being changed to closer cooperation. Industrial robots now can detect humans in their work-envelope and reduce their speed according to the motion of the human. This is a radical change to the previously in-fenced and no human in work-envelope concept. This paper is investigating today's policy and standards in human - robot interaction along with solutions for security of production cells. An example demo setup will also be shown, where the utilization of the newest technologies is emphasized. The paper also deals with introduction of high level control of security through simulation software.
KEYWORDS: Robot Safety, VALIP, Flexible Robotic Cell, Safeguards

INTRODUCTION

It has been said that the only constant in life is change. The ever changing field of robotic engineering and robot application is gaining new followers each day. In accordance to this, the safety standards and trends must be continuously updated and revised.

From the first robot idea to modern robot systems, two fundamental robot attributes are: the power to handle super-human payloads and the flexibility enabled by full range of motion. And exactly these main attributes pose a danger to people working with them. At first, robots were caged up, distancing the robot from the operator to prevent injuries. If the operator needed to interface with the robot - to load or unload parts within the machine's work area- the safety control system would need to help to confirm that the robot was in a safe state. This often meant full stop for the robot and cutting its power source, resulting in reduced productivity.

New software-based safety systems slow down a robot to a safe speed or direct robot's motion to a safe position, allowing people to share the same workspace with far less risk of injury. New technologies require, so called "collaborative robots", allowing the robot and the people to share the same workspace and work side-by-side. In accordance to this, safety solutions and standards must follow these upturns.

The organization of the paper is as follows: section 2provides a brief overview of the main characteristics of the most commonly used protective devices in robotic cells. Section 3presents most important standards relevant to designing the safety solution for robotic cell. Section 4 shows the practical use of previous two sections while designing flexible robotic cell at Narvik University College. Section 5 explains the integration of safety with VALIP system while section 6 concludes the paper.

SAFETY SOLUTIONS

Depending on the purpose of the robot system, there is a broad range of safety solutions. Within this paper we will retain focus on safety requirements for small robotic cells, as well as using robots in educational purposes.

The choice of selecting the best safety solution depends on the specific job that the robot is performing, the working area and the possibility of injuries for the people. The best choice for protective measure is a device or a system that provides maximum protection with the minimum impact on normal machine operation.

Safety-rated programmable logic controllers (PLCs) play a crucial role in a robotic work cells. They collect input data from sensors about a status of a person within the robot work space, as well as inputs from safety devices such as e-stops, pendants, sensors and interlock switches. PLC outputs help control the robot power circuit, robot servos, as well as any other devices within the cell.

Physical protection - guards

If the robot is performing a task that does not need human interference, the best solution is to use this form of protection. The good aspect of using physical protection is distancing the operator from the hazard and protection from flying objects.

The guards often have a door with interlock switch fitted to the guard door. While the door is open, the robot is not moving. The operating process starts once the doors are closed and locked. If the doors are opened during the operating process of the robot, robot stops, and to have it started again, it is needed

to press the reset button. This button is located outside the protected area to prevent trapping the personnel inside the robot working area.
Figure 1 shows robotic cell safeguarded by guards, safety mats and light curtains.

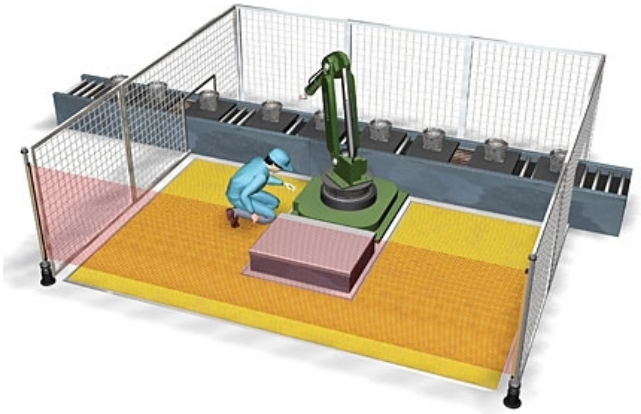

Fig. 1. Example of the robotic cell [9]

Optical protection

This form of protection is suitable when objects are to be passed in and out of the risk area, without stopping the industrial process. The main advantage of optical protection is the overall visibility of the robot and the working process.

☐ ***Laser scanners***

Safety laser scanners use pulses of light complemented with rotation mirror that deflects light pulses over an arc, thus creating a plane of detection. These scanners are based on the principle of "time-of-flight" measurement. The scanner emits very short pulses of light and at the same time an electronic stopwatch is started. If the light strikes an object, it is reflected and received by the safety laser scanner. The safety laser scanner calculates the distance to the object based on the time between sending and reception of the pulse.
Laser scanners create two zones: 1) a warning zone and 2) a safety zone (fig. 2). The warning zone provides a signal that does not shut down the hazard but informs personnel that they are approaching the safety zone, by optical or soundalarm. Objects entering or detected inside the safety zone cause the laser scanner to initiate a machine stop signal.
The main advantage of the laser scanners over horizontal light curtains or mats is the ability to reconfigure the scanning area. The shape and the size of the protected area is configured by corresponding software and downloaded to the scanner. They can also be programmed to accept specific intrusions that meet a certain shape profile, using additional sensors. Laser scanners support multi-zone safeguarding, where the overall scanning range of one device is divided in max 4 zones, with each zone supporting a warning and safety zone. They can be mounted either horizontally or vertically.
Disadvantage of the laser scanners is slower response time and lower level of resolution compared to light curtains.

☐ ***Camera systems***

Safety camera systems are electro-sensitive protective devices that use image processing technology to detect intrusion into hazardous area. These cameras can be used to monitor rectangular horizontal or vertical planes of nearly any size. When the camera detects intrusion, it sends a signal to the safety controller. They can be used for hand or body detection.

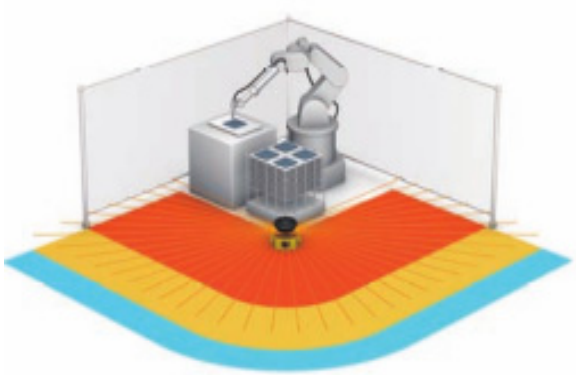

Fig. 2. Laser scanner [9]

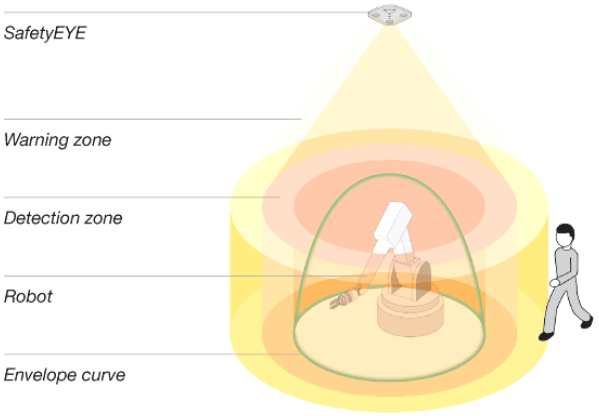

Fig. 3. Safety camera [13]

☐ ***Light curtains***

Light curtains are most simply described as photoelectric presence sensors. They must be placed at such distance to prevent the user from reaching the hazardous area before the danger is eliminated.
Safety light curtains consist of emitter and receiver pair that creates a multi-beam barrier of infrared light in front of, or around, a robotic cell (fig. 4). To eliminate susceptibility to interference from other opto-electronic devices, the LEDs in the emitter are pulsed at a specific rate, with each LED pulsed sequentially so that an emitter can only affect the specific receiver associated with it.
The working process is compound of scans, where every beam is checked. When any of the beams get blocked, the light curtain control circuit turns its output signal off. The output signal is used to control the hazard, whether to reduce robot speed or to stop it completely. In case of the failure of one of the components of the light curtain, the output signal is sent to stop the robot movement and to the control unit.
Light curtains are often integrated into the safety system by connecting them to the safety PLC. In that case the PLC handles switching the loads, the start/restart interlock and external device monitoring.
One of the important criteria when selecting a light curtain is the resolution. Resolution is the theoretical maximum size that an object must have to always trigger the light curtain. Most frequently used resolutions are:

- *14mm - commonly used for finger detection*
- *30mm - used for hand detection*
- *50mm to 70mm - commonly used for limb detection*
- *>70mm - larger values are used for full body detection.*

Important advantage of the light curtains is function for blanking and muting of the beams. Blanking function allows few of the beams to be disabled to accommodate objects typically associated with the process. These objects must be ignored by the light curtain, while the light curtain still provides detection of the operator. There are two types of blanking:

- *Fixed blanking-used for blanking the portion of the light curtain because of the machine fixture, work piece or the conveyor. This function requires for the object to be in the specific area at all times. If any of the beams programmed as "blanked" are not blocked, a stop signal is sent to the machine;*
- *Floated blanking - this option allows an object to penetrate the sensing field at any point without stopping the machine. This is accomplished by disabling up to two beams anywhere within the sensing field of the curtain. The number of blanked beams depends on the resolution of the light curtain.*

Muting function allows for the beams to be blocked for a programmed period of time. This is often used for loading/unloading the cells. To use this function the curtains must be equipped with horizontally positioned sensors to detect the object entering the robotic cell. After receiving signal from the sensors, the beams are blocked for a programmed period of time. After this time has passed the protection is turned on again.

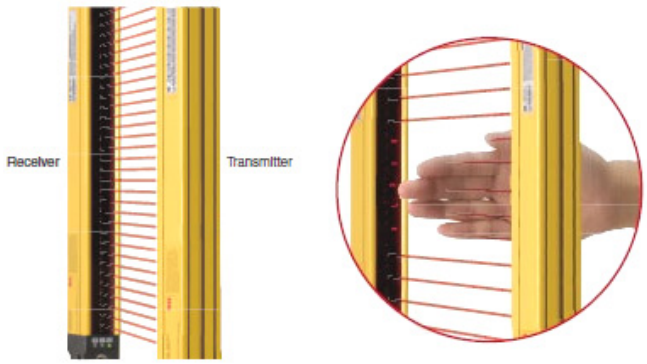

Fig. 4. Light curtain [9]

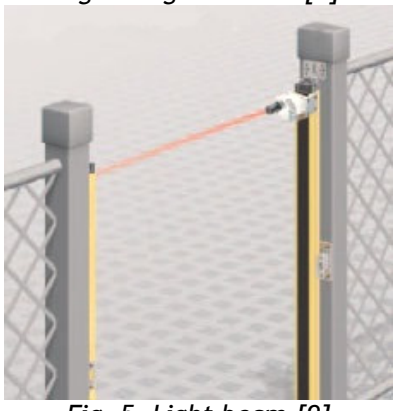

Fig. 5. Light beam [9]

Light curtains can be mounted horizontally or vertically, depending on the type of the protection needed. Also, the important advantage of the light curtains is the use of mirrors. Mirrors are used to deflect the beams, guarding two sides of a robotic cell with one pair of the light curtains. It has to be emphasized that the use of two or more mirrors is not recommendable because of signal loss and difficulties in the alignment of the beams.

- ***Light beams***

Light beams are photoelectric presence sensors, used for long scanning range. Theycan be designed with a single beam or with multiple beams barrier. Light beams are mainly used to detect personnel or objects entering the robotic cell. If the beam is blocked, the stop signal is sent to the robot.

The main difference between multiple light beams and light curtains is the resolution. Multiple light beams have a minimum resolution of 150mm and are used for long scanning range, up to 70m.

Mirrors can also be used to deflect the beams, thus simplifying the overall layout of the cell.

Safety mats

Presence sensing mats and controls are used where perimeter access guarding of a smaller area is required. Less downtime occurs because it is not necessary to set up or remove mechanical safety barriers during operation and maintenance. Multiple safety mats can be wired in series to form a complete floor-level guarding system. A signal is transmitted through the upper and lower plates separately via two wires connected to each plate. The signals through the safety mats are monitored by a controller. When the sufficient pressure is applied to the active mat area, the conductive plates touch causing the output relays in the controllers to de-energize and a stop signal is issued to the machine. If the wire should brake, or be at any way disconnected from the controller, or should the safety mat be punctured, the stop signal will be sent. The controller will not restart until the malfunction is removed.

Safety mats are completely sealed thus liquids presents no danger to the safeguarding of the cell.

SECURITY STANDARDS

In order for a machine to be made safe it is necessary to assess the risk that can result from its use. Risk assessment and risk reduction are described in EN ISO 12100:2010 and ISO/TR 14121. Note that the significance of a hazard depends upon both damage and probability of occurence.

When a risk assessment shows that a machine or process carries a risk of injury, the hazard must be eliminated or contained. In basic terms this means preventing any access to the relevant parts while they are in a dangerous condition. To achieve this, we can choose either: preventing access during dangerous motion or preventing dangerous motion during access.

Two main standards that deal with this question are EN ISO 13855:2010 and EN ISO 13857:2008.

EN ISO 13855:2010 deals with positioning of safeguards with respect to the approach speeds of parts of the human body. The position of the

safeguard depends on calculated minimum distance. Minimum distance is defined as calculated distance between the safeguard and the hazard zone necessary to prevent a person or part of a person reaching the hazard zone before the termination of the hazardous machine function [2]. One of the main aspects for calculating the minimum distance between robot and safeguard is the overall system stopping time. This time consists of two components:

- *Maximum time between the occurrence of the actuation of the safeguard and the output signal achieving the OFF-state*
- *Maximum time required to terminate the hazardous machine function after the signal from the safeguard achieves the OFF-state. The response time of the control system of the machine shall be included in this component.*

General equation for calculating minimum distance to the hazard:

$$S = (K \cdot T) + C$$

where:

S is the minimum distance, in millimetres (mm);

K is a parameter, in millimetres per second (mm/s), derived from data on approach speeds of the body or parts of the body whose value depends on the resolution of the safeguard;

T is the overall system stopping performance, in seconds (s);

C is the intrusion distance, in millimetres (mm), and depends on the resolution of the safeguard.

There are also specific requirements for the orthogonal approach to the detection zone, parallel approach, and also arrangements for angled approach or for the approach where the path from the detection zone to the hazard zone is restricted by the obstacles.

The minimum distance value obtained this way should be measured from the robots most extended position, maximum arm reach.

This standard also addresses the calculation of the minimum distance requirement for preventing circumventing of the protective equipment by reaching over the safeguard.

$$S = (K \cdot T) + C_{RO}$$

where:

CRO is additional distance which a part of the body can be moving towards the hazard zone prior to the actuation of the safeguard (values are listed in the standard).

EN ISO 13857:2008 standard defines the safety distances to prevent hazard zones being reaches by upper and lower limb. The calculation of the distance depends on the risk assessment by ISO 12100 and ISO 14121, whether the risk is low or high, on the height of the hazard zone and height of the protective structure. After collecting this information, standard offers values of different safety distances in the table.

The important question that has to be answered is if the person can be between the safeguard and the hazard. If this is possible the reset switches should be positioned outside the hazard zone. In this case the operator has to be outside of the hazard zone to reset the protection.

ROBOTIC CELL AT NARVIK UNIVERSITY COLLEGE

Utilization of these standards and above mentioned safety technologies will be reflected in the design of flexible robotic cell in the laboratory at Narvik University College.

Laboratory at NUC consists of three robots:

- *KUKA K30-3*
- *ABB FlexPicker IRB340*
- *ABB IRB 1500*

For designing the robotic cell, primary task was to define work assignment for the robots which will include synchronized operation for all three robots. The assignment consists of the following (fig. 6):

- *KUKA robot will be placing plates on one of the conveyors*
- *ABB IRB 1500 robot will be placing small part on the other conveyor*
- *ABB FlexPicker will place the parts on the plate in a specified pattern.*

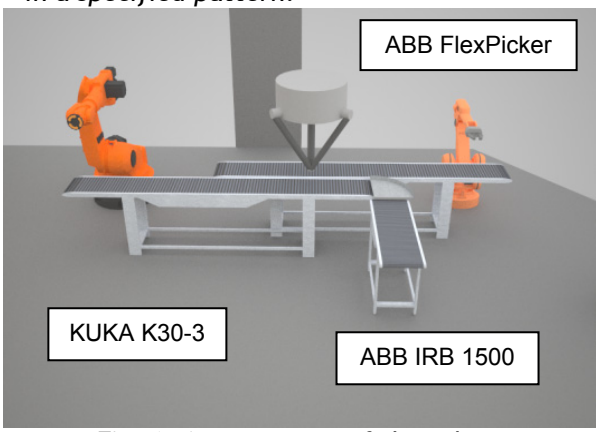

Fig. 6. Arrangement of the robots

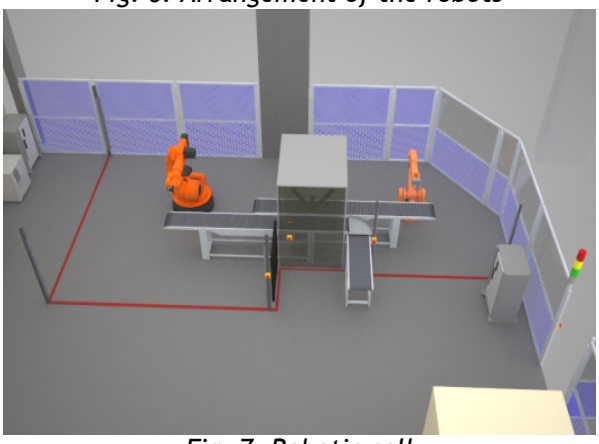

Fig. 7. Robotic cell

After a few versions of the robotic cell, the final decision about safeguards involves using partly physical and partly optical fence. The reason why the fully physical fence was not used primary lies in the function of these robots. Robots will be used for educational purposes, so the programming of the robot and the robot movement and task execution should be easily seen. The reason why the full optical fence is not used is simply the cost of these devices. With this solution, robot movement can be monitored with the operator standing at the safety distance. Figure 7 shows the final layout of the cell.

The robotic cell is surrounded by physical fence, with a door containing a lock to prevent unauthorized access. ABB FlexPicker has its own housing due to its construction. The ABB IRB 1500 robot is protected by

one pair of the light curtains with hand detection resolution. KUKA robot is protected by one pair of light curtains with a deflecting mirror on the corner. Emergency stops are placed at the entrance of the cell and at the main points near the robots.
In the process of designing this robotic cell, the distances between the robot and the guards are calculated according to the standard ISO 13855:2010.
The robotic cell will be monitored and controlled by safety PLC. It will be possible to give command to the PLC through specially designed user interface. This interface will be installed on one of the computers in the laboratory. Next section explains the operating principles of this interface.

INTEGRATION WITH VALIP

VALIP is an acronym which stands for Virtual Joint Laboratory for Advanced ICT (Information and Communication Technology) in Production. It represents a virtual copy of the real environment, e.g. laboratory or production environment with machines, robots and industrial equipment, allowing the collaborators to remotely access the resources that would otherwise be unavailable to them [1].
The important part of this virtual reality is the safety of the robots, equipment and personnel. If the operator from e.g. Banja Luka is using VALIP to remotely access robots in Narvik, he will see the robotic cell in virtual reality, but cannot be aware of every angle and every danger that can happen as he is using virtual reality and cameras have blind spots. For that reason, integration of safety is important part of VALIP. This is a new born idea, and will first be integrated with robotic cell in Narvik.
The primary idea is to have a program that will communicate with safety PLC on one side, and virtual reality generator on other side. This program will represent one of the main components in VALIP system.

Fig. 8. Example of GUI for VALIP system

When the safety light beams are blocked, PLC will stop the robot and send a signal to designated component in VALIP system which will further inform the whole system about the new state of the cell. Virtual reality generator will reflect this information to visual presentation of the cell.
The reverse communication will also be possible. Person who is remotely operating the cell will be able to send commands to the PLC to power the robots or the conveyors, through user interface rendered in virtual reality.
This way the operator has a complete understanding of the robotic cell, movement of the robot and its safety. The visualization of this program is represented in the next figure.

CONCLUSIONS

Human safety in robotic cells is one of the most important aspects when it comes to designing the robotic cell. The market today offers a broad range of security equipment and solutions. The final choice depends on the specific robot task, the robot surroundings and the level of human interference. Above mentioned standards should be consulted when designing the robotic cell and choosing the safeguard for the maximum protection.
Integration of security in VALIP system represents new concept of visualization of the robotic cell. As security is important part of robotic cell it also represent important part of virtual reality, to safeguard the robot, equipment and persons who might find themselves in the surroundings. It is also important for the remote operator to be aware of these facts and this is where this VALIP component has a primary role.

ACKNOWLEDGMENT

This work has been supported by BANOROB project, funded by the Royal Norwegian Ministry of Foreign Affairs.

REFERENCES

[1] Malešević, N., Sziebig, G., Solvang, B., Latinovic, T. (2013). Simulation of robotic tasks with VALIP system - Practical application. DEMI 2013 Conference Proceedings, in press.
[2] EN ISO13855:2010.Safety of machinery: Positioning of safeguards with respect to the approach speeds of parts of the human body. International Organization for Standardization. Geneva.
[3] EN ISO 13857:2008.Safety of machinery: Safety distances to prevent hazard zones being reached by upper and lower limbs. International Organization for Standardization. Geneva.
[4] EN ISO 12000:2010.Safety of machinery: General principles for design, Risk assessment and risk reduction. International Organization for Standardization. Geneva.
[5] Robotic Industries Association. Safety Mats, from http://www.robotics.org, accessed on 2013-04-09.
[6] Rockwell Automation. Protective Measures and Complementary Equipment, from http://www.rockwellautomation.com, accessed on 2013-04-10.
[7] ABB. Focus II Original Instructions, from http://www.abb.com, accessed on 2013-04-10.
[8] ABB. Light Curtains, Light Grids and Light Beams, from http://www.abb.com, accessed on 2013-04-10

[9] OMRON Industrial Automation, http://www.omron.com, accessed on 2013-04-11.
[10] SICK Sensor Intelligence. Safety Laser Scanners, from http://www.sick.com, accessed on 2013-04-11.
[11] SICK Sensor Intelligence. Safety Light Curtains, from http://www.sick.com, accessed on 2013-04-11
[12] Robotic Industries Association. Robot Safeguarding Devices Embody Higher Functionality at Lower Cost, from http://www.robotics.org, accessed on 2013-04-12.
[13] Pilz. SafetyEYE monitors KUKA's RoboTeam, from http://www.pilz.com, accessed on 2013-04-13.

ACTA TECHNICA CORVINIENSIS - BULLETIN of ENGINEERING

ISSN: 2067-3809 [CD-Rom, online]

ACTA TECHNICA CORVINIENSIS – Bulletin of Engineering
Tome VI (Year 2013) – FASCICULE 4 [October–December]
ISSN 2067–3809

[1.] Petar ČISAR, [2.] Sanja MARAVIĆ ČISAR

IMPROVEMENT OF EXPONENTIAL SMOOTHING USING SIMULATED NETWORK ENVIRONMENT

[1.] ACADEMY OF CRIMINALISTIC AND POLICE STUDIES, BELGRADE – ZEMUN, SERBIA
[2.] SUBOTICA TECH, SUBOTICA, SERBIA

ABSTRACT: This paper gives a general overview of the EWMA statistics. In addition to already known concepts, the paper presents a comparative analysis of different smoothing schemes. The optimization possibilities of this statistics are also discussed. With intention to improve the process of exponential smoothing, the behavior of the moving trimmed mean and moving median in computer network environment was examined in relation to the most commonly used moving average. For this purpose, several different types of distribution are used to model network traffic. Using the software package "Matlab", sequences of random numbers are generated for each type of distribution, as the way to simulate network traffic. It is shown that the moving average and moving trimmed mean better follow the curve of original traffic. At the same time, comparing the situation with and without outliers, the smallest relative jump of MSE was determined for moving average and moving median. This conclusion justifies their use for the elimination of the negative impact of outliers and positively affects the general level of traffic control in computer networks.
KEYWORDS: computer networks, mean square methods, optimization, smoothing methods, statistical distributions

INTRODUCTION

Inherent in the collection of data taken over specific time is some form of random value variation. There exist various methods for reducing the unwanted effect due to random variation. An usual statistical technique is smoothing. This technique, when properly applied, detects more clearly the underlying trend, seasonal and cyclic components. There are two different categories of smoothing methods: averaging and exponential smoothing. Taking averages is the simplest way to smooth data. Given a series of numbers and a fixed subset size, the moving average can be obtained by taking the average of the first subset. The fixed subset size is then shifted forward, forming a new subset of numbers, which is averaged. This process is repeated over the entire data series. The line connecting all the calculated partial averages is the graphical representation of moving average. A moving average is a set of numbers, each of which is the average of the corresponding subset of a larger set of data points.

The exponentially weighted moving average (EWMA) is a statistic for monitoring the process that averages the data in a way that gives adjustable weight to data as they are further removed in time. For the EWMA control technique, the decision regarding the state of control of the process depends on the EWMA statistic, which is an exponentially weighted average of all prior data, including the most recent measurements.

By the choice of weighting factor λ, the EWMA control procedure can be made sensitive to a small or gradual drift in the process.

The statistic that is calculated is the following:

$$EWMA = \lambda Y_t + (1-\lambda)\cdot EWMA_{t-1} \qquad (1)$$

for t=1, 2, …, n

where

- EWMA0 is the mean of historical data
- Yt is the observation at time t
- n is the number of observations to be monitored including EWMA0
- $0 < \lambda \leq 1$ is a constant that determines the depth of memory.

This equation has been established by Roberts as described in [1]. The parameter λ determines the rate at which "older" data enter into the calculation of the EWMA statistic. A value of λ = 1 implies that only the most recent measurement influences the EWMA. Thus, a large value of λ = 1 gives more weight to recent data and less weight to older data - a small value of λ gives more weight to older data. The value of λ is usually set between 0.2 and 0.3 [2], although this choice is somewhat arbitrary. Lucas and Saccucci [3] have shown that although the smoothing factor λ used in an EWMA chart is usually recommended to be in the interval between 0.05 to 0.25, in practice the optimally designed smoothing factor depends not only on the given size of the mean shift δ, but also on a given in-control Average Run Length (ARL). ARL represents the average number of determined process points before the first point indices the appearance of out-of-control state (exceeding one of the control limits).

The estimated variance of the EWMA statistic is approximately [4]:

$$\sigma^2_{EWMA} = \frac{\lambda}{2-\lambda} \cdot \sigma^2 \qquad (2)$$

where σ is the standard deviation calculated from the historical data.

The center line for the control chart is the target value or $EWMA_0$. The upper and lower control limits are:

$$UCL = EWMA_0 + k\sigma_{EWMA} \qquad (3)$$

$$LCL = EWMA_0 - k\sigma_{EWMA} \qquad (4)$$

where the factor k is either set equal 3 (the 3-sigma control limits) or chosen using the Lucas and Saccucci tables (ARL = 370).

In addition to the aforementioned authors, the publications [5]-[12] have also dealt with the topic of EWMA statistics and the application of statistical anomaly detection in computer networks.

Control charts are specialized time series plots, which assist in determining whether a process is in statistical control. Some of the most widely used forms of control charts are X-R charts and Individuals charts. These are frequently referred to as "Shewhart" charts after the control charting pioneer Walter Shewhart who introduced such techniques. These charts are sensitive to detecting relatively large shifts in the process (i.e. of the order of 1.5σ or above). In computer network practice, shifts can be caused by intrusion or attack, for example. Two types of charts are usually used to detect smaller shifts (less than 1.5σ), namely cumulative sum (or CUSUM) charts and EWMA charts. A CUSUM chart plots the cumulative sums of the deviations of each sample value from a target value. An alternative technique to detect small shifts is to use the EWMA methodology. This type of chart has some very attractive properties, in particular:

1. Unlike X-R and Individuals charts, all of the data collected over time may be used to determine the control status of a process.
2. Like the CUSUM, the EWMA utilizes all previous observations, but the weight attached to data exponentially decreases as the observations become older and older.
3. The EWMA is often superior to the CUSUM charting technique due to the fact that it detects larger shifts better.
4. EWMA schemes may be applied for monitoring standard deviations in addition to the process mean.
5. EWMA schemes can be used to forecast values of a process mean.
6. The EWMA methodology is not sensitive to normality assumptions.

In real situations, the exact value of the shift size is often unknown and can only be reasonably assumed to vary within a certain range. Such a range of shifts deteriorates the performance of existing control charts.

COMPARISON OF SMOOTHING SCHEMES

Calculating the optimal value of parameter λ is based on the study of authentic samples of network traffic. Random variations of network traffic are normal phenomena in the observed sample. In order to decrease or eliminate the influence of individual random variations of network traffic on occurrence of false alarms, the procedure of exponential smoothing is applied, as an aspect of data preprocessing.

For any time period t, the smoothed value St is determined by computing:

$$S_t = \lambda \cdot y_{t-1} + (1-\lambda) \cdot S_{t-1} \qquad (5)$$

where $0 < \lambda \leq 1$ and $t \geq 3$.

This is the basic equation of exponential smoothing. The formulation here is given by Hunter [2]. It should be noted that there is an alternative approach, in which, according to Roberts [1], y_t is used instead of y_{t-1}.

This smoothing scheme starts by setting S_2 to y_1, where S_i stands for smoothed observation or EWMA, and yi stands for the original observation. The subscripts refer to the time periods 1, 2, ..., n. For example, the third period is $S_3 = \lambda y_2 + (1 - \lambda) S_2$ and so on. There is no S_1. The optimal value for λ is the value which results in the smallest sum of the squared errors (SSE) or mean of the squared errors (MSE).

Comparative analysis of two different approaches (Roberts and Hunter) can be shown using the example of a process (y_t), with adopted values $EWMA_0 = 50$ and $\lambda = 0.3$. EWMA values in the table below correspond to Roberts's and S_t to Hunter's equation.

Table 1. Comparison of smoothing schemes.

time	y_t	EWMA	S_t
1	52.00	50.60	
2	47.00	49.52	52.00
3	53.00	50.56	50.50
4	49.30	50.18	51.25
5	50.10	50.16	50.67
6	47.00	49.21	50.50
7	51.00	49.75	49.45
8	50.10	49.85	49.91
9	51.20	50.26	49.97
10	50.50	50.33	50.34
11	49.60	50.11	50.39
12	47.60	49.36	50.15
13	49.90	49.52	49.39
14	51.30	50.05	49.54
15	47.80	49.38	50.07
16	51.20	49.92	49.39
17	52.60	50.73	49.93
18	52.40	51.23	50.73
19	53.60	51.94	51.23
20	52.10	51.99	51.94
21			51.99

In Table 1 the fields with approximately equal values are marked with lighter colour, while fields with equal values are marked with darker colour. From this analysis it can be concluded that after a certain number of samples (in this case about the 16th sample) both schemes give the same smoothed values.

The behaviour of both smoothing schemes will be examined also with SSE values. After calculating SSE for different λ, results were as follows.

Analysis of the obtained results has shown that approximately similar values were obtained, with greater coincidence at higher values of smoothing factor.

Table 2. Comparison of values for SSE according to Roberts and Hunter

λ	SSE (Roberts)	SSE (Hunter)
0.1	62.81	75.01
0.2	49.95	55.86
0.3	39.28	42.16
0.4	30.25	31.62
0.5	22.40	23.01
0.6	15.50	15.71
0.7	9.55	9.57
0.8	4.70	4.66
0.9	1.31	1.29

The initial EWMA plays an important role in computing all the subsequent EWMA's. There are several approaches to define this value:

1. Setting S_2 to y_1
2. Setting S_2 to the target of the process
3. Setting S_2 to average of the first four or five observations

It can also be shown that the smaller the value of λ, the more important is the selection of the initial EWMA.

ARL CURVES

Using a graphical method, the EWMA chart can be designed to have minimal ARL for the out-of-control situation, for the known shift of the mean δ and given ARL for the in-control situation. This chart has two parameters - λ and k (derives from the definition of control limits).

Figures below show the dependence of λ and k of the mean shift δ, for ARL as parameter. Using appropriate curves, values k = 2.7878 and λ = 0.1417 were determined as the optimal choice for the earliest detection of shift δ = 1σ.

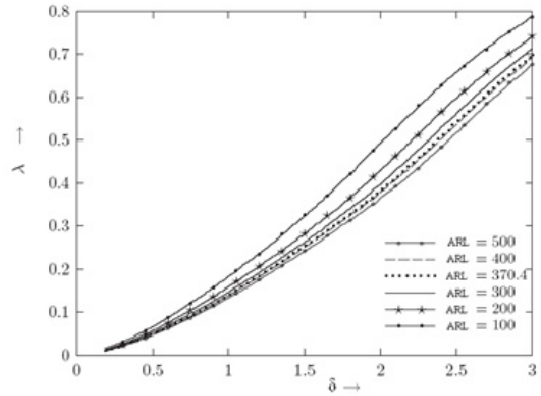

Figure 1. Optimal choice of λ in function of the mean shift [13]

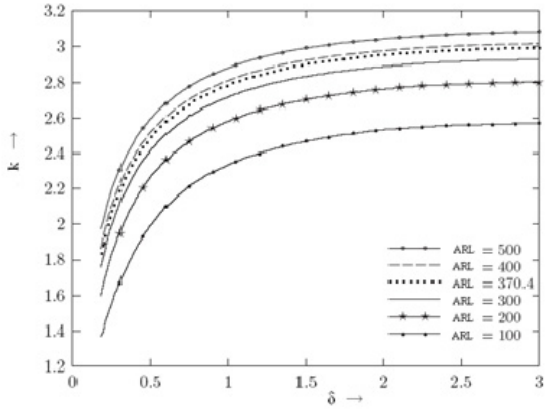

Figure 2. Optimal choice of k in function of the mean shift [13]

MOVING AVERAGE, MOVING MEDIAN AND MOVING TRIMMED MEAN IN SIMULATED NETWORK ENVIRONMENT

The calculation of moving average, based on time series network data, represents the basis of the application of EWMA statistics in network environment. This chapter will focus on the difference between moving average, moving trimmed mean and moving median, with the ambition to examine their behavior in a simulated network environment.

The changes in the computer network traffic are identified by analyzing time series information for one or more variables which indicates how the monitored variable changes over time. Network operators sometimes visually inspect such time series information to detect and characterize operational problems. However, it can be advantageous to inspect such time series information in an automated manner.

Unfortunately, outliers, data entry errors, or glitches exist in almost all real data. An outlier is an observation that lies an abnormal distance from other values in a random sample. In a sense, this definition leaves it up to the analyst to decide what will be considered abnormal. Before abnormal observations can be singled out, it is necessary to characterize normal observations. The sample mean is sensitive to these problems. One extreme data value can move the average away from the center of the rest of the data by an arbitrarily large distance, causing the situation of statistical anomaly or false alarm. The median and trimmed mean are two measures that are resistant (robust) to outliers. The median is the 50th percentile of the sample, which will only change slightly if you add a large perturbation to any value. The idea behind the trimmed mean is to ignore a small percentage of the highest and lowest values of a sample when determining the center of the sample. The geometric mean and harmonic mean, like the average, are not robust to outliers.

From a statistical point of view, the moving average, when used to estimate the underlying trend in a time series, is susceptible to rare events such as rapid shocks or other anomalies. A more robust estimate of the trend is the simple moving median. Statistically, the moving average is optimal for recovering the underlying trend of the time series when the fluctuations about the trend are normally distributed. However, the normal distribution does not place high probability on very large deviations from the trend which explains why such deviations will have a disproportionately large effect on the trend estimate.

There is no one single model that can be used effectively for modeling traffic in all kinds of computer networks. The type of network and the traffic characteristics dominantly influence the choice of the traffic model used for analysis. In the available literature the following types of distributions are used to model traffic: Poisson, normal, lognormal, Pareto, chi-square, Rayleigh, Weibull and gamma distribution. Using the software

package "Matlab" [15], sequences of 500 random numbers are generated for each type of mentioned distributions, as the way to simulate network traffic. For purpose of this research, the occurrence of outliers was simulated with 5 equal values, two times greater than the maximum value of all generated samples and distributed on every hundredth sample locations. Calculating the moving average, moving trimmed mean (10%, i.e. 5% of the highest and 5% of the lowest observations are excluded) and moving median, with width of the interval of 40 values (statistically large sample), the following values for the mean of the squared error (MSE) are obtained (values in brackets are MSE for the case without outliers):

Table 3. MSE for different distributions.

Distribution	MSE (moving average)	MSE (moving trimmed mean)	MSE (moving median)
Pareto	2.92 (0.84)	2.99 (0.85)	3.16 (0.95)
Normal	2.1 (0.976)	2.112 (0.975)	2.119 (0.986)
Poisson	8.41 (4.72)	8.57 (4.75)	8.63 (4.86)
Lognormal	0.473 (0.196)	0.481 (0.196)	0.487 (0.199)
Rayleigh	3.15 (1.715)	3.19 (1.717)	3.26 (1.749)
Chi-square	10.5 (4.32)	10.8 (4.41)	11.5 (4.86)
Weibull	0.396 (0.209)	0.401 (0.209)	0.412 (0.214)
Gamma	20.19 (7.65)	20.67 (7.67)	21.49 (8.08)

Analyzing the above table, it can be concluded that for all the observed types of distribution, moving average and moving trimmed mean generates lower MSE than moving median, which implies that the moving average and moving trimmed mean better follow the curve of original network traffic. Besides, in the context of absolute values, the smallest MSE is obtained using Weibull, lognormal and normal distribution. Comparing the situation with and without outliers, the smallest relative jump of MSE (corresponds to the best robustness) was determined for moving average and moving median. The smallest values for relative jump are calculated for Poisson (about 80%), Rayleigh (about 85%) and Weibull distribution (about 90%).

CONCLUSIONS

In addition to already known concepts about EWMA statistics, this paper presents a comparative analysis of different smoothing schemes. It was shown that after a certain number of samples (approximately after the 15^{th} sample), both known schemes provide the same smoothed value. With aim to improve the process of exponential smoothing, the behavior of the moving trimmed mean and moving median in computer network environment was examined in relation to the most commonly used moving average. For this purpose, network traffic is simulated using different types of distribution. It is shown that the moving average and moving trimmed mean curves better follow the curve of original traffic. At the same time, comparing the situation with and without outliers, the smallest relative jump of MSE (corresponds to the best robustness) was determined for moving average and moving median. This conclusion justifies their use for the elimination of the negative impact of outliers in the field of statistical anomaly detection and positively affects the general level of traffic control in computer networks.

REFERENCES

[1.] S.W. Roberts, "Control Chart Tests Based on Geometric Moving Averages", Technometrics, 1959., Vol. 42, No. 1, Special 40th Anniversary Issue, pp. 97-101, 2000.

[2.] J.S. Hunter, "The exponentially weighted moving average", Journal of Quality Technology 18: 203-210, 1986.

[3.] J.M. Lucas and M.S. Saccucci, "Exponentially weighted moving average control schemes: Properties and enhancements", Technometrics 32, pp. 1-29., 1990.

[4.] Engineering Statistics Handbook-EWMA Control Charts, http://www.itl.nist.gov/div898/handbook/pmc/section3/pmc324.htm

[5.] G. Fengmin, "Deciphering Detection Techniques: Part II Anomaly-Based Intrusion Detection", White Paper, McAfee Security, 2003.

[6.] S. Sorensen, "Competitive Overview of Statistical Anomaly Detection", White Paper, Juniper Networks, 2004.

[7.] X. Wu, V.A. Mahadik and D.S. Reeves, "A summary of detection of denial-of-QoS attacks on DiffServ networks", DARPA Information Survivability Conference and Exposition, 2003., Proceedings, Vol. 2, pp. 277-282.

[8.] A.S. Neubauer, "The EWMA Control Chart: Properties and Comparison with other Quality-Control Procedures by Computer Simulation", Clinical Chemistry, Vol. 43, pp. 594-601, 1997.

[9.] D. Seibold, "Enterprise Campus Security-Addressing the Imploding Perimeter", http://www.itsa.ufl.edu/2003/presentations/IntSec.ppt

[10.] S. Vasilios and F. Papagalou, "Application of Anomaly Detection Algorithms for Detecting SYN Flooding Attacks", Global Telecommunications Conference, 2004. GLOBECOM 04 IEEE, Vol. 4, pp. 2050-2054.

[11.] J. Viinikka and H. Debar, "Monitoring IDS Background Noise Using EWMA Control Charts and Alert Information", Recent Advances in Intrusion Detection, Lecture Notes in Computer Science, 2004, Volume 3224/2004, pp. 166-187.

[12.] Y. Zhao, F. Tsung and Z. Wang, "Dual CUSUM Control Schemes for Detecting a Range of Mean Shifts", IEEE Transactions 2005 (37), pp. 1047-1057.

[13.] S.B. Vardeman and J.M. Jobe, "Statistical Quality Assurance Methods for Engineers", John Wiley & Sons, New York 1999.

[14.] V. Ivanova, MIT Academic Computing, "MATLAB Tutorials", http://web.mit.edu/acmath/matlab/course16/16.62x/16.62x_Matlab.pdf

ACTA TECHNICA CORVINIENSIS - BULLETIN of ENGINEERING

ISSN: 2067-3809 [CD-Rom, online]

ACTA TECHNICA CORVINIENSIS – Bulletin of Engineering
Tome VI (Year 2013) – FASCICULE 4 [October–December]
ISSN 2067–3809

[1.] Krisztián LAMÁR, [2.] András Gergő KOCSIS

IMPLEMENTATION OF SPEED MEASUREMENT FOR ELECTRICAL DRIVES EQUIPPED WITH QUADRATURE ENCODER IN LabVIEW FPGA

[1.] INSTITUTE OF AUTOMATION, ÓBUDA UNIVERSITY, BUDAPEST, HUNGARY
[2.] DEPARTMENT OF ELECTRICAL MACHINES AND DRIVES, BUDAPEST UNIVERSITY OF TECHNOLOGY & ECONOMICS, BUDAPEST, HUNGARY

ABSTRACT: The paper introduces the basics of speed measurement with quadrature encoders. It explains the theory of the basic sensor types, and the signals of the quadrature encoder. It introduces the theory of the two main methods for speed measurement with quadrature encoders: the time based, and the frequency based method. It describes the quantization and relative errors of these two methods, and the considerations of their implementation. Finally it gives a short example of the practical implementation in LabVIEW FPGA, for the frequency based speed measurement method.
KEYWORDS: quadrature encoder, speed measurement, LabVIEW FPGA

INTRODUCTION

Controlling the speed of a motor is a basic functionality of modern electric drives. In order to precisely control the speed of an electric motor, it is necessary to measure the actual speed of the motor. This measurement can be done with various tools and methods. In most cases it is usually done with a sensor built in the motor or mounted to its shaft externally. These sensors vary in their principle, output signal, and resolution. Some of them are suitable for position measurement either. Selecting the right sensor is crucial, since this decision greatly influences the quality and the total cost of the drive [3].

In the past, tachogenerators were widely used for speed measurement purposes. This sensor is basically a small DC generator, which produce a voltage proportional to its speed [7]. Measuring its output voltage the speed can be calculated easily. With precise design and construction, good accuracy can be achieved in wide speed ranges. Determining the position of the shaft is not possible by measuring the output voltage of the tachogenerator.

THE QUADRATURE ENCODER

Nowadays mostly optical encoders are used for position and speed measurement of electric motors [3]. The theory of their operation is the following: in the sensor, there are phototransistor and LED couples facing each other [2]. Between them there is a disc which is mounted on the shaft of the encoder. On this disc, there are alternating transparent and non-transparent zones. When the motor is rotating, the light of a LED can reach the corresponding phototransistor depending on the type of zone which is between them at the moment [6].

There are two main types of optical encoders: absolute and incremental. With simply reading the signals of an absolute encoder it is possible to determine the position of the shaft [7]. This kind of sensor is more complex, thus more expensive than the incremental encoder.

In the incremental encoder there are three couples of phototransistors and LEDs. The disc between them has three different bands of alternating transparent and non-transparent zones. The disc and the position of the phototransistor and LED couples are designed to produce the following signals when the motor is rotating with constant speed:

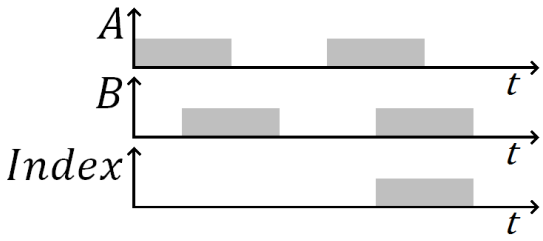

Figure 1. The typical signals of the incremental encoder

The signals of channel A and B are square waves, and there is a 90 degrees phase shift between them [1][2]. Based on this feature, incremental encoders are usually referred to as quadrature encoders. The index channel has only one impulse per revolution. Most of the applications use only the first two channels for speed measurement purposes. The Index channel can be used to get absolute position after the first revolution [1].

USING THE INCREMENTAL ENCODER

One of the most important properties of an incremental encoder is its resolution, what is equal

with the total number periods of the signals of channel A or B, under one revolution. The information about the motion of the motor is carried by the changes in the state of channel A and B. Hence this, there are four main points of every period of the signals:

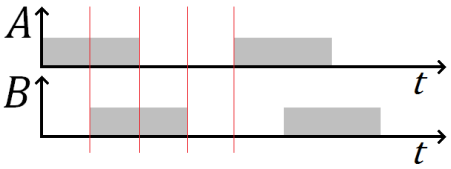

Figure 2. The main points of the two channel

By measuring the frequency of these points or the elapsed time between them, the speed of the motor can be calculated [3]. Based on how many of these points are used for the measurement, there are three different types of evaluation methods. The single evaluation method uses only one channels rising or falling edges, the double evaluation method using only one channel, but both its rising and falling edges, and the quadruple evaluation method uses every edges of the two channels. The selected evaluation method must be considered when the speed is calculated from the measured value.

A. Determining the direction of the rotation

This function can be easily realized with basic logic operations. When detecting a rising or falling edge on one of the channels, the current state of the other channel gives the direction [6]. For example: when there is a rising edge on channel A, the level of channel B is always high in one direction, and always low in the other one [1]. This information then can be stored in a Boolean variable, or in the sign of the measured value of the motors speed.

B. Time based speed measurement

One solution for measuring speed with incremental encoder is to measure the elapsed time between two of the main points shown in Figure 2 [3] [6]. Time measurement can be done by counting clock cycles:

$$T_1 = \frac{X \cdot E}{f_{clk}} \qquad (3.1)$$

Where T_1 is the elapsed time between the two points, E is the evaluation multiplier (E = 1, 2, 4), f_{clk} is the frequency of the used clock in Hz, and X is the count of clock cycles. From this, the time needed for one revolution can be calculated the following way:

$$T_{rev} = R \cdot T_1 \qquad (3.2)$$

Where T_{rev} is the time needed for one revolution and R is the resolution of the sensor. The speed of the motor is the reciprocal of this value:

$$w[rpm] = \frac{60}{T_{rev}} = \frac{60 \cdot f_{clk}}{R \cdot X \cdot E} \qquad (3.3)$$

Since this method basically calculates from the time needed for one revolution, the quantization error of the measurement is the following:

$$\Delta T_{rev} = \frac{E \cdot R}{f_{clk}} \qquad (3.4)$$

C. Frequency based speed measurement

Another solution for speed measurement is counting the main points (shown in Figure 2) for a certain amount of time, called the measurement time [3] [6]. From the result of the counting the time needed for one revolution can be calculated based on the following equation:

$$\frac{E \cdot R}{T_{rev}} = \frac{X}{T_m} \qquad (3.5)$$

Where E is the evaluation multiplier (E = 1, 2, 4), R is the resolution of the sensor, T_{rev} is the time needed for one revolution in seconds, X is the counted number of edges, and T_m is the measurement time in seconds. The speed can be calculated the following way:

$$w[rpm] = \frac{60}{T_{rev}} = \frac{60 \cdot X}{T_m \cdot E \cdot R} \qquad (3.6)$$

The quantization error of the measurement is the following [3] [6]:

$$\Delta w[rpm] = \frac{60}{T_m \cdot E \cdot R} \qquad (3.7)$$

CONSIDERATIONS OF THE SPEED MEASUREMENT METHODS

One most important property of the speed measurement is the quantization error. When using the frequency based method, it is recommended to use the quadruple evaluation if it is possible. Choosing the correct measurement time is essential. Basically, the longer the measurement time, the better the results are. In exchange for the longer measurement, the speed controller will be slower and this will decrease the quality of the drive [3]. This method is ideal for drives with high resolution encoders, because the higher resolution decreases the quantization error. Another advantage of this method that the measurement always as long, as we want it to be. The relative error of the measurement can be calculated, by dividing the quantization error with the actual speed of the motor [3]:

$$e_{rel\_freq} = \frac{\Delta w_{freq}}{w} \qquad (4.1)$$

Because the actual speed is in the denominator, the precision of this method increases with the speed.

With the time based method, the quantization error is smaller when low resolution encoders are used. The length of the measurement depends on the speed being measured: the lower the speed, the longer the measurement. Usually there is a maximum measurement time, and above that, the result is set to zero. The relative error is calculated by dividing the quantization error with the actual time what is needed for one revolution:

$$e_{rel\_time} = \frac{\Delta T_{rev}}{T_{rev}} \qquad (4.2)$$

Because the measured speed value is calculated from T_{rev} by division, the relative error of the speed measurement is the same. Since the time of one whole rotation decreases as the speed is higher, this method is more precise at lower speeds.

Because of the link between the speed and the relative errors, the two methods are often used together [3] [6]. Based on the speed of the motor, the software can switch between the two methods. The speed where the two methods have the same relative error can be calculated (in Fig 3. this point is

at 21 rpm) [3]. The switching point, or points should be somewhere around this speed.

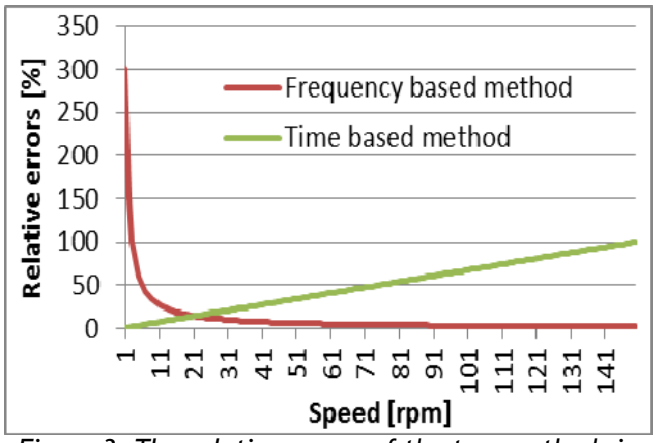

Figure 3. The relative errors of the two methods in the the function of the speed

If the drive is operating in position controlled mode, then the minimum speed the drive can measure gets very important at the end of the positioning. This value can be reduced by using higher-resolution encoders, better evaluation method, or increasing the length of the measurement. Both of the frequency and time based methods takes the same time when the drive is at the minimum speed. It is possible to reduce the effect of the quantization error if the start of measurement is synchronized with the signals of the quadrature encoder. For example: after the frequency based method finished the counting the edges of the signals and calculating the actual speed of the motor, the next measurement starts with the next edge. This function can also be important when the time based method is being used.

IMPLEMENTATION OF SPEED MEASUREMENT WITH THE FREQUENCY BASED METHOD IN LABVIEW FPGA

Practical implementation of speed measurement methods in LabVIEW FPGA is really simple. The following example will describe the algorithm and programming of the speed measurement with the frequency based method. The used quadrature encoder has a resolution of 5000 pulses per revolution. The example uses quadruple evaluation and a three milliseconds long measuring time. Based on the equation (3.7), the quantization error is one revolution per minute.

The whole code is in a "Single-Cycle Timed Loop". The clock associated with the loop has an 80 MHz frequency. This means that the loop is executed in every 12.5 nanosecond [4]. The channel A and B of the quadrature encoder is read by the purple colored "FPGA I/O Node" block shown in Fig. 4. Then the two signals are compared to their value from the last cycle saved by shift registers [5]. The comparison is made by the exclusive or gates. The signals of the exclusive-or gates then connected to an or gate which produces a signal that contains every impulse shown in Fig. 2. The case structure (the box with the black border) is in "Standby" state by default. When an edge is detected on one of the two channels of the encoder, the "Counting" state will be activated by the select element.

The "Counting" state is shown in Fig. 5. In this state the edges of the encoder are counted in a variable (the lower blue shift register). Another variable is incremented in every cycle. This variable is then compared to a constant outside the case structure. When the variable is greater/equal to the constant, it means that 240000 cycles have been elapsed (it equals with 3 milliseconds).

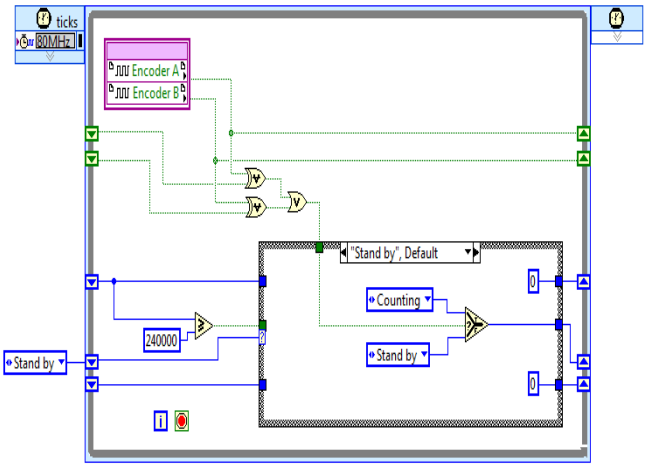

Figure 4. The timed loop of the frequency based speed measurement software with the "Standby" case

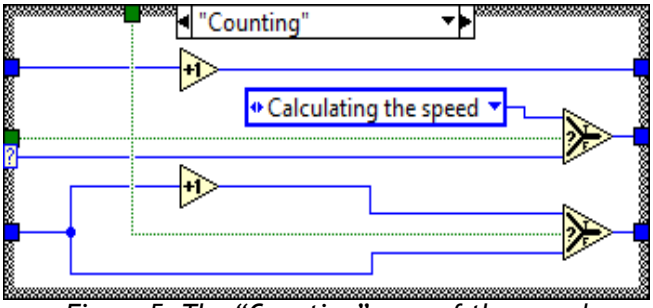

Figure 5. The "Counting" case of the speed measurement software

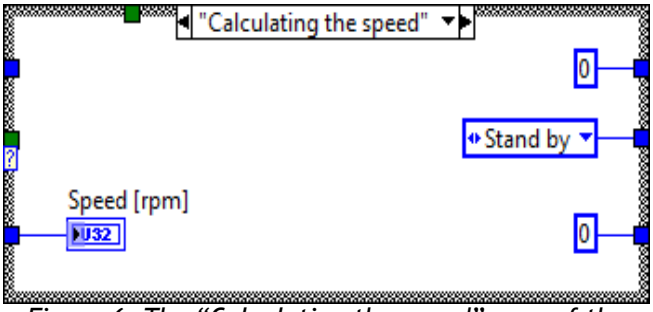

Figure 6. The "Calculating the speed" case of the speed measurement software

After this, the case structure will switch to the "Calculating the speed" case, shown in Fig. 6. In this case the speed is calculated from the variable that contains the count of the edges. In this example the speed in revolutions per minute equals with the count.

CONCLUSIONS

Speed measurement with quadrature encoder is a basic function of modern electric drives. As it can be seen in this paper, the basic theory of this function is simple, and it can be easily implemented. In simple cases, where only speed control is required (and the drive is not operating in the lower speed ranges), it is sufficient to use only the frequency based method

[6]. This makes the practical implementation easy and reliable. When positioning is required, it is recommended to use the two methods together, with an appropriate switching method to reduce the effect of the quantization and relative errors [3] [6]. This is also advised when the motor is equipped with a low-resolution sensor.

REFERENCES

[1] National Instruments, "Quadrature encoder fundamentals" Aug 27, 2008, http://www.ni.com/white-paper/4763/en/ (accessed 06-08-2013)

[2] National Instruments, "Encoder measurements: how-to guide" Mar 27, 2012, http://www.ni.com/white-paper/7109/en/ (accessed 06-08-2013)

[3] Petrella, R., Tursini, M., Peretti, L., Zigliotto, M.., Speed measurement algorithms for low-resolution incremental encoder equipped drives: a comparative analysis, Proceedings of International Aegean Conference on Electrical Machines and Power Electronics,. ACEMP '07, pp.780-787, 2007

[4] National Instruments, "LabVIEW FPGA module user manual" Mar, 2004, http://www.ni.com/pdf/manuals/370690b.pdf (accessed 06-08-2013)

[5] National Instruments, "LabVIEW user manual" Apr, 2003, http://www.ni.com/pdf/manuals/320999e.pdf (accessed 06-08-2013)

[6] Incze, I.I., Negrea, A., Imecs, M., Szabó, C.,"Incremental encoder based position and speed identification: modeling and simulation" Acta Universitatis Sapientiae, Series Electrical and Mechanical Engineering, Vol.2, pp.27-39, 2010

[7] Schmidt, I., Vincze, G., Veszprémi, K., Villamos szervo- és robothajtások, Műegyetemi Kiadó, 2000.

[8] Kiraly, I., Determination of correction coefficients of the slot leakage inductance for multi-phase machines, COMPEL-The International Journal for Computation and Mathematics in Electrical and Electronic Engineering, Vol.32, No.3, pp. 961-976, 2013

[9] Varga, A., Rácz, E., Kádár, P., New Experimental Method for Measuring Power Characteristics of Photovoltaic Cells at Given Light Irradiation, Proceedings of 8th IEEE International Symposium on Applied Computational Intelligence and Informatics, SACI-2013, Timisoara, Romania, pp.405-409, 2013

[10] Fuerstner, I., Gogolak, L., Pletl, S., Solution Diversity for a Specified Project in Mechatronics, Proceedings of the International Conference Science in Parctice, 2012

[11] Novak-Marcincin, J., Janak, M., Barna, J., Torok, J., Novakova-Marcincinova, L., Fecova, V., Verification of a program for the control of a robotic workcell with the use of AR, International Journal of Advanced Robotic Systems, Vol.9, Art. No. 54, 2012

[12] Rădac, M.-B., Precup R.-E., Petriu, E. M., Preitl, S., Experiment-based Performance Improvement of State Feedback Control Systems for Single Input Processes, Acta Polytechnica Hungarica, Vol.10, No.3, pp.5-24, 2013

[13] Sárosi, J., Accurate Positioning of Humanoid Upper Arm, International Journal of Engineering, Annals of Faculty of Engineering Hunedoara, Vol. 9, No. Extra, pp. 33-36, 2011

[14] Durovsky, F., Fedak, V., Integrated mechatronic systems laboratory, Proceedings of the 14th International Power Electronics and Motion Control Conference (EPE-PEMC 2010), pp.S51-S55, 2010

[15] Suto, J., Oniga, S., Remote controlled data collector robot, Carpathian Journal of Electronic and Computer Engineering., Vol.5. pp.117-120, 2012

[16] Balázs, G. Gy., Horváth, M., Schmidt, I., New Current Control Method for Grid-Connected Inverter of Domestic Power Plant, Proceedings of the 15th International Power Electronics and Motion Control Conference (EPE-PEMC 2012), pp.1-5. 2012

[17] Gyeviki J., Sárosi J., Csikós S., Position Control of Pneumatic Actuators with PLC 2011, Proceedings of the IEEE/ASME International Conference on Advanced Intelligent Mechatronics (AIM2011), pp.742-747, 2011

ACTA TECHNICA CORVINIENSIS – BULLETIN of ENGINEERING

ISSN: 2067-3809 [CD-Rom, online]

ACTA TECHNICA CORVINIENSIS – Bulletin of Engineering
Tome VI (Year 2013) – FASCICULE 4 [October–December]
ISSN 2067–3809

[1.] F.A. AISIEN, [2.] N.A. AMENAGHAWON, [3.] R. ADEBOYEJO

POTENTIAL APPLICATION OF RECYCLED RUBBER FROM SCRAP TIRE IN THE REMOVAL OF PHENOL FROM AQUEOUS SOLUTION

[1-3.] DEPARTMENT OF CHEMICAL ENGINEERING, FACULTY OF ENGINEERING, UNIVERSITY OF BENIN, PMB 1154, BENIN CITY, NIGERIA

ABSTRACT: The adsorption of phenol from aqueous solution using waste tire rubber granules (WTRG) was investigated in a batch system. The effect of various factors such as initial concentration of phenol, amount of adsorbent, size of adsorbent particles, pH and temperature of solution on the adsorption capacity of WTRG and percentage removal of phenol was studied. The equilibrium time for a phenol concentration of 700mg/l was obtained to be 60 minutes indicating fast adsorption. The percentage removal of phenol and adsorption capacity of WTRG increased from 20.5 to 40% and 5 to 10.6 mg/g respectively with decrease in particle size from 2.36 to 0.30mm. The adsorption capacity of WTRG was observed to decrease from 13.4 to 9.9 mg/g with increase in solution temperature from 5 to 45°C indicating that low temperatures favoured the adsorption of phenol. Maximum adsorption was recorded at a pH of 8.5 and an adsorbent dosage of 4g. Isotherm data were analysed using Langmuir and Freundlich isotherm models. The equilibrium data for phenol adsorption on WTRG was observed to fit Langmuir isotherm best with an R^2 value of 0.995.
KEYWORDS: Adsorption, Phenol, waste tire, adsorption capacity, isotherm

INTRODUCTION

One of the most important types of municipal solid wastes (MSW) is waste tires resulting from the increase in vehicle ownership and traffic volume around the world. These waste tires represent a major environmental problem as a result of their volume, non-biodegradability and indiscriminate disposal (Mousavi et al, 2010). An estimated 5 million tires from trucks, cars and motorcycles existed in Nigeria the early 1980s (Ebewele et al, 1990). As the country's population and economy grow, so does the amount and type of scrap tires generated. With an annual generation rate of 15%, between 700,000 and 850,000 scrap tires are added to the waste stream each year. Recently, Aisien et al, (2006) estimated that about 15 million scrap tires are now in existence in Nigeria.

Although some recycling methods for waste tire are currently employed such as uses in road pavement, rubber roofs, floor mats, liquid waste treatment, playground surfaces and as solid fuels for cement kiln and paper mill, still a huge amount of tires are discarded improperly (Aisien et al, 2002; Aisien et al, 2006). It is therefore imperative to explore other possible applications such as use as adsorbents.

The improper discharge of industrial organic effluents contaminates the environment. Phenol is a predominant aromatic compound usually contained in industrial wastewater. It is the basic structural unit of a variety of synthetic organic compounds found in wastewater originating from industrial operations such as oil refineries, pesticide and dye manufacture, phenolic resin manufacture, textile, plastic, tanning, rubber, pharmaceuticals etc (Mahvi et al, 2004; Manojlovic et al, 2007; Nagda et al, 2007). It is important to remove phenol from wastewater before discharge into any naturally occurring water body because it is highly hazardous, carcinogenic and resistant to degradation (Dabhade et al, 2007; Mahvi et al, 2004).

Conventional methods for removing phenolic compounds from industrial wastewater include solvent extraction, steam distillation, irradiation as well as chemical techniques such as electrochemical oxidation, reverse osmosis photocatalytic degradation and adsorption on activated carbon, ion exchange resins and silicates (Carmona et al, 2006; Goncharuk et al, 2002; Mokrini et al, 1997; Nagda et al, 2007; Polcaro et al, 1997). The major drawback with these methods is the cost associated with start-up and subsequent sustainability. Adsorption remains the best option for phenol removal as it can generally remove all types of phenolic compounds in a simple and easy operation. However, conventional adsorption using activated carbon is costly and its use is sometimes restricted on economic considerations. In comparison with conventional adsorbent, waste tire rubber granules offers an excellent alternative in that it is cheap and readily available. Recently interests has been shown in the use of waste tire rubber granules in the treatment of industrial wastewater (Aisien et al, 2002; Mousavi et al, 2010)

Hence the objective of this work is to investigate the potential use of recycled waste tire rubber as adsorbent in the removal of phenol from industrial wastewater. The study was focused on the sorption capability of waste tire rubber for phenol from aqueous solution by testing the effect of various

operational variables such as initial phenol concentration, adsorbent dosage, adsorbent particle size, pH and temperature of the aqueous solution.

MATERIALS & METHODS - Preparation of Adsorbent

Scrap tires were collected from Uwelu scrap tire dump site in Benin City, Nigeria. The tires were washed with water to remove dirt and were subsequently air dried. The cleaned sides of the tire free from steel breeds were cut into sections with the aid of a hacksaw and later into small pieces using very sharp knives. The size of the tire chips were further reduced using an electric grinding machine. The resulting tire particles were mechanically sieved to obtain particles in the size range 2.36 to 0.075 mm using different sieve trays as shown in Tables 1 and 2. The tire granules were then washed with distilled water to remove any foreign materials by agitating it with a mechanical shaker operating at 150 rpm for 3 hours. It was subsequently oven dried at 60°C for 5 hours and stored in airtight containers for subsequent use.

Table 1: Modified design gradations and Federal Ministry of Works (FMW) specification

Sieve size	FMW specification limit (% passing)	Gradation used (% passing)
19mm (3/4 in.)	100	100
12.5mm (1/2 in.)	85-100	85
9.5mm (3/8 in.)	75-92	77
4.75mm (#4)	65-82	65
2.36mm (#8)	50-65	50
1.18mm (#16)	36-61	41
0.6mm (#30)	26-40	26
0.3mm (#50)	18-30	21.5
0.15mm (#100)	13-24	13
0.075mm (#200)	7-14	8

Table 2: Rubber gradation

Sieve size	(% passing)
2.36mm (#8)	100
1.18mm (#16)	90
0.60mm (#30)	75
0.425mm (#40)	50
0.212mm (#75)	20

Solution Preparation

All chemicals used in this study were of analytical reagent grade and were used without further purification. Phenol solutions were prepared by diluting stock solution of phenol to the desired concentrations. A stock solution containing 1000mg/l of phenol was prepared by dissolving 1g of phenol (British Drug Houses Ltd, England) in 1000ml of distilled water.

Analysis of Phenol

The concentration of un-adsorbed phenol in the sorption medium was measured using a UV-Vis spectrophotometer (PG Instruments model T70) at a wavelength of 248nm. The instrument response was periodically checked by using standard phenol solutions.

Batch Adsorption Study

Adsorption of phenol on dried waste tire rubber granules was studied in batch experiments. The experiments were carried out in mechanically agitated 250ml Erlenmeyer flasks containing 2g of WTRG in 100ml of an aqueous solution of phenol of the desired concentration. The effects of pH, adsorbent dosage, contact time, initial phenol concentration and temperature on the adsorption capacity and percentage phenol removal were investigated. At the end of each experiment the agitated solution mixture was filtered using Whatmann No.1 filter paper and the residual concentration of phenol was determined spectrophotometrically.

The percentage removal of phenol from solution was calculated as follows:

$$\%\ \text{Removal} = \frac{Co - Ce}{Co} \times 100 \qquad (1)$$

where Co and Ce are the initial and equilibrium concentration of adsorbate respectively.

The adsorption capacity of the WTRG for phenol was expressed in terms of the ratio of the mass of phenol retained by the WTRG to that of the recycled rubber i.e.

$$\text{Adsorption capacity} = \frac{\text{Mass of phenol retained (mg)}}{\text{Mass of WTRG (g)}} \qquad (2)$$

RESULTS AND DISCUSSION - Effect of contact time on the adsorption of phenol on WTRG

The rate of adsorption is one of the influential factors that must be taken into consideration before planning batch adsorption experiments, hence the need to carry out time dependent studies. The profile of time dependent study of adsorption of phenol by WTRG is shown in Figure 1.

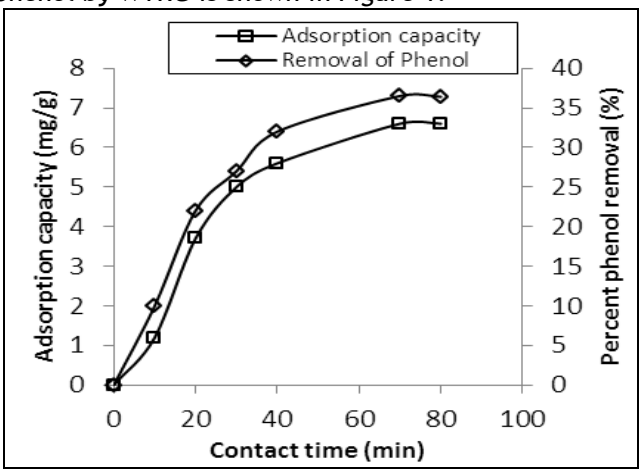

Figure 1: Effect of contact time on the removal of phenol from solution (pH 7; initial phenol concentration, 700 mg/l; WTRG dose, 2g; temperature, 31°C).

It can be observed from Figure 1 that adsorption was rapid within the first 40 minutes as indicated by the steep increase in both the adsorption capacity and percentage phenol removal. The profile flattens out after 60 minutes of contact indicating that equilibrium has been reached. Therefore, for further studies, the contact time was set at 60 minutes. The fast kinetic process observed at the initial stage can be attributed to the abundant availability of active binding sites on the adsorbent, which are later occupied as the adsorption process progresses, thereby resulting in the inability of the WTRG to

remove phenol at later stages of the adsorption process (Mahvi et al, 2004). Aisien et al, (2002) reported fast adsorption of crude oil on WTRG as is mostly observed in adsorption of organic solvent on WTRG.

Effect of initial phenol concentration on the adsorption of phenol on WTRG

The efficiency of WTRG in removing phenol from aqueous solution at different initial phenol concentrations was determined. The equilibrium sorption capacities of WTRG for different concentrations of phenol are presented in Figure 2.

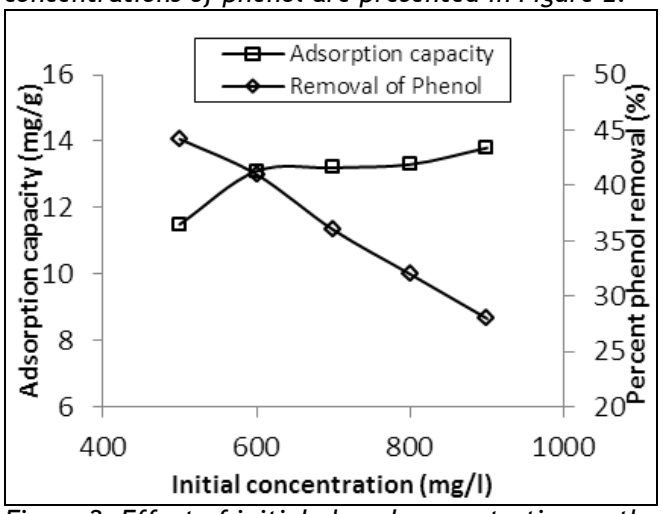

Figure 2: Effect of initial phenol concentration on the removal of phenol from solution (pH 7; WTRG dose, 2g; temperature, 31°C).

It can be observed from Figure 2 that the adsorption capacity increased with increase in initial phenol concentration. This indicates that there is a direct relationship between the uptake of phenol and the concentration of phenol in solution. The trend observed can be explained by the fact that increasing the concentration of phenol in solution increases the mass transfer driving force and therefore the rate at which phenol molecules pass from the bulk solution to the adsorbent surface (Mahvi et al, 2004). A different trend was however observed for the percentage removal of phenol from solution in relation to the initial phenol concentration as shown in Figure 2. The percentage removal decreased from 44.2 to 27.3% when the initial phenol concentration was increased from 500 to 1000mg/l because at high concentrations of phenol, the ratio of phenol present in solution to the available surface area for adsorption is high (Dabhade et al, 2007).

Effect of adsorbent dosage on the adsorption of phenol on WTRG

Adsorbent dose has a great influence on the adsorption process. Dosage of adsorbent added into the solution determines the number of binding sites available for adsorption (Zafar et al., 2007). Figure 3 shows the effect of adsorbent dosage on the adsorption capacity of WTRG for phenol and the percentage removal of phenol. It is evident from the Figure that for an initial phenol concentration of 1000 mg/l, increasing the adsorbent dose led to the enhancement of phenol uptake as a result of the greater surface area provided and availability of more active sites (Ho et al., 1995; Nagdah et al, 2007). Maximum removal of phenol was observed with an adsorbent dose of 4g.

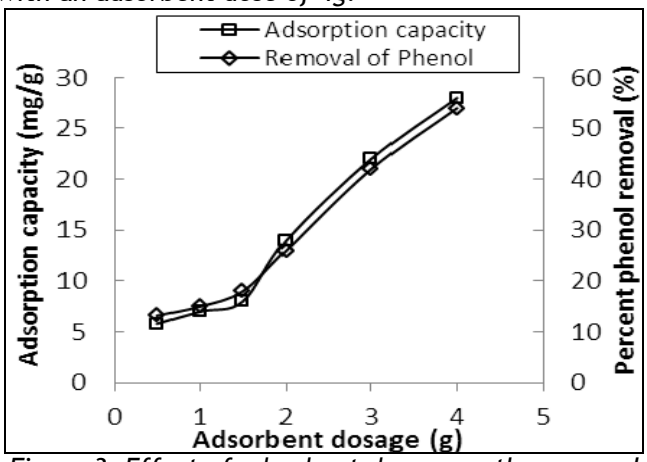

Figure 3: Effect of adsorbent dosage on the removal of phenol from solution (pH 7; initial phenol concentration, 1000 mg/l; temperature, 31°C).

Effect of pH on the adsorption of phenol on WTRG

Adsorption of phenol by WTRG is pH dependent as shown in Figure 4. The Figure shows that adsorption of phenol increases as the pH of the solution increases up to a maximum value of 8.5 after which it decreased.

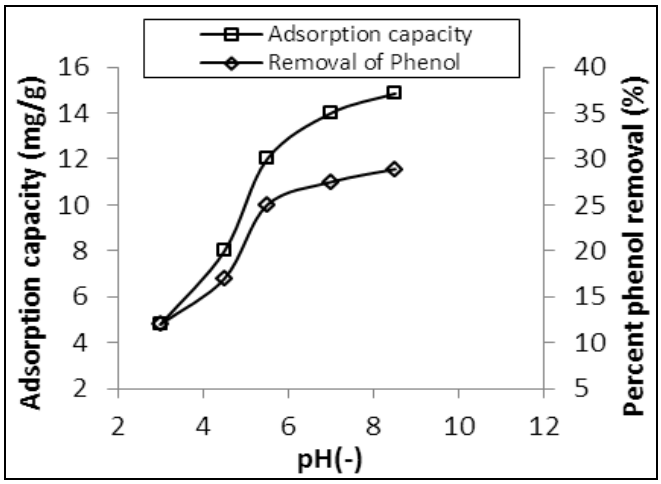

Figure 4: Effect of pH on the removal of phenol from solution (initial phenol concentration, 1000 mg/l; WTRG dose, 2g; temperature, 31°C).

The same trend was observed for both the adsorption capacity and percentage phenol removal. Atef et al, (2009) reported similar trends for the effect of pH on the adsorption of phenol on activated phosphate rock. Banat et al, (2010) also reported a similar trend for the effect of pH on the adsorption of phenol on bentonite. Phenol which is a weak acid (PKa=9.89) will be adsorbed to a lesser extent at pH values higher than its PKa value due to repulsive forces between negative surface charge on the adsorbent and the phenolate ion prevailing at such high pH values. This observation is explained by the fact that at pH values higher than its PKa value, phenol forms salts which readily ionize leaving a negative charge on the phenolic group. At the same time, the presence of the hydroxyl ions (OH^-) on the adsorbent limits the uptake of phenol (Atef et al, 2009). On the other hand, at low pH values, the surface of the adsorbent will also be surrounded by the hydroxyl ions but is less negative compared to surface charge

on the adsorbent at higher pH, which reduces the attraction of the phenolic group towards it (Tiemann et al., 2002).

Effect of adsorbent particle size the adsorption of phenol on WTRG

Figure 5 shows the percentage removal of phenol and adsorption capacity of WTRG at various sizes of adsorbent particles. The trend observed indicate that as the particle size increases, percentage phenol removal and adsorption capacity decreases. The percentage removal of phenol and adsorption capacity of WTRG decreased from 40 to 20.5% and 10.6 to 5mg/g respectively with increase in particle size from 0.30 to 2.36mm. The smaller the size of the adsorbent particles, the greater the interior surface area and micro pore volume and consequently more active sites are available for adsorption (Annadurai et al, 2000). However, for larger particles, the pore diffusion resistance to mass transfer is higher and most of the internal surfaces of the particle may not be utilized for adsorption and consequently the amount of phenol adsorbed is small (Annadurai et al, 2000). Aisien et al, (2002) reported similar trends for the uptake of crude oil by WTRG.

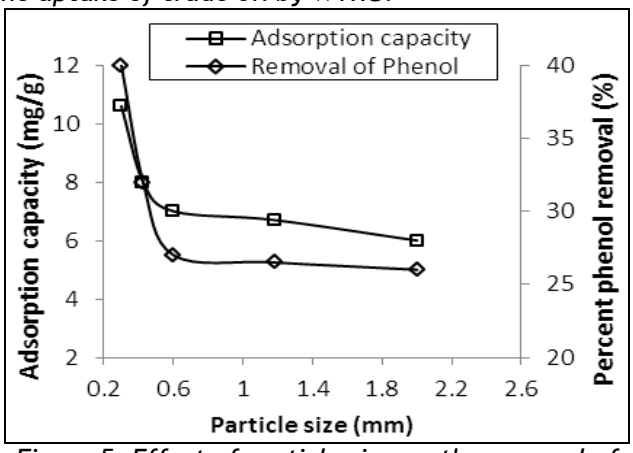

Figure 5: Effect of particle size on the removal of phenol from solution (initial phenol concentration, 1000 mg/l; pH 7; WTRG dose, 2g; temperature, 31˚C).

Effect of solution temperature the adsorption of phenol on WTRG

The effect of temperature on the WTRG/phenol system is shown in Figure 6. Percentage removal of phenol and adsorption capacity of WTRG decreased with increase in temperature. The adsorption capacity of WTRG was observed to decrease from 13.4 to 9.9 mg/g and the percentage removal of phenol from solution from 49.6 to 37.4 % with increase in temperature from 5 to 45°C. This indicates that a lower temperature is more favorable for the adsorption of phenol on WTRG. The trend observed is due to the weakening of the attractive force between phenol molecules and the adsorbent on the one hand and due to enhancement of thermal energies of the adsorbate on the other hand thus making the attractive force between the adsorbate (phenol) and adsorbent insufficient to retain the adsorbed molecules at the binding sites (Jadhav et al, 2003). Babarinde et al, (2012) reported similar trend for the adsorption of Nickel, Chromium and Cobalt ions from Aqueous Solutions using Cocoyam (Colocasia esculenta) Leaf. Aisien et al (2003) also reported similar results for the use of WTRG in the treatment of crude oil contaminated water.

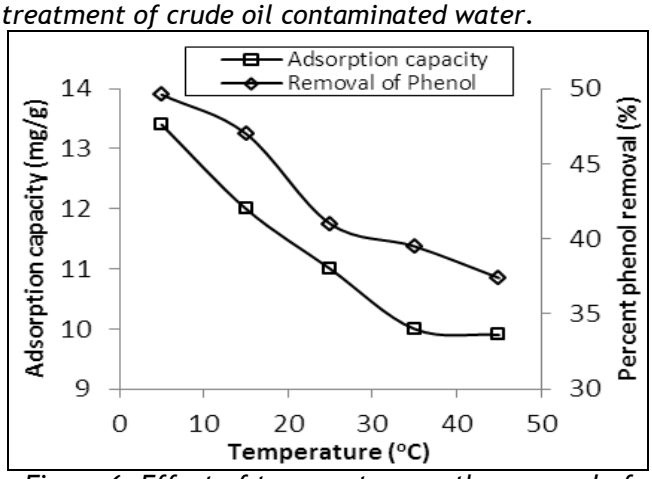

Figure 6: Effect of temperature on the removal of phenol from solution (initial phenol concentration, 1000 mg/l; WTRG dose, 2g; pH 8.5; temperature, 31˚C).

Isotherm Study

To examine the relationship between phenol uptake (Qe) and its equilibrium concentration in the solution (Ce), adsorption isotherm models are widely employed for fitting experimental data, of which the Langmuir and Freundlich isotherm equations are the most widely used. The curves of the related adsorption isotherms are regressed and parameters of the equation are thus obtained.

Langmuir Isotherm

The Langmuir model (Langmuir, 1918) has been used empirically because it contains the two useful parameters (Qo and b), which reflect the two important characteristics of the sorption system (Holan and Volesky, 1994; Volesky and Holan, 1995). It provides information on uptake capabilities and is capable of reflecting the usual equilibrium adsorption process behavior.

The linear form of the Langmuir equation is given as:

$$\frac{Ce}{Qe} = \frac{1}{bQo} + \frac{Ce}{Qo} \qquad (3)$$

Qo is the maximum sorption capacity (mg/g) of the adsorbent while b is the sorption constant (l/mg) at a given temperature. A linear plot of Ce/Qe against Ce as shown in Figure 7 was employed to obtain the values of Qo and b from the slope and intercept of the plot respectively. The essential characteristics of the Langmuir isotherm model can also be explained in terms of a dimensionless constant referred to as the separation factor (R_L) defined in Equation (4).

$$R_L = \frac{1}{(1+bCo)} \qquad (4)$$

Co is the initial concentration of phenol. The dependence of the nature of adsorption on the value of R_L is presented in Table 3. For the highest initial phenol concentration of 1000mg/l, R_L was calculated to be 0.0000115. Since this value is between zero and one, it implies that the adsorption is favourable.

The values of the Langmuir isotherm parameters as well as the correlation coefficient (R^2) of the Langmuir equation for the adsorption of phenol by WTRG are given in Table 4.

Table 3: R_L values and type of isotherm

R_L	Type of isotherm
R_L >1	Unfavourable
R_L =1	Linear
0< R_L <1	Favourable
R_L =0	Irreversible

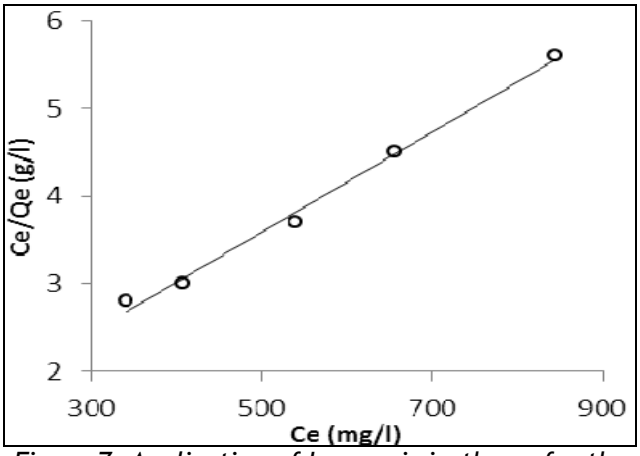

Figure 7: Application of Langmuir isotherm for the adsorption of phenol on WTRG

Table 4: Values of Langmuir isotherm constants for WTRG/phenol system

Qo (mg/g)	b (l/mg)	R^2
15.6	87.09	0.995

Freundlich Isotherm

The Freundlich isotherm is an empirical equation employed to describe heterogeneous systems. The Freundlich equation is expressed as:

$$Qe = K_f (Ce)^{1/n} \quad (5)$$

This equation can be expressed in linear form as follows:

$$\ln Qe = \ln K_f + 1/n \ln Ce \quad (6)$$

K_f and n are the Freundlich constants related to the adsorption capacity and adsorption intensity respectively. The intercept and slope of the linear plot of log Qe against log Ce at given experimental conditions as shown in Figure 8 provides the values of K_f and n. Values of n between 1 and 10 represent beneficial adsorption. The values of these parameters as well as the correlation coefficient (R^2) of the Freundlich equation for the adsorption of phenol by WTRG are given in Table 5.

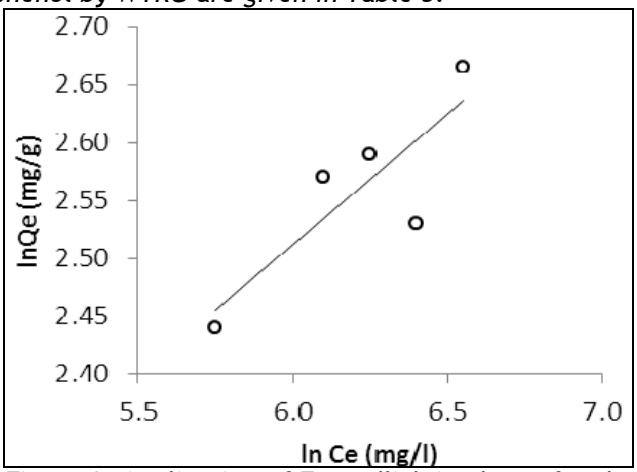

Figure 8: Application of Freundlich isotherm for the adsorption of phenol on WTRG

Table 5: Values of Freundlich isotherm constants for WTRG/phenol system

K_f (mg/g)	n	R^2
2.710	6.369	0.721

Comparison of the results presented in Tables 4 and 5 indicate that the experimental data fitted the Langmuir isotherm better than the Freundlich isotherm as evident in the higher R^2 value obtained for the Langmuir isotherm. This suggests that the adsorption of phenol by WTRG is of the mono-layer type and agrees with the observation that the phenol ions adsorbed from an aqueous solution usually forms a layer on the surface of the adsorbent.

CONCLUSIONS

The present study investigated the adsorption of phenol from aqueous solution using waste tire rubber granules in a batch system. The following conclusions can be drawn.

- ☐ Adsorption of phenol by WTRG is affected by operational parameters such as contact time, initial phenol concentration, adsorbent dosage and solution temperature.
- ☐ The excellent capability of WTRG as adsorbent for organic pollutants like phenol in aqueous solutions has been verified.
- ☐ The equilibrium contact time was obtained as 60 minutes indicating that the adsorption process was a fast kinetic process.
- ☐ Maximum removal efficiency was achieved at a pH of 8.5 and an adsorbent dosage of 4g.
- ☐ A low temperature (5°C) and small adsorbent particle size (0.212mm) favored the adsorption process.
- ☐ The adsorption of phenol by WTRG is of the mono-layer type and this was best described by the Langmuir isotherm with an R^2 value of 0.995.
- ☐ This study has revealed that the low cost WTRG can be widely used for removal of phenol from aqueous solution.

ACKNOWLEDGEMENT

The authors express their gratitude to the Authorities of the Technical Laboratory of the Chemical Engineering Department, University of Benin, Benin City, Nigeria for providing the facilities utilized in carrying out this study.

REFERENCES

[1.] Aisien, F.A; Hymore, F.K, and Ebewele, R.O: Potential Application of Recycled Rubber in Oil Pollution Control. Indian Journal of Engineering and Materials Science. 11, 179-190, 2002.

[2.] Aisien, F.A., Ebewele, R.O. and Hymore, F.K: Potential Application of Recycled Rubber in Oil Pollution Control. Environmental Monitoring and Assessment, 85, 175-190, 2003.

[3.] Aisien, F.A; Hymore, F.K, and Ebewele, R.O: Application of Ground Scrap Tire Rubbers in Asphalt Concrete Pavement. Indian Journal of Engineering and Materials Science. 13, 333-338, 2006.

[4.] Annadurai, G; Rajesh., B.S; Mahesh, K.P.O, and Murugesan, T: Adsorption and Biodegradation of Phenol by Chitosan-Immobilised Pseudomonas Putida. Bioprocess Engineering. 22, 493-501, 2000.

[5.] Atef, S; Alzaydien, S, and Waleed. M: Equilibrium, Kinetic and Thermodynamic Studies

on the Adsorption of Phenol onto Activated Phosphate Rock. International Journal of Physical Sciences.4(4), 172-181, 2009.

[6.] Babarinde, A; Babalola, J.O; Adegoke, J; Osundeko, A.O; Ibidapo, T.J; Nwabugwu, C.A, and Ogundimu. O.F: Biosorption of Ni(II), Cr(III), and Co(II) from Aqueous Solutions using Cocoyam (Colocasia esculenta) Leaf: Kinetic, Equilibrium, and Thermodynamic Studies. Pacific Journal of Science and Technology. 13(2), 272-282, 2012.

[7.] Banat, F.A., and Al-Asheh, S: The Use of Human Hair as a Phenol Biosorbent. Adsorption Science and Technology.19, 599-608, 2001.

[8.] Dabhade, M.A; Saidutta, M.B, and Murthy, D.V.R. Adsorption of Phenol on Granular Activated Carbon from Nutrient Medium: equilibrium and kinetic study. International Journal of Environmental Research. 3(4), 557-568, 2007.

[9.] Ebewele, R.O., and Ozing, L.H: Potential Application of Recycled Rubber. Nigerian Journal of Engineering. 6(1), 1-3, 1990.

[10.] Ho, Y.S; Wase, D.A.J, and Forster, C.F: Batch Nickel Removal from Aqueous Solution by Sphagnum Moss Peat. Water Resources. 29, 1327-1332, 1995.

[11.] Holan, Z.R. and Volesky, B: Biosorption of Pb and Ni by Biomass of Marine Algae. Biotechnology and Bioengineering. 43, 1001-1009, 1994.

[12.] Jadhav, D.N, and A.K. Vangara, A.K: Removal of Phenol from Wastewater using Sawdust and Sawdust Carbon. Indian Journal of Chemical Tchnology.11, 35-45, 2004.

[13.] Langmuir, I: The Adsorption of Gases on the Plane Surfaces of Glass, Mica, and Platinum. Journal of the American Chemical Society. 40, 1361-1403, 1918.

[14.] Mahvi, A.H; Maleki, A, and Eslami, A: Potential of Rice Husk Ash for Phenol Removal in Aqueous Systems. American Journal of Applied Sciences. 1(4), 321-326, 2004.

[15.] Manojlovic, D; Ostojic, D.R; Obradovic, B.M; Kuraica, M.M; Krsmanovic, V.D, and Puric. J: Removal of Phenol and Chlorophenols from Water by new Ozone Generator. Desalination.213:116-122, 2007.

[16.] Mousavi, H.Z; Hosseynefar. A; Jaheed, V and Dehghani, S.A: Removal of Lead from Aqueous Solution using Waste Tire Rubber Ash as Adsorbent. Brazillian Journal of Chemical Engineering. 27(1), 79-87, 2010.

[17.] Polcaro, A.M, and Palmas, S: Electrochemical Oxidation of Chlorophenols. Industrial Engineering and Chemical Research. 36(5), 1791-1798, 1997.

[18.] Tiemann, K.J; Gamez, G; Dokken, K; Parsons, J.G, and Gardea-Torresdey, J.L: Chemical Modification and X-ray Absorption Studies for Lead(II) binding by Medicago sativa (Alfalfa) Biomass. Microchemical Journal. 71, 291-292, 2002.

[19.] Volesky, B, and Holan, Z.R: Biosorption of Heavy Metals. Biotechnology Progress. 11, 235-250, 1995.

[20.] Zafar, M.N; Nadeem, R, and Hanif. M.A: Biosorption of Nickel from Protonated Rice Bran. Journal of Hazardous Materials. 143, 478-485, 2007.

ACTA TECHNICA CORVINIENSIS - BULLETIN of ENGINEERING

ISSN: 2067-3809 [CD-Rom, online]

ACTA TECHNICA CORVINIENSIS – Bulletin of Engineering
Tome VI (Year 2013) – FASCICULE 4 [October–December]
ISSN 2067–3809

[1.] Sorin PARPUCEA

THE BAROQUE HISTORICAL LOAD-BEARING STRUCTURE – A CASE STUDY: THE GREEK CATHOLIC CATHEDRAL "SCHIMBAREA LA FAȚĂ" FROM THE CITY OF CLUJ-NAPOCA, TRANSYLVANIA

[1.] DEPT. OF CIVIL CONSTRUCTIONS & MANAGEMENT, FACULTY OF CONSTRUCTIONS, TECHNICAL UNIVERSITY OF CLUJ-NAPOCA, ROMANIA

ABSTRACT: The Greek-Catholic Cathedral "Schimbarea la Față" it is one of the most important and well-known baroque historical monuments from the city of Cluj-Napoca, in Transylvania. From the beginning of the construction, until the end of the 90's this church had a tumultuous history and it survived in very good conditions. What the author presents are the structure with its three main historic load-bearing sub-units, the historic structural elements, where there are positioned and how they work. All this is made with an analysis based on photos, measurements and other information collected from the site.
KEYWORDS: baroque, historic structure, masonry, suspended dome

INTRODUCTION

The Minorite Order came to the city of Cluj-Napoca in 1486. Only in 1724 they received the construction authorization to build their own church. After almost 60 years of struggle with money problems, authorizations and construction problems, they finished the Greek Catholic Cathedral named "Schimbarea la Față". [1]

In the city of Cluj-Napoca, the Greek-Catholic Cathedral, it is a well-known historical monument. The architecture it is baroque and it is one of the most well preserved historical buildings of its kind. As far as the plane geometry, the cathedral has a rectangular shape, with a basillical structural system in the coir section. It is a brick masonry structure, with arches, suspended domes, pilasters and a load-bearing wall with direct foundation. [2]

The author presents during this article, the structure with its main historic load-bearing structure subunits.

METHODOLOGY OF RESEARCH

The research is an analysis of the structure from an historic structure engineering point of view. It is divided in three sections: the roof framing, the main nave and the choir section. The author presents the most representatives baroque historical load-bearing structures and elements.

In the analysis where used photos and blueprints made by the author in order to understand what are the elements that are used, where are they and what role they play. Every historic load-bearing structure sub-unit is analysed and historical load-bearing baroque elements are explained.

RESULTS

In this section the author describes in details the three historic load-bearing structure sub-units of the building:

- *The roof framing: is made out of soft wood with truss frames doubled by rafters until the level of the crossbar, double king strut and tie-beam. All the main trusses and the secondary trusses are held together with intermediate purlins and eaves purlins, both having crossbars in the rafters section between the two purlins. A system of double wall plate supports the whole roof framing structure. Between the suspended domes there are two main trusses, with one secondary truss in the middle of them. Along of the each suspended dome, there are four secondary trusses held with crossbars in the rafter section. [1], [2] View Figure 1, 2, 3.*
- *The main nave: In the main nave there are four vault segments (or bays). The first one is also divided in three, forming three covered spaces with a balcony sustained by two pillars. On the masonry structure, on pillars and arches, there are suspended domes that discharge their forces. View Figure 4, 5.*

The bays are limited by pilasters built in curve-reversed curve system. On top of these pilasters there are brick masonry arches which support the suspended dome. At each window from the main nave there is an archivolt that starts from the pilaster and on which discharges the short arm of the dome. View Figure 8.

Figure 1. The roof framing

Figure 2. Main and secondary (the short ones) trusses

Figure 3. Crossbars in the rafter section

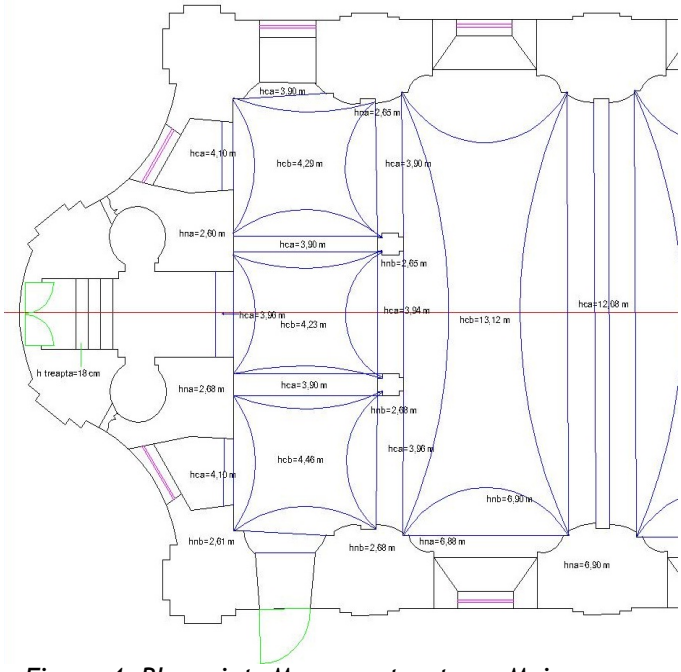

Figure 4. Blueprint. Masonry structure. Main nave, first vault segment.

Figure 5. First vault segment

All the vaults are suspended domes. They have a distinctive characteristic: the rectangular plane geometry with a proportion of 1 to 3. Because of this they look more like torus dome than a sphere dome. View Figure 6.

Another important characteristic of the vaults is that they do not have ribs on the back of it, and the construction technology is in swallow-tailed style. [2] View Figure 7.

The Triumphal Arch is situated at the end of the main nave and the beginning of the choir section of the church. It is defined by two stronger pilasters, which are more robust then all the other ones. These two pilasters are united, at the main nave side, by an amplified arch, an archivolt. [1], [2] View Figure 8.

- *The choir section: presents a retraction towards the main nave and it ends with a sanctuary section that has a straight wall. View Figure 9.*

In the choir section there are two bays (or vault segments) and two suspended domes. View Figure 10.

Figure 6. Suspended domes with rectangular plane geometry

Figure 7. Swallow-tailed technology

Figure 8. Maine nave. The triumphal Arch, suspended domes and pilasters

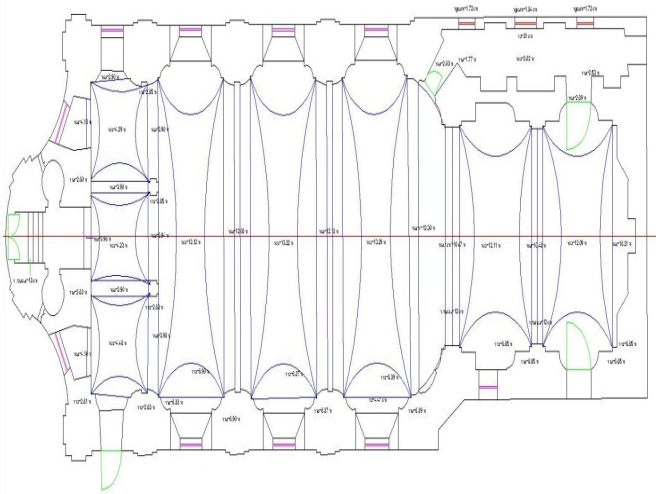

Figure 9. Blueprint. The ground floor.

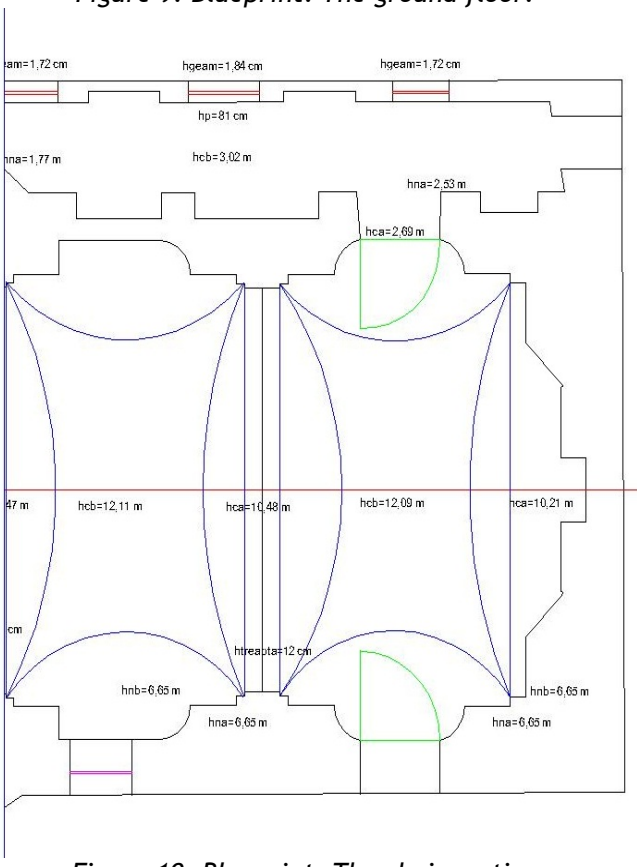

Figure 10. Blueprint. The choir section

CONCLUSIONS

In the case study of the Greek-Catholic Cathedral "Schimbarea la Față", the baroque historical load-bearing structure is divided in three historic load-bearing structure sub-units: the roof framing, the main nave and the choir section. Each of these is also divided in other structure elements. The roof framing is made in specific baroque style, and is supported by the masonry structure, which also supports the suspended domes, held by arches, that discharge on walls and pilasters.

Acknowledgment

This paper was supported by the project "Improvement of the doctoral studies quality in engineering science for development of the knowledge based society-QDOC" contract no. POSDRU/107/1.5/S/78534, project co-funded by the European Social Fund through the Sectorial Operational Program Human Resources 2007-2013

REFERENCES

[1.] Mircea Toca, 1983, The Baroque Cluj (Clujul Baroc), 34-40 p.

[2.] Balint Szabo, 2005, Illustrated dictionary of historic load-bearing structures (Dicționar ilustrat de structuri portante istorice) Kriterion & Utilitas, 113-168 p.

[3.] Daniel Borden, Jerzy Elzanowsky, Cornelia Lawrenz, Daniel Miller, Adele Smith, Joni Taylor: Architecture - evolution, style, personality. From Renaissance to the XIX century (Arhitectura - evolutie, stiluri, personalitati. De la Renastere la secolul XIX), Vol 2, Publishing Company Litera, 2010

[4.] J.P. Laurent, "History de techniques Renaissance", 2008

[5.] Hermann Fabini,"The Univers of fortified churches in Transylvania", Monumenta, 2009

[6.] *** „The Fifth Scientific Symposium on historical load-bearing structures - masonry historical load-bearing structures (Al 5-lea Simpozion ▫tiin▫ific de Structuri Portante Istorice - Structuri portante istorice din zidărie)", Utilitas, 2001

[7.] Balint Szabo, „Illustrated dictionary of intervention on historic load-bearing structures" (Dictionar ilustrat de interventii la structuri portante istorice), Utilitas, 2008

[8.] Ching Francis D. K., Adams Cassandra, „A visual dictionary of Arhitecture", New York, Van Nostrand Reinhold, 1995-1997

[9.] Constantinescu Dinu Teodor, „Monumental buildings (Constructii Monumentale)", Bucuresti, Editura Stiintifica si Enciclopedica, 1989.

[10.] Fleming John, Honour Hugh, Pevsner Nicolaus, „The Penguin dictionary or Arhitecture", London, Penguin Books, 1991.

ISSN: 2067-3809 [CD-Rom, online]

ACTA TECHNICA CORVINIENSIS – Bulletin of Engineering
Tome VI (Year 2013) – FASCICULE 4 [October–December]
ISSN 2067–3809

[1.] Naqib DANESHJO, [2.] Cristian Dan STRATYINSKI, [3.] Baryalai TAHZIB, [4.] Christian DIETRICH

PROPOSED CONSTRUCTION OF AN UNMANNED RESEARCH VEHICLE

[1,2,4.] TECHNICAL UNIVERSITY, FACULTY OF AERONAUTICS, DEPARTMENT OF AVIATION ENGINEERING, KOŠICE, SLOVAKIA
[3.] TECHNICAL UNIVERSITY, FACULTY OF CIVIL ENGINEERING, DEPARTMENT OF ENVIRONMENTAL ENGINEERING, KOŠICE, SLOVAKIA

ABSTRACT: The main scope of this article is to describe the structural design unmanned reconnaissance vehicle to 80kg. Apart from the design and technical and visual documentation of the work is also a detailed description of each component. This work proposes a suitable design for a simplified UAV system which promotes the autonomous movement of an UAV and includes the optimal selection of its components (avionics), such as a (Javelin Stamp) processor, GPS module, motors, gyroscopes and maneuvering equipment for an optically remote controlled drone. In the proposal, the most important part is the selection of the profile's wings, because it imparts its aerodynamic characteristics and as a result, its lift.
KEYWORDS: CATIA, GPS module, UAV, 3D structure

INTRODUCTION

The main objective of this work is to plan the construction of an unmanned vehicle with a mass limited to 80kg. At present, unmanned aerial vehicles (UAV's) are currently in use by almost all national defence forces. This work proposes a suitable design for a simplified UAV system which promotes the autonomous movement of an UAV and includes the optimal selection of its components (avionics), such as a (Javelin Stamp) processor, GPS module, motors, gyroscopes and maneuvering equipment for an optically remote controlled drone.

In the proposal, the most important part is the selection of the profile's wings, because it imparts its aerodynamic characteristics and as a result, its lift. This allows us to create a wing dependent on the dimensions of the aircraft. When calculating the lift and resistance coefficient, the course of pressure around the wing, depends on the angle at which it strikes the wing and the results of the calculation of Reynolds number. The program, Catia V5, was used to model the 3D structure. Unmanned technology is playing an increasingly important role in modern armies. Unmanned aircraft take pride of place as they can conduct surveillance, identify targets and eliminate them.

PROPOSED CONSTRUCTION OF AN UNMANNED FUSELAGE

The fuselage requiresbearing assembly which consists of parts necessary for a stable and controlled-flight. The airframe houses the power plant which is responsible for carrying the load.

A simple fuselage consists of the following main parts: airframe, fuselage, tailfin, control system and landing gear.

The optimal shape places the propeller and engine at the rear of the hull with simple rectangular wings attached to the fuselage, but remarkably the tail is detached, joined only by connecting beams which is unlike most modern aircraft. The main load-bearing members consist of simple rectangular wings with transverse rudders. The wings are connected to the hull with a varying profile. The internal combustion engine is located in the rear of the fuselage. Stabilizers are not directly attached to the hull, because of the location of the engine. The tailfin acts as stabilizers which are located in the same plane and consist of a horizontal tail surface, which is located above the two vertical tail fins. The horizontal tail consists of a lateral surface that houses the elevator rudder which is supported by two vertical surfaces that house the yaw rudders.

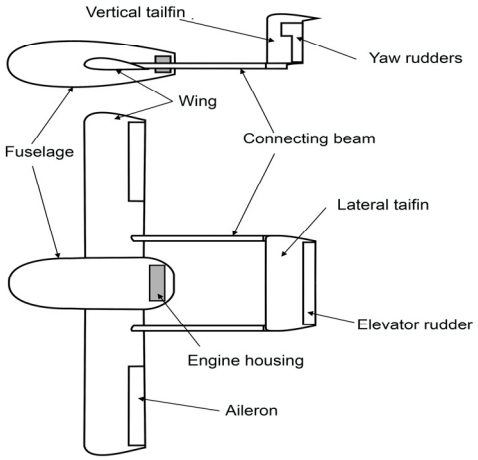

Figure 1. Preliminary design of the aircraft shape

The calculation of the dimensions of the aircraft should be based on its designed take-off weight. For this particular case, the take-off mass is m = 80kg. The maximum takeoff weight is defined as the limit at which an aircraft is able to take off with (empty aircraft, crew, cargo and fuel weight).

The profile of the airfoil (wing cross-section in the vertical plane) depends on its geometrical dimensions and aerodynamic characteristics.
The basic dimensions of the wing include the calculation of the chord length, its relative thickness, the relative curvature, the radius of the leading edge and trailing edge thickness.
Relative profile thickness has a considerable effect on the degree of aerodynamic characteristics of the profile, especially drag coefficient.

$$\overline{c} = \frac{c_{\max}}{b}. \qquad (1)$$

where: $\overline{c}$ - [-] relative profile thickness, c_{max} - [mm] max profile thickness, b - [mm] length of profile chord
Parameters of the wings profile:
max lift factor c_L: 1,847
max lift coefficient at angle: 15°
angle of zero lift : -4,5°
The calculation of the wing area is based on the calculation of the minimum airspeed. A minimum flight speed of 60 kph was selected-1 (16.667 ms-1).

$$v_{\min} = \sqrt{\frac{G}{\frac{1}{2}\cdot\rho\cdot c_{L\max}\cdot S}}. \qquad (2)$$

$$S = \frac{G}{\frac{1}{2}\cdot\rho\cdot c_{L\max}\cdot v_{\min}^{2}} = \frac{80\,9,81}{\frac{1}{2}\cdot 1,2\cdot 1,847\cdot 16,667^{2}} = 2,549 m^{2}. \qquad (3)$$

where: S - wing area [m^2], G - mass of aircraft [kg], ρ - air density, cLmax - maximum coefficient of lift for a given profile, vmin - minimum flight speed[ms^{-1}]
The shape of the wing is a simple rectangle.
Wing dimensions:

- *wingspan: 4m,*
- *chord length: 0,650m*
- *max wing thickness : 0,137m*

CALCULATION OF THE OPTIMAL FLIGHT SPEED

The optimal lift coefficient is based on the NACA profile 4421. The polar profile corresponds to the optimal value of the maximum strike angle, 6°, where the lift coefficient cL = 1.0758. It is then possible to calculate the flight speed using the relation:

$$v_{let} = \sqrt{\frac{G}{\frac{1}{2}\cdot\rho\cdot c_{L}\cdot S}} = \sqrt{\frac{80\cdot 9,81}{\frac{1}{2}\cdot 1,2\cdot 1,0758\cdot 2,6}} = 21,62 m.s^{-1} = 77,84 km.h^{-1}. \qquad (4)$$

CALCULATION OF REYNOLDS NUMBER

The profile V2.22a was used for the calculation of Reynolds number: airspeed: 78km.h^{-1}, wing chord: 0,65m
Reynolds number for the given parameters equals:
Re=964136
This Re is sufficient for the rectangular wing. Reynolds numbers on actual gliders ranges between 600,000 and 3500 000.

PROPOSED FUSELAGE USING CATIA V5 - Proposed fuselage structure, wing attachment and engine fitting

The fuselage which is constructed around the aircraft's frame plays a very important function. In terms of design, the wings, tail, landing gear, management, power train parts and equipment and weapons are integrated into a single unit. Certain requirements are placed on the fuselage which needs to be considered from the outset. These include: aerodynamics (optimal aero-dynamic characteristics of the fuselage, regarding the reduction of drag caused by the unfavorable effect created were the fuselage joins the wing, tail, and possibly other parts of the aircraft), strength, design, manufacture and service.
Aerodynamic requirements call for optimal fuselage aerodynamic characteristics, especially the minimization of resistance due to an adverse effect on the body where it joins with the wing, tail, and possibly other parts of the aircraft.
This can be avoided by shaping the body and using a well-designed transition between the wing, fuselage and tail.

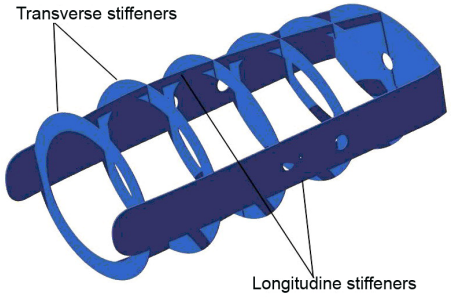

Figure 2. Supporting structure of the fuselage

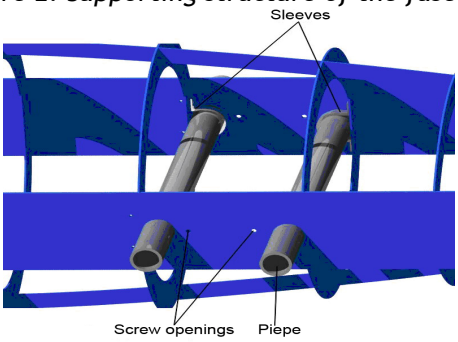

Figure 3. Supporting structure of the wings

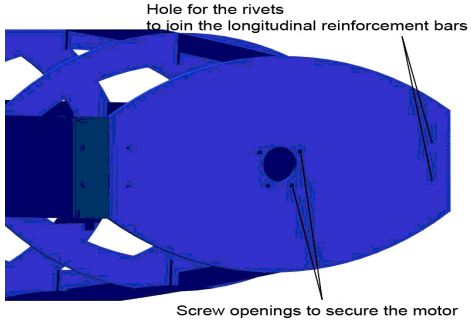

Figure 4. Supporting structure of the engine mount

A well-designed structure should have a minimum weight in relation to its size and use advanced materials and manufacturing technologies. An optimal solution is to preferably implement a circular cross section or circular parts.
The supporting structure of the fuselage has undergone various forms of organization over the years. At present, two forms are used. Rod (rarely used) and semi shell hull structures which house the load-bearing part of the transverse and longitudinal direction and cover the carrier).

The wing will be constructed from two load bearing beams and exhibit a circular cross section. The mountings consist of two aluminum tubes with an outer diameter Ø50mm and thickness of 5 mm. The Limbach L 275 E engine was selected.

Proposed wing construction

The whole wing beam design requires suitably spaced supporting parts, reinforced using longitudinal stiffeners and ribs. The main beam withstands substantial bending moment induced by normal forces.

The wings are composed of one auxiliary beam, three longitudinal stiffeners, one of which performs as the leading edge and eight ribs. The main and auxiliary beams are made of tubes with an outer diameter of Ø40mm and a thickness of 3 mm.

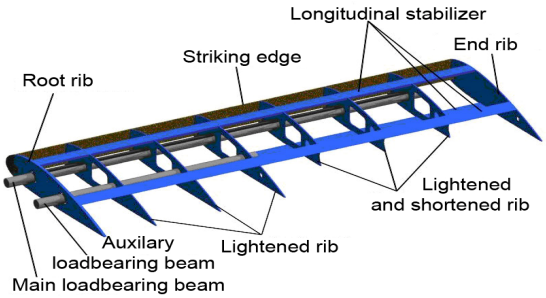

Figure 5. Wing construction

Lateral control rudders (ailerons) are control bodies whose activities produce a moment about the longitudinal axis of the aircraft, causing the aircraft to roll. The most common type of wings currently used are normally designed as deflective and located at the end of the trailing edge.

The frequent use of an aileron is justified, because it is structurally similar to the wing construction. Besides shortcomings in the moment, there are also limitations due to torque which is created by moment. Lateral control is provided by one aileron deflecting upwards, while the other deflects downwards.

The ailerons have the same plan outline as the main rectangular wing. Its dimensions differ from the wings through simple relative values, where the length of the wings, is ¼ the wingspan and the width is ¼ leaf the width.

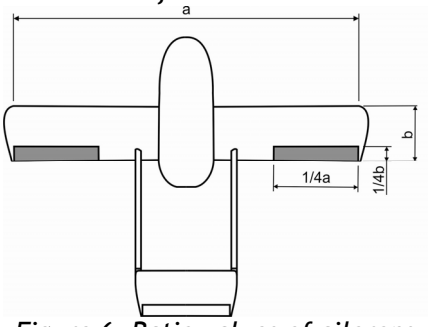

Figure 6. Ratio values of ailerons

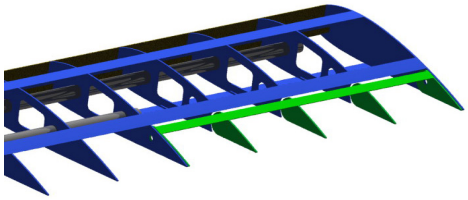

Figure 7. Model of the ailerons - lateral rudder

Length of aileron:

$$a_k = \frac{1}{4} \cdot a = \frac{1}{4} \cdot 4 = 1\text{m}. \quad (5)$$

where: a_k - [m] length of aileron[m], a -wingspan[m]

Width of aileron:

$$b_k = \frac{1}{4} \cdot b = \frac{1}{4} \cdot 0{,}65 = 0{,}1625\text{m}. \quad (6)$$

where: b_k-width of aileron[m], b-width of aileron[m]

Length 1m and width 0,165m, which results in an aileron area of 0,165m^2.

Proposed connections of stabilizers and wings

The aircraft's fuselage is independent to the stabilizers which are anchored to the supporting surface (wings):

- wing rib attachments
- connecting beam (cylindrical)
- stabilizer attachment

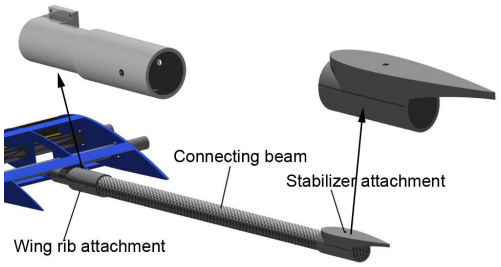

Figure 8. Wing stabilizer connections

Proposed stabilizer

Stabilizers are usually separated into horizontal and vertical wing segments which are located at the end of the fuselage. Horizontal tail surfaces provide longitudinal stability and maneuverability of the aircraft, while the vertical tail surfaces provide directional stability and maneuverability of the aircraft. Both areas consist of fixed and flexible parts. The fixed horizontal surface act as the stabilizer and the movable surface acts as the elevator. The fixed vertical part acts as a fin and the movable part is used to change direction (yaw).

A. Vertical tail area:

The vertical tail surface area is 0.066 times the wing area.

$$A_{zp} = 0{,}066 \cdot S = 0{,}066 \cdot 2{,}6 = 0{,}1716\text{m}^2. \quad (7)$$

where:A_{zp} - area of vertical tail fin [m^2], S - area of load bearing wing [m^2]

The selected rectangular shape has a vertical tail surface width of a = 0.36 m. The height B should be calculated from the width of the selected area b and vertical tail area A_{zchp}.

$$b_{zp} = \frac{A_{zp}}{a_{zp}} = \frac{0{,}1716}{0{,}36} = 0{,}477\text{m}^2. \quad (8)$$

where:

A_{zp}- vertical tail area [m^2],

a_{zp}- width of vertical tail surface [m]

b_{zp} - height of vertical tail surface [m]

According to previous calculations b_{zp} = 0.48m and width a_{zp} = 0.36m was selected.

The resulting single vertical tail surface area of Azp = 0.1728 square meters.

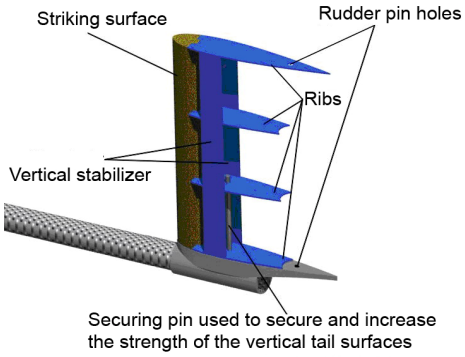

Figure 9. Vertical tail surface construction

B. Yaw rudders:

When calculating the directional (yaw) surface area we used the same ratio values that were used previously which is ¼ of the vertical tail surface area.

$$A_{sk} = \frac{1}{4} \cdot A_{zp} = \frac{1}{4} \cdot 0{,}1728 = 0{,}0432\text{m}^2. \quad (9)$$

where: A_{sk} - area of the yaw rudders [m²]

The rudder height bs is determined by the height of the construction of the vertical tail surface and will therefore be equal to its height, ie:

$b_{sk} = b_{zp} = 0{,}48\text{m}.$

The width of the yaw rudder should be calculated according to the equation:

$$a_{sk} = \frac{A_{sk}}{b_{sk}} = \frac{0{,}0432}{0{,}48} = 0{,}09\text{m}. \quad (10)$$

where: a_{sk} - width of yaw rudder [m],
b_{sk} - height of yaw rudder [m],

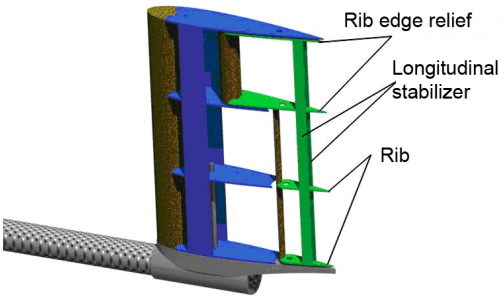

Figure 10. Construction of yaw rudder

C. Horizontal tail surface:

The calculation of the tail area is based on the ratio of the values that were previously calculated. The horizontal tail surface area is 0.2 times the wing area.

$$A_{vp} = 0{,}2 \cdot S = 0{,}2 \cdot 2{,}6 = 0{,}52\text{m}^2. \quad (11)$$

where: A_{vp}- horizontal surface area [m²],
S-area of load bearing wing [m²]
A rectangle with a length b_{vp}= 1m was chosen for the shape of the horizontal tail surfaces. The width of the a_{vp} must be calculated according to the equation:

$$a_{vp} = \frac{A_{vp}}{b_{vp}} = \frac{0{,}52}{1} = 0{,}52\text{m}. \quad (12)$$

where: a_{vp} - width of the horizontal tail surface [m]
b_{vp} - length of the horizontal tail surface [m]

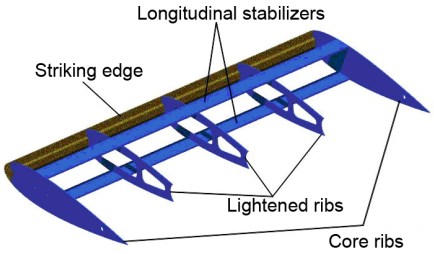

Figure 11. Construction of horizontal tail surface

D. Elevator rudder:

When calculating the area of the elevator rudder, we use the same ratio values that were used for the calculation of yaw and transverse rudder (aileron) which is ¼ the horizontal tail surface area.

$$A_{vk} = \frac{1}{4} \cdot A_{vp} = \frac{1}{4} \cdot 0{,}52 = 0{,}13\text{m}^2. \quad (13)$$

where: A_{vk} -area of the elevator [m²]

The length of the elevator bvk is determined by the construction of the horizontal tail surface and is therefore equal to its length, ie:

$b_{vk} = b_{vp} = 1\text{m}.$

Width of the elevator rudder is calculated as:

$$a_{vk} = \frac{A_{vk}}{b_{vk}} = \frac{0{,}13}{1} = 0{,}13\text{m}. \quad (14)$$

where: a_{vk} - width of horizontal [m]
b_{vk} - length of horizontal [m]

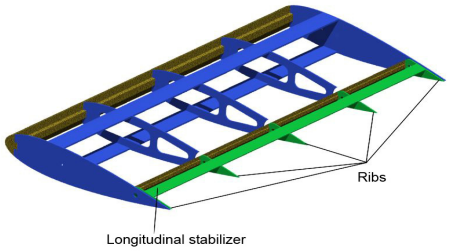

Figure 12. Longitudinal stabilizers; - ribs
Construction of elevator rudder

Figure 13. Complete construction of the drone (UAV)

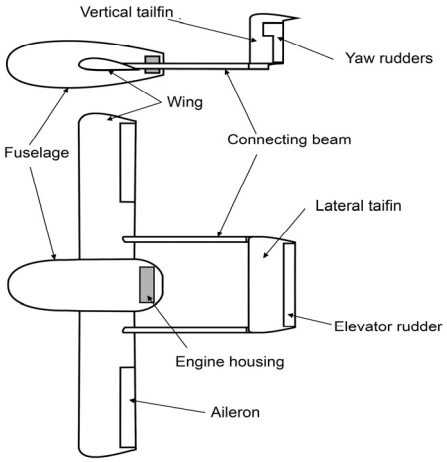

Figure 14. Proposed and calculated dimensions of the drone (UAV)

The flow diagram illustrates the results of the calculations.

Mass and centre of gravity

- ☐ total construction mass: m_D=39kg
- ☐ dry mass of engine: m_m=7,2kg
- ☐ avionics weight without battery: m_s=0,25kg

The total mass of the drone (UAV) was calculated with the aid of CATIA V5 program where the construction materials were chosen according to their material density. The mass of the engine and avionics are specified by the manufacturer. Since the total mass of the exploratory UAVs are limited to 80 kg, fuel, batteries and other equipment are limited to 33.55 kg, which is a sufficient margin. An increase in the mass would also increase the minimum flight speed. The centre of gravity is indicated in Figure 22.

Centre of gravity coordinates:

x_T=1334mm, y_T=0mm, z_T=28mm

Additional transfer of gravity and balance may be set by the positioning fuel, batteries and avionics of the aircraft.

CONCLUSIONS

The work deals with UAVs. It clarifies current issues regarding UAVs, their use and continuous development. The work proposes a step by step structural design for an aircraft and provides descriptions and pictures, which can also be used as a guide in designing new types of UAVs. Special effort was paid to create an interesting and simple design. The structural design is not final and may be further modified and extended.

REFERENCES

[1] Čalkovský, A.- Pávek, J.- Daněk, V.: Konstrukce a pevnost letadel 1.díl. 1984, 547 s. U-1165/1.

[2] Hlubeňová, Jana - Líška, Ondrej Hlubeň, Daniel:Metodika výberu simulačného programu. 2009. 1 elektronický optický disk(CD-ROM).

[3] [3] Pauliková, A.: Modelovanie dynamických systémov pracovného prostredia technologickej prevádzky, habilitačná práca, Košice, 2008, 166 s.

[4] Michal Fabian, Róbert Boslai, Jaroslav Šeminský Reverse engineering na báze 2D pohľadovpomocou intuitívneho modelára: Imagine&Shape v CATIA V5, 2010. - 1 elektronický optický disk (CD-ROM).

[5] Kopas, M. - Pauliková,A.: Specifics of belt conveyor as part of checkout counters and their impacts on operational staff, In: Zdvihací zařízení v teorii a praxi. No. 2 (2009), p. 41-45.ISSN 1802-2812.

[6] Ižaríková, G.: Matematické modelovanie pracovných priestorov výrobných prostriedkov a systémov. In: Transfer inovácií. Č. 14 (2009), s. 181-184. - ISSN 1337-7094

[7] Kuderjavý, P.: Modelovanie a simulácia automatizovaných výrobných systémov v edukačnom procese. In: Perspective Directions and Ways of Realizing Innovative Technologies in the System of European Higher Education: international scientific herald: the collection of scientific articles containing the materials of the 19th International scientific - practical conference: (December 8-11, 2009), Uzhhorod (Ukraine) - Vysoke Tatry (Slovakia): book 1. - Uzhhorod: Ministry of Education and Science of Ukraine, 2010 P. 177-186.

[8] http://www.slavetind.cz/stavba/konstrukce/kridlo/Profil_kridla.aspx

ACTA TECHNICA CORVINIENSIS – BULLETIN of ENGINEERING

ISSN: 2067-3809 [CD-Rom, online]

ACTA TECHNICA CORVINIENSIS - BULLETIN of ENGINEERING

ISSN: 2067-3809 [CD-Rom, online]

ACTA TECHNICA CORVINIENSIS - BULLETIN of ENGINEERING

ISSN: 2067-3809 [CD-Rom, online]

copyright © UNIVERSITY POLITEHNICA TIMISOARA,
FACULTY OF ENGINEERING HUNEDOARA,
5, REVOLUTIEI, 331128, HUNEDOARA, ROMANIA
http://acta.fih.upt.ro

ACTA TECHNICA CORVINIENSIS – Bulletin of Engineering
Tome VI (Year 2013) – FASCICULE 4 [October–December]
ISSN 2067–3809

Scientific Events in 2013

1. THE 5th INTERNATIONAL CONFERENCE ON GEARS WITH EXHIBITION – GEARS 2013 7 – 9thOctober, 2013, Garching (near Munich), GERMANY

The fifth international conference on gears and transmissions in Germany will become a broad platform for equipment manufacturers and producers and researchers of gear and transmission systems to present new solutions and their latest research results.

Climate change is one of the big issues in public discussion, in politics and industry. The conference will show, what the transmission and drive train industry can contribute to increase energy efficiency. Gears are vital in the efficiency of different applications. They transmit and vary torque between prime movers and applications.

There is still room for improvement, which will be demonstrated by the presenters. New concepts for drive trains of energy supply systems provide answers to the increasing demand for energy worldwide. These concepts must be introduced to global markets more quickly. Therefore, new designs are necessary and will be presented at the conference.

The state-of-the-art of industrial applications will be demonstrated at an exhibition beside the conference.

The conference will last three days, comprising keynote addresses and presentations in a series of plenary and parallel sessions. The official language of the conference will be English. No simultaneous translation will be provided. The conference program and the registration form will be available in June 2013.

Detailed informations here: www.vdi-gears.eu

2. THE 7th INTERNATIONAL SCIENTIFIC-PROFESSIONAL CONFERENCE – SB 2013 "CONTEMPORARY PRODUCTION PROCESSES, EQUIPMENT AND MATERIALS FOR WELDED CONSTRUCTIONS AND PRODUCTS" 23 – 25th October, 2013, Slavonski Brod, CROATIA

During last six meetings this conference had gathered number of experts and scientists who presented and introduced novelty in welding profession. Due to that, for the seventh time, organizers call everyone who can give their contribution to the area of welding technology and welding related techniques, automation and robotization in production of welded constructions, and all others that can, in any other way, give their contribution to development of welding practice, to present their scientific and professional knowledge and experiences. This year, also, there will be the exhibition of welding devices, filler metals and equipment, and all presented papers will be published i the conference proceedings and CD media. We thank to all our present partners of this conference for their contribution and welcome you in Slavonski Brod.

Topics of interest for the conference should be related but not limited to the following thematic focuses:

- *New technologies and materials*
- *Welding processes*
- *Robotization and automation*
- *Pressure vessels*
- *Welding related techniques*
- *Manufacturing of welded construction*
- *Quality control of welded products*
- *Reliability and safety of welded productions and constructions*
- *Weldability of materials*
- *Filler metals*
- *Equipment for welding and welding related techniques*
- *Personnel and education in welding*
- *Metallurgy*
- *Ecology and occupational health*
- *Economical aspects of welding*

Detailed informations here: http://www.sfsb.hr/dtzsb/

3. INDUSTRIAL ENGINEERING AND ENVIRONMENTAL PROTECTION
30th October, 2013, Zrenjanin, SERBIA

The conference provides forum for discussion and exchange of experiences between people from government, state agencies, universities and research institutions, and practitioners from industry.
Framework scientific topics of the conference:
1. Process Technology
2. Engineering Environmental Protection and safety at work
3. Manufacturing technologies and materials
4. Maintenance
5. Design and maintenance of process plants
6. Basic operations, machinery and processes
7. Computer technologies and engineering education
8. Biotechnology
9. Reengineering and project management
10. Process management
For any further information, we recommend you the website: http://www.tfzr.uns.ac.rs/ieep/index.php

4. THE 7th INTERNATIONAL CONFERENCE INTERDISCIPLINARITY IN ENGINEERING - INTER-ENG 2013
10 - 11th October, 2013, Tirgu Mures, ROMANIA

It is with great pleasure that the "Petru Maior" University of Tîrgu Mures - Faculty of Engineering in collaboration with Romanian Academy of Technical Sciences invites you to the International Conference Interdisciplinarity in Engineering INTER-ENG 2013. The conference will be jointly organized and hosted by the Department of Industrial Engineering and Management and the Department of Electrical Engineering and Computer Science of "Petru Maior" University of Tîrgu Mures.
The main theme of the Conference is announced as: "Advanced technologies for the next-generation manufacturing processes". The conference scope is to provide a professional and scientific forum for engineers and research scientists from universities, research centers and to present research works, contributions and recent developments as well as current practices in engineering. The INTER-ENG conference will also offer the opportunity for companies in engineering to present their products and services. This conference aims to bring together the researchers, scientists, professors, graduate students and civil society organizations and their representatives to share and to discuss theoretical and practical knowledge in the scientific environment. In this edition special attention will be given to young professional orientation to technical studies, that will be invited to participate in plenary sessions, but a Workshop will also be hold for both teachers and students from high schools, with the theme of Vocational education and training in engineering and industrial management.
The conference will promote dialogue on how to comprehend and develop advanced engineering technologies and achieve next-generation industrial manufacturing in the interdisciplinary context from different fields: mechanics, electronics, informatics, etc. The Inter-Eng Conference drives innovation and enterprise, creating new technologies and developing applications and intellectual property for the benefit of the society. The event will develop thinking on modeling for future engineering technologies.
For any further information, we recommend you the INTER-ENG 2013 conference website: http://www.inter-eng.upm.ro/2013/

5. INTERNATIONAL ELECTRICAL ENGINEERING CONFERENCE FOR YOUNG RESEARCHERS - IEECYR2013
23 - 26th October, 2013, Cluj Napoca, ROMANIA

It is a great pleasure and an honor to extend you a warm invitation to attend the 2013 International Electrical Engineering Conference for Young Researchers organised by Technical University of Cluj-Napoca, to be held October 23-26, 2013 in Cluj-Napoca, Romania.
The role of Electric Engineering and Power Systems is becoming more and more important as most domains are directly dependent of it. Whether your interests are in Electrical Engineering, Power Systems, Computer Science, Telecomunications, Robotics or Automations join hundreds of fellow PhDs, young academic staff and researchers from throughout the world to engage in a focused, 2-day series of workshops, presentations, technical sessions and seminars covering the main topics of interests.
The conference will be held from 23rd to 26th of October, 2013 in Cluj-Napoca, the heart of Transylvania and the European Youth Capital (2015), Romania.
For any further information, we recommend you the conference website: http://www.ieecyr2013.org/

6. THE 16th INTERNATIONAL SYMPOSIUM ON THERMAL SCIENCE AND ENGINEERING OF SERBIA - SIMTERM 2013
22 - 25thOctober, 2013, Sokobanja, SERBIA

Department of Thermal Engineering of the Faculty of Mechanical Engineering Niš and the Society of Thermal Engineers of Serbia, continuing scientific research in the field of Energetics-Efficiency-Ecology, organize the International Symposium on Thermal Science and Engineering of Serbia - SIMTERM 2013, under the patronage of the Ministry of Education, Science and Technological Development of the Republic of Serbia. It is expected that SIMTERM 2013 will gather researchers, engineers, experts, representatives of local and central government and companies from Serbia and abroad, interested in the exchange of scientific and practical information and experience from the thematic fields.
We are inviting you and looking forward to your participation in the 16th Symposium on Thermal Science and Engineering of Serbia, under title: Energy - Efficiency - Ecology.
For any further information, see at: http://simterm.masfak.ni.ac.rs/index-en.html

7. THE FIRST INTERNATIONAL SYMPOSIUM ON AGRICULTURAL ENGINEERING
4 - 6th October 2013, Belgrade – Zemun, SERBIA

It is a great honor to call You to participate in the work of The First International Symposium on Agricultural Engineering (ISAE—2013) in order to give Your professional contribution in the area of future development of the agricultural engineering. The symposium is organized by Faculty of Agriculture, University of Belgrade, Serbia, in Association with Faculty of Agricultural and Food Sciences, Sarajevo, Bosnia and Herzegovina and University of Basilicata – School for Agricultural, Forestry, Food and Environmental, Sciences, Potenza, Italy, under support of The European Society of Agricultural Engineers (EurAgEng). It will be held on October, 4-6, 2013, at the Faculty of Agriculture, University of Belgrade, Belgrade-Zemun, Serbia.
For any further information, we recommend you the website: http://www.agrif.bg.ac.rs/events

8. THE 11th INTERNATIONAL CONFERENCE ON TELECOMMUNICATIONS IN MODERN SATELLITE, CABLE AND BROADCASTING SERVICES – TELSIKS 2013
16 - 19th October 2013, Belgrade - Nis, SERBIA

The Conference TELSIKS is a highly competent scientific and professional meeting aimed at the efficient exchange of results in the area of telecommunications, through presentation of current scientific results, development trends, etc.
TELSIKS 2013 is organized by University of Niš, Faculty of Electronic Engineering.
For any further information, we recommend you the website: http://www.telsiks.org.rs/

9. THE 11th SYMPOSIUM ON NOVEL TECHNOLOGIES AND ECONOMIC DEVELOPMENT
22 – 23rd October 2013, Belgrade, SERBIA

Symposium on Novel Technologies and Economic Development would be going to be held at University of Belgrade in Serbia. The main mission to attend this Conference is dedicated towards to build and formulate the effective strategic advancement for economic research and development. The primary show would be concerned with the issue of indigenous economic development issues related to it. The International meeting is also decked with effective keynote sessions and workshops which will reduce all contentions from the minds of the conferees. The Technologies event will provide an unprecedented opportunity to the individual researchers to share their thoughts; opinion and challenges therefore develop a perfect harmony in this domain of interest. Organizer is the Faculty of Technology in Leskovac, University of Belgrade.
For any further information, we recommend you the website: http://www.ni.ac.rs/en/events

10. THE 5th INTERNATIONAL CONFERENCE ON COMPUTATIONAL MECHANICS AND VIRTUAL ENGINEERING - COMEC 2013
24 - 25th October 2013, Brasov, ROMANIA

Topics:
- *Computational Methods (Finite Element Method, Boundary Element Methods, Mesh less Methods, Multiscale Methods, Optimization Methods and Sensitivities, Discretization Methods, Mathematical Foundations, High Performance Computing, Inverse Problem, Visualization);*
- *Computational Solid Mechanics (Material Modeling, Finite Deformations and Localization, Micromechanics and Multiscale Modeling, Nanomechanics, Nonlinear Analysis of Structures, Multibody Dynamics and Robotics, Composite Structures, Structural Optimization, Experimental Mechanics);*
- *Composites Materials and Industrial Applications;*
- *Biomechanics (Biosolid Modeling, Modeling of Biofluids, Multiscale Modeling, Medical Imaging and Modeling, Medical Applications, Experimental Methods);*

For any further information, see at: https://sites.google.com/site/comec2013brasov/home

11. INTERNATIONAL CONGRESS ON ENERGY EFFICIENCY AND ENERGY RELATED MATERIALS (ENEFM)
9 - 12nd October, 2013, Kemer / Antalya, TURKEY

ENEFM is traditional annual congress for scientists and expected to collect a wide audience of participants and listeners. We hope that the scientific program, including a wide array of topics will live to your expectations, and that participation in the Congress will offer you an opportunity to meet up with your colleagues, friends and renowned specialists from all over the world.
For any further information, see at: http://www.enefm.org/

12. THE 12th INTERNATIONAL SCIENTIFIC CONFERENCE ON INFORMATICS - INFORMATICS'2013,
5 - 7th November, 2013, Spišská Nová Ves, SLOVAKIA

The 12th International Conference on Informatics INFORMATICS'2013 is an international forum for presenting original research results, sharing the experience and to exchange ideas from transferring theoretical concepts into real-life domains by scientists and experts working in Computer Science and Informatics.
The 12th International Conference on Informatics INFORMATICS'2013 is a biennial international forum which gives room for scientists, experts in computer science and professionals in new emerging fields of informatics to present original research results, to share experience and to exchange ideas about transferring theoretical concepts into real life. The conference provides a unique opportunity for establishing and maintaining professional relationships of widely recognized scientists between each another in specific areas of computer science.
For any further information, we recommend you the website: http://informatics.kpi.fei.tuke.sk/

13. 2nd REGIONAL CONFERENCE - MECHATRONICS IN PRACTICE AND EDUCATION – MechEdu 2013
5 - 6th December, 2013, Subotica, SERBIA

MECHEDU was born in the frame of IPA cross-border program with the aim of promoting activities in various areas of mechatronics by providing a forum for exchange of ideas, presentation of technical achievements and discussion of future directions.

The first MECHEDU conference in 2011 aroused much attention and positive feedback from the participants. Therefore, the representatives of Subotica Tech and Faculty of Technical Sciences from Serbia, together with F-AR and Mechatronik Plattform from Austria, agreed to jointly organize this conference in the future.
We hope that the MECHEDU 2013 Conference will bring together an international community of experts from the region to discuss the state-of-the-art, latest research results, perspectives of future developments, and innovative applications relevant to mechatronics.
For any further information, we recommend you the website: http://www.vts.su.ac.rs/sr/mechedu

14. INTERNATIONAL CONFERENCE ON FRONTIERS OF ENVIRONMENT, ENERGY & BIOSCIENCE - ICFEEB 2013
24 - 25th October, 2013, Beijing, CHINA

ICFEEB 2013 is one of the leading international conferences for presenting novel and fundamental advances in the fields of Environment, Energy and Bioscience. The purpose of the conference is for the scientists, scholars, engineers and students from the universities and the research institutes all around the world to present ongoing research activities, and hence to foster research relations. This conference provides opportunities for the delegates to exchange new ideas and application experiences face to face, to establish research or business relations and to find global partners for future collaboration. It also serves to foster communication among researchers and practitioners working in a wide variety of scientific areas with a common interest in improving Environment, Energy and Bioscience related techniques.
For any further information, we recommend you the website: http://www.icfeeb.org/

15. INTERNATIONAL CONFERENCE ON APPLIED SCIENCES
26 - 27th October 2013, Wuhan, CHINA

On behalf of Military Economy Research Center of Chinese People's Liberation Army, Military Economy Academy, Romania "Politehnica" University of Timisoara, Wuhan University, Huazhong University of Science and Technology, we are pleased to invite you to attend 2013 International Conference on Applied Sciences, which will be held in Wuhan of Hubei Province in China.
It will be focused on several fields of application, operation and influence of the applied science and technology on defense economy.
Warmly welcome researchers and postgraduates submit your papers and communicate on conference.
For any further information, we recommend you the website: http://www.icoas2013.net/index.htm

16. INTERNATIONAL CONFERENCE ON ENGINEERING : ENGINEERING FOR ECONOMIC DEVELOPMENT - ICEUBI2013
27 – 29 November, 2013, Covilhã, Portugal

ICEUBI 2013 aims to promote the contribution of Engineering for economic development, ensuring contact between researchers and practitioners from different fields of engineering and allowing the dissemination of its research, innovation and development within the various sectors of economic activity.
This event comes in the sequence of the successful "ICEUBI2011" (www.iceubi2011.ubi.pt), where more than 170 communications (and 150 participants) have been presented assuming a reference position in the international context of scientific meetings dedicated to engineering.
For any further information, we recommend you the website: http://193.136.66.103/iceubi2013

ACTA TECHNICA CORVINIENSIS – BULLETIN of ENGINEERING

ISSN: 2067-3809 [CD-Rom, online]

ACTA TECHNICA CORVINIENSIS – Bulletin of Engineering
Tome VI (Year 2013) – FASCICULE 4 [October–December]
ISSN 2067–3809

MANUSCRIPT PREPARATION - General Guidelines

These instructions are written in a form that satisfies all of the formatting requirements for the author manuscript. Please use them as a template in preparing your manuscript. Authors must take special care to follow these instructions concerning margins. The basic instructions are simple:

- *Manuscript shall be formatted for an A4 size page.*
- *The top and left margins shall be 25 mm.*
- *The bottom and right margins shall be 25 mm.*
- *The text shall have both the left and right margins justified.*

The original of the technical paper will be sent through e-mail as attached document (.doc, Windows 95 or higher). Manuscripts should be submitted to e-mail: redactie@fih.upt.ro, with mention "for **ACTA TECHNICA CORVINIENSIS – Bull. of Eng."**.*

STRUCTURE

The manuscript should be organized in the following order: Title of the paper, Authors' names and affiliation, Abstract, Key Words, Introduction, Body of the paper (in sequential headings), Conclusion, Acknowledgements (where applicable), References, and Appendices (where applicable).

THE TITLE

The title is centered on the page and is CAPITALIZED AND SET IN BOLDFACE (font size 14 pt). It should adequately describe the content of the paper. An abbreviated title of less than 60 characters (including spaces) should also be suggested.

AUTHOR'S NAME AND AFFILIATION

The author's name(s) follows the title and is also centered on the page (font size 11 pt). A blank line is required between the title and the author's name(s). Last names should be spelled out in full and succeeded by author's initials. The author's affiliation (in font size 11 pt) is provided below. Phone and fax numbers do not appear.

ABSTRACT

A nonmathematical abstract, not exceeding 200 words, is required for all papers. It should be an abbreviated, accurate presentation of the contents of the paper. It should contain sufficient information to enable readers to decide whether they should obtain and read the entire paper. Do not cite references in the abstract.

KEY WORDS

The author should provide a list of three to five key words that clearly describe the subject matter of the paper.

TEXT LAYOUT

The manuscript must be typed single spacing. Use extra line spacing between equations, illustrations, figures and tables. The body of the text should be prepared using Georgia or Times New Roman. The font size used for preparation of the manuscript must be 11 points. The first paragraph following a heading should not be indented. The following paragraphs must be indented 10 mm. Note that there is no line spacing between paragraphs unless a subheading is used. Symbols for physical quantities in the text should be written in italics.

FIGURES AND TABLES

Figures (diagrams and photographs) should be numbered consecutively using Arabic numbers. They should be placed in the text soon after the point where they are referenced. Figures should be centered in a column and should have a figure caption placed underneath. Captions should be centered in the column, in the format "Figure 1" and are in upper and lower case letters. When referring to a figure in the body of the text, the abbreviation "Figure" is used Illustrations must be submitted in digital format, with a good resolution. Table captions appear centered above the table in upper and lower case letters. When referring to a table in the text, "Table" with the proper number is used. Captions should be centered in the column, in the format "Table 1" and are in upper and lower case letters. Tables are numbered consecutively and independently of any figures. All figures and tables must be incorporated into the text.

EQUATIONS AND MATHEMATICAL EXPRESSIONS

Equation numbers should appear in parentheses and be numbered consecutively. All equation numbers must appear on the right-hand side of the equation and should be referred to within the text.

CONCLUSION

A conclusion section must be included and should indicate clearly the advantages, limitations and possible applications of the paper. Discuss about future work.

ACKNOWLEDGEMENTS

An acknowledgement section may be presented after the conclusion, if desired. Individuals or units other than authors who were of direct help in the work could be acknowledged by a brief statement following the text.

REFERENCES

References should be listed together at the end of the paper in alphabetical order by author's surname. List of references indent 10 mm from the second line of each references. Personal communications and unpublished data are not acceptable references.

***Journal Papers**: Surname 1, Initials; Surname 2, Initials and Surname3, Initials: Title, Journal Name, volume (number), pages, year.*

***Books**: Surname 1, Initials and Surname 2, Initials: Title, Edition (if existent), Place of publication, Publisher, year.*

***Proceedings Papers**: Surname 1, Initials; Surname 2, Initials and Surname 3, Initials: Paper title, Proceedings title, pages, year.*

ACTA TECHNICA CORVINIENSIS - BULLETIN of ENGINEERING

ISSN: 2067-3809 [CD-Rom, online]

ACTA TECHNICA CORVINIENSIS – Bulletin of Engineering
Tome VI (Year 2013) – FASCICULE 4 [October–December]
ISSN 2067–3809

Indexes & Databases

ACTA TECHNICA CORVINIENSIS - BULLETIN of ENGINEERING

*is accredited and ranked in the **"B+" CATEGORY** Journal by **CNCSIS - The National University Research Council's Classification of Romanian Journals (poz. 940)**. The Journal is a part of the **SCIPIO - The Romanian Editorial Platform.***

ACTA TECHNICA CORVINIENSIS - BULLETIN of ENGINEERING

is indexed and covered in the following databases and directories:

INDEX COPERNICUS - JOURNAL MASTER LIST
http://journals.indexcopernicus.com/

GENAMICS JOURNALSEEK Database
http://journalseek.net/

DOAJ - Directory of Open Access Journals
http://www.doaj.org/

EVISA Database
http://www.speciation.net/

CHEMICAL ABSTRACTS SERVICE (CAS)
A division of the American Chemical Society
http://www.cas.org/

EBSCO Publishing
http://www.ebscohost.com/

GOOGLE SCHOLAR

http://scholar.google.com

SCIRUS - Elsevier

http://www.scirus.com/

ULRICHSweb - Global serials directory

http://ulrichsweb.serialssolutions.com

getCITED

http://www.getcited.org

BASE - Bielefeld Academic Search Engine

http://www.base-search.net

Electronic Journals Library

http://rzblx1.uni-regensburg.de

Open J-Gate

http://www.openj-gate.com

ProQUEST Research Library

http://www.proquest.com

ACTA TECHNICA CORVINIENSIS - BULLETIN of ENGINEERING

ISSN: 2067-3809 [CD-Rom, online]

ACTA TECHNICA CORVINIENSIS
– BULLETIN of ENGINEERING

ACTA TECHNICA CORVINIENSIS
– BULLETIN of ENGINEERING
ISSN: 2067-3809 [CD-Rom, online]

ACTA TECHNICA CORVINIENSIS
BULLETIN OF ENGINEERING

ISSN: 2067-3809

fascicule 4
[October-December]

TOME VI
[2013]